Author:
Ouyang, Huiling

Title:
Investigating the Impact of Titanium Dioxide Nanoparticles on Estuarine Benthic Diatoms

Investigating the Impact of Titanium Dioxide Nanoparticles on Estuarine Benthic Diatoms

Huiling Ouyang

A dissertation submitted to the University of Bristol in accordance with the requirements for award of the degree of Doctor of Philosophy in the Faculty of Life Science.

School of Biological Sciences

September 2019

57345 words

Abstract

The dramatically escalating increase in the production and application of titanium dioxide nanoparticles (nano-TiO_2) has raised concerns of their risk, due to their extremely small size and high surface area to volume ratio. Increasing amounts of nano-TiO_2 are released into the environment intentionally or accidentally, and they are anticipated to accumulate in the estuarine sediments and could impact microorganisms in biofilms. The negative impacts of nano-TiO_2 on algae have been widely recorded. However, most of the previous studies have been carried out with planktonic species, with little focus on the benthic species. This research focused on the impact of a commercially available nano-TiO_2 product, P25, on selected species of estuarine benthic diatoms from Portishead, Severn Estuary, UK.

Ultraviolet radiation (UVR) was found to play an importance role in determining the impact of nano-TiO_2 on the estuarine benthic diatoms. In the presence of fluorescent lighting containing a negligible amount of UVR, the cell density yield and growth rate of *Nitzschia* cf. *clausii*, *Navicula gregaria*, and *Cylindrotheca closterium* were significantly stimulated by the presence of 100 mg/L nano-TiO_2. In the presence of lighting containing a considerable amount of UVR, the cell density yield and growth rate of *Cylindrotheca closterium* were significantly inhibited by the presence of nano-TiO_2, with the 72 h-IC50 being 8.73 mg/L (95% confidence interval of 8.54 – 8.94 mg/L). In the presence of lighting containing a considerable amount of UVR, the total chlorophyll *a* content in an estuarine microphytobenthos (MPB) community (dominated by benthic diatoms) exposed to 50 – 200 mg/L nano-TiO_2 was not significantly different from the untreated MPB, but the phaeopigment concentrations in the treated MPBs were significantly higher, after 1 week and 2 weeks of exposure to nano-TiO_2. The genera composition of the MPB diatom community, derived from field samples exposed to 50 – 200 mg/L nano-TiO_2, was not significantly different from the untreated MPB, after 1 week of exposure; however, after 2 weeks of exposure, a significant shift was recorded in the genera composition of the diatom community in the treated MPB, with an increase in the relative abundance of the genus *Entomoneis* and decreases in the relative abundance of genus *Navicula* and *Cylindrotheca*, compared to the untreated MPB.

Estuarine benthic diatoms growing on mudflats are subjected to UVR exposure, especially when the tide goes out. Results from this research highlighted that nano-TiO_2 could negatively impact the benthic diatom community in the intertidal mudflats of estuaries, which may have further impacts on estuarine primary production.

Dedication and Acknowledgements

First of all, I would like to thank my primary supervisor, Professor Marian Yallop: thanks very much for your supervision in the past six years; without your help, guidance, instruction and pushing, I could never get this thesis done. I would also like to thank my other supervisors, Professor Andy Radford and Professor Tom Scott for all the help and guidance during the project.

I would like to thank every current or former members in Yallop's group and Scott's group, in particular Dan Fagan, Ria Woodfield, Chong Liu, Jasmina Majit, Huw Pullin, Peter Martin, Keith Hallam, Annette Richer, Christopher Williamson, Bunmi Ogunjemilusi, Amy Ockenden, Deirdre McLachlan and Ian Griffiths. Thanks Deirdre McLachlan for the help with proof-reading. My thanks also go to all my friends, thanks for bringing me all the happiness. I would also like to thank my examiners, Prof. Mike Allen and Dr Gary Barker for the helpful and inspiring comments and suggestions.

Finally, I would like to thank my family for their support. I want to thank my boy for coming into my life with all the joy and pain, turning my life into a "hard" mode. I also want to thank my husband for pushing me forward every day and night.

This research was funded by a University of Bristol Postgraduate Scholarship. I would also like to acknowledge the grants provided by the British Phycological Society and the University of Bristol Alumni, which supported my attendance at the 6th European Phycological Congress (EPC6).

Author’s declaration

I declare that the work in this dissertation was carried out in accordance with the requirements of the University's *Regulations and Code of Practice for Research Degree Programmes* and that it has not been submitted for any other academic award. Except where indicated by specific reference in the text, the work is the candidate's own work. Work done in collaboration with, or with the assistance of, others, is indicated as such. Any views expressed in the dissertation are those of the author.

SIGNED: ..... DATE: .....

Table of Contents

Abstract i
Dedication and Acknowledgements ii
Author's declaration iii
Table of Contents iv
List of Figures ix
List of Tables xiii
Chapter 1 General introduction on nanoparticles 1
1.1 Definition of a nanoparticle 1
1.2 Sources of nanoparticles 1
1.3 Concerns about ENPs 3
1.4 Engineered nano-TiO_2 in the environment 5
1.4.1 Forms of nano-TiO_2 5
1.4.2 Application of nano-TiO_2 7
1.4.3 Fate of nano-TiO_2 7
1.4.4 Environmental concentration of nano-TiO_2 9
1.5 General information for the impact of nano-TiO_2 on the biota 10
1.6 Current knowledge regarding the impact of nano-TiO_2 on algae 11
1.6.1 Varied results on the impact of nano-TiO_2 on algae 11
1.6.2 Possible mechanisms for the impact of nano-TiO_2 16
1.6.3 The importance of illumination on the impact of nano-TiO_2 18
1.7 Knowledge gaps and aims of this thesis 18
1.7.1 Knowledge gaps 18
1.7.2 The importance of estuarine benthic diatoms 19
1.7.3 Aims of this thesis 20
Chapter 2 The aggregation and sedimentation behavior of nano-TiO_2 (P25) in an artificial estuarine environment 21
2.1 Introduction 21
2.1.1 The aggregation of NPs in the aqueous environment 21
2.1.2 Measurements of aggregation behavior of NPs 23
2.1.3 The aggregation of nano-TiO_2 in the aqueous environment 23
2.1.4 Aims and hypotheses 24
2.2 Methods 26
2.2.1 Characterization of nano-TiO_2 26
2.2.2 Selecting the best wavelength for estimating the concentration of nano-TiO_2 suspended in the water 28
2.2.3 Sedimentation studies of nano-TiO_2 in the estuarine waters 29
2.2.4 Hydrodynamic diameter of nano-TiO_2 aggregates 32
2.2.5 Zeta-potential measurement 33
2.2.6 Data analysis 33
2.3 Results 34

2.3.1 Characterization of nano-TiO_2 powder ····· 34
2.3.2 Relationship between absorbance and concentration of nano-TiO_2 ····· 37
2.3.3 Sedimentation of nano-TiO_2 under different salinity and pH ····· 39
2.3.4 Hydrodynamic diameter and zeta-potential of nano-TiO_2 aggregates in the AEW ····· 41
2.3.5 Sedimentation of nano-TiO_2 particles under different particle concentrations in seawater ····· 42
2.3.6 Summary of results ····· 45
2.4 Discussion ····· 45
2.4.1 Characteristics of nano-TiO_2 ····· 45
2.4.2 Determination of nano-TiO_2 concentration by absorbance ····· 47
2.4.3 The impact of salinity and pH on the sedimentation of nano-TiO_2 ····· 48
2.4.4 The impact of particle concentration on the sedimentation of nano-TiO_2 in seawater ····· 50
2.4.5 Limitations and suggestions ····· 52
2.5 Conclusion ····· 53
Chapter 3 Critical evaluation of the methods for measuring growth parameters of three estuarine benthic diatom isolates in the presence of nano-TiO_2 ····· 55
3.1 Introduction ····· 55
3.1.1 Quantification of the impact of a substance on algal growth ····· 55
3.1.2 Quantification of the impact of nano-TiO_2 on algal growth ····· 56
3.2 Materials and Methods ····· 59
3.2.1 Estuarine benthic diatom cultures ····· 59
3.2.2 Test nanoparticles ····· 62
3.2.3 Could cell enumeration using light microscopy provide reliable results for quantification of algal biomass in estuarine benthic diatoms in the presence of nano-TiO_2? ····· 63
3.2.4 Could chlorophyll *a* content measurement determined using a spectrophotometer provide reliable results for quantification of algal biomass in estuarine benthic diatoms in the presence of nano-TiO_2? ···· 65
3.2.5 Could *in vivo* fluorescence measurement provide reliable results for quantification of algal biomass in estuarine benthic diatoms in the presence of nano-TiO_2? ····· 66
3.2.6 Data analysis ····· 67
3.3 Results ····· 67
3.3.1 Could cell enumeration using light microscopy provide reliable results for quantification of algal biomass in estuarine benthic diatoms in the presence of nano-TiO_2? ····· 67
3.3.2 Could chlorophyll *a* content determined using a spectrophotometer provide reliable results for quantification of algal biomass in estuarine benthic diatoms in the presence of nano-TiO_2? ····· 71
3.3.3 Could *in vivo* fluorescence measurement provide reliable results for quantification of algal biomass in estuarine benthic diatoms in the presence of nano-TiO_2? ····· 72
3.4 Discussion ····· 73
3.4.1 Could cell enumeration using light microscopy provide reliable results for quantification of algal biomass in estuarine benthic diatoms in the presence of nano-TiO_2? ····· 73
3.4.2 Could chlorophyll *a* content determined using a spectrophotometer provide reliable results for quantification of algal biomass in estuarine benthic diatoms in the presence of nano-TiO_2? ····· 74
3.4.3 Could *in vivo* fluorescence measurements provide reliable results for quantification of algal biomass in estuarine benthic diatoms in the presence of nano-TiO_2? ····· 75
3.5 Conclusion ····· 75
Chapter 4 Investigation on the growth of three estuarine benthic diatoms exposed to nano-TiO_2 in the

presence of fluorescent lighting ····· **77**
4.1 Introduction ····· 77
Section 1: The impact of nano-TiO_2 on the growth of three estuarine benthic diatoms in the presence of fluorescent lighting ····· 78
4.2 Method ····· 79
4.2.1 Estuarine benthic diatoms ····· 79
4.2.2 TiO_2 particles ····· 79
4.2.3 The impact of TiO_2 particle type on the growth of estuarine benthic diatoms in the presence of fluorescent lighting ····· 80
4.2.4 Cell density measurement ····· 81
4.2.5 Chlorophyll *a* content measurement ····· 82
4.2.6 Data analysis ····· 82
4.3 Results ····· 82
4.3.1 Characteristics of TiO_2 particles ····· 82
4.3.2 The impact of TiO_2 particle type on the biomass yield of three estuarine benthic diatoms in the presence of fluorescent lighting ····· 85
4.3.3 The impact of TiO_2 particles on the growth rate of three estuarine benthic diatoms in the presence of fluorescent lighting ····· 87
4.3.4 The impact of TiO_2 particles on the chlorophyll *a* concentration per cell of three estuarine benthic diatoms in the presence of fluorescent lighting ····· 88
4.3.5 Summary of results ····· 89
Section 2: Investigation on the possible mechanisms for the stimulated growth of estuarine benthic diatoms in the presence of nano-TiO_2 and fluorescent lighting ····· 91
4.4 Methods ····· 94
4.4.1 The impact of light intensity on the growth rate of estuarine benthic diatoms in the presence of fluorescent lighting ····· 94
4.4.2 The impact of nutrient availability on the growth of *Nitzschia* cf. *clausii* in the presence of fluorescent lighting ····· 95
4.4.3 Data analysis ····· 95
4.5 Results ····· 96
4.5.1 The impact of light intensity on the growth of estuarine benthic diatoms in the presence of fluorescent lighting ····· 96
4.5.2 The impact of nutrient concentration on the growth of *Nitzschia* cf. *clausii* in the presence of fluorescent lighting ····· 97
4.5.3 Summary of results ····· 98
4.6 Discussion ····· 99
4.6.1 The impact of nano-TiO_2 on the growth of estuarine benthic diatom in the presence of fluorescent lighting ····· 99
4.6.2 The possible mechanisms to account for the stimulated growth of estuarine benthic diatoms observed in the presence of 100 mg/L nano-TiO_2 and fluorescent lighting ····· 103
4.6.3 The impact of TiO_2 on estuarine benthic diatoms in the presence of fluorescent lighting: was primary particle size a key factor for the stimulation impact of TiO_2? ····· 105
4.6.4 The impact of TiO_2 on estuarine benthic diatoms in the presence of fluorescent lighting: was there a species-specific response? ····· 106

4.6.5 Limitations and suggestions ····· 107
4.7 Conclusion ····· 108
Chapter 5 Investigation on the response of estuarine benthic diatom *Cylindrotheca closterium* exposed to nano-TiO_2 in the presence of ultraviolet radiation ····· 110
5.1 Introduction ····· 110
5.2 Methods ····· 113
5.2.1 Culture condition ····· 113
5.2.2 TiO_2 particles ····· 114
5.2.3 The impact of TiO_2 particle type on the growth of *Cylindrotheca closterium* in the presence of UV lighting ····· 114
5.2.4 The impact of nano-TiO_2 on the growth of *Cylindrotheca closterium* in relation to particle concentration and cultivation time in the presence of UV lighting ····· 115
5.2.5 The impact of nano-TiO_2 on the photophysiology of *Cylindrotheca closterium* in the presence of UV lighting ····· 115
5.2.6 Growth measurements and calculations ····· 116
5.2.7 PAM measurements and calculations ····· 117
5.2.8 Data analyses ····· 118
5.3 Results ····· 119
5.3.1 Impact of TiO_2 particle type on the growth of *Cylindrotheca closterium* in the presence of UV lighting ····· 119
5.3.2 The impact of nano-TiO_2 on the growth of *Cylindrotheca closterium* in relation to particles concentration and cultivation time in the presence of UV lighting ····· 120
5.3.3 Impact of nano-TiO_2 on the photophysiology of *Cylindrotheca closterium* ····· 124
5.3.4 Summary of results ····· 126
5.4 Discussion ····· 126
5.4.1 The impact of TiO_2 on estuarine benthic diatoms in the presence of UV lighting: was primary particle size a key factor for the growth inhibition of TiO_2? ····· 126
5.4.1 The IC50 value of nano-TiO_2 for *Cylindrotheca closterium* in the presence of UV lighting ····· 128
5.4.2 The temporal change of growth inhibition of nano-TiO_2 in the presence of UV lighting ····· 131
5.4.3 The impact of nano-TiO_2 on the photophysiology of *Cylindrotheca closterium* in the presence of UV lighting ····· 132
5.4.4 Limitations and suggestions ····· 133
5.5 Conclusion ····· 135
Chapter 6 Investigation on the response of an estuarine microphytobenthic community dominated by benthic diatoms exposed to nano-TiO_2 in the presence of ultraviolet radiation ····· 136
6.1 Introduction ····· 136
6.1.1 The importance of microphytobenthic biofilms in the estuarine ecosystem ····· 136
6.1.2 The presence of benthic diatoms in the intertidal MPB ····· 136
6.1.3 The impact of nano-TiO_2 on the intertidal MPB ····· 137
6.2 Methods ····· 139
6.2.1 Test nanoparticles ····· 139
6.2.2 Intertidal MPB preparation ····· 139
6.2.3 Experimental setup ····· 141
6.2.4 Biomass measurements ····· 142

6.2.5 Diatom composition analysis ····· 143
6.2.6 Diatom community diversity index calculation ····· 144
6.2.7 Data analysis ····· 144
6.3 Results ····· 145
6.3.1 The impact of nano-TiO_2 on the chlorophyll *a* content of the intertidal MPB in the presence of UV lighting ····· 145
6.3.2 The impact of nano-TiO_2 on the phaeopigment content of the intertidal MPB in the presence of UV lighting ····· 146
6.3.3 The impact of nano-TiO_2 on the richness of the diatom community in the intertidal MPB in the presence of UV lighting ····· 148
6.3.4 The impact of nano-TiO_2 on the diversity of the diatom community in the intertidal MPB in the presence of UV lighting ····· 149
6.3.5 The impact of nano-TiO_2 on the diatom composition in the intertidal MPB in the presence of UV lighting ····· 152
6.3.6 Summary of results ····· 160
6.4 Discussion ····· 161
6.4.1 The impact of nano-TiO_2 on the biomass of the intertidal MPB in the presence of UV lighting ·· 161
6.4.2 The impact of nano-TiO_2 on the diatom composition in the intertidal MPB in the presence of UV lighting ····· 163
6.4.3 Environmental relevance and implications of the present study ····· 165
6.4.4 Limitations and suggestions ····· 167
6.5 Conclusion ····· 167
Chapter 7 Synthesis and recommendations for future studies ····· 169
7.1 The importance of illumination type when determining the impact of nano-TiO_2 ····· 169
7.2 Species-specific sensitivity to the presence of nano-TiO_2 ····· 170
7.3 Is *Cylindrotheca closterium* a good model species for investigating the impact of nano-TiO_2? ····· 172
7.4 Considerations for selecting suitable endpoints to address the risk of nano-TiO_2 ····· 173
Abbreviations ····· 176
Reference ····· 178

List of Figures

Figure 1.1 Illustrating a range of examples for the application of nanoparticles, modified from Tsuzuki (2009). 2
Figure 1.2 Generalized trend for the particle reactivity (the tendency of a particle to undergo chemical reactions) as a function of particle size, modified from Wigginton et al. (2007). 4
Figure 1.3 Photoreaction on the surface of a TiO_2 particle, when irradiated by photons with energy higher than the band gap. Modified from Chong et al. (2010). 6
Figure 1.4 Illustration for the possible mechanisms for the impact of nano-TiO_2 on an algal cell, modified from Chen et al. (2019). OH●, O_2^-●, H_2O_2 are short for OH radicals, superoxide radical anions and hydrogen peroxide, respectively, which are reactive oxygen species (ROS). 17
Figure 2.1 Flow chart for measuring the absorption of nano-TiO_2 suspension and the time interval between each step. 28
Figure 2.2 (A) Scanning electron microscopy images and (B) transmission electron microscopy images of nano-TiO_2 powder. The TEM image was taken by Dr Ian Griffiths, School of Physics, University of Bristol, UK. 34
Figure 2.3 Size distribution of primary nano-TiO_2 particles. The x-axis shows the size of a particle and is in log-scale. 35
Figure 2.4 X-ray powder diffraction (XRD) pattern of (A) nano-TiO_2 (P25) and reference pattern (downloaded from http://rruff.info/) of (B) pure anatase (RRUFF ID: R060277.9), (C) pure rutile (RRUFF ID: R050031.1) and (D) pure brookite (RRUFF ID: R050363.1). 36
Figure 2.5 Absorption spectra of 10 mg/L nano-TiO_2 in the Milli-Q water (black line) and AEW 8-30 (artificial estuarine water, pH = 8, salinity = 30 ‰) (red line) within range of 280 to 800 nm. Results are shown as mean values (lines) and 95% confidence interval (grey areas, n = 3). 37
Figure 2.6 The variation of coefficient of determination (R^2) of the linear regression between the concentration of nano-TiO_2 (1 – 100 mg/L) and absorbance value of nano-TiO_2 suspension as a function of wavelength (nm). Nano-TiO_2 was dispersed in Milli-Q water (black line) or AEW 8-30 (artificial estuarine water, pH = 8, salinity = 30 ‰) (red line). 38
Figure 2.7 The state of nano-TiO_2 (100 mg/L) suspension in 30 AEW samples within 72 h. The salinity of AEW samples varied from 0 to 35 ‰. Images were taken at (A-E) < 10 min, (F-J) 1 h, (K-O) 4 h, (P-T) 24 h, (U-Y) 72 h for samples with pH of (A, F, K, P, U) 5, (B, G, L, Q, V) 6, (C, H, M, R, W) 7, (D, I, N, S, X) 8 or (E, J, O, T, Y) 9. 40
Figure 2.8 Sedimentation profile of nano-TiO_2 in 30 different AEW samples with salinity being (A) 0, (B) 10 ‰, (C) 20 ‰, (D) 25 ‰, (E) 30 ‰, (F) 35 ‰. The pH value of AEW samples is denoted by colour. Results are shown as mean ± standard deviation (n = 3). When the standard deviation is not visible, it is smaller than the symbol. 41
Figure 2.9 The state of nano-TiO_2 suspensions in the AEW 8-30 (pH = 8, salinity = 30 ‰) with different initial concentrations after (A) < 10 min, (B) 1 h, (C) 2 h, (D) 4 h, (E) 7 h, (F) 24 h. 43
Figure 2.10 Sedimentation of nano-TiO_2 in the AEW 8-30 (pH = 8, salinity = 30 ‰) as a function of time with 3 different initial particle concentrations (C_0). Results are shown as mean ± standard deviation (n = 6). When the standard deviation is not visible, it is smaller than the symbol. 44
Figure 2.11 The relationship between suspension absorbance at 330 nm (dashed lines) or 421 nm (solid lines) with the concentration of nano-TiO_2, when nano-TiO_2 was dispersed in the Milli-Q water (black lines) or AEW 8-30 (red lines). 48

Figure 3.1 (A, C, E) Light microscopy images and (B, D, F) scanning electron microscopy images of three estuarine benthic diatom clones isolated from the Severn Estuary. (A, B) *Navicula gregaria*, (C, D) *Nitzschia* cf. *clausii*, (E, F) *Cylindrotheca closterium*. Scale bar = 10 µm. 61
Figure 3.2 Growth curve of (A) *Navicula* gregaria, (B) *Nitzschia* cf. *clausii*, (C) *Cylindrotheca closterium*. over a 6-day period. The values represent the means ± 1 standard deviation. N = 3. 62
Figure 3.3 Images of diatom cells and TiO_2 aggregates in the haemocytometer counting chamber under (A, C, E) light microscopy and (B, D, F) fluorescence microscopy. (A, B) *Navicula gregaria*; (C, D) *Nitzschia* cf. *clausii*; (E, F) *Cylindrotheca closterium*. Purple circles highlighted the cells completely invisible under light microscopy. The width of the square on the grid is 250 µm. 69
Figure 3.4 Cell density of *Navicula gregaria* cultures cultivated with and without nano-TiO_2 for 72 h. Results obtained without sonication were shown in white bars. Results obtained after sonication with H_2SO_4 were shown in grey bars. Results are shown as mean ± standard deviation (n = 6). Significance of the difference between bars were determined by independent-samples T tests (between two white bars or two grey bars) or paired-samples T tests (between white and grey bars within the same group). 71
Figure 3.5 Calculated chlorophyll *a* content of *Navicula gregaria* cultures with and without the presence of nano-TiO_2. Results are shown as mean ± standard deviation (n = 6)..... 72
Figure 3.6 *In vivo* fluorescence intensity of *Navicula gregaria* cultures with and without the presence of nano-TiO_2. Results are shown as mean ± standard deviation (n = 6)..... 73
Figure 4.1 (A, B) Transmission electron microscopy (TEM) images and (C, D) scanning electron microscopy (SEM) images of (A, C) nano-TiO_2 and (B, D) micro-TiO_2. The TEM images were taken by Dr Ian Griffiths, School of Physics, University of Bristol, UK. 83
Figure 4.2 Energy-dispersive X-ray (EDX) spectra of (A) micro-TiO_2 and (B) nano-TiO_2.The presence of element titanium (Ti), oxygen (O) and chlorine (Cl) respond to the peaks are marked in the figure. The EDX spectra were taken by Dr Chong Liu, School of Physics, University of Bristol, UK. 84
Figure 4.3 Z-average hydrodynamic size (measured by Zetasizer Nano-S90) of nano-TiO_2 and micro-TiO_2 (100 mg/L) aggregates in the f/2 medium at 5 different time points. Results are shown as mean ± standard deviation (n = 3). 85
Figure 4.4 The biomass yield of diatom cultures grown with no TiO_2 (control), 100 mg/L micro-TiO_2 and 100 mg/L nano-TiO_2, after 72 h of cultivation in the presence of fluorescent lighting. Three different species (*Nitzschia* c.f. *clausii*, *Navicula gregaria* and *Cylindrotheca closterium*) were tested. Results are shown as mean ± standard deviation (n = 12). Within each species, bars with the same letter are not significantly different (Tukey HSD *post-hoc* test). 87
Figure 4.5 The chlorophyll *a* concentration per cell of diatoms grown with no TiO_2 (control), 100 mg/L micro-TiO_2 and 100 mg/L nano-TiO_2, in the presence of fluorescent lighting. Three different species (*Nitzschia* c.f. *clausii*, *Navicula gregaria* and *Cylindrotheca closterium*) were tested. Results are shown as mean ± standard deviation (n = 12). 89
Figure 4.6 The relative growth rate (µ) of diatom cultures cultivated under a series of light intensities (30 – 70 µmol m^{-2} s^{-1}), compared to the growth rate of the control group cultivated at 80 µmol m^{-2} s^{-1} in the presence of fluorescent lighting. Three different species (*Nitzschia* c.f. *clausii*, *Navicula gregaria* and *Cylindrotheca closterium*) are marked by the colour of the bars. Results are shown as mean ± standard deviation (n = 6). 97
Figure 4.7 The average growth rate within 72 h of *Nitzschia* c.f. *clausii* grown in the normal f/2 medium (control) and nitrate, phosphate, silicate and trace metal enriched f/2 media, in the presence of fluorescent lighting. Results are shown as mean ± standard deviation (n = 4). Bars with the same letter are not significantly different (Tukey HSD *post-hoc* test). 98

Figure 5.1 An example of a typical rapid light curve. 118
Figure 5.2 The average growth rate within 72 h for *Cylindrotheca closterium* cultures in the control group (without TiO_2) and treatments with 100 mg/L micro-TiO_2 and 100 mg/L nano-TiO_2, in the presence of fluorescent lighting (grey bar) or UV lighting (white bars). Results are shown as mean ± standard deviation (n = 6). 120
Figure 5.3 The growth curves of *Cylindrotheca closterium* cultures with varying concentrations of nano-TiO_2 in the presence of UV lighting, indicated by temporal change in cell density. The concentration of nano-TiO_2 is denoted by different symbols. Results are shown as mean ± standard deviation (n = 4). The Y-axis is shown in log-scale. Significant difference compared to the control group was marked as * ($0.01 \leq p < 0.05$) and ** ($p < 0.01$) next to the symbol, based on TukeyHSD *post-hoc* test, at each measuring time point. 121
Figure 5.4 Dose-response curves of *Cylindrotheca closterium* to the presence of nano-TiO_2 after different periods of cultivation (denoted by colour), in the presence of UV lighting. Responses are defined as the inhibition percentage on growth rate (IP) in the treatment group compared to the control group grown without TiO_2. Results are shown as mean ± standard deviation (n = 4). Curves were fitted with a log-logistic model. The R^2 values indicate the goodness of curve fitting are shown in the figure. The IC50 values are shown as mean and 95% confidence interval in the parentheses in the figure. 123
Figure 5.5 Rapid light curves (RLCs) of *Cylindrotheca closterium* cultures with varying concentrations of nano-TiO_2 (denoted by different symbols), in the presence of UV lighting. Results are shown as mean ± standard deviation (n = 4). The RLC curve was fitted with the model of Eilers and Peeters (1988). 125
Figure 6.1 (A) An example of the MPBs from the Severn Estuary (brown colour, located with red arrows) on the surface of the mudflat. (B) MPB isolation process with lens-tissue method and additional cover glasses (10 mm in diameter). (C) Visualization of MPBs biofilms grown at the bottom of microplate wells (brown colour, located with red arrows). 140
Figure 6.2 The biomass (indicated by chlorophyll *a* concentration) in the initial intertidal MPB (denoted as Time 0) and in MPBs following cultivation with varying concentrations of nano-TiO_2 for 1 week (denoted as Week 1) and 2 weeks (denoted as Week 2), in the presence of UV lighting. Results are shown as mean ± standard deviation (n = 6). 146
Figure 6.3 The phaeopigment concentration in the initial intertidal MPB (denoted as Time 0) and in MPBs following cultivation with varying concentrations of nano-TiO_2 after 1 week (denoted as Week 1) and 2 weeks (denoted as Week 2), in the presence of UV lighting. Results are shown as mean ± standard deviation (n = 6). Bars sharing a same lowercased-letter or uppercased-letter are not significantly different (TukeyHSD *post-hoc* test). 148
Figure 6.4 Scanning electron microscopy images of frustules belongs to genus (A) *Amphora*, (B) *Cylindrotheca*, (C) *Entomoneis*, (D) *Gyrosigma*, (E) *Navicula*, (F) *Nitzschia*, in the intertidal MPB. 149
Figure 6.5 The relative abundance of each diatom genus (marked by colour) in the initial intertidal MPBs (Time 0) and in the MPBs cultivated with varying concentrations of nano-TiO_2, after 1 week (Week 1) and 2 weeks of cultivation (Week 2), in the presence of UV lighting. Results are shown as the mean value of 6 replicates. 150
Figure 6.6 The diversity of diatom community in the initial intertidal MPB (Time 0) and in MPBs cultivated with varying concentrations of nano-TiO_2 for 1 week (Week 1) and 2 weeks (Week 2) in the presence of UV lighting. The diversity of diatom community was indicated by Shannon diversity index (H'). Results are shown as mean ± standard deviation (n = 6). 152
Figure 6.7 NMDS plot based on the relative abundance of 6 diatom genera in intertidal MPBs cultivated with varying concentration of nano-TiO_2 (marked by colour) for 1 week in the presence of UV lighting. Each point indicates an individual replicate in the group. 153

Figure 6.8 Bubble NMDs plots showing the relative abundance of genus (A) *Amphora*, (B) *Cylindrotheca*, (C) *Entomoneis*, (D) *Gyrosigma*, (E) *Navicula*, (F) *Nitzschia* in the initial intertidal MPB (Time 0) and in the MPBs cultivated with varying concentration of nano-TiO_2 (mg/L) for 1 week (Week 1) in the presence of UV lighting. The concentration of nano-TiO_2 are denoted by numbers in the parentheses in the legend. Each point indicates an individual replicate in the group. Within each genus, larger bubbles indicate a relatively higher relative abundance. Bubble sizes are not comparable between genera. The Spearman's rank correlation coefficient (SR) and *P* value between Axis 1 values and the RA of each genus are shown in the Figure. 155
Figure 6.9 Bubble NMDS plots showing the relative abundance (RA) of genus (A) *Amphora*, (B) *Cylindrotheca*, (C) *Entomoneis*, (D) *Gyrosigma*, (E) *Navicula*, (F) *Nitzschia* in the intertidal MPBs cultivated with varying concentration of nano-TiO_2 (denoted by colour) for 2 weeks in the presence of UV lighting. Each point indicates an individual replicate in the group. Within each genus, larger bubbles indicate a relatively higher RA. Bubble sizes are not comparable between genera. The Spearman's rank correlation coefficient (SR) and *P* value between Axis 1 values and the RA of each genus are shown in each figure. 157
Figure 6.10 NMDS plot based on the relative abundance of 6 diatom genera in the intertidal MPBs cultivated with varying concentration of nano-TiO_2 (mg/L) for 1 week (Week 1) and 2 weeks (Week 2). The concentration of nano-TiO_2 are denoted by numbers in the parentheses in the legend. Each point indicates an individual replicate in the group. 159
Figure 6.11 Bubble plots showing the relative abundance of genus (A) *Amphora*, (B) *Cylindrotheca*, (C) *Entomoneis*, (D) *Gyrosigma*, (E) *Navicula*, (F) *Nitzschia* in the intertidal MPBs cultivated after 1 week or 2 weeks of cultivation (marked by different colour). Each point indicates an individual replicate in the group. Within each genus, larger bubbles indicate a relatively higher relative abundance. Bubble sizes are not comparable between genera. The Spearman's rank correlation coefficient (SR) and *P* value between Axis 1 values and the RA of each genus are shown in the figure. 160

List of Tables

Table 1.1 Examples of the applications of nano-TiO_2 in our daily lives. 7
Table 1.2 Estimated environmental concentrations of nano-TiO_2 in different compartments..... 10
Table 1.3 The 72 h-IC50 values for nano-TiO_2 (concentration of nano-TiO_2 at which the inhibition percentage on the growth rate is 50% after 72 h of exposure) on freshwater green alga *Pseudokirchneriella subcapitata* in the presence of fluoresent lighting. Data are presented in the order of increasing 72 h-IC50 values. Data are shown as the mean value or the range of the value. "–" indicates that the information is not available. 13
Table 1.4 The details of three growth container and the corresponding 72 h-IC50 values of nano-TiO_2 (concentration of nano-TiO_2 at which the inhibition percentage on the growth rate is 50% after 72 h of exposure) on freshwater green alga *Pseudokirchneriella subcapitata* in the study conducted by Nicolas et al. (2016)..... 14
Table 2.1 Components in the base medium for artificial estuarine water (AEW) samples, adopted from the f/2 medium recipe (Guillard and Ryther 1962)..... 29
Table 2.2 Five primary stocks for making trace metal stock of f/2 medium (Guillard and Ryther 1962)..... 30
Table 2.3 Skewness, kurtosis and normality test results provided by SPSS for the primary particle size distribution of nano-TiO_2. 35
Table 2.4 Z-average hydrodynamic diameter, zeta-potential of nano-TiO_2 (100 mg/L) dispersed in 3 AEW samples. Results are shown as mean ± standard deviation (n = 3). For sample codes, see section 2.2.3.1..... 42
Table 2.5 The sedimentation rate constant (k) and the coefficient of determination (R^2) for the sedimentation curve of nano-TiO_2 in the AEW 8-30 (pH = 8, salinity = 30 ‰), according to first-order kinetics..... 45
Table 2.6 The properties of nano-TiO_2 (P25) measured in the present study compared to the manufacture information and other studies. Results are shown as the mean value, or mean value ± standard deviation, or the range of the value. "–" denotes the information is not available. 46
Table 2.7 Remaining percentage of nano-TiO_2 suspended in various solutions after 5 h with different initial concentration. Studies with seawater samples are shown first, followed by studies with freshwater samples. ... 51
Table 4.1 Characteristics of the TiO_2 particles in the powder form..... 83
Table 4.2 The average specific growth rate (μ, day^{-1}) within 72 h for diatom cultures grown with no TiO_2 (control), 100 mg/L micro-TiO_2 and 100 mg/L nano-TiO_2, in the presence of fluorescent lighting. Results are shown as mean ± standard deviation (n = 12). Within each species, numbers with the same letter was not significantly different (Tukey HSD *post-hoc* test). 88
Table 4.3 Studies recording the growth stimulation effect of nano-TiO_2 in the presence of fluorescent lighting. **SP =** Stimulation percentage of growth rate. **IP =** Inhibition percentage of growth rate. Studies with diatoms are marked in bold and shown first, followed by studies with green algae. "–" denotes the information is not available. 92
Table 4.4 Impact of nano-TiO_2 on the growth rate of different algal species cultivated under laboratory conditions with fluorescent lighting. Studies with nano-TiO_2 (P25, the type of particles used in the present investigation) are shown first, marked by underlined species names. For the other studies, studies with diatoms are shown first with species names marked in bold. Within the same species, studies with smaller nano-TiO_2 are shown first. **IC50** (mg/L) = the concentration of nano-TiO_2 at which the inhibition percentage on growth rate is 50%. **IC10** (mg/L) = the concentration of nano-TiO_2 at which the inhibition percentage on growth rate is 10%. **SP (X)** = Stimulation percentage of growth rate with the presence of **X** mg/L nano-TiO_2**. IP (X)** = Inhibition percentage of growth rate with the presence of **X** mg/L nano-TiO_2. "–" denotes the information is not available. 101

Table 5.1 The daily growth rate of *Cylindrotheca closterium* with varying concentrations of nano-TiO_2 in the presence of UV lighting. Results are shown as mean ± standard deviation (n = 4). Significant differences compared to the control group are marked as * ($0.01 \leq p < 0.05$) and ** ($p < 0.01$), based on TukeyHSD *post-hoc* test..... 122
Table 5.2 The chlorophyll *a* concentration (pg per cell) of *Cylindrotheca closterium* with varying concentrations of nano-TiO_2 in the presence of UV lighting, after different cultivation time. Results are shown as mean ± standard deviation (n = 4). Significant difference compared to the control group was marked as * ($0.01 \leq p < 0.05$) and ** ($p < 0.01$), based on TukeyHSD *post-hoc* test. 124
Table 5.3 The maximum quantum yield of PSII after dark-adaption (Fv/Fm), maximum electron transport rate ($rETR_{max}$), maximum light use coefficient (α) and light saturation coefficient (E_k) of *Cylindrotheca closterium* with varying concentration of nano-TiO_2 in the presence of UV lighting, after 72 h of cultivation. Results are shown as mean ± standard deviation (n = 4). 126
Table 5.4 Impact of nano-TiO_2 on different algae cultivated with the presence of UVR. Studies with marine species are shown first, followed by studies with freshwater species. Studies with diatoms were marked in bold. **IC50** (mg/L) = the concentration of nano-TiO_2 at the inhibition on the growth rate is 50%. **IP (X)** = Inhibition percentage of growth rate in the presence of **X** mg/L nano-TiO_2. 130

Chapter 1 General introduction on nanoparticles

1.1 Definition of a nanoparticle

A nanoparticle (NP) is defined as a particle with all three dimensions (British Standards Institution 2007; International Organization for Standardization 2008) or at least two dimensions (American Society for Testing and Materials 2012) in the size range of 1 – 100 nm. In a broad sense, NP refers to a particle with at least one dimension within 1 – 100 nm (Martin and Mitchell 1998; Makoto et al. 2010; Caruso et al. 2011; Beer et al. 2012; Singh 2016; Han et al. 2017; Notter et al. 2018; Manangama et al. 2019). In the present study, the broad definition of NP was adopted.

1.2 Sources of nanoparticles

Nanoparticles (NPs) are present throughout the history of the Earth, rather than being a unique human creation (Handy et al. 2008a). Based on the source, the NPs can be classified as natural NPs (NNPs), incidental NPs (INPs) and engineered NPs (ENPs) (Singh 2016). The NNPs can be created in processes such as volcanic eruptions (Lee and Richards 2004), oceanic evaporation (Obernosterer et al. 2005) and forest fires (Sapkota et al. 2005). For example, some carbon nanotubes and fullerene nanocrystals were found in an ice core sample dated from 10,000 years ago; they were assumed to come from natural fires (Murr et al. 2004). Some NNPs, likely originated from the natural weathering byproducts of minerals, have been detected almost everywhere in the environment (Wigginton et al. 2007).

The INPs are unintentionally released NPs from anthropogenic activities such as firing, frying, fuel combustion and mining (Navarro et al. 2008; Lagally et al. 2012), or from wear and corrosion processes (Westerhoff et al. 2018). The INPs are generally heterogeneous in size and morphology. The ENPs are produced by human industrial activities and they generally have controlled size, morphology and composition (Singh 2016). For instance, EVONIK INDUSTRIES manufactured a nanostructured titanium dioxide (TiO_2) product with high photocatalytic activity named AEROXIDE® TiO_2 P25, which had an average primary particle size around 21 nm (https://www.aerosil.com/sites/lists/RE/DocumentsSI/TI-1243-Titanium-Dioxide-as-Photocatalyst-EN.pdf; accessed 03/05/2019). A wide variety of ENPs have been

produced for various applications including medicine (Salata 2004; Zhang et al. 2008; Rudramurthy and Swamy 2018), water treatment (Tiwari et al. 2008; Simeonidis et al. 2016; Prathna et al. 2018), environmental remediation (Zhang and Elliott 2006; Das et al. 2014; Liu et al. 2014a; Dhasmana et al. 2019), cosmetics (Kokura et al. 2010; Mu and Sprando 2010; Bowman et al. 2018), electronics (Lee et al. 2008; Karmakar et al. 2011; Liu et al. 2018) and packaging (Espitia et al. 2012; Carbone et al. 2016; Souza and Fernando 2016; Morris 2018). Some examples for the applications of ENPs are shown in Figure 1.1. For example, gold NPs were added in the MRI contrast agents to increase the sensitivity of imaging (Tiquia-Arashiro and Rodrigues 2016); TiO_2 NPs were added in the cosmetics to block UV light (Jaroenworaluck et al. 2006); silver, copper, zinc oxide NPs could be used as broad-spectrum pesticides in agriculture (Chhipa 2017); barium titanate NPs were used in the preparation of multi-layered ceramic capacitors, carbon black NPs were produced per year mainly for adding into rubber as a reinforcing agent, amorphous silica were produced per year with major use of functional filler in polymers (European commission 2012a); silver, carbonaceous, iron, gold and TiO_2 NPs were used in the wastewater treatment to remove pollutants and germs (Esakkimuthu et al. 2014); lithium titanate NPs and tin oxide NPs were used in the lithium-ion battery for improvement in energy, power and cycle life (Venugopal et al. 2010).

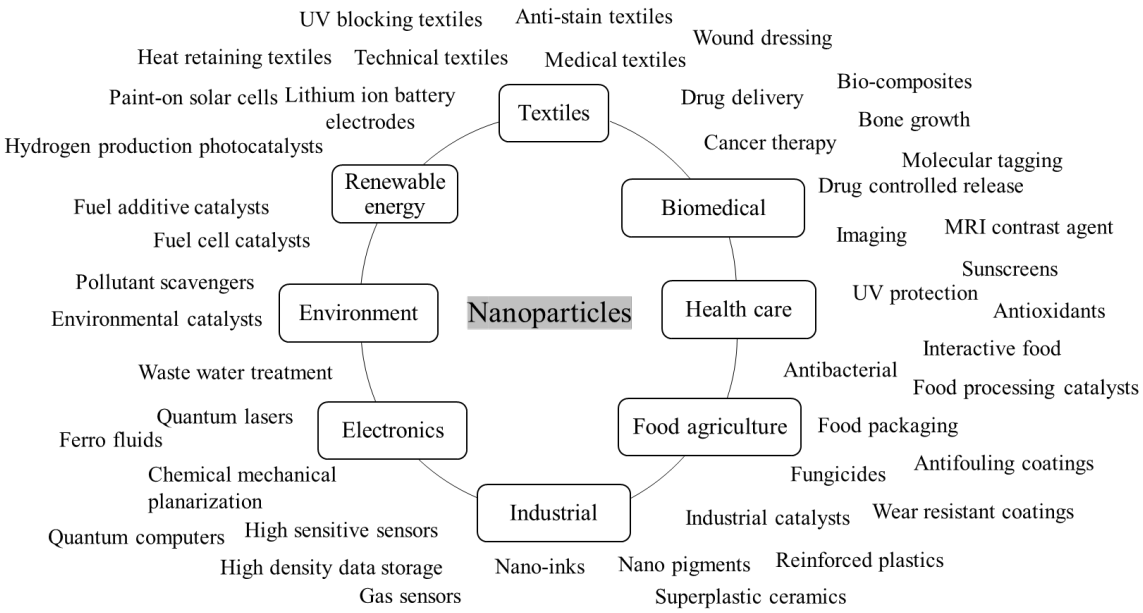

Figure 1.1 Illustrating a range of examples for the application of nanoparticles, modified from Tsuzuki (2009).

The ENPs may be released into the environment intentionally, through direct application in the water treatment process, agriculture or for environmental remediation. They may also enter the environment accidentally during synthesis or processing. The major release may come from the unintentionally release from the daily application, aging or degradation of products containing ENPs. For example, the TiO_2 ENPs added in sunscreens, once applied on the skin, could be released into surface waters directly during bathing activities (Botta et al. 2011; Gondikas et al. 2014), or be released to sewage system after washing (Johnson 2011). Silver ENPs added to textiles are also known to enter the environment during washing activities (Windler et al. 2012; Mitrano et al. 2014). Carbon black NPs are anticipated to come out from the rubber due to aging (European commission 2012a). As a result of the unintentional release at point sources, the amount of ENPs in the environment is highly unknown, yet it is believed to increase dramatically due to the rapid development of nanotechnology.

1.3 **Concerns about ENPs**

Due to their small size and high surface area to volume ratio, NPs have a much higher reactivity and thus exhibit outstanding characteristics, relative to macroscopic particles (Figure 1.2) (Wigginton et al. 2007; Singh 2016). This facilitates the development of nanotechnology, making it one of the most promising technologies (Tegart 2004). However, on the other hand, environmental concerns have been raised regarding the ecological risks of ENPs (Hett 2004; Royal Society 2004; Tsuji et al. 2005; UNEP 2007; Suh et al. 2009; Batley et al. 2013; Bundschuh et al. 2016; Maurizi et al. 2018).

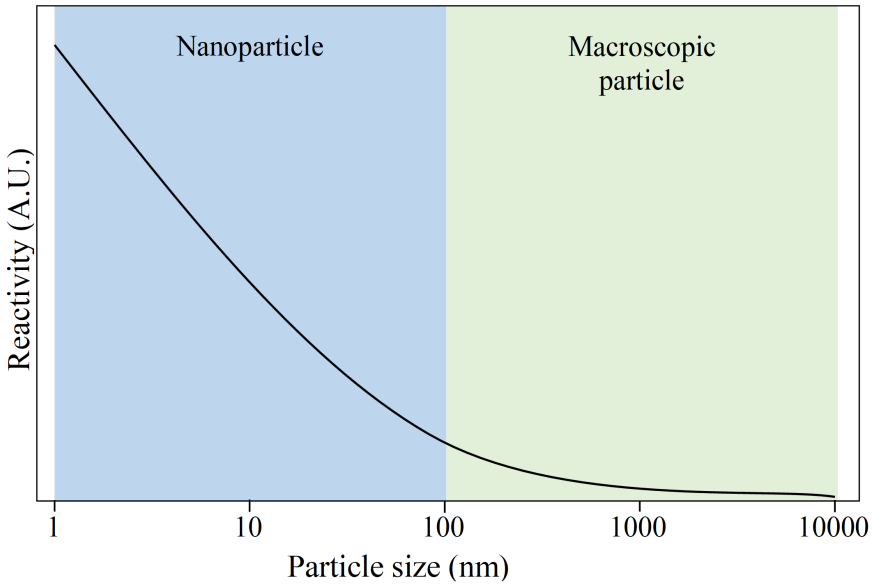

Figure 1.2 Generalized trend for the particle reactivity (the tendency of a particle to undergo chemical reactions) as a function of particle size, modified from Wigginton et al. (2007).

It has been debated whether special attention should be paid to ENPs, considering NNPs are naturally created all the time and the production of NNPs out-weighs the production of ENPs (Handy et al. 2008a). It should be noted, the ENPs are generally designed with unique structure, size, morphology and coating to achieve particular physico-chemical properties. For instance, silicate-coated gold NPs was designed for enhanced thermodynamic stability for application as contrast agent in photoacoustic imaging (Chen et al. 2011). The superparamagnetism effect of iron oxide and manganese oxide NPs was found to present at particle sizes smaller than 30 nm only and thus particles smaller than 30 nm were fabricated as additives in magnetic resonance imaging (MRI) agents to increase the contrast (Kandasamy and Maity 2015). Carbon-based NPs were designed to form 3D ordered hierarchical porous structures to boost their electrochemical properties in lithium-ion batteries (Geng et al. 2020). As a result of the special design, the ENPs may have different environmental behaviour compared to the NNPs (Handy et al. 2008b; Sharifi et al. 2012; Wagner et al. 2014). Many NNPs have a short life time in the environment; they may disappear through dissolution or aggregation (Handy et al. 2008a). However, ENPs can remain in the environment for a much longer time if they have been designed to have certain coating and structural properties (Handy et al. 2008b).

A number of studies have been conducted to investigate the ecological risks associated with presence of

ENPs. The negative impact of ENPs has been reported in a variety of organisms including algae (e.g. Hund-Rinke and Simon 2006; Franklin et al. 2007; Wang et al. 2008; Aruoja et al. 2009; Miao et al. 2010; Peng et al. 2011; Miller et al. 2012; Clement et al. 2013; Xia et al. 2015; Nicolas et al. 2016; Sendra et al. 2017a; Saxena and Harish 2018), higher plants (e.g. Navarro et al. 2008; Ma et al. 2010; Larue et al. 2012; Pokhrel and Dubey 2013; Du et al. 2017a), primary consumers (e.g. Heinlaan et al. 2008; Amiano et al. 2012; Adam et al. 2014; Salieri et al. 2015; Xiao et al. 2015; Brami et al. 2017), fishes (e.g. Federici et al. 2007; Xiong et al. 2011; Yue et al. 2015; Rajkumar et al. 2016; Pitt et al. 2018) and bacteria (e.g. Sondi and Salopek-Sondi 2004; Thill et al. 2006; Heinlaan et al. 2008; Tong et al. 2013; Erdem et al. 2015; Nuzzo et al. 2017; Hao et al. 2018; Kim et al. 2018). These findings support the idea that guidelines for regulating ENPs should be developed to assess and guarantee the environmental safety of ENPs.

In Europe, the development of risk assessments for ENPs started in 2004, led by the Scientific Committee on Emerging and Newly Identified Health Risks (SCENIHR), the Scientific Committee on Consumer Safety (SCCS), the European Food Safety Authority (EFSA) and the European Medicines Agency (EMA) (European Commission 2012a), yet, to my knowledge, a conclusion is yet to be reached. The risk of a substance is determined by its inherent hazards, concentration in the environment and the dose of exposure to organisms (https://www.epa.gov/risk/about-risk-assessment#whatisrisk, accessed 23/05/2019). The environmental concentration of ENPs and their potential biotic impact remain highly uncertain and further work in these areas is required to fill in the knowledge gap.

1.4 Engineered nano-TiO_2 in the environment

Nano-TiO_2 is amongst the most widely used ENPs (Boxall et al. 2007) and the most widely produced metal oxide ENPs (Miller et al. 2012). This thesis focuses on the impact of engineered nano-TiO_2. If not specifically mentioned, nano-TiO_2 refers to engineered nano-TiO_2 in the present thesis.

1.4.1 Forms of nano-TiO_2

TiO_2 may present in crystal forms (anatase, rutile and brookite) or amorphous form in nature. Though they share the same chemical composition, different crystal structures exhibit varied characteristics. A mixture of

anatase and rutile are the typical forms in the engineered nano-TiO_2 (EPA 2010). With a higher refractive index, rutile provides an enhanced whiteness, brightness and opacity and is a better whitening pigment than anatase (Dupont Report 2015). With a higher photocatalytic ability, anatase is a better photocatalyst than rutile (Chong et al. 2010; Skocaj et al. 2011; Luttrell et al. 2014). Photocatalysis refers to the catalysis of a chemical reaction by absorption of light. When TiO_2 is irradiated by light with energy greater than the band gap (defined as the energy difference between the valence band and conduction band), photoreactions would occur on the surface of TiO_2 particles and charge carriers (e^- and h^+) are created. In general, UVR could effectively photoactivate TiO_2 (Skocaj et al. 2011). With a series of oxidative-reductive reactions, oxygen can be turned into superoxide radical anions ($O2^{-}\bullet$) and water molecular can be turn OH radicals ($OH\bullet$). (Figure 1.3, Chong et al. 2010). $O2^{-}\bullet$ and $OH\bullet$ may further react and form hydrogen peroxide (H_2O_2). The $OH\bullet$, $O_2^{-}\bullet$, H_2O_2 are highly oxidative reactive oxygen species (ROS). The creation of ROS on the surface of TiO_2 by simply introducing UVR lighting makes TiO_2 a promising photocatalytic material for degrading pollutants and decomposing cells (Lee et al. 2013).

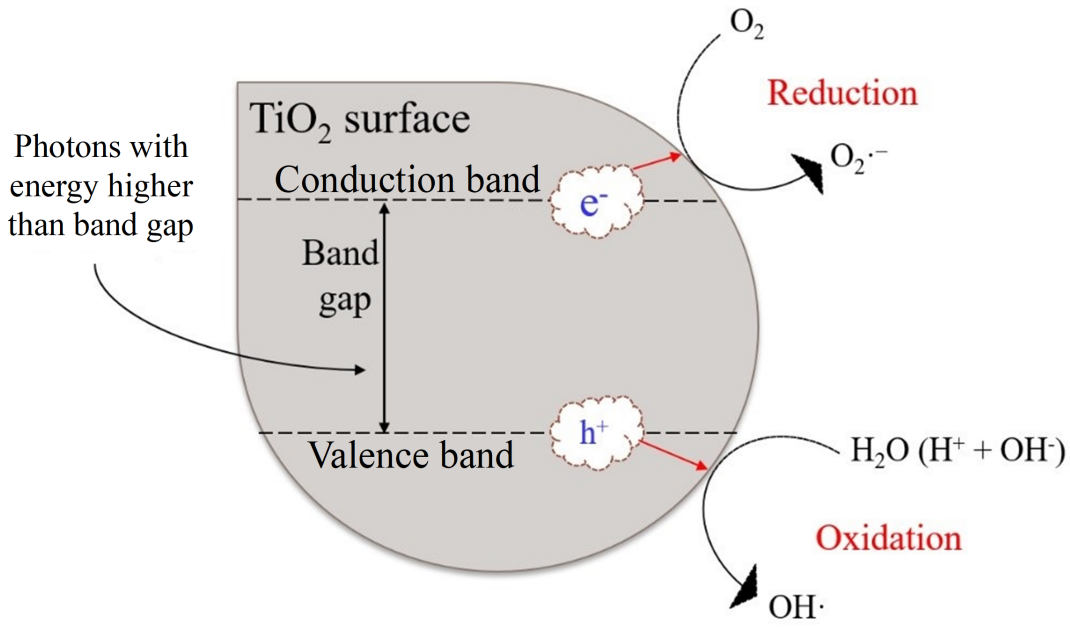

Figure 1.3 Photoreaction on the surface of a TiO_2 particle, when irradiated by photons with energy higher than the band gap. Modified from Chong et al. (2010).

1.4.2 Application of nano-TiO_2

Nano-TiO_2 is widely used in our lives (Table 1.1). The production of nano-TiO_2 has increased dramatically in the past decade. The annual production of nano-TiO_2 increased from 5,000 tons in 2006 (UNEP 2007) to 10,000 tons in 2012 (European commission 2012b), and may reach 2.5 million tons in 2025, by when bulk-TiO_2 industry may be completely converted to nano-TiO_2 industry (Robichaud et al. 2009).

Table 1.1 Examples of the applications of nano-TiO_2 in our daily lives.

Application	Particle property	Reference
Cosmetics and personal care products	Absorb and reflect ultraviolet (UV) light; being transparent to visible light	Popov et al. (2005)
Self-clean coatings	Photocatalytic capacity: inhibit biofouling of microalgae	Graziani et al. (2013)
Water purification and bioremediation	Photocatalytic capacity: degradation of organic compounds	Nagaveni et al. (2004)
Catalysts	Photocatalytic capacity: convert light energy into electrical or chemical energy	Wang et al. (2016a)
Food and food packaging	White pigment	Weir et al. (2012)
White paints	Whitening pigment; high refractive index with a high degree of transparency of visible lights	Dupont Report (2015)
Biomedical application	High biocompatibility and chemical stability	Zi et al. (2013)

1.4.3 Fate of nano-TiO_2

Nano-TiO_2 may be released into the environment accidentally from factories during the production processes, due to abnormal events such as explosion, spillage or equipment malfunction (Aitken et al. 2004). Nano-TiO_2 can be released from its associated products. For example, nano-TiO_2 in the cosmetics and sunscreens can enter the aquatic environment due to bathing and washing activities (Botta et al. 2011; Gondikas et al. 2014; Jeon et al. 2016). Nano-TiO_2 in paints, coatings and textiles can be released into the environment due to aging, abrasion and weathering washing (Kaegi et al. 2008; Golanski et al. 2011; Windler et al. 2012; Al-Kattan et al. 2014; Mitrano et al. 2014). In addition, nano-TiO_2 in packages can be released during degradation (Lin et al. 2014).

Water is the ultimate sink for most of the chemicals (Koumanova 2006). The nano-TiO_2 released into the environment may accumulate in the aquatic environment through processes such as deposition, wastewater discharge and direct input (Boxall et al. 2007; Klaine et al. 2008; Koelmans et al. 2009; Donia and Carbone

2019). Upon entering the aquatic environment, the particles may be carried by the water until reaching the ocean or settle out into the sediments during the transition process. The retention time of nano-TiO_2 in the water column is determined by its chemical and physical characteristics. TiO_2 is said to be chemically inert and therefore would not be expected to react with other chemicals (Skocaj et al. 2011; Rawski and Bhuiyan 2017). Therefore, it is considered that nano-TiO_2 would only go through physical changes in the environment, such as aggregation or disaggregation. The stability of nano-TiO_2 in the water column depends on the characteristics of the particle (e.g. size, morphology, crystal structure, coating) (Handy et al. 2008a; Klaine et al. 2008; Hotze et al. 2010; Baalousha 2017), the concentration of particles (Taboada-Serrano et al. 2005; Allouni et al. 2009; Keller et al. 2010), and the properties of the aqueous environment (e.g. pH, ionic strength, monovalent ions and divalent ions, dissolved organic matter, alkalinity and dispersing agents) (Hotze et al. 2010; OECD 2010; Zhu et al. 2014).

Under natural conditions, the physico-chemical properties of water play an important role in determining the stability and the fate of nano-TiO_2 (French et al. 2009; Keller et al. 2010; Wang et al. 2014a; Li et al. 2016). Studies have revealed that the aggregation and sedimentation of nano-TiO_2 is much more rapid in seawater compared to freshwater; the higher ionic strength (salinity) in seawater is believed to be the main reason for the quicker sedimentation rate, because it promotes the aggregation of NPs (Keller et al. 2010; Sillanpää et al. 2011; Li et al. 2016). Researchers have also highlighted that the nano-TiO_2 in the water column may settle down to the sediments within a few hours, once in the seawater (Keller et al. 2010; Sillanpää et al. 2011; Li et al. 2016).

Estuaries, where seawater and freshwater merge together, may be the first place where nano-TiO_2 molecules encounter a saline environment. Nano-TiO_2 carried by the water is anticipated to settle out in estuaries. Moreover, the biofilms on the surface of estuarine muds, which are a matrix of sediments, algae and other protists, bacteria and extracellular polymeric substances (EPS) (Underwood and Paterson 1993a), are capable of trapping particles and prevent them resuspending (Yallop et al. 2000; Stal and de Brouwer 2003; Friend et al. 2008; Gerbersdorf et al. 2009). Investigations have recognized the importance of biofilms in binding NPs (Battin et al. 2009; Ferry et al. 2009; Kroll et al. 2014; Ikuma et al. 2015). Therefore, the intertidal areas in the estuaries, mudflats and sandflats, where biofilms are largely formed (Decho 2000;

Yallop et al. 2000), are expected to be an important sink for nano-TiO_2.

1.4.4 Environmental concentration of nano-TiO_2

There is a lack of information on the concentrations of nano-TiO_2 in the environment. One of the major difficulties is to distinguish ENPs from NNPs. TiO_2 is a natural mineral with a content of 0.8 – 1.2% in continental crust (Taylor 1964). Natural TiO_2 NPs are widely present in the environment. Another difficulty relates to the instability of nano-TiO_2. Nano-TiO_2 is most likely to present as bound particles in the environment, rather than separated single particles (French et al. 2009; Keller et al. 2010; Loosli et al. 2015; Li et al. 2016; Roy et al. 2016). Keller et al. (2010) reported that nano-TiO_2 (mean particle diameter of 27 nm) immediately aggregated to larger particles with diameter of 190 – 230 nm once dispersed in deionized water. In seawater, the nano-TiO_2 formed aggregates with an average particle diameter of around 500 nm within a few minutes, and the size of aggregates further increased to over 1000 nm after 60 mins (Keller et al. 2010). Li et al. (2016) measured that the average particle diameter of nano-TiO_2 increased from 21 nm to 200 – 276 nm after dispersing the particles into lake waters, and the diameter of particles increased to 607 – 1179 nm when dispersing particles into brackish waters. The aggregation behavior makes the detection of particle existence and the measurement of particle concentration very difficult.

Determining the concentration of nano-TiO_2 in the environment is a necessity for understanding its risk (https://www.epa.gov/risk/about-risk-assessment#whatisrisk, accessed 23/05/2019). Due to the limited number of observations on environmental concentrations, models have been developed to estimate the possible environmental concentration of nano-TiO_2 (Table 1.2). The nano-TiO_2 added in the cosmetics (e.g. sunscreens) was considered to be the largest source of nano-TiO_2 released into the environment (Gottschalk et al. 2009). To be noted, these predictions were made several years ago and only a few applications were taken into account during the prediction. However, considering the dramatic increase in the production and application of nano-TiO_2 in the past 10 years, the environment concentration of nano-TiO_2 may be much higher than those summarized in Table 1.2.

Table 1.2 Estimated environmental concentrations of nano-TiO_2 in different compartments.

Region	Predicted concentration	Compartment	Source of nano-TiO_2	Reference
UK	24.5 µg/L	Water	Sunscreens, paint products	Boxall et al. (2007)
	701 mg/kg	Sludge		
	1030 µg/kg	Soil		
	7 mg/m^3	Air		
	0.25 – 8.8 µg/L	Water	Sunscreens	Johnson et al. (2011)
Europe	0.012 – 0.057 µg/L	Water	Plastics, cosmetics, coatings, metals, energy storage/production and paints	Gottschalk et al. (2009)
	100 – 433 mg/kg	Sludge		
	< 0.005 µg/m^3	Air		
U.S.	0.002 – 0.010 µg/L	Water	Plastics, cosmetics, coatings, metals, energy storage/production and paints	
	107 – 523 mg/kg	Sludge		
	< 0.005 µg/m^3	Air		
Switzerland	0.016 – 0.085 µg/L	Water	Plastics, cosmetics, coatings, metals, energy storage/production and paints	
	172 – 802 mg/kg	Sludge		
	0.0007 – 0.003 mg/kg	Air		
	0.7 – 16 µg/L	Water	Plastics, cosmetics, coatings, metals, energy storage/production and paints	Mueller and Nowack (2008)
	0.4 – 4.8 µg/kg	Soil		
	0.0015 – 0.042 µg/m^3	Air		
Ireland	0.0018 – 2.7 µg/L	Drinking water	Paints, coatings, plastics and packaging	O'Brien and Cummins (2010)
South Africa	0.0003– 0.89 µg/L	Water	Cosmetics	Musee (2010)

1.5 General information for the impact of nano-TiO_2 on the biota

The impact of nano-TiO_2 has been widely investigated in organisms including bacteria, algae, plants, invertebrates and vertebrates. The biotic effects of nano-TiO_2 have been reviewed recently (Iavicoli et al. 2011; Menard et al. 2011; Shi et al. 2013; Minetto et al. 2014; Zhang et al. 2015; Cox et al. 2016; Hou et al. 2019). The presence of nano-TiO_2 has been reported to damage cell membranes and induce oxidative stress, inflammatory responses and even genotoxicity at the cellular level (Liu et al. 2010; Tong et al. 2013; Hong and Zhang 2016; Relier et al. 2017; Gandamalla et al. 2019); inhibit growth, decrease biomass, reduce mobility and induce cell death on the organism level (Warheit et al. 2007; Aruoja et al. 2009; Sadiq et al. 2011; Amiano et al. 2012; Dalai et al. 2013; Kumari et al. 2014; Xia et al. 2015; Roy et al. 2016; Sendra et al. 2017b; Priyanka et al. 2018); and alter bacterial and algal composition at the community level (Ge et al. 2011; Fan et al. 2016; Du et al. 2017b; Sendra et al. 2017a; Auguste et al. 2019; Ockenden 2019).

Importantly, adverse effects have not always been detected when investigating the impact of nano-TiO_2. Heinlaan et al. (2008) reported that the presence of nano-TiO_2 at an unrealistic concentration of 20 g/L, showed no toxic effect on bacterium V*ibrio fischeri* or crustaceans *Daphnia magna* and *Thamnocephalus*. In addition, the beneficial effects of nano-TiO_2 were recorded by some researchers. For examples, Zheng et al. (2005) observed that the presence of nano-TiO_2 increased the germination rate of spinach seeds, as well as the weight of spinach, compared to the control. Nogueira et al. (2015) reported significantly higher growth rates of the green alga *Raphidocelis subcapitata* in the presence of 16 and 20 mg/L nano-TiO_2, after 72 h of exposure, compared to the control. Li et al. (2019) also noticed that dinoflagellate alga *Alexandrium tamarense* had a higher growth rate in the presence of 20 and 40 mg/L nano-TiO_2 after 96 h of exposure, compared to the control.

1.6 **Current knowledge regarding the impact of nano-TiO_2 on algae**

Algae are ubiquitous primary producers in aquatic ecosystems. They play a crucial role in ecosystem functioning by contributing up to half of the total primary production in the world (Giordano et al. 2005). Due to their wide prevalence, algae are likely the first organisms to be in contact with any artificial substance. Therefore, to investigate the risks of a substance in the environment, it is reasonable to start with experiments determining its impact on algae. Amongst all the studies investigating the risk of nano-TiO_2, algae have received the most attention.

1.6.1 **Varied results on the impact of nano-TiO_2 on algae**

The impact of nano-TiO_2 on algae is generally investigated by a growth inhibition test, which examines the change of biomass in algal cultures exposed to varying concentrations of nano-TiO_2, according to the protocols suggested by Organization for Economic Cooperation and Development (OECD) in the Guidelines for the Testing of Chemicals, Test No. 201: Alga, Growth Inhibition Test (OECD 1984, 2011). Quite a few studies have been conducted to investigate the impact of nano-TiO_2 on algae. Some studies reported the toxicity of nano-TiO_2 in inhibiting algal growth and photosynthesis, leading to decreased cell number (e.g. Chen et al. 2012; Manzo et al. 2015; Xia et al. 2015), reduced chlorophyll *a* content (e.g. Aruoja et al. 2009; Lee and An 2013; Li et al. 2015), damaged cell membrane (e.g. Dalai et al. 2013; Xia et al. 2015; Roy et al.

2016), lowered fluorescence intensity (e.g. Hund-Rinke and Simon 2006; Kulacki and Cardinale 2012) and suppressed photosynthetic rate (e.g. Deng et al. 2017; Middepogu et al. 2018). In contrast, there are some studies claiming that nano-TiO_2 is not harmful (e.g. Blaise et al. 2008; Ji et al. 2011; Hartmann et al. 2013; Joonas et al. 2019), whilst a few studies had detected stimulation effects of nano-TiO_2 on algal growth (Hartmann et al. 2010; Kulacki and Cardinale 2012; Clement et al. 2013; Nogueira et al. 2015). Despite the different tolerance of the test algae, the different conclusions on the impact of nano-TiO_2 on algal growth may be linked to the differences in the experimental setups (e.g. growth container, initial algal density) and the different properties of the test nano-TiO_2. For instance, for green alga *Pseudokirchneriella subcapitata*, one of the most widely studied algae, a wide range of protocols and particle types were used and the outcomes vary considerably, which are summarized in Table 1.3. It supports the idea that understanding the degree of impact of just one single nanoparticle is not straightforward, as there are a very wide range of IC50 values (concentration of a substance at which the inhibition percentage on the growth rate is 50%) reported.

Table 1.3 The 72 h-IC50 values for nano-TiO_2 (concentration of nano-TiO_2 at which the inhibition percentage on the growth rate is 50% after 72 h of exposure) on freshwater green alga *Pseudokirchneriella subcapitata* in the presence of fluoresent lighting. Data are presented in the order of increasing 72 h-IC50 values. Data are shown as the mean value or the range of the value. "–" indicates that the information is not available.

Particle property			Growth container	Initial biomass (cells/ml)	72 h-IC50 (mg/L)	Reference
Particle size (nm)	Surface area (m^2/g)	Crystal structure				
21	55.13	72.6% anatase, 18.4% rutile, 9% amorphous	24-well microplates	10^4	2.53	Lee and An (2013)
< 10	250 – 320	98.5% anatase, 1.5% rutile	Cylindrical vials	–	2.7	Nicolas et al. (2016)
20 – 40	30 – 60	–	–	2.6×10^5	4.16	Ozkaleli and Erdem (2018)
< 10	250 – 320	98.5% anatase, 1.5% rutile	24-well microplates	–	8.5	Nicolas et al. (2016)
25 – 70	–	–	Cylindrical vials	10^4	9.73	Aruoja et al. (2009)
< 5	–	Mainly anatase	Glass scintillation vials	10^4	14.8	Joonas et al. (2019)
20	60	11% anatase, 89% rutile	Cylindrical vials	–	39	Nicolas et al. (2016)
30	47	72.6% anatase, 18.4% rutile, 9% amorphous	Polystyrene cylindrical vials	10^4	71.1	Hartmann et al. (2010)
< 10	250 – 320	98.5% anatase, 1.5% rutile	Erlenmeyer flasks	–	> 50	Nicolas et al. (2016)
14	90	90% anatase, 10% rutile	Microplates	3×10^6	> 50	Fekete-Kertész et al. (2016)
20	60	11% anatase, 89% rutile	24-well microplates	–	> 50	Nicolas et al. (2016)
20	60	11% anatase, 89% rutile	Erlenmeyer flasks	–	> 50	Nicolas et al. (2016)
< 100	–	–	96-well microplate	10^4	> 100	Blaise et al. (2008)
< 10	288	67.2% anatase, 32.8% amorphous	Polystyrene cylindrical vials	10^4	241	Hartmann et al. (2010)

1.6.1.1 Influence of the experimental setup on the impact of nano-TiO_2

Type of Growth Container

Nicolas et al. (2016) investigated the impact of growth container on the growth inhibition effect of nano-TiO_2 on green alga *Pseudokirchneriella subcapitata*. The authours reported that 72 h-IC50 of nano-TiO_2 (particle size < 10 nm) obtained with different containers followed an order of "cylindrical vials" < "24-well microplates" < "Erlenmeyer flasks" (Table 1.4). They attributed the differences in the IC50 values to the differernt aggregation of nano-TiO_2 in the three containers (Nicolas et al. 2016). They observed visible particle aggregates in the microplates and flasks but not in the vials, and therefore concluded that the aggregation of nano-TiO_2 may be much more severe in the microplates and flasks, leading to relatively lower concentrations of particles remaining in the nanosizes in these two containers and thus different IC50 values (Nicolas et al. 2016).

Table 1.4 The details of three growth container and the corresponding 72 h-IC50 values of nano-TiO_2 (concentration of nano-TiO_2 at which the inhibition percentage on the growth rate is 50% after 72 h of exposure) on freshwater green alga *Pseudokirchneriella subcapitata* in the study conducted by Nicolas et al. (2016).

	Cylindrical vials	**24-well microplates**	**Erlenmeyer flasks**
72 h-IC50 (mg/L)	2.7	8.5	>50
Composition	Glass	Polystrene	Glass
Shape and size	Cylinder 7.5 cm height 2.5 cm diameter	Cylinder 16.5 mm height 15.7 mm diamter	Wild neck Erlenmeyer 250 mL in capacity
Working volume	25 mL	2.5 mL	100 mL

Intial biomass

In Table 1.3, most of studies started with initial algal biomass of 10^4 cells/ml, which was recommended by the protocols of OECD (2011), except for two studies, where initial biomass was greater than 10^4 cells/mL (Fekete-Kertész et al. 2016; Ozkaleli and Erdem, 2018). For these two studies with higher biomass, the 72h-IC50 values were not very differernt from the other studies listed in Table 1.3. Nevertheless, Metzler et al. (2018) reported that the growth inhibition of 100 mg/L nano-TiO_2 (particle size of 35.1 nm) on the green alga *Pseudokirchneriella subcapitata* significantly decreased with increasing initial cell density (biomass).

They attributed the lower inhibition of nano-TiO_2 on the higher biomass culture to a reduced nano-TiO_2 quota on a per cell basis. At a given concentration of nano-TiO_2, an increase in the algal biomass (cell density) would decrease the quota/burden of nano-TiO_2 per cell, resulting in reduced average stress on an individual cell and thus a lower growth inhibition (Metzler et al. 2018).

1.6.1.2 Influence of particle properties on the impact of nano-TiO_2

Particle size, morphology and surface area

Size is the major concern in terms of the impact of NPs. The surface area to volume ratio of a particle increases dramatically as particle size decreases. For a spherical particle, a 10 times difference in particle size would result in a 100 times difference in surface area, on a per mass basis. With a higher surface area to volume ratio, small particles are more likely to exhibit higher surface reactivity than large particles, on a per mass basis (Figure 1.2). In addition, particle morphology also has an impact on the surface area to volume ratio of the particle. Spherical particles have the smallest surface area to volume ratio amongst all the morphologies. Therefore, in the case of two different sized particles with the same mass concentration, spherical particles may have the lowest reactivity.

Crystal structure

TiO_2 has three crystal forms (anatase, rutile and brookite) and an amorphous form, among which anatase and rutile are the most widely present forms of nano-TiO_2 (EPA 2010). Though they share the same chemical composition, different crystal structures exhibit varied photocatalytic potential in generating reactive oxygen species (ROS) on the particle surface (Chong et al. 2010; Skocaj et al. 2011). ROS may be toxic to organisms (Simon et al. 2000; Nordberg and Arner 2001; Fleury et al. 2002; Kimura et al. 2005; Auten and Davis 2009). Anatase is generally reported to be a better photocatalyst than rutile (Kakinoki et al. 2004; Jiang et al. 2008; Luttrell et al. 2014; Odling and Robertson 2015), and therefore anatase is likely to induce a higher production of ROS and thus greater toxicity.

Particle aggregation state

Nano-TiO_2 is unstable in aqueous solution and tends to aggregate into larger particles as a result of van der Waals attraction (Handy et al. 2008a; Hotze et al. 2010). Once added into algal culture, nano-TiO_2 is subject to aggregation, which may lead to a change in particle availability. The aggregation between particles is referred to as homoaggregation and the aggregation between particles and algal cells is referred to as heteroaggregation (Handy et al. 2008a; Hotze et al. 2010). The aggregation of NPs depends on a variety of factors that influence the particle-particle interaction, including the characteristics of the NP itself (e.g. size, morphology, crystal structure, coating), the concentration of the particles, the property of the aqueous solution (e.g. pH, ionic strength, monovalent ions and divalent ions, dissolved organic matter, alkalinity and dispersing agents), algal status (e.g. species type, cell density, the ability to secrete extracellular polymeric substance) and experimental setup (e.g. growth container, shaking). Once aggregated, particle size increases with reduced total surface area, resulting in a lowered particle reactivity.

For studies summarized in Table 1.3, the influence of particle size, surface area, crystal structure on the impact of nano-TiO_2 was not straightforward. It is likely that the impact of nano-TiO_2 on algae is a combined effect of these factors.

1.6.2 **Possible mechanisms for the impact of nano-TiO_2**

The negative impacts of nano-TiO_2 have mainly been attributed to physical constraints and increased oxidative stress. The figure below illustrates potential mechanisms of the impact of nano-TiO_2 on an algal cell, after passing through the barrier of the cell wall, if there is a wall. (Figure 1.4).

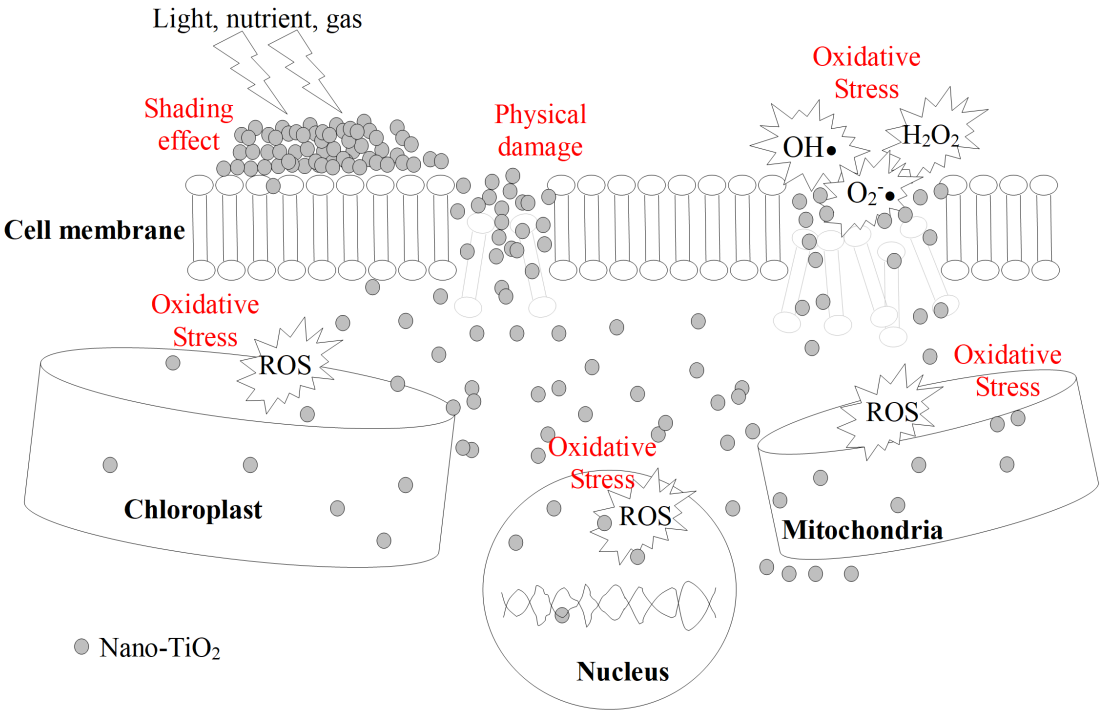

Figure 1.4 Illustration for the possible mechanisms for the impact of nano-TiO_2 on an algal cell, modified from Chen et al. (2019). OH•, O_2^-•, H_2O_2 are short for OH radicals, superoxide radical anions and hydrogen peroxide, respectively, which are reactive oxygen species (ROS).

1.6.2.1 Physical constraints due to the presence of nano-TiO_2

The interaction between nano-TiO_2 and algal cells may result in physical constraints. One type of physical constraints refers to the adsorption of nano-TiO_2 onto the cell surface (Figure 1.3) or the entrapment of cells by particle aggregates (heteroaggregation) which may limit nutrient uptake, gas exchange, as well as contribute to a lowered light received by cells (Hund-Rinke and Simon 2006; Aruoja et al. 2009; Hartmann et al. 2010; Li et al. 2015; Wang et al. 2016b; Morelli et al. 2018). This type of physical constraints is commonly referred to as the "shading effect". Another type of physical constraints comes from the physical interactions between NPs and cells (Figure 1.3), which may cause physical damage such as cell wall damage and membrane damage (Wang et al. 2016b).

1.6.2.2 Increased oxidative stress due to the presence of nano-TiO_2

The negative impact of nano-TiO_2 has been commonly attributed to an increased oxidative stress, associated with a high level of reactive oxygen species (ROS) (Chen et al. 2012; Miller et al. 2012; Dalai et al. 2013;

Li et al. 2015; Xia et al. 2015; Roy et al. 2016; Deng et al. 2017; Sendra et al. 2017b; Sendra et al. 2017a; Middepogu et al. 2018; Jia et al. 2019; Wu et al. 2019). The ROS may be produced biologically by the cells in response to the presence of nano-TiO_2 (Li et al. 2015), or produced chemically on the surface of TiO_2 particles (Figure 1.3). The presence of excessive ROS may induce several adverse effects at the cellular level such as membrane lipid peroxidation, impairment of photosynthesis in the chloroplasts, impairment of mitochondria, DNA damage and even cell apoptosis (Simon et al. 2000; Nordberg and Arner 2001; Fleury et al. 2002; Kimura et al. 2005; Auten and Davis 2009).

1.6.3 The importance of illumination on the impact of nano-TiO_2

Studies have revealed a significantly higher growth inhibition of nano-TiO_2 on algae in the presence of ultraviolet radiation (UVR, wavelength < 400 nm) for 72 h or longer (Miller et al. 2012; Graziani et al. 2013; Roy et al. 2016; Sendra et al. 2017b; Sendra et al. 2017a), highlighting the importance of UVR in determining the impact of nano-TiO_2. The influence of UVR on the impact of nano-TiO_2 is mainly associated with the photocatalytic property of nano-TiO_2, as the presence of UVR determines whether TiO_2 would be photoactivated and how much ROS would be produced (Chong et al. 2010; Skocaj et al. 2011).

1.7 Knowledge gaps and aims of this thesis

1.7.1 Knowledge gaps

Owing to the photocatalytic property, the type of illumination is crucial with respect to impact of nano-TiO_2. Significantly greater negative impacts of nano-TiO_2 have been recorded in the presence of UVR, compared to the absence of UVR (Miller et al. 2012; Graziani et al. 2013; Roy et al. 2016; Sendra et al. 2017b; Sendra et al. 2017a). However, up until now, most of the laboratory investigations on the impacts of nano-TiO_2 have been performed with fluorescent lighting only and these lights are reported to emit a negligible level of UVR. Considering UVR may be present in natural conditions, experiments conducted with fluorescent lighting might have underestimated the impact of nano-TiO_2. Therefore, there is a potential knowledge gap regarding the impact of nano-TiO_2 on algae in the presence of UVR.

Up to now, most studies investigating the impact of nano-TiO_2 on algae were performed with freshwater

species (Menard et al. 2011; Tang et al. 2018). The green algae *Pseudokirchneriella subcapitata* (also named as *Selenastrum capricornutum* or *Raphidocelis subcapitata*), *Desmodesmus subspicatus* and *Chlamydomonas reinhardtii*, the model species of green algae suggested by the Organization for Economic Co-operation and Development (OECD 2011), were the most widely studied algae (e.g. Warheit et al. 2007; Blaise et al. 2008; Wang et al. 2008; Aruoja et al. 2009; Metzler et al. 2011; Chen et al. 2012; Hartmann et al. 2013; Lee and An 2013; Nicolas et al. 2016; Sendra et al. 2017b). Other studied freshwater species included *Chlorella* sp., *Scenedesmus* sp., and *Desmodesmus* sp. (e.g. Ji et al. 2011; Sadiq et al. 2011; Dalai et al. 2013; Roy et al. 2016; Iswarya et al. 2017; Middepogu et al. 2018). Recently, studies have been conducted with marine species, such as *Phaeodactylum tricornutum*, *Dunaliella tertiolecta*, *Skeletonema costatum* and *Thalassiosira pseudonana* (e.g. Miller et al. 2010; Miller et al. 2012; Li et al. 2015; Manzo et al. 2015; Xia et al. 2015; Deng et al. 2017). While most studies were conducted with planktonic species, there is a lack of studies on the impact of nano-TiO_2 on benthic algal species. Considering the potential sedimentation and the accumulation of nano-TiO_2 in the sediments of estuaries, the benthic algae inhabiting estuarine environment are likely to be associated with a higher risk of exposure. In estuaries, benthic diatoms are the key primary producers, especially for estuaries with high turbidity (Underwood and Paterson 1993a). To my knowledge, the impact of nano-TiO_2 on the estuarine benthic diatoms has not been reported yet. Therefore, there exists a knowledge gap regarding the impact of nano-TiO_2 on the estuarine benthic diatoms.

1.7.2 The importance of estuarine benthic diatoms

Estuarine benthic diatoms are referring to the group the diatoms living within the intertidal areas in estuaries. They play an especially important role for estuaries with high turbidity, as they may not be able to support a high biomass of phytoplankton in the water column (Underwood and Paterson 1993a). Besides making a large contribution to the overall primary production (Admiraal et al. 1983; MacIntyre et al. 1996; Underwood and Kromkamp 1999), estuarine benthic diatoms also support estuarine secondary production as a direct food source as thus regarded as important biofuels for estuarine food webs (Pinckney and Zingmark 1991; MacIntyre et al. 1996). In addition, together with self-secreted extracellular polymeric substances (EPS), estuarine benthic diatoms usually form extensive biofilms on the surface of intertidal areas, which have been found to serve several ecological functions including increasing sediment stability and reducing sediment erosion (Underwood and Paterson 1993; Yallop et al. 1994; Miller et al. 1996). These makes benthic diatoms

a precious asset for estuaries.

1.7.3 **Aims of this thesis**

To fill in those knowledge gaps, the impacts of nano-TiO_2 on the estuarine benthic diatoms were investigated in this thesis. A commercial nano-TiO_2 product, P25, was selected as the test particle, as it was previously tested in a few studies, facilitating for the cross-study comparisons. The impact of nano-TiO_2 was explored under two different illumination conditions, the commonly used fluorescent lighting which contained a negligible level of UVR and a UV lighting which contained a considerable amount of UVR.

The aims of this thesis include:

(1) To investigate the impact of salinity, pH and particle concentrations on the aggregation and sedimentation behavior of nano-TiO_2 in a synthetic estuarine environment;
(2) To examine whether the presence of nano-TiO_2 interferes with the biomass determination of the estuarine benthic diatoms test in the present thesis;
(3) To assess the impact of nano-TiO_2 on the growth of three estuarine benthic diatoms through single-species testing under fluorescent lighting and to discuss the possible mechanisms for their impact;
(4) To investigate the impact of nano-TiO_2 on the growth of estuarine benthic diatom through single-species testing under UV lighting and their impact with respect to particle concentration and cultivation time;
(5) To investigate the impact of nano-TiO_2 on the growth and diatom composition of a field derived estuarine microphytobenthos community dominated by benthic diatoms, in the presence of UV lighting.

Chapter 2 The aggregation and sedimentation behavior of nano-TiO_2 (P25) in an artificial estuarine environment

2.1 Introduction

2.1.1 The aggregation of NPs in the aqueous environment

When NPs enter into the aqueous environment, the particle-particle interactions including the particle-particle collision frequency and the particle-particle forces (e.g. Borne repulsion, diffuse double layer potential, van der Waals attraction) determine whether NPs stay as single particles or form aggregates (Handy et al. 2008a; Hotze et al. 2010). Generally, NPs are unstable in the water and they tend to aggregate. Even in the ultrapure water, nano-TiO_2 with a primary particle diameter of 21 nm rapidly formed aggregated particles with a diameter of 216.0 ± 3.0 nm (Chekli et al. 2015); nano-TiO_2 with a primary particle size of 15 – 30 nm immediately formed aggregates with a diameter of 190 – 230 nm (Keller et al. 2010); nano-TiO_2 with a primary particle size of 67 nm immediately formed aggregates with a diameter of 192.1 ± 5.8 nm (Nur et al. 2015). Studies have shown that aggregation of NPs depends on a variety of factors that influence the particle-particle interaction, including the characteristics of the NP itself, the concentration of the particles, and the property of the aqueous solution (Hotze et al. 2010; Almusallam et al. 2012; Batley et al. 2013; Li et al. 2016; Baalousha 2017).

The characteristics of the NPs including size, morphology, chemical composition, crystal structure and coating have been reported to have an impact on the tendency of particle aggregation (Handy et al. 2008a; Klaine et al. 2008; Hotze et al. 2010; Baalousha 2017). For example, hematite NPs with an average size of 12 nm (aggregates with diameter of 1000 – 1650 nm), were reported to form larger aggregates than particles with an average size of 32 nm (aggregates with diameter of 800 – 1100 nm) and particles with an average size of 65 nm (aggregates with diameter of 650 – 1050 nm), in 1mM NaCl at pH of 9, after a 10 min incubation period (He et al. 2008), suggesting a greater aggregation tendency at a smaller particle size. Zhou et al. (2013) observed a similar phenomenon for anatase nano-TiO_2 (primary size ranged from 6 to 54 nm) where smaller NPs were more prone to aggregate. Apart from size, morphology also plays a role in determining the stability of NPs. The hydrodynamic diameter of spherical nano-ZnO (20 nm in diameter) in

a saline solution (salinity = 0.6 ‰, pH = 9) was 2 μm after 1 h incubation, which was 1.33 times larger than the hydrodynamic diameter (1.5 μm) of a mixture of rod-like nano-ZnO (200 nm in length by 20 nm in radius) and slab-like nano-ZnO (200 nm by 200 nm by 20nm) (Zhou and Keller 2010). Nano-TiO_2 of anatase and brookite structure were found to have a higher aggregation tendency than nano-TiO_2 of rutile structure (Lebrette et al. 2004; French et al. 2009), indicating that there is an impact of crystal structure on the nanoparticle aggregation behavior. PVP-coated nano-Ag was found to be more stable than citrate-coated nano-Ag in the solutions containing NaCl or $CaCl_2$ (Huynh and Chen 2011; Wang et al. 2014a), highlighting the impact of coating on nanoparticle aggregation behavior.

For a given NP, the composition of the dispersing solution including pH, ionic strength, monovalent ions and divalent ions, dissolved organic matter (DOM), alkalinity and dispersing agents, is of great importance in determining the aggregation tendency of the NPs (OECD 2010; Wang et al. 2014a; Loosli et al. 2015). For instance, when the pH of solution approaches to the point of zero charge (pH_{PZC}, the pH value at which the zeta-potential of the NP dispersion is zero), the aggregation tendency of NPs will increase due to lowered electrostatic repulsion (Zhu et al. 2014). Zhu et al. (2014) found that the rate of increase in the size of nano-TiO_2 aggregates (at concentration of 20 mg/L) at pH of 6 (pH_{PZC} = 6, approximately 22 nm/min) was 1 order of magnitude higher than the rate of increase in the size of nano-TiO_2 at pH of 4 or 8 (1 – 1.5 nm/min). For ionic strength, the aggregation tendency of NPs normally increases as ionic strength increases (Domingos et al. 2009; Keller et al. 2010), due to reduced size of the electrostatic double layer and reduced repulsive forces (Hotze et al. 2010). Divalent cations were reported to have a greater impact on promoting the aggregation of NPs compared to monovalent cations (Shih et al. 2012; Baalousha et al. 2013). The presence of organic matter may also influence the aggregation of NPs, including promoting aggregation, hindering the aggregation, as well as being independent of NP stability (Chen and Elimelech 2007; Domingos et al. 2009; Zhu et al. 2014; Luo et al. 2018). Zhu et al. (2014) reported that the addition of humic acid (HA) promoted the aggregation of nano-TiO_2 at pH =4, hindered the aggregation of nano-TiO_2 at pH = 6, and showed no impact on the aggregation of nano-TiO_2 at pH = 8. The contradictory impact of HA on the aggregation of nano-TiO_2 observed by Zhu et al. (2014) was attributed to the differences in the surface charge of nano-TiO_2 at different pH values. The presence of HA increased the negative charge of the nano-TiO_2 surfaces. At pH = 4, when nano-TiO_2 surfaces were originally positively charged, the addition of HA neutralized the surface

charge and brought it closer to zero, resulting in an increased particle aggregation. At pH = 6, when the particle charge was close to zero, the addition of HA resulted in more negatively charged particles, and thus increased the stability of nano-TiO_2. At pH = 8, when nano-TiO_2 surfaces were highly negatively charged, the addition of HA barely changed the surface charge, and therefore did not have a significant impact on the stability of nano-TiO_2 (Zhu et al. 2014).

In addition, particle concentration plays an important role in determining the aggregation tendency of the NPs in the water. Generally, a higher particle concentration would result in a smaller distance between particles, increasing the possibility of particle collision (Taboada-Serrano et al. 2005). An increase in the aggregation of NPs has been reported with an increase in particle concentration, for NPs including nano-TiO_2 (10 – 200 mg/L, Keller et al. 2010; 30 – 500 mg/L, Allouni et al. 2009), nano-ZnO (10 – 100 mg/L, Zhou and Keller 2010; 10 – 200 mg/L, Keller et al. 2010), nano-FeO (13 – 440 mg/L, He et al. 2008), nano-CeO_2 (10 – 200 mg/L, Keller et al. 2010) and nano-Fe_2O_3 (13 – 440 mg/L, He et al. 2008).

2.1.2 Measurements of aggregation behavior of NPs

Once aggregated into large particles, NPs may settle out of the water column due to gravity. The setting velocity of particles has been found to be positively related with particle diameter (Cheng 1997). Therefore, the aggregation behavior of NPs is a crucial factor influencing the fate and transport of NPs in the aquatic environment, and it may further determine which organisms may be threatened under the risk of NPs exposure. A few investigations have been conducted to study the aggregation behavior of NPs. The aggregation behavior of NPs is normally measured in two ways. The direct way monitors the increase of particle size over time, through dynamic light scattering (DLS) measurements (He et al. 2008; French et al. 2009; Keller et al. 2010; Adam et al. 2016; Lin et al. 2017; Luo et al. 2018). The indirect way monitors the sedimentation of NPs, through the change of particle concentration in the solution over time, by the technique of UV-vis spectrophotometry (Allouni et al. 2009; Keller et al. 2010; Sillanpää et al. 2011; Li et al. 2016) or nephelometry (Ottofuelling et al. 2011; Brunelli et al. 2013; Wang et al. 2014b).

2.1.3 The aggregation of nano-TiO_2 in the aqueous environment

Quite a few studies have been carried out to investigate the aggregation behavior of nano-TiO_2 in the

environment (Allouni et al. 2009; French et al. 2009; Keller et al. 2010; Ottofuelling et al. 2011; Sillanpää et al. 2011; Brunelli et al. 2013; Wang et al. 2014a; Wang et al. 2014b; Zhu et al. 2014; Loosli et al. 2015; Adam et al. 2016; Li et al. 2016; Luo et al. 2018). Five of these studies were conducted with the commercial nano-TiO_2 (P25), the test NP used in the present thesis (Ottofuelling et al. 2011; Sillanpää et al. 2011; Brunelli et al. 2013; Wang et al. 2014a; Li et al. 2016). Wang et al. (2014a) studied the impact of salinity, dissolved organic carbon (DOC) and particle concentration (1 – 10 mg/L) on the aggregation of nano-TiO_2 by following the change of particle size in synthetic waters over a 240-h period, yet provided little information on the sedimentation profile of nano-TiO_2 in the water. Sillanpää et al. (2011) monitored the sedimentation profile of nano-TiO_2 (10 and 100 mg/L) within 5 h in four natural freshwater and brackish water samples. Brunelli et al. (2013) followed the sedimentation profile of nano-TiO_2 (0.01 – 10 mg/L) within 50 h in 6 natural and synthetic freshwater and seawater samples. Li et al. (2016) monitored the sedimentation profile of nano-TiO_2 (10 mg/L) within 3 h in 34 lake and brackish water samples. While these three studies provided useful information on the behaviour of nano-TiO_2 (P25) in different types of natural water with varied properties, it remains unclear how would water pH and salinity affect the sedimentation behaviour of nano-TiO_2 (P25). Some investigations were conducted by Ottofuelling et al. (2011) to explore the impact of pH and salinity on the stability of nano-TiO_2 (P25), yet they only did a one-time measurement of the concentration of particles remaining suspended in the water sample after 15 h. There remains a knowledge gap regarding the sedimentation behaviour of nano-TiO_2 (P25) as a function of time in typical estuarine environment along a gradient from the upper region (freshwater condition) to the lower region (seawater condition) remains unclear.

2.1.4 **Aims and hypotheses**

In the present chapter, the sedimentation behaviour of nano-TiO_2 was investigated in various synthetic estuarine media samples, which mimicked the change of salinity and pH typically recorded from the upper estuary to the lower estuary.

Aim 1: The sedimentation of nano-TiO_2 over time was generally followed by measuring the particle concentration suspended in the water, commonly via the absorbance of the particle suspension. Allouni et al. (2009) selected absorbance at 337 nm to represent the concentration of nano-TiO_2, while others chose an

absorbance of 378 nm as the index (Keller et al. 2010; Sillanpää et al. 2011; Li et al. 2016). To find out the best wavelength to estimate the concentration of nano-TiO_2 suspended in the water, the relationship between the particle concentration and the absorbance of nano-TiO_2 suspension was examined.

Hypothesis 1: Generally, the wavelength at which the absorption of light peaks is used to predict the concentration of a compound. It was hypothesized that the wavelength at which the absorption of the particle suspension peaks would be the best wavelength to estimate the concentration of nano-TiO_2 suspended in the water.

Aim 2: To investigate the impact of salinity and pH on the sedimentation of nano-TiO_2, the concentration of nano-TiO_2 suspended in various samples with different salinity and pH were followed over a 72-h period. Six salinity levels were tested from 0 to 35 ‰, representing a salinity gradient from the upper estuary (freshwater condition) to the lower estuary (seawater condition). Five pH levels were tested between 5 and 9, representing the typical variation of pH within natural waters (Deluchat et al. 1997; Hudson et al. 2007).

Hypothesis 2.1: It was hypothesized that the sedimentation rate of nano-TiO_2 would be positively related to increasing salinity.

Hypothesis 2.2: It was reported that the pH_{PZC} value of nano-TiO_2 in the water was affected by the salinity (Ottofuelling et al. 2011). Therefore it was hypothesized that the impact of pH on the sedimentation of nano-TiO_2 would be influenced by salinity level.

Aim 3: It has been reported that the decrease of nano-TiO_2 in the seawater followed a first-order decay equation (Keller et al. 2010; Brunelli et al. 2013; Li et al. 2016). To investigate the impact of particle concentration on the sedimentation of nano-TiO_2 in seawater, the sedimentation of nano-TiO_2 in a seawater sample with different initial concentrations was followed and the sedimentation rate was compared.

Hypothesis 3: An increase in particle concentration would increase the possibility of particle collision (Taboada-Serrano et al. 2005; Allouni et al. 2009). As a result, NPs at higher concentrations are more likely

to form larger aggregates, and therefore higher sedimentation rates would be expected. It was hypothesized that the sedimentation rate of nano-TiO_2 would be positively related to the initial particle concentration.

2.2 Methods

2.2.1 Characterization of nano-TiO_2

Nano-TiO_2 powder (Aeroxide® P25, product no.718467) was bought from Sigma-Aldrich. Some characterizations were conducted to determine its properties.

2.2.1.1 Primary particle size

The primary particle size of nano-TiO_2 powder was examined by a transmission electron microscope (TEM, JEOL 2010, JEOL LTD. UK). The particle powder was dispersed in pure ethanol to create a suspension and then sonicated to avoid clumping. A 3 µl drop of the suspension was deposited onto a carbon TEM grid and allowed to dry under atmospheric condition. Several images were taken at 160 KV with a tungsten filament. The imaging of nano-TiO_2 on TEM was conducted by Dr Ian Griffiths, School of Physics, University of Bristol, UK. Primary particle size was determined based on the TEM images by measuring 120 randomly selected particles using Image-J software (Zip archive, version ij152).

2.2.1.2 Particle morphology

Particle morphology was examined by a field emission scanning electron microscope (FESEM, Sigma HD VP, ∑IGMA™, Zeiss, Germany). Particle powder was dispersed in pure ethanol to create a suspension and sonicated to avoid clumping. A 10 µl drop of the suspension was deposited onto a cover glass (12 mm in diameter, cleaned with ethanol) and allowed to dry under atmospheric condition. The cover glass was then mounted onto a stub with carbon tape. To avoid accumulation of static electric charges, sample was sputter-coated with gold (Edwards Scancoat Gold Sputter Coater, Edwards Laboratories, Milpitas, USA) for 20 seconds before examination on the FESEM. Images were taken at 5 KV with SE2 sensor under standard (30 µm) aperture. Particle morphology was judged from the FESEM images.

2.2.1.3 Surface area

The surface area of nano-TiO_2 was determined by Brunauer, Emmett, Teller (BET) surface area analysis (Brunauer et al. 1938). The measurement was conducted with a Quantachrome Nova 1200 analyzer (Quantachrome Corp., USA). Prior to the measurement, an overnight degas operation was applied to NPs to remove surface moisture and volatilize surface contamination (such as carbon dioxide). The degas operation was done in a glass cell at 105°C under low vacuum (1 x 10^2 mbar) on the instrument degassing station. Afterwards, three replicate measurements were performed using nitrogen as the adsorbative gas. The BET measurements were conducted by Dr Huw Pullin, School of Physics, University of Bristol, UK. The surface area results were obtained from the manufacturer-supplied Quantachrome NovaWin analytical software.

2.2.1.4 Crystal structure

The crystal structure of nano-TiO_2 was examined by X-ray powder diffraction (XRD) analysis using a Phillips Xpert Pro diffractometer with a CuKα radiation source (Philips Analytical, The Netherlands). Particle powder was dispersed in ethanol to create a suspension. Several drops of suspension were transferred onto the middle of a clean glass slide and air dried to create an even particle film. X-ray diffraction scanning angle (2θ) was set from 5 to 80 degrees and the spectrum was recorded with a step size of 0.02 degree under room temperature. The XRD measurements were conducted by Dr Keith Hallam, School of Physics, University of Bristol, UK. The crystal structure of nano-TiO_2 was analyzed by Quanto software (provided by Institute of Crystallography, Bari; http://www.ba.ic.cnr.it/content/quanto), through comparing the obtained XRD spectrum with built-in dataset of spectra from pure anatase, rutile or brookite TiO_2.

2.2.1.5 Light absorption properties

The light absorption properties of nano-TiO_2 in the water were determined using a spectrophotometer (Biochrom WPA Biowave II, Biochrom Cambridge, UK) following the steps illustrated in Figure 2.1. A fresh stock of nano-TiO_2 (1 g/L) was made with Milli-Q water. After sonicating the nano-TiO_2 stock in a water bath (110W, 40 kHz, Bransonic CPX3800H-E ultrasonic bath, Branson Ultrasonic SA, Switzerland) for 15 min, 100 µl of nano-TiO_2 stock (1 g/L) was immediately dispersed into 9.9 mL water (Milli-Q water or seawater) to achieve a final concentration of 10 mg/L nano-TiO_2. Three replicate nano-TiO_2 suspensions

were prepared with Milli-Q water or seawater, respectively. Each nano-TiO_2 suspension was vigorously vortexed for 30 s and 3 mL of suspension was transferred into a cuvette (UV grade PMMA cuvette, suitable for 280 – 800 nm, Fisherbrand, Thermo Fisher Scientific, UK) for the absorption measurement. The absorption spectrum of nano-TiO_2 suspension was recorded with a spectrophotometer (Biochrom WPA Biowave II) within the range of 280 to 800 nm, after zeroing the machine with the corresponding dispersing water (Milli-Q or seawater). The absorption of particle suspension was measured within 10 min after dispersing nano-TiO_2 stock into the water. All measurements were run in triplicates. The seawater used in the present experiment was the same as the artificial estuarine water 8-30 (AEW 8-30) used in the section 2.2.3. A detailed composition of the AEW 8-30 is described in section 2.2.3.

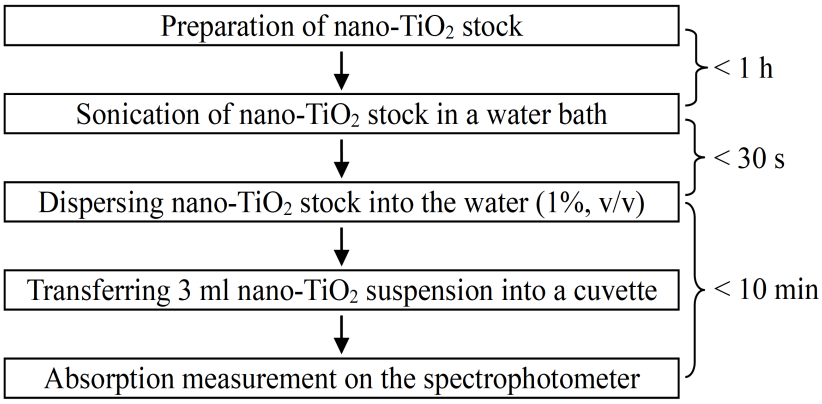

Figure 2.1 Flow chart for measuring the absorption of nano-TiO_2 suspension and the time interval between each step.

2.2.2 Selecting the best wavelength for estimating the concentration of nano-TiO_2 suspended in the water

To find out the best wavelength for estimating the concentration of nano-TiO_2 remaining suspended in the water, the relationship between the particle concentration (0.1 – 100 mg/L) and the absorbance of nano-TiO_2 suspension was examined. Nano-TiO_2 suspensions at different particle concentrations (0.1, 1, 5, 10, 25, 50, 100 mg/L) were prepared and their absorption spectra (280 – 800 nm) were measured following steps outlined in Figure 2.1.

Simple linear regression was adopted to analyze the relationship between particle concentration and the

absorbance of nano-TiO_2 suspension at each wavelength, by constraining the intercept to zero. The value of coefficient of determination from each linear regression was used to select the best wavelength for determining the particle concentration from the measured absorbance of particle suspension.

2.2.3 Sedimentation studies of nano-TiO_2 in the estuarine waters

2.2.3.1 Preparation of estuarine water samples

The AEW (artificial estuarine water) was made up using a based medium (Table 2.1), adopted from the commonly used f/2 culture medium, according to the following procedure.

Table 2.1 Components in the base medium for artificial estuarine water (AEW) samples, adopted from the f/2 medium recipe (Guillard and Ryther 1962).

Components	Concentration (mol/L)
$NaNO_3$	8.83×10^{-4}
NaH_2PO_4 H_2O	3.63×10^{-3}
Na_2SiO_3 $9H_2O$	1.07×10^{-4}
$FeCl_3$ $6H_2O$	1.17×10^{-5}
$EDTANa_2$ $2H_2O$	1.17×10^{-5}
$CuSO_4$ $5H_2O$	3.93×10^{-8}
$ZnSO_4$ $7H_2O$	7.65×10^{-8}
$CoCl_2$ $6H_2O$	4.20×10^{-8}
$MnCl_2$ $4H_2O$	9.10×10^{-7}
Na_2MoO_4 $2H_2O$	2.60×10^{-8}
Thiamine HCl (vit. B1)	2.96×10^{-7}
Biotin (vit. H)	2.05×10^{-9}
Cyanocobalamin (vit. B12)	3.69×10^{-10}

2.2.3.1.1 Preparation of stock solution

Five working stock solutions were prepared with Milli-Q water.

(1) $NaNO_3$ stock: 75 g/L.

(2) NaH_2PO_4 H_2O stock: 5 g/L.

(3) Na_2SiO_3 $9H_2O$ stock: 30 g/L.

(4) Trace metal stock: To make up a 1 L stock, first dissolving 4.36 g $EDTANa_2$ $2H_2O$ and 3.15 g $FeCl_3$ $6H_2O$ in 950 mL Milli-Q water, then added 1 mL of each stock shown in Table 2.2, and finally brought

the final volume to 1 L with Milli-Q water.

Table 2.2 Five primary stocks for making trace metal stock of f/2 medium (Guillard and Ryther 1962).

Stocks	Concentration (g/L)
$CuSO_4$ $5H_2O$	9.8
$ZnSO_4$ $7H_2O$	22
$CoCl_2$ $6H_2O$	10
$MnCl_2$ $4H_2O$	180
Na_2MoO_4 $2H_2O$	6.3

(5) Vitamin stock: To make up 1 L stock, first dissolving 0.2 g Thiamin HCl (vit. B_1) in 950 mL Milli-Q water, then added 10 mL of biotin stock (0.1 g/L) and 1 mL of cyanocobalamin stock (1 g/L), and finally brought the final volume to 1 L with Milli-Q water.

Stocks (1) – (4) were filtered-sterilized (0.22 μm, PVDF syringe filters, Fisherbrand, Thermo Fisher Scientific, U.K.) and stored at 4 ^{0}C at dark until use. Stock (5) was filter-sterilized (0.22 μm) and stored at -20 ^{0}C until use. All stocks were brought to room temperature before using.

2.2.3.1.2 Preparation of 30 different AEW samples

The AEW samples were prepared by mixing the stocks (1) – (5) prepared as stated in section 2.2.3.1.1 with artificial seawater. The artificial seawater was made up by dissolving Tropic Marin salt (Underwood and Provot 2000; Ast et al. 2009) in Milli-Q water to achieve desire salinity (0 ‰, 10 ‰, 20 ‰, 25 ‰, 30 ‰, or 35 ‰). To make up 1 L AEW, added 1 mL of stock (1), 1 mL of stock (2), 1 mL of stock (3), 1 mL of stock (4) and 0.5 mL of stock (5) in sequence into artificial seawater at different salinity and brought the final volume to 1 L. The mixture was then adjusted with 1 M HCl or NaOH to achieve desire pH (5, 6, 7, 8, 9). A total of thirty different AEW samples were prepared for each combination of five pH levels and six salinity levels, mimicking a salinity and pH gradient from the upper estuary to the lower estuary. Each AEW was coded as AEW p-s, where p refers to the pH value and s refers to the salinity level. For example, AEW 8-30 refers to the artificial estuarine water sample with pH of 8 and salinity of 30 ‰, which was the culture medium (f/2 medium) used to cultivate estuarine benthic diatoms in the present thesis. AEW 8-30 was selected as a representative of seawater in the present study. All AEW samples were then filtered-sterilized (0.22 μm) and ready for test.

2.2.3.2 The impact of pH and salinity on the sedimentation of 100 mg/L nano-TiO_2

To investigate the impact of medium pH and salinity on the sedimentation of nano-TiO_2 (aim 2), the sedimentation profiles of 100 mg/L nano-TiO_2 in 30 AEW samples were followed within the period of 72 h. Nano-TiO_2 suspensions at concentration of 100 mg/L was prepared with 30 AEW samples and their absorptions at 421 nm (A_{421}) were measured according to Figure 2.1 (see section 2.4.2 for the reason of selecting 421 nm as the measuring wavelength). The measuring point was set at the center of the particle suspension. The first measurement was made within 10 min after dispersing nano-TiO_2 into the AEW sample. Afterwards, nano-TiO_2 suspensions were allowed to settle down in the cuvette at 18℃, with minimum disturbance and movement. Caps were applied onto the cuvettes to minimize the evaporation within the period of 72 h. The A_{421} of each AEW sample in the cuvette was re-measured after 1 h, 4 h, 24 h, 48 h and 72 h, counting from the moment nano-TiO_2 stock was dispersed into the AEW sample. All measurements were run in triplicates. Images of each AEW were taken at time < 10 min, 1 h, 4 h, 24 h and 72 h with the back camera (13 MP, f/2.0) of a smartphone (Model A0001, OnePlus One, China).

The sedimentation curve of nano-TiO_2 in the water sample was constructed by plotting the concentration of nano-TiO_2 suspended in the AEW as a function of time. The concentration of nano-TiO_2 (C, mg/L) suspended in the water was obtained using equation 2.1:

$$C\ (\text{mg/L}) = C_0 \times (A_t/A_0)_{421} \qquad \text{(eq 2.1)}$$

where C_0 is the starting particle concentration of nano-TiO_2, A_t is the absorbance of nano-TiO_2 suspension at 421 nm at time t and A_0 is the initial absorbance of nano-TiO_2 suspension at 421 nm measured at t < 10 min.

2.2.3.3 The impact of particle concentration on the sedimentation of nano-TiO_2 in the AEW 8-30

To investigate the impact of particle concentration on the sedimentation of nano-TiO_2 in seawater (aim 3), the sedimentation profile of nano-TiO_2 in AEW 8-30 was followed for 24 h. Nano-TiO_2 suspensions at concentrations of 10, 50, 100 mg/L were prepared with AEW 8-30 and their absorption at 421 nm (A_{421}) was

measured according to section 2.2.3.2. Afterwards, nano-TiO_2 suspensions were allowed to settle down in the cuvette as described in section 2.2.3.2. The absorption of each sample was re-measured at 1, 2, 3, 4, 5, 7, 9 and 24 h, counting from the moment nano-TiO_2 stock was dispersed into the AEW 8-30. All measurements were run in six replicates. Images of each AEW were taken at time < 10 min, 1 h, 2 h, 4 h, 7 h, and 24 h with the back camera (13 MP, f/2.0) of a smartphone (Model A0001, OnePlus One, China).

The sedimentation curve of nano-TiO_2 in the AEW 8-30 was constructed by plotting the concentration of nano-TiO_2 suspended in the sample as a function of time. The concentration of nano-TiO_2 (mg/L) suspended in the water was obtained using equation 2.1.

The sedimentation rate constant (k) was calculated by fitting the sedimentation curve with the following first-order equation (equation 2.2).

$$C = C_0 e^{-kt} \qquad \text{(eq 2.1)}$$

where C is the concentration of nano-TiO_2 at time t, C_0 is the starting concentration of nano-TiO_2 at $t = 0$ and k is the first-order rate constant.

2.2.4 Hydrodynamic diameter of nano-TiO_2 aggregates

To investigate the link between sedimentation rate and the hydrodynamic diameter of nano-TiO_2 aggregates, the diameter of TiO_2 particles in the water at several different time points was measured by dynamic light scattering (DLS). Three AEW samples (AEW 7-0, AEW 8-0 or AEW 8-30) were tested to represent three types of water (see section 2.3.3 for details).

Nano-TiO_2 suspensions at concentration of 100 mg/L were prepared with AEW 7-0, AEW 8-0 or AEW 8-30 according to Figure 2.1. After vortex mixing for 30 s, 1.2 mL of particle suspension was transferred into a measuring cuvette (DTS0012). The hydrodynamic diameter of nano-TiO_2 aggregates was measured with a Zetasizer Nano-S90 (Malvern-ZEN-1690, Malvern Instruments, UK). The Zetasizer instrument was operated with a He-Ne laser at 633 nm and light scattering was detected at an angle of 90°. The measuring

temperature was set at 18°C, the temperature used to cultivate estuarine benthic diatoms in the present thesis. Each cuvette was measured once only and was not re-measured. Until measurements were made, the cuvettes were set aside to allow the sedimentation of nano-TiO_2 with minimum disturbance and movement. Prior to the measurement, the cuvette was shaken to resuspend all the particle aggregates at the bottom of the cuvette. The DLS measurement was carried out at time < 10 min, 1 h, 4 h and 24 h, counting from the moment nano-TiO_2 stock was dispersed into the AEW sample. All measurements were run in triplicates. The hydrodynamic diameter (z-average mean) of TiO_2 aggregates was obtained from the manufacturer-supplied Malvern software. As indicated by the Malvern software, all measurements met the quality criteria.

2.2.5 **Zeta-potential measurement**

To investigate the relationship between sedimentation rate and the zeta-potential of nano-TiO_2 particles, the zeta-potential of nano-TiO_2 suspended in the water was measured. Three AEW samples (AEW 7-0, AEW 8-0 or AEW 8-30) were tested to represent three types of water (see section 2.3.3 for details).

Nano-TiO_2 suspensions at concentration of 100 mg/L were prepared with AEW 7-0, AEW 8-0 or AEW 8-30 according to Figure 2.1. After a vigorous vortex mixing for 30 s, particle suspension was loaded into a folded capillary cell (DTS1070). The zeta-potential of nano-TiO_2 suspension was immediately measured with a Zetasizer Nano Z (Malvern-ZEN-2600, Malvern Instruments, UK). The measuring temperature was set at 18°C. All measurements were run in triplicates. The zeta-potential values were obtained from the manufacturer-supplied Malvern software. As indicated by the Malvern software, all measurements met quality criteria.

2.2.6 **Data analysis**

Normality tests and tests for the statistical significance between values were performed using SPSS software (version 24.0 of SPSS for Windows). After checking the homogeneity of variance by Levene's test and the normality of the residuals by Kolmogorov-Smirnov test, parametric tests (e.g. independent-samples T tests, ANOVA tests) were applied to determine the difference between groups. The linear regression curves and the first-order curves were fitted in the GraphPad Prism 6.0 software (https://www.graphpad.com/, GraphPad Software). The values of the coefficient of determination and the first-order rate constants were determined

by GraphPad Prism 6.0 software. Results were shown as mean values ± standard deviation, unless otherwise stated. The significance level was set at < 0.05.

2.3 Results

2.3.1 Characterization of nano-TiO_2 powder

2.3.1.1 Morphology

According to the SEM and TEM images (Figure 2.2), the nano-TiO_2 powder had an irregular morphology.

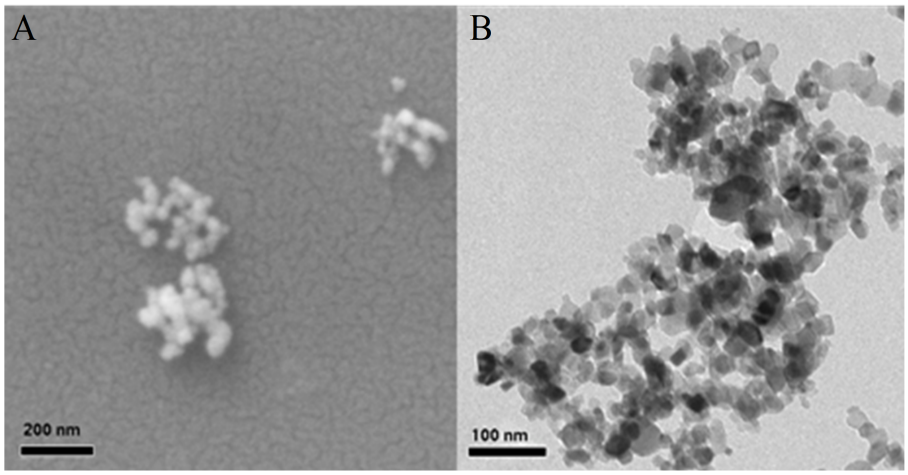

Figure 2.2 (A) Scanning electron microscopy images and (B) transmission electron microscopy images of nano-TiO_2 powder. The TEM image was taken by Dr Ian Griffiths, School of Physics, University of Bristol, UK.

2.3.1.2 Primary particle size

A total of 120 particles was measured for their sizes based on the TEM pictures. The number distribution of the primary particle size followed a log-normal distribution, instead of a normal distribution (Table 2.3). The nano-TiO_2 had a geometric mean of 24.4 nm with a standard deviation of 1.4 nm (Figure 2.3).

Table 2.3 Skewness, kurtosis and normality test results provided by SPSS for the primary particle size distribution of nano-TiO_2.

		Original data	Log-transformed data
Skewness	Statistic	0.696	-0.028
	Standard error	0.221	0.221
Kurtosis	Statistic	0.157	-0.408
	Standard error	0.438	0.438
Kolmogorov-Smirnov Test with Lilliefors Correction	Statistic	0.083	0.039
	Df	120	120
	p	0.04	0.2
Shapiro-Wilk Test	Statistic	0.962	0.994
	Df	120	120
	p	0.002	0.873

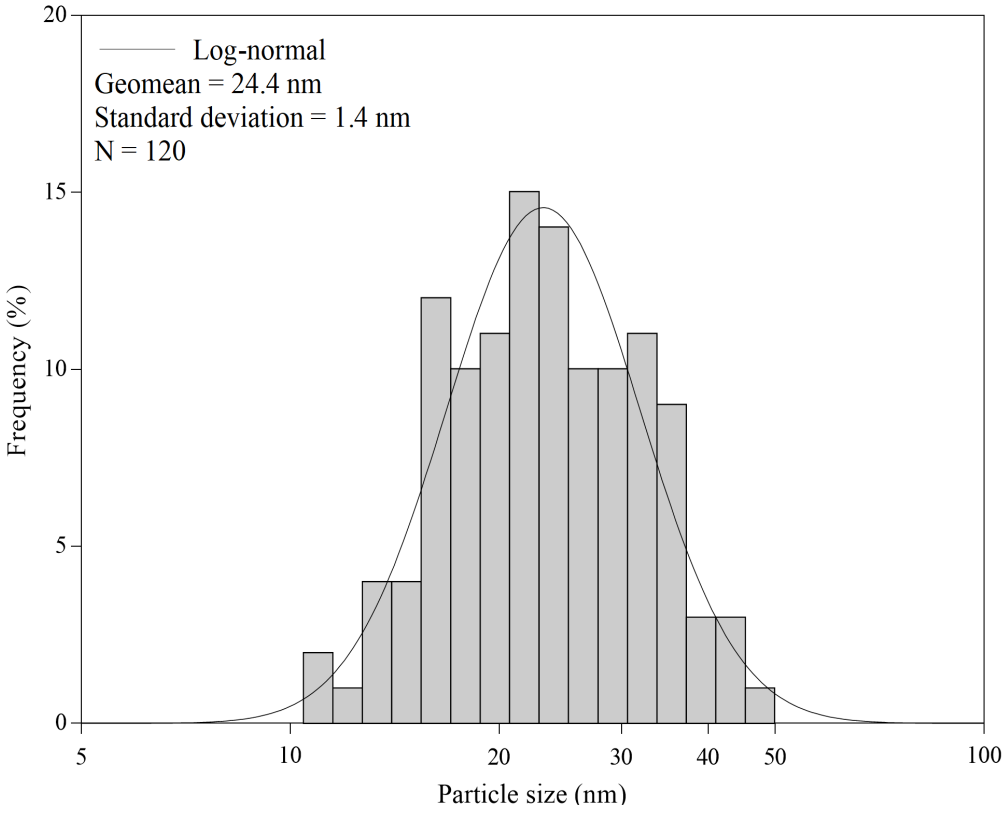

Figure 2.3 Size distribution of primary nano-TiO_2 particles. The x-axis shows the size of a particle and is in log-scale.

2.3.1.3 Surface area

BET (Brunauer, Emmett, Teller) measurements showed that the surface area of nano-TiO_2 was 44.83 ± 0.93 m^2/g (n = 3).

2.3.1.4 Crystal structure

The XRD pattern of nano-TiO_2 is illustrated in Figure 2.4A, with peaks around 25°, 27°, 38°, 48°, 53°, 55° and 63°. Pure anatase phase is marked by peaks located around 25°, 38°, 48°, 53° and 55° (Figure 2.4B). Pure rutile phase has main peaks around 27°, 36°, 53° and 56° (Figure 2.4C). Pure brookite phase has intense peaks located around 25°, 26°, 31°, 36°, 47° and 55 (Figure 2.4D). As indicated by the diffraction peaks, the nano-TiO_2 was composed of a mixture of anatase and rutile phase, and rarely brookite phase. Quanto software calculated that nano-TiO_2 consists of 85.8% anatase and 14.2% rutile.

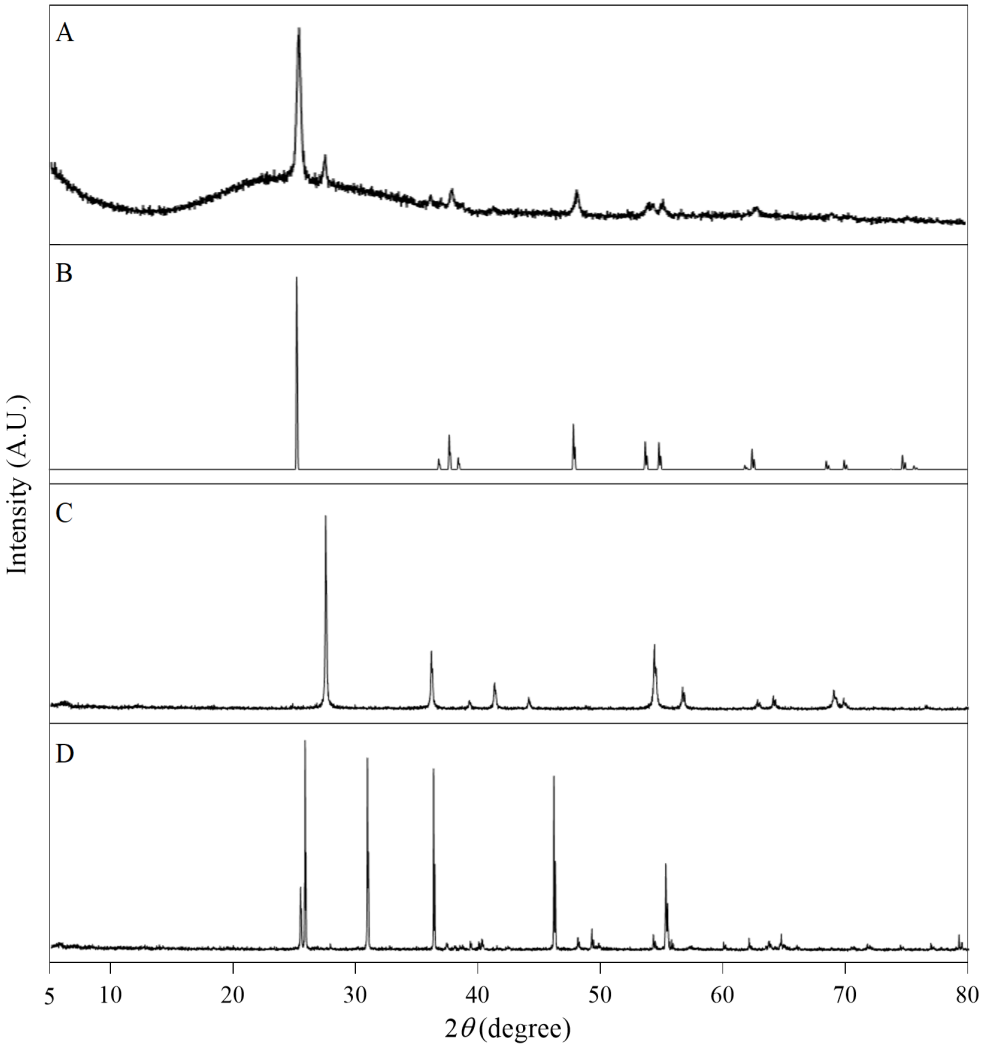

Figure 2.4 X-ray powder diffraction (XRD) pattern of (A) nano-TiO_2 (P25) and reference pattern (downloaded from http://rruff.info/) of (B) pure anatase (RRUFF ID: R060277.9), (C) pure rutile (RRUFF ID: R050031.1) and (D) pure brookite (RRUFF ID: R050363.1).

2.3.1.5 Light absorption properties of nano-TiO_2

The light absorption spectra for 10 mg/L nano-TiO_2 suspended in Milli-Q water (in relative to Milli-Q water) and 10 mg/L nano-TiO_2 suspended in AEW 8-30 (in relative to AEW 8-30) was found to be different (Figure 2.5). In the AEW 8-30, an absorption peak was recorded at around 330 nm. In the Milli-Q water, the absorption of nano-TiO_2 suspension continuously decreased from 280 nm to 800 nm, with 330 nm being a turning point and thereafter the rate of decrease in absorbance increased.

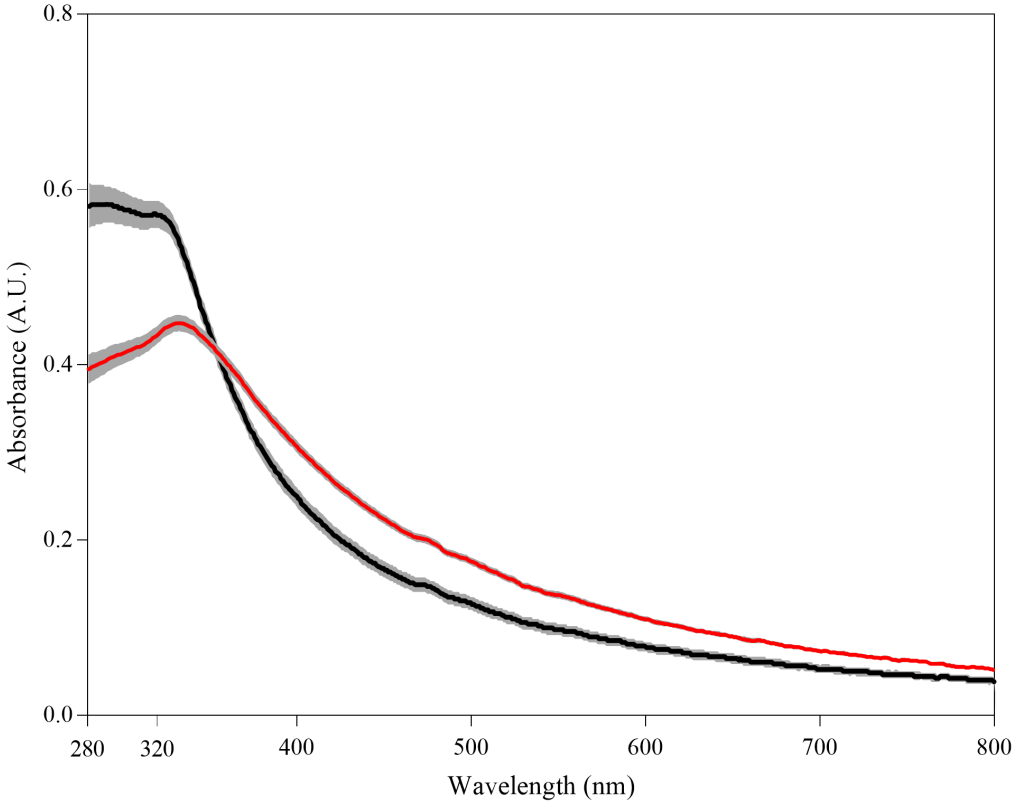

Figure 2.5 Absorption spectra of 10 mg/L nano-TiO_2 in the Milli-Q water (black line) and AEW 8-30 (artificial estuarine water, pH = 8, salinity = 30 ‰) (red line) within range of 280 to 800 nm. Results are shown as mean values (lines) and 95% confidence interval (grey areas, n = 3).

2.3.2 Relationship between absorbance and concentration of nano-TiO_2

To find out the best wavelength for estimating the concentration of nano-TiO_2 suspended in the water, the relationship between the particle concentration and the absorbance of nano-TiO_2 suspension was explored.

The absorption spectra of nano-TiO_2 in Milli-Q water and AEW 8-30 at 7 particle concentrations (0.1, 1, 5, 10, 25, 50, 100 mg/L) were recorded. It was measured that the absorbance values of nano-TiO_2 suspension at the lowest concentration of 0.1 mg/L were not different from zero. The coefficient of determination (R^2) of the linear regression between the concentration of nano-TiO_2 (1 – 100 mg/L) and the absorbance value of the nano-TiO_2 suspension at each wavelength was calculated. The variation of the value of R^2 as a function of wavelength is shown in Figure 2.6. When nano-TiO_2 was dispersed in Milli-Q water, the R^2 reached the highest value (0.9993) at 427 nm. When nano-TiO_2 was dispersed in AEW 8-30, the R^2 reached the highest value (0.9999) at 421 nm. The sum of two coefficients of determination peaked at 421 nm, being 1.9991.

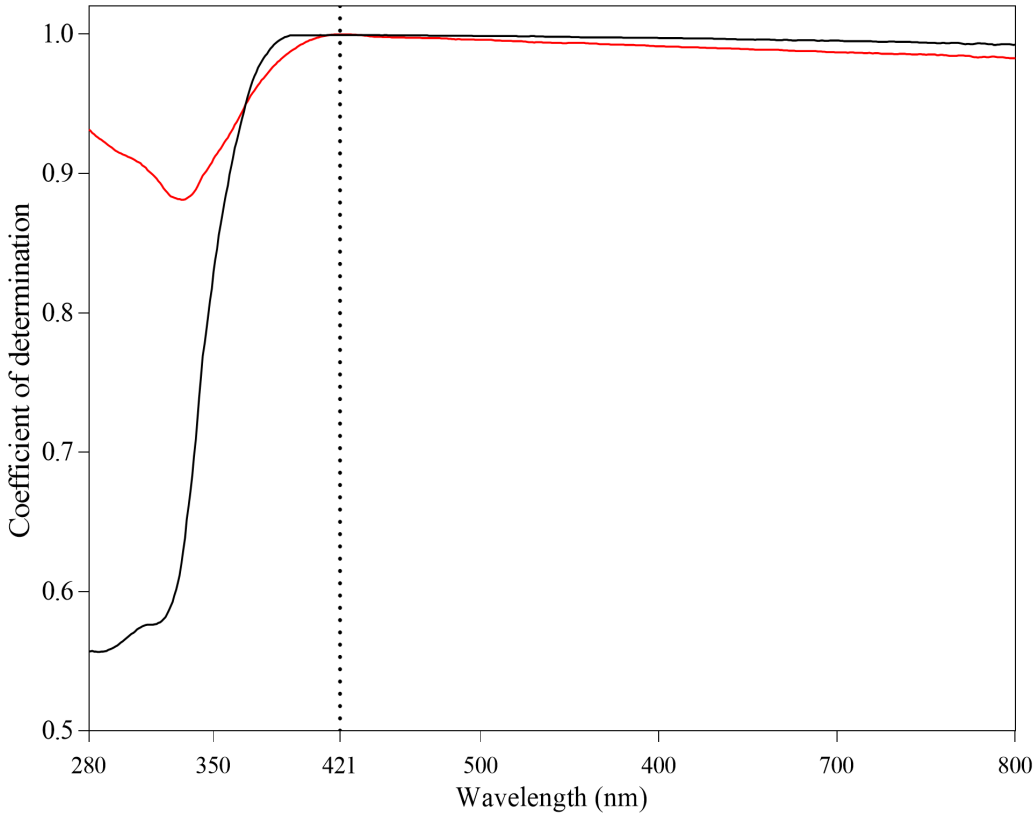

Figure 2.6 The variation of coefficient of determination (R^2) of the linear regression between the concentration of nano-TiO_2 (1 – 100 mg/L) and absorbance value of nano-TiO_2 suspension as a function of wavelength (nm). Nano-TiO_2 was dispersed in Milli-Q water (black line) or AEW 8-30 (artificial estuarine water, pH = 8, salinity = 30 ‰) (red line).

2.3.3 **Sedimentation of nano-TiO_2 under different salinity and pH**

To investigate the impact of salinity and pH on the sedimentation of 100 mg/L nano-TiO_2 in the water, the sedimentation profiles of 100 mg/L nano-TiO_2 in 30 AEW samples were followed.

The change in suspended nano-TiO_2 in 30 AEW samples within the period of 72 h is illustrated in Figure 2.7. Nano-TiO_2 dispersed in the saline AEW samples (salinity ≥ 10 ‰) quickly settled down regardless of the pH value. The sedimentation of nano-TiO_2 in the AEW 5-0 (pH = 5, salinity = 0) was similar to that in the saline AEW samples. However, in other freshwater samples (salinity = 0, pH > 5), the sedimentation of nano-TiO_2 was much slower, with considerable amount of TiO_2 remaining suspended after 72 h.

The residual concentration of nano-TiO_2 in the sample as a function of time is shown in Figure 2.8. Two distinct sedimentation profiles were observed. The first type appeared in the AEW 5-0 and all the saline AEW samples, in which the concentration of nano-TiO_2 rapidly decreased by approximately 80% within 4 h, with sedimentation rate being approximately 20 mg/L/h, and more than 99% of the particles settled out after 24 h. In this group, the salinity (10 – 35 ‰) and pH (5 – 9) showed no impact on the sedimentation behavior of nano-TiO_2. The second type was recorded in the freshwater samples with pH between 6 and 9, in which the concentration of nano-TiO_2 slightly decreased by 2% only within 4 h and 26 – 62% of the particles remained suspended after 72 h. In this group, the decrease of nano-TiO_2 was in proportion to time ($p < 0.001$, $R^2 > 0.9784$). The highest sedimentation rate of 100 mg/L nano-TiO_2 was 1.09 (± 0.04) mg/L/h at pH of 8, followed by 0.87 (± 0.01) mg/L/h at pH of 6 and 0.72 (± 0.01) mg/L/h at pH of 9, and the slowest was 0.51 (± 0.01) mg/L/h at pH of 7.

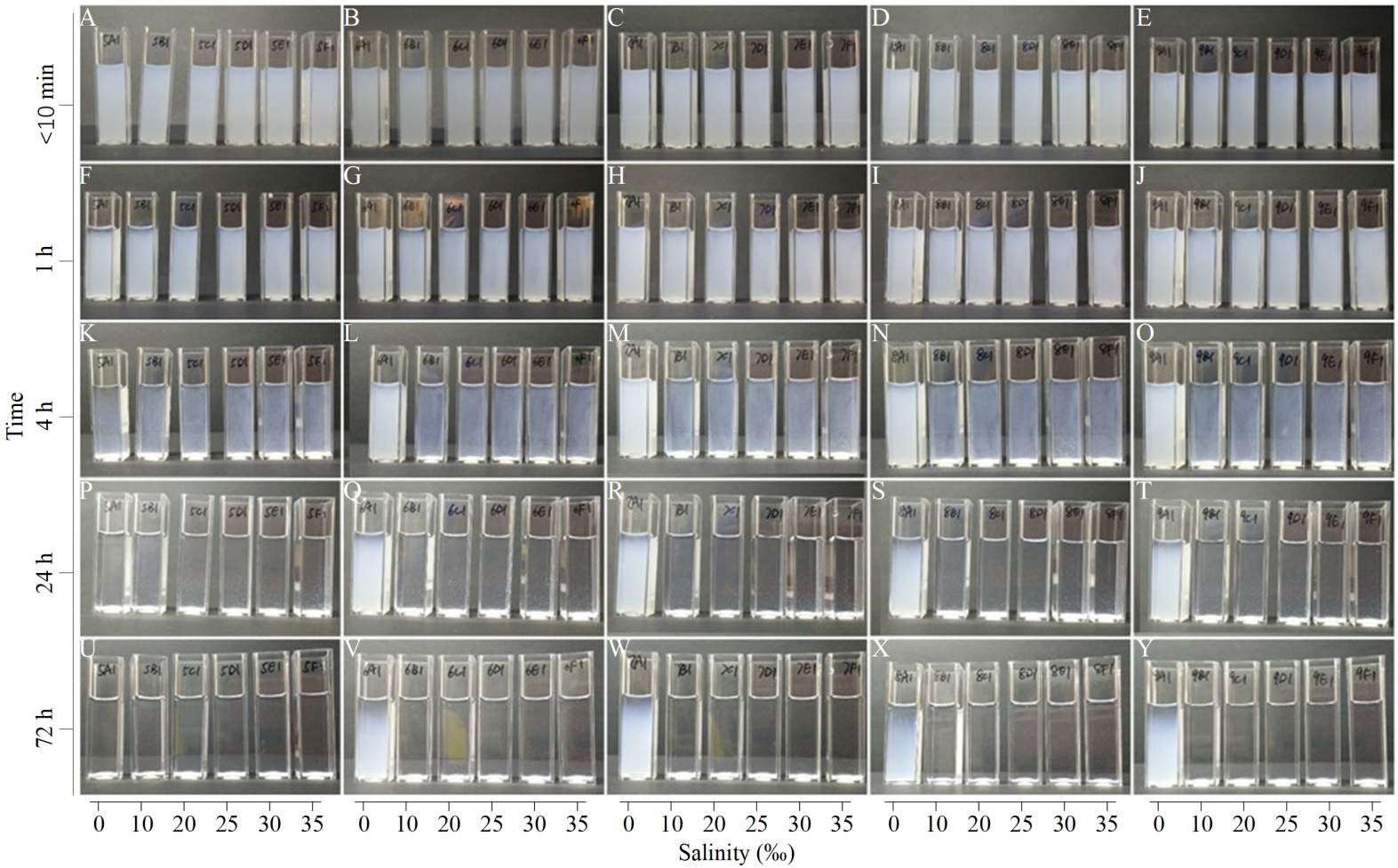

Figure 2.7 The state of nano-TiO_2 (100 mg/L) suspension in 30 AEW samples within 72 h. The salinity of AEW samples varied from 0 to 35 ‰. Images were taken at (A-E) < 10 min, (F-J) 1 h, (K-O) 4 h, (P-T) 24 h, (U-Y) 72 h for samples with pH of (A, F, K, P, U) 5, (B, G, L, Q, V) 6, (C, H, M, R, W) 7, (D, I, N, S, X) 8 or (E, J, O, T, Y) 9.

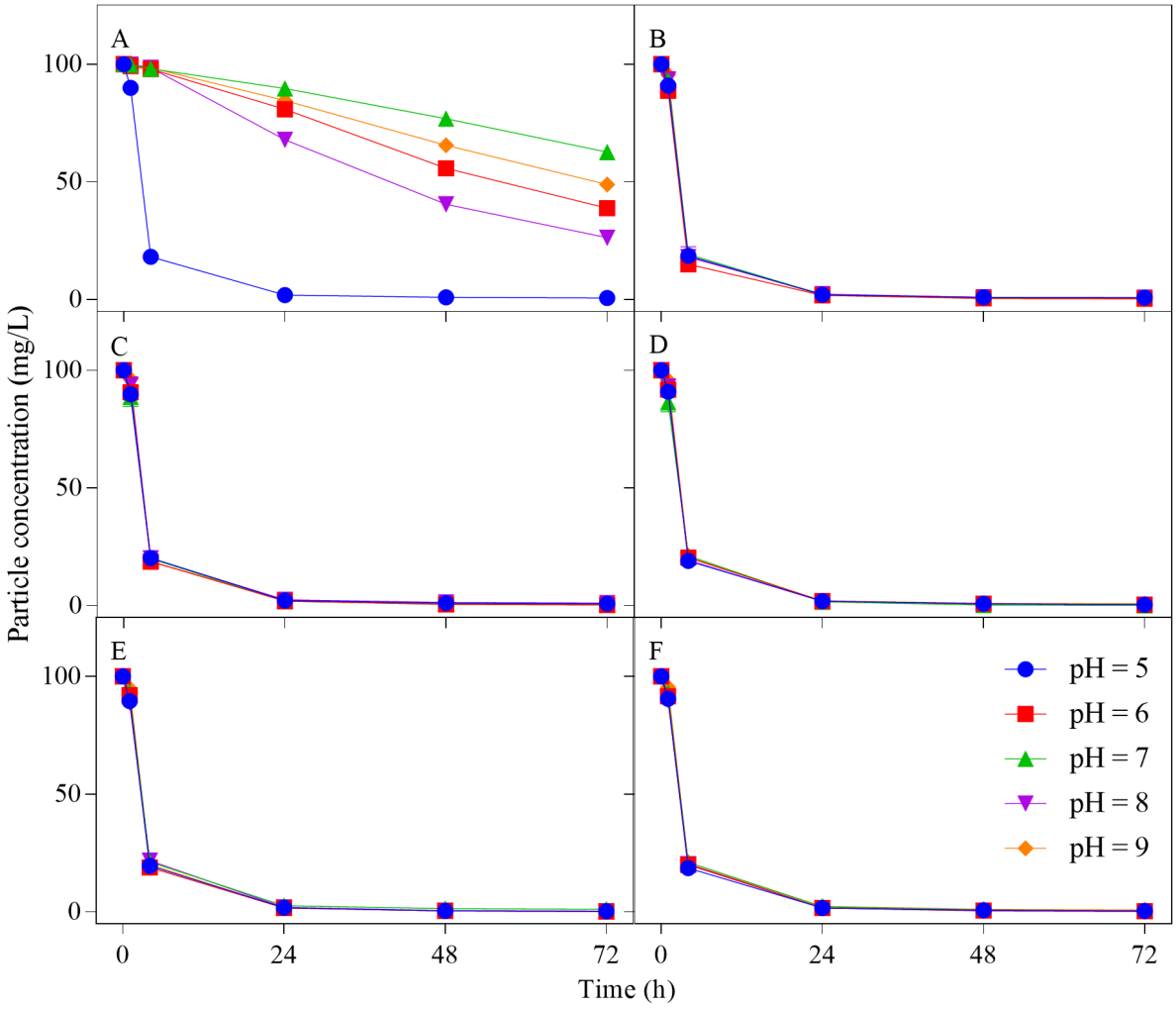

Figure 2.8 Sedimentation profile of nano-TiO_2 in 30 different AEW samples with salinity being (A) 0, (B) 10 ‰, (C) 20 ‰, (D) 25 ‰, (E) 30 ‰, (F) 35 ‰. The pH value of AEW samples is denoted by colour. Results are shown as mean ± standard deviation (n = 3). When the standard deviation is not visible, it is smaller than the symbol.

2.3.4 Hydrodynamic diameter and zeta-potential of nano-TiO_2 aggregates in the AEW

To investigate the link between sedimentation rate and the hydrodynamic diameter and zeta-potential of nano-TiO_2 particles, the hydrodynamic diameter and zeta-potential of nano-TiO_2 aggregates in three AEW samples were measured and compared in Table 2.4. The formation of nano-TiO_2 aggregates happened very quickly. According to the first DLS measurement (< 10 min after dispersing nano-TiO_2 into the water), the average particle size had increased from 24 nm (average primary particle size) to 320 nm in freshwater

samples (AEW 7-0 and AEW 8-0) and had increased to 1130 nm in the seawater sample (AEW 8-30). In the freshwater samples (AEW 7-0 and AEW 8-0), the size of nano-TiO_2 aggregates was stable within 24 h. According to a two-way ANOVA test, the incubation time ($F_{3,16} = 0.138$, $p = 0.936$) and water pH ($F_{1,16} = 0.649$, $p = 0.432$) showed no significant impact on the size of the aggregates in the freshwater samples. By contrast, the size of nano-TiO_2 aggregates in the seawater sample (AEW 8- 30) increased by 60% within 4 h and were stable thereafter. The zeta-potential was highly negative for nano-TiO_2 in the freshwater samples (AEW 7-0 and AEW 8-0), but was positive and close to zero in the seawater sample (AEW 8-30).

Table 2.4 Z-average hydrodynamic diameter, zeta-potential of nano-TiO_2 (100 mg/L) dispersed in 3 AEW samples. Results are shown as mean ± standard deviation (n = 3). For sample codes, see section 2.2.3.1.

Sample	pH	Salinity	Hydrodynamic particle size (nm)				Zeta-potential (mV)
			< 10 min	1 h	4 h	24 h	
AEW 7-0	7	0	324 ± 9	328 ± 9	323 ± 11	327 ± 16	-34.37 ± 0.09
AEW 8-0	8	0	319 ± 7	321 ± 12	325 ± 10	324 ± 6	-32.97 ± 0.82
AEW 8-30	8	30 ‰	1130 ± 161	1443 ± 195	1793 ± 260	1586 ± 287	1.56 ± 0.18

2.3.5 Sedimentation of nano-TiO_2 particles under different particle concentrations in seawater

To investigate the impact of particle concentration on the sedimentation of nano-TiO_2 in seawater, the sedimentation of nano-TiO_2 in a seawater sample (AEW 8-30) was followed and shown in Figure 2.9. Particles gradually settled down within 24 h. After 24 h, all samples looked similar without any visible cloudiness, due to the low amount of TiO_2 remaining suspended in the water.

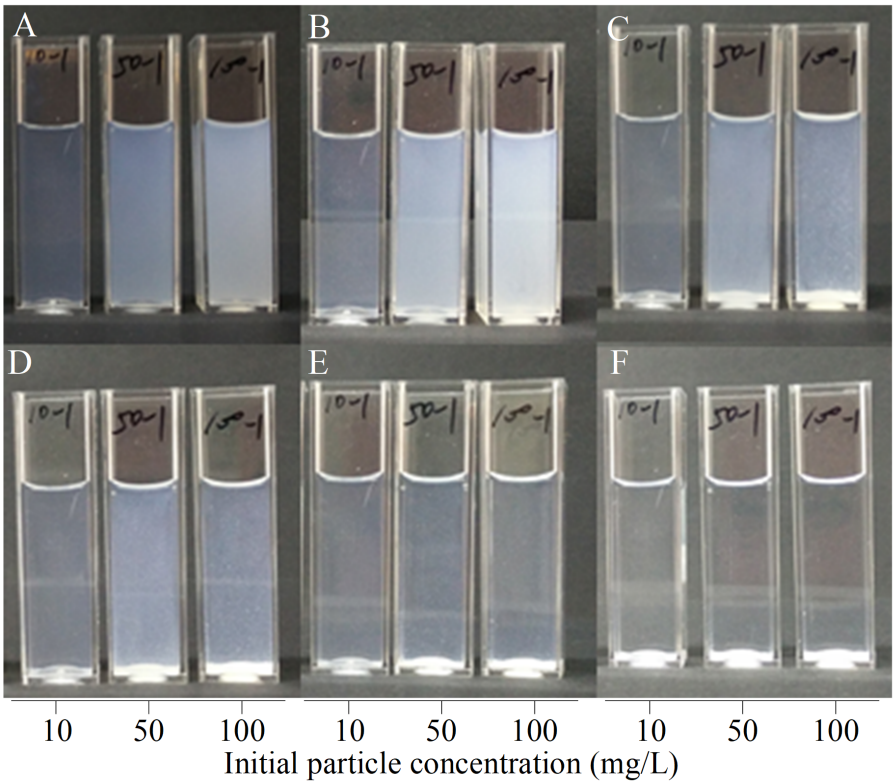

Figure 2.9 The state of nano-TiO_2 suspensions in the AEW 8-30 (pH = 8, salinity = 30 ‰) with different initial concentrations after (A) < 10 min, (B) 1 h, (C) 2 h, (D) 4 h, (E) 7 h, (F) 24 h.

The sedimentation curve was constructed by plotting the concentration of nano-TiO_2 suspended in the AEW 8-30 versus time (Figure 2.10). Particle concentration decreased more rapidly with a higher initial particle concentration. Regardless of the initial particle concentration, the concentration of nano-TiO_2 suspended in the water became similar after 9 h, and fell below detection limit of 1 mg/L after 24 h.

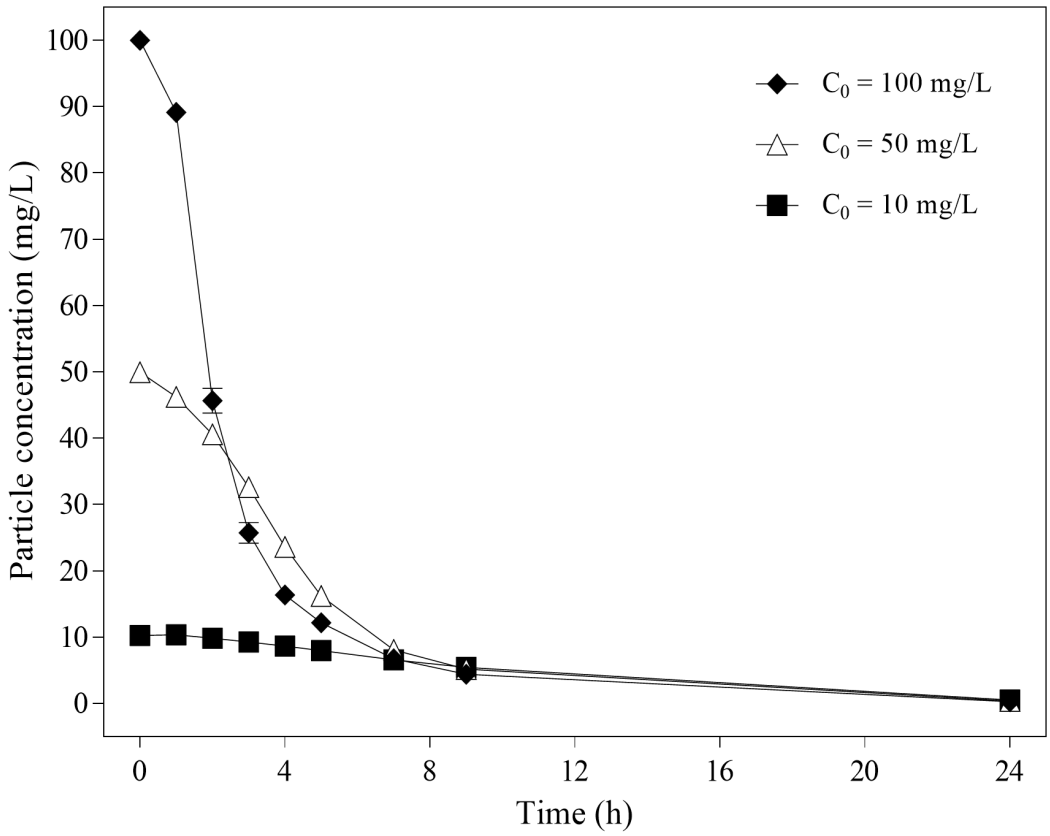

Figure 2.10 Sedimentation of nano-TiO_2 in the AEW 8-30 (pH = 8, salinity = 30 ‰) as a function of time with 3 different initial particle concentrations (C_0). Results are shown as mean ± standard deviation (n = 6). When the standard deviation is not visible, it is smaller than the symbol.

The sedimentation rate was calculated by fitting the sedimentation curves in Figure 2.10 with first-order kinetics. The sedimentation rate constant (k) was found to be positively related to the initial particle concentration (Table 2.5). As particle concentration increased from 10 mg/L to 100 mg/L, the k increased by 5.8-fold.

Table 2.5 The sedimentation rate constant (k) and the coefficient of determination (R^2) for the sedimentation curve of nano-TiO_2 in the AEW 8-30 (pH = 8, salinity = 30 ‰), according to first-order kinetics.

Initial particle concentration (mg/L)	k (h^{-1})	R^2
10	0.065 ± 0.003	0.9258
50	0.191 ± 0.008	0.9491
100	0.379 ± 0.016	0.9536

2.3.6 Summary of results

- The absorbance of nano-TiO_2 suspension at 421 nm was found to provide the best estimation of the concentration of nano-TiO_2 suspended in the different types of water.
- At pH of 5, the sedimentation rate of 100 mg/L nano-TiO_2 in the water was not affected by the water salinity within the range of 0 – 35 ‰. At pH of 6 – 9, the sedimentation rate of 100 mg/L nano-TiO_2 in the freshwater samples (salinity = 0) was much slower than that in the saline samples (salinity = 10 – 35 ‰). The sedimentation rates in the saline samples were not different, regardless of salinity (10 – 35 ‰) and pH (5 – 9).
- The sedimentation rate of nano-TiO_2 in seawater increased as particle concentration increased from 10 mg/L to 100 m/L.

2.4 Discussion

2.4.1 Characteristics of nano-TiO_2

The nano-TiO_2 tested in the present study is a commercially available product, which is one of the most widely tested nano-TiO_2 type by researchers. The properties of nano-TiO_2 measured in the present study fell within the range provided by the manufacture and were similar with those reported in the other studies (Table 2.6).

Table 2.6 The properties of nano-TiO_2 (P25) measured in the present study compared to the manufacture information and other studies. Results are shown as the mean value, or mean value ± standard deviation, or the range of the value. "–" denotes the information is not available.

Properties	The present study	Manufacture[a]	Brunelli et al. (2013)	Wang et al. (2014a)	Ottofuelling et al. (2011)
Morphology	Spherical-like	–	Semi-spherical	Spheroid	–
Size (nm)[b]	24.4 ± 1.4	21	10 – 60	21	19.8
Surface area (m^2/g)[c]	44.83 ± 0.93	35 – 65	61	50 ± 15	52.2
Crystal structure[d]	85.8% anatase, 14.2% rutile	approximately 80% anatase, 20% rutile	–	86% anatase, 14% rutile	88% anatase, 12% rutile

a) Information obtained from https://www.sigmaaldrich.com/catalog/product/aldrich/718467?lang=en&region=GB, accessed 01/02/2019.

b) Size values were based on transmission electron microscopy

c) Surface area values were based on BET measurement.

d) Crystal structure information was based on XRD measurements.

The absorption spectra of nano-TiO_2 in the Milli-Q water and seawater sample (AEW 8-30) was found to be different. A clear absorption peak at around 330 nm was recorded for the nano-TiO_2 (P25) suspension in the AEW 8-30. This spectrum was similar to that recorded by Dalai et al. (2012) but with a different type of nano-TiO_2. They recorded that the absorbance of nano-TiO_2 (primary particle size < 25 nm, 99.7% anatase) peaked at 336 nm in a lake water (Dalai et al. 2012). In the current investigation, a different absorption pattern was recorded when nano-TiO_2 (P25) were dispersed in the Milli-Q water, compared to that in the seawater. As the wavelength decreased from 330 nm to 280 nm, instead of a decrease, the absorption of nano-TiO_2 (P25) in the Milli-Q water slightly increased until it reached a plateau. A similar pattern was found by Keller et al. (2010), with nano-TiO_2 (primary particle size of 27 nm, 82% anatase and 18% rutile), though the type of dispersion water used in their experiment was not mentioned. Chen et al. (2013) also observed a similar absorption plateau between 280 and 325 nm by dispersing nano-TiO_2 (P25) into deionized water. It was reported that the interaction between metal ions and organic compounds could affect the absorbance value of the solution within the UV range (Yin et al. 2016). Studies showed that metal ions and organic compounds may gather around the NPs and affect the surface properties of the NPs (Hotze et al. 2010). Tropic Marin salt, the salt used to prepare AEW 8-30, contains a variety of types of trace metals and some organic compounds (Atkinson and Bingman 1997). Therefore, it is postulated that the interaction between nano-TiO_2, metal ions and organic compounds in the AEW 8-30 could change the absorption characteristics

of the solution, resulting in the different absorption spectra recorded in two nano-TiO_2 suspensions.

2.4.2 Determination of nano-TiO_2 concentration by absorbance

It was hypothesized that the wavelength at which the absorption of the particle suspension peaks would be the best wavelength to estimate the concentration of nano-TiO_2 suspended in the water. In the present investigation, the absorbance of nano-TiO_2 in the seawater sample (AEW 8-30) peaked at 330 nm. However, the coefficient of determination (R^2) between absorbance of nano-TiO_2 suspension and the concentration of nano-TiO_2 (P25), determined by linear regression, was low ($R^2 = 0.6$ when dispersed in the Milli-Q water, $R^2 = 0.88$ when dispersed in the AEW 8-30) (Figure 2.11), which was not in agreement with the hypothesis. The low value of R^2 was due to the absorption saturation at 50 – 100 mg/L, making the absorbance at 330 nm a bad option for estimating the concentration of nano-TiO_2 suspended in the water. It is noted in Figure 2.6 that the determination of nano-TiO_2 concentration by the suspension absorbance optimized at 421 nm, based on the linear regression. Therefore, the absorbance of nano-TiO_2 suspension at 421 nm (A_{421}) was used as an index to indicate the residual concentration of nano-TiO_2 (P25) in the water sample.

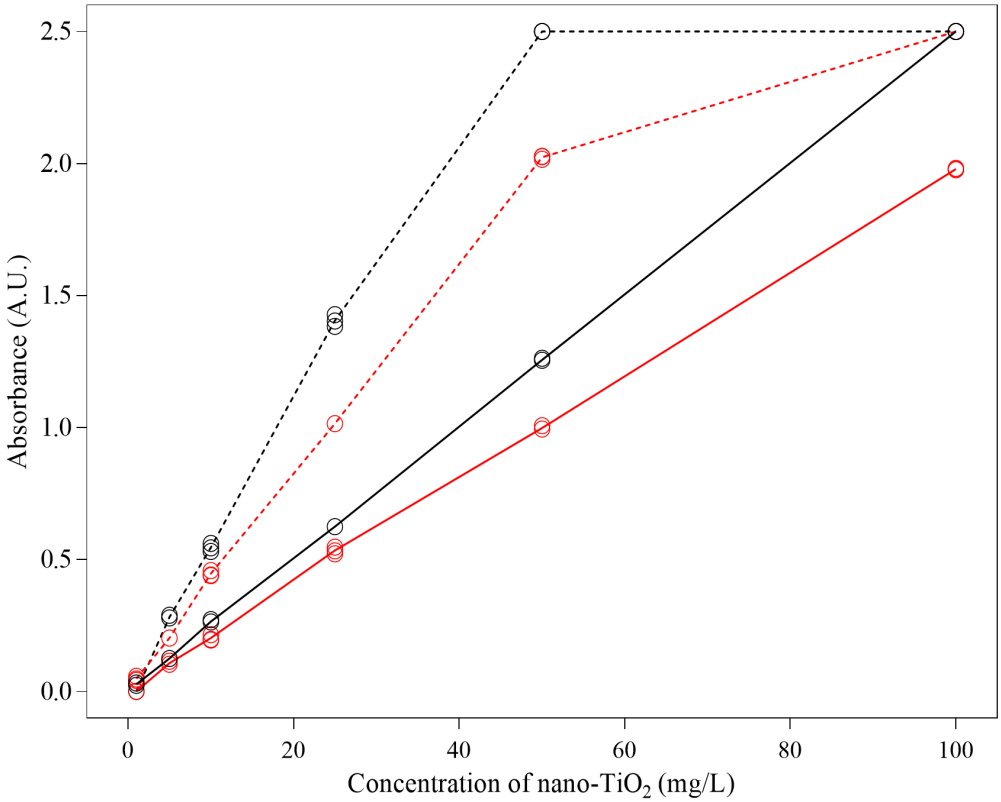

Figure 2.11 The relationship between suspension absorbance at 330 nm (dashed lines) or 421 nm (solid lines) with the concentration of nano-TiO_2, when nano-TiO_2 was dispersed in the Milli-Q water (black lines) or AEW 8-30 (red lines).

2.4.3 The impact of salinity and pH on the sedimentation of nano-TiO_2

It was hypothesized that the sedimentation rate of nano-TiO_2 in the water would be positively related to increasing salinity. At pH of 5, the sedimentation rate of nano-TiO_2 in the water was not affected by water salinity within the range of 0 – 35 ‰, in contrary to the hypothesis. At pH of 6 – 9, the sedimentation of nano-TiO_2 in the freshwater samples (salinity = 0) was much slower than that in the saline samples (salinity = 10 – 35 ‰), but the sedimentation rates in the saline samples were not different, which was partly in accordance with the hypothesis.

At pH of 6 – 9, the differences in the sedimentation rate of nano-TiO_2 in the freshwater samples and saline samples was likely to be linked with the differences in the size of particle aggregates. Take samples at pH of 8 for an example, in the freshwater sample AEW 8-0, the immediate nano-TiO_2 aggregates were around 325

nm and remained unchanged for 24 h; in the seawater sample AEW 8-30, the immediate nano-TiO_2 aggregates were 1130 nm, which was 3.5 times larger than the size of particle aggregates in the freshwater sample AEW 8-0. The size of aggregates in seawater even increased to 1793 ± 260 nm after 4 h, which was 5.5 times larger than the size of aggregates in the freshwater sample AEW 8-0. The aggregation tendency of NPs has been reported to increase as ionic strength increases, due to reduced size of the electrostatic double layer and reduced repulsive forces (Hotze et al. 2010). In the present investigation, the sedimentation rate of nano-TiO_2 was not further accelerated by the increase of salinity within the range of 10 to 35 ‰. It is possible that the size of electrostatic double layer and the repulsive forces between nano-TiO_2 was reduced to a minimum level at salinity of 10 ‰, and thus any further increases in the salinity showed no impact on the particle aggregation behavior. Wang et al. (2014a) reported that the size of nano-TiO_2 (P25) aggregates in the water with salinity of 1 ‰ was not significantly different from that in the water with salinity of 30 ‰, suggesting that the ionic strength at salinity as low as 1 ‰ could be high enough to maximize the aggregation tendency of nano-TiO_2.

The similar sedimentation rate of nano-TiO_2 between the AEW 5-0 and other saline samples may be linked to the high aggregation tendency of nano-TiO_2 at pH of 5. Ottofuelling et al. (2011) reported that the pH_{PZC} for nano-TiO_2 (P25) was 5 in Milli-Q water, confirming that nano-TiO_2 (P25) has a higher aggregation tendency at pH of 5, compared to other pH values, when water salinity was zero.

It was hypothesized that the impact of pH on the sedimentation of nano-TiO_2 would be influenced by the salinity level. In the present study, at salinity of 0, the impact of pH on the sedimentation rate was obvious, with an order of 5 > 8 > 6 > 9 > 7; at salinity ≥ 10 ‰, the impact of pH on the sedimentation rate was not evident, in accordance to the hypothesis.

It was surprising to find that although the sedimentation rate of nano-TiO_2 in the AEW 8-0 was 2.2 times higher than the sedimentation rate in the AEW 7-0 (pH = 7, salinity = 0) (Figure 2.8), the hydrodynamic size of particle aggregates in the AEW 8-0 and AEW 7-0 was not significantly different within 24 h (Table 2.4). Nevertheless, the zeta-potential value of nano-TiO_2 in the AEW 7-0 (-34.37 ± 0.09 mV) was found to be more negative than that in the AEW 8-0 (-32.97 ± 0.82 mV), which matched the observation that nano-TiO_2

was more stable in AEW 7-0 compared to AEW 8-0; it was reported that higher absolute zeta-potential value indicates higher stability (Kitahara 1973; Cosgrove 2010; Larsson et al. 2012). These results indicated that z-average size may not provide a good indication of the sedimentation behavior of NPs, though it provides useful information regarding the extent of particle aggregation.

In the saline samples, the impact of pH on the sedimentation rate of nano-TiO_2 was not evident. This was possibly due to the overwhelming impact of salinity (ionic strength) on particle aggregation tendency, compared to the impact of pH. A similar result was reported by Ottofuelling et al. (2011), who found that the influence of pH on the sedimentation of nano-TiO_2 was significant when the NaCl concentration was below 5 mM (equals to a salinity of 3 ‰) but disappeared at salinities higher than 3 ‰.

In summary, the results from the present investigation suggested that rapid aggregation and sedimentation of nano-TiO_2 was likely to occur once the nano-TiO_2 was in contact with saline water, at the upper parts of the estuaries, posing a greater threat to benthic organisms inhabiting estuaries. Once the nano-TiO_2 is in the estuary, aggregation and sedimentation may not be affected by water salinity or pH.

2.4.4 The impact of particle concentration on the sedimentation of nano-TiO_2 in seawater

It was hypothesized that the sedimentation rate of nano-TiO_2 would be positively related to the initial particle concentration. In the present study, the calculated first-order sedimentation constant (k) was positively correlated with initial particle concentration ($R^2 = 0.9975$, $p < 0.001$), suggesting a greater sedimentation rate of nano-TiO_2 in the AEW 8-30 (pH = 8, salinity = 30 ‰) with a higher initial particle concentration, which was consistent with the hypothesis.

The positive relationship between particle concentration and the sedimentation rate has been reported in previous studies with seawater samples at relatively high particle concentrations (≥10 mg/L) (Table 2.7). However, as shown in Table 2.7, when the concentration of nano-TiO_2 was relatively low (≤ 10mg/L), the impact of particle concentration on the sedimentation rate in seawater became less obvious (Brunelli et al. 2013). In the present study, the zeta-potential of nano-TiO_2 (P25) in the AEW 8 -30 (1.56 mV) was close to

zero, indicating a high tendency of particle-particle attachment. An increase in particle concentration would increase the possibility of particle collision (Taboada-Serrano et al. 2005; Allouni et al. 2009). As a result, NPs at higher concentrations are more likely to form larger aggregates, and therefore higher sedimentation rates would be expected. At concentrations of 10 mg/L or lower, the increase of particle numbers may not be high enough to induce a marked change in the particle-particle interaction. As a result, the increase of initial particle concentration on the sedimentation rate may become less obvious (Table 2.7).

However, in the freshwater samples, the impact of particle concentration on the sedimentation rate was not notable (Table 2.7). In the AEW 8-0 (freshwater sample), the zeta-potential of nano-TiO_2 (-32.97 mV) was far away from zero, indicating high repulsion between particles (Kitahara 1973; Cosgrove 2010; Larsson et al. 2012). Under this circumstance, the increased possibility of particle collision may not change the particle attachment efficiency. Therefore, the increase of particle concentration may have limited impact on the particle aggregation, and consequently does not have a notable impact on the particle sedimentation rate.

Table 2.7 Remaining percentage of nano-TiO_2 suspended in various solutions after 5 h with different initial concentration. Studies with seawater samples are shown first, followed by studies with freshwater samples.

Dispersing solution		**Primary particle size (nm)[a]**	**Initial particle concentration (mg/L)**	**Remaining percentage**	**Reference**
Salinity (‰)	**pH**				
30	8	24.4 ± 1.4	10	78%	The present study
			50	32%	
			100	12%	
> 0	6.9 – 7.4	15 – 350	30	42%	Allouni et al. (2009)
			50	35%	
			100	25%	
			500	10%	
32	7.99	27 ± 4	10	75%	Keller et al. (2010)
			50	33%	
			100	15%	
			200	10%	
3.89	8	21	10	80%	Sillanpää et al. (2011)
			100	20%	
5.55	8.1	21	10	80%	
			100	18%	
32	8.14	21	0.01	89%	Brunelli et al. (2013)

			0.1	82%	
			1	68%	
			10	79%	
33	8.10	21	0.01	86%	
			0.1	81%	
			1	85%	
			10	84%	
35	8.08	21	0.01	86%	
			0.1	85%	
			1	81%	
			10	83%	
35	8.17	21	0.01	89%	
			0.1	89%	
			1	79%	
			10	65%	
Freshwater	5.0	21	10	100%	Sillanpää et al. (2011)
			100	99%	
	8.14	21	0.01	95%	Brunelli et al. (2013)
			0.1	81%	
			1	89%	
			10	91%	
	8.06	21	0.01	81%	Brunelli et al. (2013)
			0.1	83%	
			1	81%	
			10	87%	
	8.38	27 ± 4	10	99%	Keller et al. (2010)
			50	98%	
			100	98%	
			200	98%	

a) Results are shown as mean value, or mean ± standard deviation, or the size range

In summary, the results from the present investigation, suggested that the released nano-TiO_2 would stay stable for a relative long time in the water column if located in a freshwater environment, regardless of variation in the particle concentration. However, once entering the saline environment, nano-TiO_2 may rapidly settle out of the water column, with the setting rate positively related to the particle concentration.

2.4.5 **Limitations and suggestions**

Water salinity is an important factor affecting the stability of nano-TiO_2. In the present study, the difference in the sedimentation rate of nano-TiO_2 was noticed between freshwater samples and saline water samples.

However, no differences were detected between saline water samples with salinity varied from 10 ‰ to 35 ‰, possibility due to the saturation effect as 10 ‰ was relatively high. It would be interesting to investigate how salinity affect the sedimentation of nano-TiO_2 with salinity level of 1 – 10 ‰, which could provide further information for a better understanding of the fate of nano-TiO_2 in the upper estuarine regions.

Due to the detection limit through absorbance measurements with a spectrophotometer (close to 1 mg/L), the sedimentation of nano-TiO_2 at concentration lower than 1 mg/L was not measured in the present study and were not measured in many previous studies. It is noted the concentration of nano-TiO_2 in the water column in the UK has been predicted to be 0.25 – 24.5 µg/L (Boxall et al. 2007; Johnson et al. 2011; Neal et al. 2011). Some studies have measured the release of nano-TiO_2 from sunscreens during bathing activities (< 5 µg Ti/L, Gondikas et al. 2014), from paints, textiles during washing process (< 600 µg TiO_2/L, Kaegi et al. 2008), and after wastewater treatment (<15 µg Ti/L, Kiser et al. 2009; 27 – 43 µg Ti/L, Shi et al. 2016). None of those concentrations had exceeded 1 mg/L. Brunelli et al. (2013) detected the presence of nano-TiO_2 by a scattering measurement using nephelometry. They reported that there is negligible impact of particle concentration on the sedimentation of nano-TiO_2 at concentrations lower than 1 mg/L. To my knowledge, the study conducted by Brunelli et al. (2013) was the only investigation which measured the behavior of nano-TiO_2 at particle concentrations below 1 mg/L. Therefore, further investigations are needed to explore the behavior of nano-TiO_2 under low concentrations of NPs, to justify whether the impact of water property and particle concentration remains effective.

2.5 **Conclusion**

- The aggregation of nano-TiO_2 in the water occurred within minutes. It can be assumed that the majority of nano-TiO_2 would unlikely stay in the aquatic environment in the nanoform.
- The sedimentation of 100 mg/L nano-TiO_2 in the saline samples (salinity ≥ 10 ‰) was 40 times higher than that in the freshwater samples, likely due to large difference in the size of particle aggregates. The rapid sedimentation of nano-TiO_2 is anticipated to occur once nano-TiO_2 enters an estuary and the freshwater mixes with saline at the upper parts of estuaries.
- The pH value had a distinct impact on the sedimentation rate of nano-TiO_2 in the freshwater environment. However, there was no clear relationship found between the sedimentation rate of

nano-TiO_2 and the pH value of the water.

- The impact of salinity (10 – 35 ‰) and pH did not affect the sedimentation rate of nano-TiO_2 when particles were placed in the saline water. An increase in particle concentration accelerated the sedimentation of nano-TiO_2 in saline water. The concentrations of nano-TiO_2 with initial concentrations higher than 10 mg/L could drop to below 1 mg/L within 24 h.
- These results implied that nano-TiO_2 was very likely to settle out of the water column rapidly in the estuaries, making estuaries a potential sink for nano-TiO_2 and posing a greater threat to benthic organisms inhabiting in this environment, compared to species found in freshwater benthic assemblages.

Chapter 3 Critical evaluation of the methods for measuring growth parameters of three estuarine benthic diatom isolates in the presence of nano-TiO_2

3.1 Introduction

3.1.1 Quantification of the impact of a substance on algal growth

The impact of a chemical or substance on algae is generally assessed by a growth inhibition test, which measures the changes of biomass in algal cultures after exposure to the substance at various concentrations. The most widely adopted protocol is the guideline recommended by Organization for Economic Cooperation and Development (OECD) in the Guidelines for the Testing of Chemicals, Test No. 201: Alga, Growth Inhibition Test (OECD 1984, 2011). The impact of the test substance is indicated by the difference in the growth rate or growth yield between the control group (without the test substance) and the treatment group (with the presence of the test substance). The growth rate (μ, day^{-1}), the more commonly used endpoint, is defined as the rate of the logarithmic increase of biomass, which can be calculated according to equation 3.1; growth yield (Y) is defined as the increase of biomass, which can be calculated according to equation 3.2 (OECD 2011).

$$\mu_{i-j}\ (\mathrm{day}^{-1}) = \frac{\ln C_j - \ln C_i}{t_i - t_i} \qquad \text{(eq 3.1)}$$

$$Y_{i-j} = C_j - C_i \qquad \text{(eq 3.2)}$$

where $\mu_{i\text{-}j}$ is the average growth rate from time i to time j, C_i and C_j is the biomass at time i and time j, t_i and t_j is the time i (day) and time j (day), $Y_{i\text{-}j}$ is the growth yield from time i to time j.

According to equations 3.1 and 3.2, quantification of the changes in algal biomass is the basis for determining the algal growth rate and biomass yield and therefore the impact of a substance. The most commonly used endpoints for estimating biomass include cell density (e.g. Stauber and Florence 1987; Huang et al. 1993;

Lam et al. 1999; Franklin et al. 2000; Moreno-Garrido et al. 2000; Araújo et al. 2010a; Liu et al. 2014b; Samadani et al. 2018), chlorophyll *a* content (e.g. Abou-Waly et al. 1991; El Jay 1996; Mayer et al. 1997; Tang et al. 1997; Shehata et al. 1999; Urrestarazu Ramos et al. 1999; Ball et al. 2001; Baun et al. 2002; Munkegaard et al. 2008; Sinang et al. 2019) and *in vivo* fluorescence (e.g. Blaylock et al. 1985; Miao et al. 2005; Cedergreen et al. 2007; Araújo et al. 2010a; Nagai et al. 2013).

Cell density (cell counts per unit volume, or per unit surface area), which is based on cell counts, provides a direct estimation of the biomass. Cell enumeration is normally done by manual counting under light microscopy. Alternatively, chlorophyll *a* content provides an indirect estimation of algal biomass. It is based on the assumption that the chlorophyll *a* content in each algal cell is constant (Tunzi et al. 1974). Chlorophyll *a* content is normally determined by extracting chlorophyll *a* in a solvent (e.g. ethanol, methanol, acetone) and then measuring the chlorophyll extract by spectrophotometry or fluorimetry (Sartory 1982; Mayer et al. 1997). Several spectrophotometric analyses have been proposed, based on the absorption value of chlorophyll pigment extracts at several wavelengths such as 629 nm, 647 nm, 665 nm and 750 nm (Lorenzen 1967; Marker 1972; Nusch 1980; Sartory 1982; Lichtenthaler and Buschmann 2001; Ritchie 2006; Ritchie 2008). Fluorometric analysis is generally based on the red/far-red fluorescence produced by chlorophyll *a* at around 670 nm (Yentsch and Menzel 1963; Holm-Hansen et al. 1965; Mayer et al. 1997). Relatively, chlorophyll *a* content determination is less labour-intensive compared to cell density determination.

In vivo fluorescence, which measures the autofluorescence of chlorophyll pigments, also offers an indirect estimation of algal biomass (Lorenzen 1966; Mayer et al. 1997). It is based on the assumption that *in vivo* fluorescence is highly correlated with chlorophyll *a* content (Tunzi et al. 1974). Considering the relationship between chlorophyll *a* content and cell density, the *in vivo* fluorescence method provides a good indication of the cell density. Once the relationship between *in vivo* fluorescence and cell density is established, *in vivo* fluorescence measurement could provide an easy and quick measure of biomass.

3.1.2 Quantification of the impact of nano-TiO_2 on algal growth

The growth inhibition test has been widely applied to address the impact of nano-TiO_2 on algae, with biomass determined by cell density measurements (e.g. Warheit et al. 2007; Wang et al. 2008; Miller et al. 2010;

Metzler et al. 2011; Chen et al. 2012; Lin et al. 2012; Yang et al. 2012; Dalai et al. 2013; Li et al. 2015; Manzo et al. 2015; Xia et al. 2015; Roy et al. 2016; Wang et al. 2016b; Deng et al. 2017; Iswarya et al. 2017; Minetto et al. 2017; Sendra et al. 2017a; Zhang et al. 2017; Gao et al. 2018; Middepogu et al. 2018), chlorophyll *a* measurements (e.g. Aruoja et al. 2009; Gong et al. 2011; Sadiq et al. 2011; Dash et al. 2012; Lee and An 2013) or *in vivo* fluorescence measurements (e.g. Hund-Rinke and Simon 2006; Wei et al. 2010; Cardinale et al. 2012; Kulacki and Cardinale 2012; Miller et al. 2012; Clement et al. 2013; Nicolas et al. 2016; Hu et al. 2017).

Nano-TiO_2 tend to aggregate in culture media and the size of aggregates may range from hundreds of nanometers to tens of micrometers (Aruoja et al. 2009; Keller et al. 2010; Sadiq et al. 2011; Sillanpää et al. 2011; Chen et al. 2012; Hartmann et al. 2013; Wang et al. 2016b; Deng et al. 2017). Due to the insolubility property and the aggregation tendency, the interference of nano-TiO_2 on the microscopic, spectrometric and fluorometric measurements has been noted (Aruoja et al. 2009; Metzler et al. 2011; Hartmann et al. 2013; Horst et al. 2013; Ong et al. 2014; Petersen et al. 2014), raising concerns of obtaining reliable biomass determinations in the presence of nano-TiO_2.

Usually, cell density determinations are based on microscopic measurements. The interference of nano-TiO_2 on the microscopic measurement mainly comes from the difficulties in cell visualization due to the obscuring effect of large particles (Hartmann et al. 2013), which is likely to cause an underestimation of the biomass. The homoaggregation of nano-TiO_2 (the aggregation between TiO_2 particles only) may lead to the formation of aggregates up to 10 μm (Keller et al. 2010; Sillanpää et al. 2011; Wang et al. 2016b), which might not have a notable interference on the microscopic measurement as many species might not be fully obscured by those aggregates. However, the heteroaggregation between nano-TiO_2 and cells may induce the formation of clumps up to hundreds of micrometers (Aruoja et al. 2009; Ji et al. 2011; Metzler et al. 2011; Sadiq et al. 2011; Ockenden 2019), which may severely interfere with cell visualization using light microscopy. The heteroaggregation depends on a number of factors including the properties of the culture medium (e.g. pH, salinity, organic matter), the characteristics of the particles (e.g. size, morphology, concentration), the property of the cells (e.g. clumping tendency, ability to produce extracellular polymeric substances (EPS)) and the interaction between particles and the cells, which can change with time. The EPS secreted by the

algae has been reported to play a predominant role in promoting the heteroaggregation of NPs due to the binding effect (Hartmann et al. 2010; Gao et al. 2018). Because the ability to produce EPS is species-specific, heteroaggregation is hypothesized to be species-specific. Therefore, the interference of nano-TiO_2 on the cell density measurement may vary across species.

Chlorophyll *a* content determinations are based on spectrophotometric or fluorometric measurements of chlorophyll extracts. *In vivo* fluorescence determination is a fluorometric measurement. The interference of nano-TiO_2 on the spectrophotometric measurements could come from the intrinsic absorbance of nano-TiO_2, which may increase the absorption value (Horst et al. 2013). Interference may occur with fluorometric measurements because the presence of particles may block the light received by algal cells and/or block the light emitted from the algal cells, due to the intrinsic light absorbance and scattering property of the particles (Farkas and Booth 2017), resulting in a reduced fluorescence intensity. The interference of nano-TiO_2 on the fluorometric measurements may also come from the intrinsic fluorescence of nano-TiO_2 (Hartmann et al. 2013; Horst et al. 2013). Therefore, the presence of nano-TiO_2 may interfere with methods based on spectrophotometric and fluorometric measurements.

In summary, it is evident from the literature, that the presence of nano-TiO_2 in the algal culture may compromise biomass measurements and any possible interference must be considered when investigating the impact of nano-TiO_2 on any previously untested algal species. To the best of my knowledge, there has been no reported measurements carried out to test impacts of NPs on estuarine benthic diatoms. Therefore, it is important to evaluate whether the presence of nano-TiO_2 would interfere with the biomass measurements or not, before conducting experiments to investigate the impact of nano-TiO_2 on the estuarine benthic diatoms.

In this chapter, the potential interference of nano-TiO_2 on three commonly used biomass determination methods, including cell enumeration using light microscopy, chlorophyll *a* content measurement using spectrophotometry and *in vivo* fluorescence measurement, were evaluated with selected species of estuarine benthic diatoms used for experiments in this thesis.

3.2 Materials and Methods

3.2.1 Estuarine benthic diatom cultures

3.2.1.1 Single cell isolation

Diatom cells were isolated from a natural assemblage in the surface sediment sampled in Sep 2014, from Portishead, Severn Estuary in the United Kingdom (51°29'34"N, 2°46'26"W). The surface sediment was transferred into a sterile petri dish together with some estuarine water to keep the sediment moist. Samples were brought back to the laboratory within 2 hours and kept in the growth room (18 ^{0}C, photosynthetically active radiation (PAR) = 80 µmol m^{-2} s^{-1}, cool white fluorescent, F58W/840, T8 Luxline® Plus, Sylvania, Hungary). The diatom assemblage was isolated from the sediment using the lens-tissue technique (Eaton and Moss 1966) and single cells were isolated with micropipettes to obtain isolates of cells (Andersen 2005). To make sure only one cell was isolated each time, the isolated materials were transferred to a clean glass slide and carefully examined under an inverted light microscopy (Olympus IM, Japan). Once the presence of only one cell was confirmed, the cell was transferred into a 12-well microplate well containing 3 mL of sterile f/2 medium. The f/2 medium was made according to the procedures stated in section 2.2.3.1, with salinity being 30 ‰ and pH being 8.0.

3.2.1.2 Clonal pre-cultivation

The isolated single cells were incubated statically with a light-dark cycle of 14 h-light (PAR = 80 µmol m^{-2} s^{-1}, fluorescence lighting) and 10 h-dark in a constant temperature (18 ± 1 ^{0}C) growth room (Reftech Climate Room). After 3 – 4 weeks, the clonal culture was sub-cultured into petri dishes (vented, 35 mm in diameter, polystyrene, Corning®). Only the cultures deemed to be free of bacteria (by confirming the absence of bacteria through streak plating on 1% agar plate made of f/2 medium) were sub-cultured and identified for further investigation.

3.2.1.3 Species identification

Light microscopy (LM) images of the cell and the scanning electron microscopy (SEM) images of the frustule were obtained for species identification. The LM images were captured by examining live cells

under Leica DM LB2 microscope (Leica Microsystems, Wetzlar, Germany) at magnification of × 400 or × 1000. The SEM images were captured by examining cleaned diatom frustules under Sigma HD VP Field Emission scanning electron microscope (FESEM), at 5 KV with SE2 sensor under standard (30 μm) aperture. The diatom cells were cleaned with saturated potassium permanganate solution and concentrated HCl (Underwood and Yallop 1994). The diluted subsample of cleaned diatom frustules was deposited onto a cover glass (12 mm in diameter, cleaned with ethanol) and allowed to dry under atmospheric condition. The cover glass was then mounted onto a stub with carbon tape. To avoid accumulation of static electric charges, samples were sputter coated with gold for 20 seconds before being examined by the SEM.

Three clones belonged to three different species commonly presented in estuarine mudflat ecosystem were selected as representatives of estuarine benthic diatoms for the investigation in the present study. The identified species were *Navicula gregaria* Donkin (16 μm in length, identified by Professor Marian Yallop); *Nitzschia* cf. *clausii* Hantzsch (35 μm in length, identified by Professor David Mann); *Cylindrotheca closterium* (Ehrenberg) Reimann & J. C. Lewin (60 μm in length, identified by Professor Marian Yallop) (Figure 3.1).

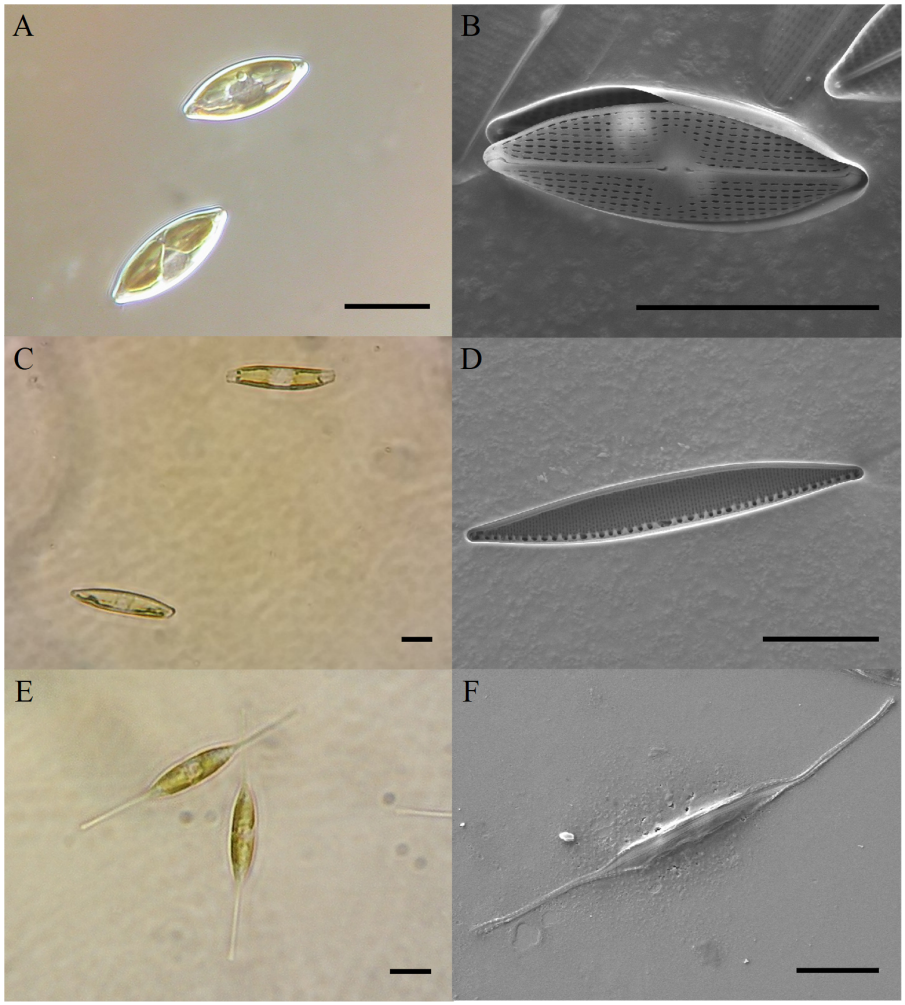

Figure 3.1 (A, C, E) Light microscopy images and (B, D, F) scanning electron microscopy images of three estuarine benthic diatom clones isolated from the Severn Estuary. (A, B) *Navicula gregaria*, (C, D) *Nitzschia* cf. *clausii*, (E, F) *Cylindrotheca closterium*. Scale bar = 10 µm.

3.2.1.4 Daily maintenance

Cultures were grown in petri dishes (vented, 35 mm in diameter, polystyrene, Corning®), using a static condition which was best suited for these estuarine benthic species. The cultures were sub-cultured every 3-4 days with fresh f/2 medium to assure cells were in exponentially growth phase according to the growth curves in Figure 3.2. Unless otherwise stated, the diatom cultures were grown at 18 ± 1 ^{0}C with a light-dark cycle of 14 h-light (PAR = 80 µmol m^{-2} s^{-1}, fluorescence lighting) and 10 h-dark in a constant growth room (Reftech Climate Room).

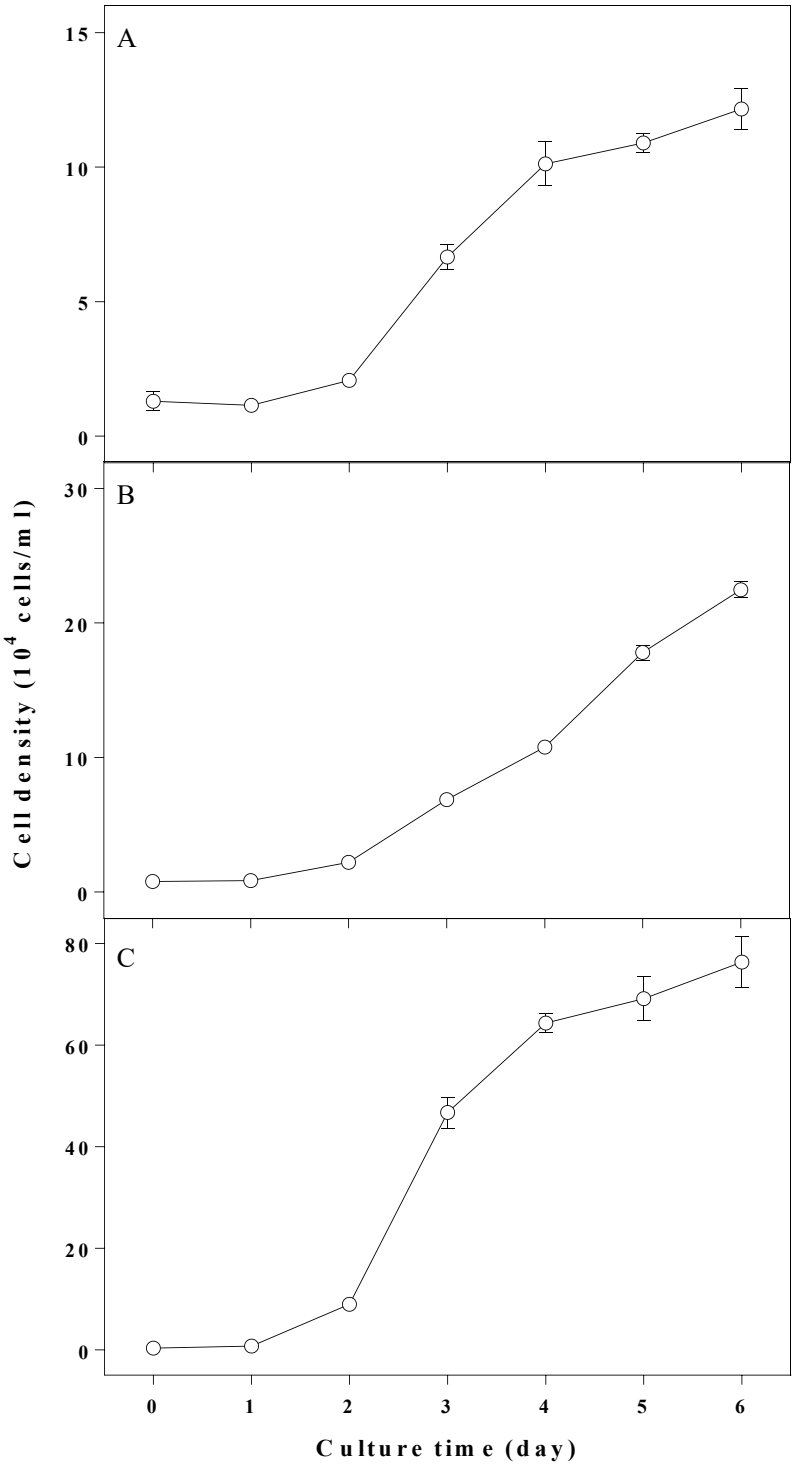

Figure 3.2 Growth curve of (A) *Navicula* gregaria, (B) *Nitzschia* cf. *clausii*, (C) *Cylindrotheca closterium*. over a 6-day period. The values represent the means ± 1 standard deviation. N = 3.

3.2.2 **Test nanoparticles**

Nano-TiO_2 (Aeroxide® P25, product no.718467) was purchased from Sigma-Aldrich. The particle powder

had a size of 24.4 ± 1.4 nm (geomean ± standard deviation) and a surface area of 44.83 ± 0.93 m^2/g (mean ± standard deviation) and consisted of 85.8% anatase and 14.2% rutile (see section 2.2.1 in Chapter 2 for the details of the measurements). A stock of nano-TiO_2 (10g/L) was prepared with Milli-Q water immediately before experiments began. The nano-TiO_2 stocks were ultrasonicated for 15 min in a water bath (110W, 40 kHz) before dispersing into fresh f/2 medium to achieve a final concentration of 100 mg/L. The particle suspension was exposed to cells within 10 minutes of preparation.

3.2.3 Could cell enumeration using light microscopy provide reliable results for quantification of algal biomass in estuarine benthic diatoms in the presence of nano-TiO_2?

3.2.3.1 Does the presence of nano-TiO_2 interfere with cell enumeration using light microscopy?

Considering the importance of EPS in promoting the heteroaggregation between particles and cells, the size of particle-cell aggregates is likely to increase as the production of EPS increases over time. Therefore, the interference of nano-TiO_2 on cell density measurement was investigated after the maximum exposure time, to maximize the potential interference. The maximum exposure time refers to the period adopted for the growth inhibition test, which was 72 h in the present investigation.

Algal cultures at the exponential stage were harvested and centrifuged at 2000 rpm (805 *g*, Eppendorf centrifuge 5810 R, Germany) for 5 min to remove the old medium. The cell pellet was resuspended in the f/2 medium containing 100 mg/L nano-TiO_2. Six replicates were prepared for each species, and each replicate contained 4.5 mL algal culture and occupied a well in the 12-well microplate (polystyrene, growth area of 3.8 cm^2/well). The initial biomass in the algal sample was set to $1 – 2 \times 10^4$ cells/ml. Microplates were incubated in static conditions at 18 ± 1 ℃ with a cycle of 14 h-light (PAR = 80 µmol m^{-2} s^{-1}, fluorescent lighting) and 10 h-dark in a growth room (Reftech Climate Room). After 72 h, cells and TiO_2 particles were harvested from the microplates and transferred into clean test tubes. The well-mixed diatom culture was loaded into a haemocytometer chamber (Mod-Fuchs Rosenthal BS748, Weber, 0.2 mm deep) and immediately examined under a fluorescence microscope (Leica DM LB2, Leica Microsystems, Germany) at a magnification of × 400. Cell enumeration was performed under bright field mode (light microscope) and

fluorescence mode (excitation light: blue, emission light: red; fluorescence microscope), respectively. Owing to the autofluorescence of chlorophyll pigments (excitation by blue light, emission of red light), the cells obscured by the large TiO_2 particles under the light microscopy could be detected by fluorescence microscopy (Aruoja et al. 2009; Sadiq et al. 2011). The interference of nano-TiO_2 was indicated by the presence of cells that only became visible in the fluorescence mode.

3.2.3.2 Is there a method to eliminate the interference of nano-TiO_2 for cell enumeration using light microscopy?

Navicula gregaria cultures were exposed to 100 mg/L nano-TiO_2 for 72 h as stated in section 3.2.3.1 (treatment group). A blank control group was setup by growing *Navicula gregaria* without nano-TiO_2. Six replicates were prepared for each group and randomly allocated to microplate wells. After 72 h of cultivation, cells and TiO_2 particles were harvested from the microplate and transferred into clean test tubes; then they were preserved in 1% Lugol's iodine solution (final concentration) and stored in the dark prior to examination.

Three methods were tested for their effectiveness in breaking the clumps of particles and cells: (a) sonication for 2 min; (b) sonication with 10 – 15 glass beads (2 mm) for 2 min; (c) sonication with 0.067 M H_2SO_4 for 2 min. Sonication was delivered through an ultrasonic water bath (110W, 40 kHz). Sonication for 2 min was applied because it was reported to be an effective and non-destructive method for dispersing benthic diatom clumps (Voltolina 1991). H_2SO_4 was tested because it was reported to be efficient for dissolving EPS, the substance facilitating the heteroaggregation of nano-TiO_2 and cells. For method (a) and (b), 0.3 mL of well-mixed subsample from the treatment group (with nano-TiO_2) was sonicated. For method (c), 0.1 mL of well-mixed subsample from the treatment group was mixed with 0.2 mL 0.1 M H_2SO_4 and was sonicated. The effectiveness of each method in breaking the particle clumps was judged by the absence of aggregates larger than the algal cells under microscopic examination. Afterwards, the influence of the effective method on cell damage was determined by measuring the cell density in the control group before and after applying the method. The cell density was obtained by manual counting under a magnification of × 400 with a light microscope (Olympus CH, Japan), after loading the well-mixed sample (before or after sonication) into a haemocytometer chamber (Mod-Fuchs Rosenthal BS748, Weber, 0.2 mm deep) and left for 2 min to allow

the settlement of cells and any particle aggregates prior to counting.

3.2.4 Could chlorophyll *a* content measurement determined using a spectrophotometer provide reliable results for quantification of algal biomass in estuarine benthic diatoms in the presence of nano-TiO_2?

To investigate whether the presence of nano-TiO_2 interfered with the chlorophyll *a* measurement, the chlorophyll *a* content in the algal culture with and without nano-TiO_2 was measured with and without the presence of nano-TiO_2. The spectrophotometric protocol recommended by Lorenzen (1967) was adopted for chlorophyll *a* measurement in the present study, which corrected for the presence of phaeopigments. The interference of nano-TiO_2 was investigated after minimum exposure time only, upon which the change of biomass in the treatment group was believed to be negligible and any difference between the treatment group (with nano-TiO_2) and the control group (without nano-TiO_2) was attributed to the interference of nano-TiO_2 only. The interference of nano-TiO_2 assessed in the present experiment was assumed to be independent of algal species, so that only one species, *Navicula gregaria*, was used to address this question.

Navicula gregaria cultures were resuspended in the fresh f/2 medium (control group) or the f/2 medium containing 100 mg/L nano-TiO_2 (treatment group) as stated in section 3.2.3.1. Six replicates were prepared for each group and each replicate contained 4 mL algal culture. Each sample was immediately centrifuged at 4000 rpm (3220 *g*) for 15 min and the pellet was extracted in 1.8 mL 100% ethanol at 4 ^{0}C for 24 h in the dark. Afterwards, the ethanol extracts were mixed and centrifuged again at 4000 rpm (3220 *g*) for 15 min to remove diatom frustules and TiO_2 particles. The absorption value of the chlorophyll extract was recorded at 665 nm and 750 nm with a spectrophotometer (Biochrom WPA Biowave II), before and after acidification with HCl (final concentration of 1×10^{-2} mol/L) (Lorenzen 1967). Pure ethanol was used as a reagent blank and 1 cm cuvette (polystyrene) was used for the measurement. The chlorophyll *a* (chl *a*) content in the algal culture was determined by equation 3.3 (Lorenzen 1967).

$$\text{chl } a \text{ (mg/L)} = \frac{k \times F \times \left(E_{665_0} - E_{665_a}\right) \times v}{l \times V} \qquad \text{(eq 3.3)}$$

where *k* (= 11.9035 µg·cm/ml, Ritchie 2006) is the absorption coefficient of chlorophyll *a* in the pure ethanol,

F (= 2.0) is the factor to equate the reduction in absorbance after acidification to the initial chlorophyll *a* concentration, E_{665_0} and E_{665_a} are adjusted absorbance values at 665 nm (turbidity-adjusted absorbance by deducting absorbance at 750 nm (A_{750}) from absorbance at 665 nm (A_{665})) before and after acidification, v (= 1.8 mL) is the volume of ethanol used for pigment extraction, l (= 1 cm) is the path length of the cuvette, V (= 4 mL) is the volume of algal culture used for pigment measurement.

The interference of nano-TiO_2 was indicated by the difference in the calculated chlorophyll *a* content between control group and the treatment group.

3.2.5 Could *in vivo* fluorescence measurement provide reliable results for quantification of algal biomass in estuarine benthic diatoms in the presence of nano-TiO_2?

3.2.5.1 Does nano-TiO_2 fluoresce under the setup for *in vivo* fluorescence measurement?

To investigate whether nano-TiO_2 fluoresce under the *in vivo* fluorescence measurement set up, the *in vivo* fluorescence of the f/2 medium containing 100 mg/L nano-TiO_2 was measured. Six replicates were prepared and each replicate containing 4.5 mL f/2 medium and occupied a well in the 12-well microplate. The f/2 medium without nano-TiO_2 was measured as blank. The *in vivo* fluorescence of each sample was measured with a plate reader (FLUOstar OPTIMA, BMG LABTECH, Germany), with excitation at 430 ± 10 nm and emission at 680 ± 10 nm (Mayer et al. 1997).

3.2.5.2 Does the presence of nano-TiO_2 interfere with *in vivo* fluorescence measurement?

To investigate whether the presence of nano-TiO_2 interfered with the *in vivo* fluorescence measurement, the *in vivo* fluorescence of the algal culture with and without nano-TiO_2 was compared. The minimum exposure time was tested only, upon which the change of biomass in the treatment group (with nano-TiO_2) was believed to be negligible and any difference between the treatment group and the control group (without nano-TiO_2) was attributed to the interference of nano-TiO_2 only. The interference of nano-TiO_2 assessed in the present experiment was assumed to be independent of algal species, so that only one species, *Navicula gregaria*, was used to address this question.

Navicula gregaria cultures were resuspended in the fresh f/2 medium (control group) or the f/2 medium containing 100 mg/L nano-TiO_2 (treatment group) as stated in section 3.2.3.1. The *in vivo* fluorescence of each sample was measured immediately as described in section 3.2.5.1. The interference of nano-TiO_2 was indicated by the difference in the fluorescence intensity between the control group and the treatment group. All assays were run in six replicates.

3.2.6 Data analysis

Tests for the statistical significance between values were performed using SPSS software (version 24.0 of SPSS for Windows). After checking the normality of the data, one-sample T test was used to compare the difference of data with zero. After checking the homogeneity of variance by Levene's test and the normality of the residuals by Kolmogorov-Smirnov test, parametric tests (e.g. independent-samples T tests, ANOVA tests) were applied to determine the difference between groups. Results were shown as mean values ± standard deviation. The significance level was set at < 0.05.

3.3 Results

3.3.1 Could cell enumeration using light microscopy provide reliable results for quantification of algal biomass in estuarine benthic diatoms in the presence of nano-TiO_2?

3.3.1.1 Does the presence of nano-TiO_2 interfere with cell enumeration under light microscopy?

Microscopy images of diatom cells and TiO_2 particles under bright field mode (light microscope) and fluorescence mode (fluorescence microscope) are shown in Figure 3.3. Despite being a white powder, TiO_2 presented black under light microscope. However, the presence of TiO_2 was not visible under fluorescence microscope. The presence of algal cells was obvious under fluorescence microscope, marked by their red chloroplasts.

As show in Figure 3.3, the size of particle aggregates and the heteroaggregation between particles and cells was species-specific. Some large particle aggregates were recorded in *Navicula gregaria* samples (Figure

3.3A) and *Cylindrotheca closterium* samples (Figure 3.3E). The size of particle aggregates was relatively small in the *Nitzschia* cf. *clausii* samples (Figure 3.3C). The heteroaggregation was recorded in the *Navicula gregaria* samples (Figure 3.3 A, B). As highlighted by the purple circles, the visualization of some *Navicula gregaria* cells under light microscopy was obscured by the presence of large particle aggregates. A low level of heteroaggregation was recorded in *Nitzschia* cf. *clausii* samples and *Cylindrotheca closterium* samples. Observations under light microscopy (control group) and fluorescence microscopy revealed that none of the *Nitzschia* cf. *clausii* cells and *Cylindrotheca closterium* cells were only visible under fluorescence microscope.

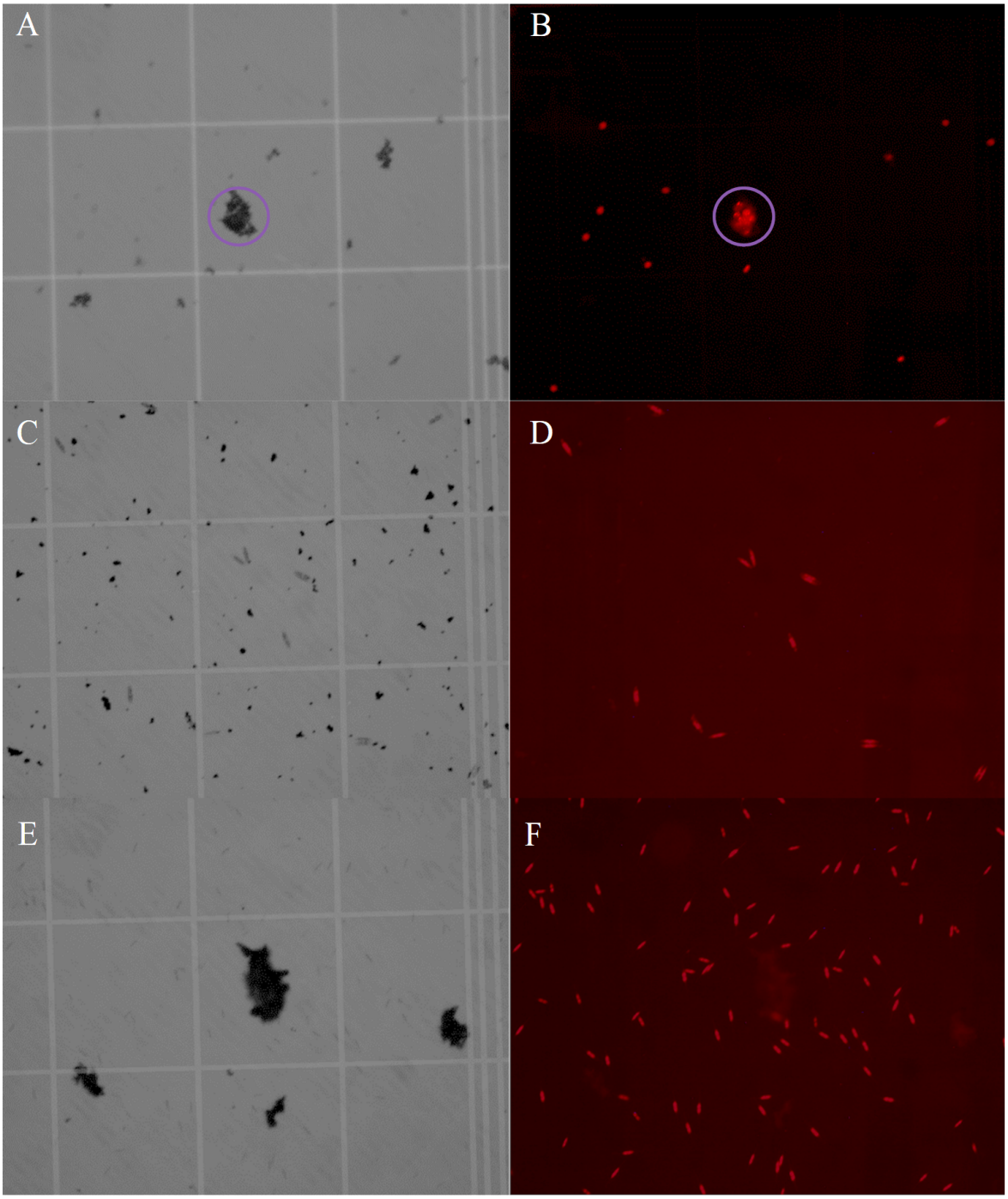

Figure 3.3 Images of diatom cells and TiO_2 aggregates in the haemocytometer counting chamber under (A, C, E) light microscopy (Control method) and (B, D, F) fluorescence microscopy (Test Method). (A, B) *Navicula gregaria*; (C, D) *Nitzschia* cf. *clausii*; (E, F) *Cylindrotheca closterium*. Purple circles highlighted the cells completely invisible under light microscopy. The width of the square on the grid is 250 µm.

3.3.1.2 Is there a method to eliminate the interference of nano-TiO_2 on the cell enumeration of *Navicula gregaria* using light microscopy?

The effectiveness of method (a) 2 min sonication and (b) 2 min sonication with glass beads in separating the heteroaggregation of particles and cells were found to be low, with the presence of particle aggregates larger than the size of *Navicula gregaria* cells, and thus cell densities after applying these methods were not obtained.

The method (c) 2 min sonication with H_2SO_4 worked effectively in breaking up larger TiO_2 aggregates into particles smaller than algal cells. The impact of application of a 2 min sonication with H_2SO_4 (method c) on the cell density in the control group (without nano-TiO_2) was found to be negligible; the difference in the cell density before and after sonication with H_2SO_4 was not significant (paired-samples T test, $t_5 = -0.002$, $p = 0.998$) (Figure 3.4). A significantly higher cell density (higher by 49%) was recorded in the treatment group (with nano-TiO_2) after sonication with H_2SO_4, compared to that obtained before sonication (paired-samples T test, $t_5 = -7.123$, $p = 0.001$). Comparably, without the sonication, the cell density in the treatment group was significantly lower (lower by 15%) than that in the control group (independent-samples T test, $t_{10} = 2.877$, $p = 0.016$); after the sonication with H_2SO_4, the cell density in the treatment group was significantly higher (higher by 30%) than that in the control group (independent-samples T test, $t_{10} = -4.082$, $p = 0.002$).

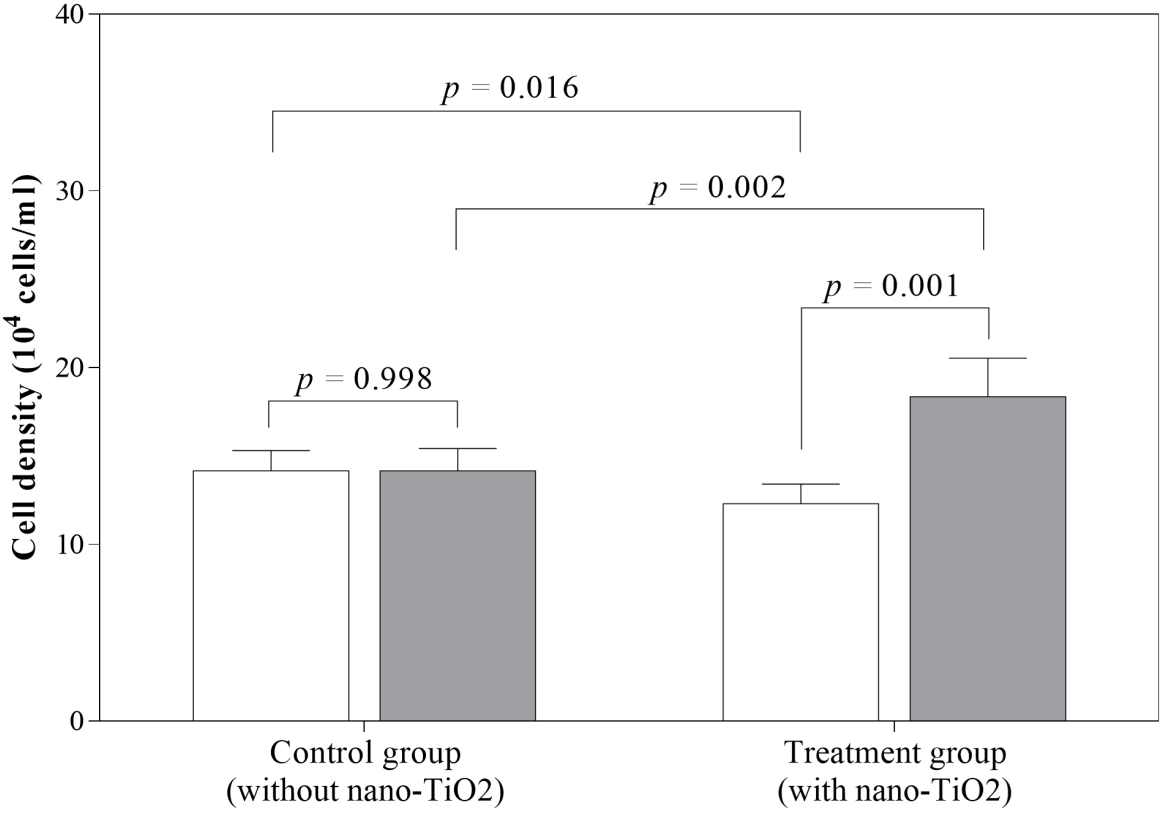

Figure 3.4 Cell density of *Navicula gregaria* cultures cultivated with and without nano-TiO_2 for 72 h. Results obtained without sonication were shown in white bars. Results obtained after sonication with H_2SO_4 were shown in grey bars. Results are shown as mean ± standard deviation (n = 6). Significance of the difference between bars were determined by independent-samples T tests (between two white bars or two grey bars) or paired-samples T tests (between white and grey bars within the same group).

3.3.2 Could chlorophyll *a* content determined using a spectrophotometer provide reliable results for quantification of algal biomass in estuarine benthic diatoms in the presence of nano-TiO_2?

As shown in Figure 3.5, the calculated chlorophyll *a* content in the treatment group (with nano-TiO_2, 0.107 mg/L) was 2% lower than that in the control group (without nano-TiO_2, 0.109 mg/L). The difference between the two groups was not significant (independent-samples T test, t_{10} = -0.415, p = 0.687).

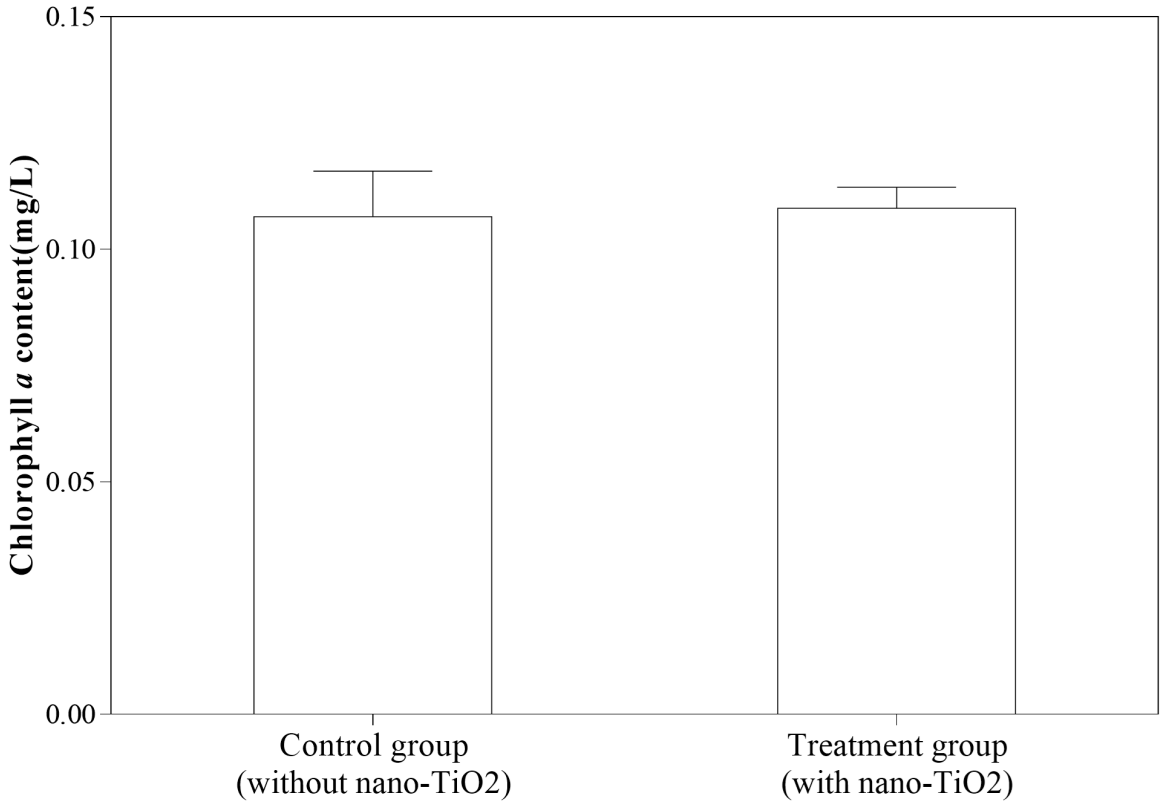

Figure 3.5 Calculated chlorophyll *a* content of *Navicula gregaria* cultures with and without the presence of nano-TiO_2. Results are shown as mean ± standard deviation (n = 6).

3.3.3 Could *in vivo* fluorescence measurement provide reliable results for quantification of algal biomass in estuarine benthic diatoms in the presence of nano-TiO_2?

3.3.3.1 Does nano-TiO_2 fluoresce under the setup for *in vivo* fluorescence measurement?

The fluorescence intensity of 100 mg/L nano-TiO_2 in the f/2 medium was found to be 0.5 ± 1.2, which was not significantly different from zero (one-sample T test, t_5 = -0.415, p = 0.235).

3.3.3.2 Does the presence of nano-TiO_2 interfere with *in vivo* fluorescence measurement?

As shown in Figure 3.6, the fluorescence from the treatment group (with nano-TiO_2, 151.6) was 10% lower than that from the control group (without nano-TiO_2, 168.0). The difference between two groups was significant (independent-samples T test, t_{10} = -6.096, p < 0.001).

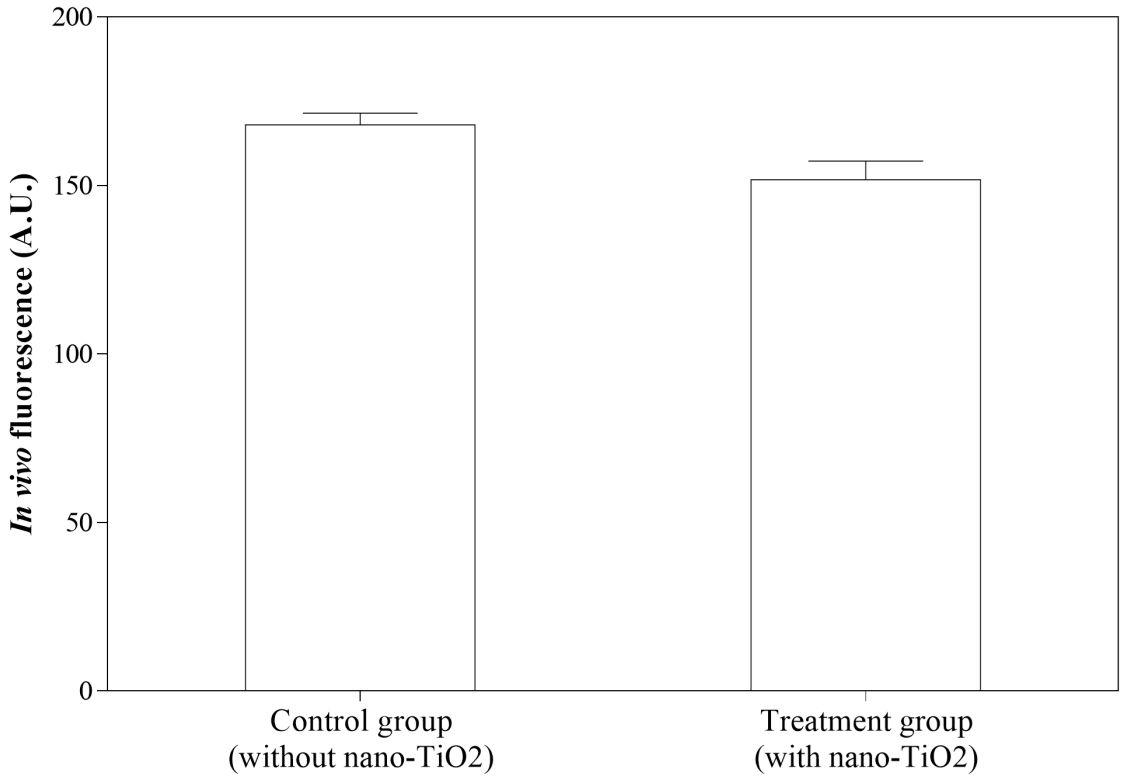

Figure 3.6 *In vivo* fluorescence intensity of *Navicula gregaria* cultures with and without the presence of nano-TiO_2. Results are shown as mean ± standard deviation (n = 6).

3.4 **Discussion**

In the present study, the interference of 100 mg/L nano-TiO_2 on three biomass determination methods were tested. The concentration of 100 mg/L, the highest concentration recommended by the OECD when conducting a growth inhibition test (OECD 2011), was selected to maximize the potential interference.

3.4.1 **Could cell enumeration using light microscopy provide reliable results for quantification of algal biomass in estuarine benthic diatoms in the presence of nano-TiO_2?**

It was hypothesized that the presence of nano-TiO_2 would interfere with cell density measurement via manual counting using light microscopy, by obscuring the visualization of cells. The interference of nano-TiO_2 was recorded on *Navicula gregaria*, which was in accordance with the hypothesis. However, the interference of nano-TiO_2 on *Nitzschia* cf. *clausii* and *Cylindrotheca closterium* was negligible, in contrast

to the hypothesis. This confirmed that the unamended cell density measurement using light microscopy could provide reliable results for *Nitzschia* cf. *clausii* and *Cylindrotheca closterium* samples grown in the presence of nano-TiO_2, but would not be a reliable method for *Navicula gregaria* samples.

The interference recorded in *Navicula gregaria* samples was found to be associated with the heteroaggregation of algal cells and NPs. As a result, several methods were trialed to reduce the heteroaggregation and to eliminate the interference. A sonication method with H_2SO_4 was found to work effectively in breaking up the clumps, without causing cell damage. This confirmed that a modified cell density measurement, with an additional sonication treatment with H_2SO_4, could provide reliable results for cell enumeration of *Navicula gregaria* cultures grown in the presence of nano-TiO_2.

3.4.2 Could chlorophyll *a* content determined using a spectrophotometer provide reliable results for quantification of algal biomass in estuarine benthic diatoms in the presence of nano-TiO_2?

It was hypothesized that the presence of nano-TiO_2 would not interfere with chlorophyll *a* measurement via spectrophotometric measurement of chlorophyll extracts. The calculated chlorophyll *a* content in the control group (without nano-TiO_2) and treatment group (with nano-TiO_2) was not significantly different, implying the absence of interference, in accordance with the hypothesis. This confirmed that the chlorophyll *a* measurement using a spectrophotometer test in the present investigation could provide reliable biomass estimates for estuarine benthic diatoms grown with the presence of nano-TiO_2.

However, some studies have revealed that the chlorophyll *a* concentration per cell increased when exposed to nano-TiO_2 (*Chlamydomonas reinhardtii*, Chen et al. 2012; *Phaeodactylum tricornutum*, Deng et al. 2017; *Chlorella pyrenoidosa*, Middepogu et al. 2018), raising the concern of whether chlorophyll *a* concentration could be a good indicator for algal biomass. Therefore, any change observed in the chlorophyll *a* concentration may be attributed to the change in the biomass, or come from the change in the cellular chlorophyll *a* concentration. As a result, the change in the chl *a* concentration may not provide reliable indication regarding the change of algal biomass, in the absence of additional measurements of cell numbers.

3.4.3 Could *in vivo* fluorescence measurements provide reliable results for quantification of algal biomass in estuarine benthic diatoms in the presence of nano-TiO_2?

It was hypothesized that the presence of nano-TiO_2 would interfere with *in vivo* fluorescence measurement. Results indicated that the background fluorescence of nano-TiO_2 was found to be negligible. However, the fluorescence of the treatment group (with nano-TiO_2) was significantly lower than that in the control group (without nano-TiO_2), implying the presence of interference, in accordance with the hypothesis. The interference was believed to be linked to the light absorbing and scattering effect of particles, which may block the light being received by algal cells and/or the light emitted from the algal cells (Farkas and Booth 2017). Because particles could not be separated from the cells, eliminating the interference of nano-TiO_2 on the *in vivo* fluorescence measurement was considered impossible. This suggested that the *in vivo* fluorescence measurement may not provide reliable results for cultures grown with the presence of nano-TiO_2.

3.4.4 Limitations and suggestions

The inference of nano-TiO_2 was found to be associated with the presence of undissolved particles in the medium. Therefore, the interference of nano-TiO_2 may be concentration-dependent. As particle concentration decreases, the inference of nano-TiO_2 may decrease and even become negligible. It is suggested that, the potential interference of nano-TiO_2 at the highest test concentration should be tested before applying any traditional methods to measure biomass.

3.5 Conclusion

In summary, the cell density measurement via cell enumeration under light microscopy and chlorophyll *a* measurement with a spectrophotometer could provide reliable results for estimating biomass for the selected estuarine benthic diatoms including *Navicula gregaria*, *Nitzschia* cf. *clausii*, and *Cylindrotheca closterium*. Considering the possible change in chlorophyll *a* concentration per cell in the presence of nano-TiO_2, cell density was selected as the preferred biomass index in subsequent investigations wherever possible. However, chlorophyll *a* concentration should be measured additionally as well, to examine whether the chlorophyll *a*

concentration per cell changes in the presence of nano-TiO_2.

Chapter 4 Investigation on the growth of three estuarine benthic diatoms exposed to nano-TiO_2 in the presence of fluorescent lighting

4.1 Introduction

The dramatically escalating increase in the production and application of NPs has raised concerns of their environmental risks, due to their extremely small size and high surface area to volume ratio, especially for the most widely used nano-TiO_2 (Boxall et al. 2007; Nowack and Bucheli 2007; Handy et al. 2008a; Handy et al. 2008b; Jain et al. 2018; Maurizi et al. 2018). Quite a few studies have been conducted to investigate the impact of nano-TiO_2 on algae. The negative impacts of nano-TiO_2 on algal growth have been widely recorded under laboratory conditions in the presence of fluorescent lighting with particle concentrations lower than 100 mg/L, the highest test concentration recommended by Organization for Economic Cooperation and Development (OECD) (OECD 2011), resulting in lower biomass yield (assessed by cell density or chlorophyll *a* content) and inhibited growth rates (e.g. Wang et al. 2008; Aruoja et al. 2009; Sadiq et al. 2011; Chen et al. 2012; Hartmann et al. 2013; Roy et al. 2016; Iswarya et al. 2017; Middepogu et al. 2018). However, most of the previous studies were carried out with planktonic species, with little focus on the benthic species, although the benthic ones are considered to be associated with higher exposure to nano-TiO_2 due to particle aggregation and sedimentation (Ferry et al. 2009; Keller et al. 2010; Wang et al. 2014a; Li et al. 2016).

Some studies have been carried out to investigate the impact of nano-TiO_2 on several marine planktonic diatom species and freshwater benthic diatom species, in laboratory conditions with lighting provided by fluorescent lights. The inhibitory effect of nano-TiO_2 on the growth of marine planktonic diatoms was reported in some investigations, with 72 h-IC50 ranging from 7 – 168 mg/L (*Phaeodactylum tricornutum*, Clement et al. 2013; Wang et al. 2016b; Deng et al. 2017; Sendra et al. 2017b; *Skeletonema costatum*, Li et al. 2015; *Nitzschia closterium*, Xia et al. 2015). In contrast, Miller et al. (2010) claimed that nano-TiO_2 in the presence of fluorescent lighting showed no impact on the growth of the marine planktonic diatom *Skeletonema costatum* and *Thalassiosira pseudonana* after 96 h of exposure, yet the highest concentration tested in their study was only 1 mg/L. The inhibitory effect of nano-TiO_2 on the growth of a freshwater

benthic diatom *Nitzschia palea* (Ockenden 2019), also using fluorescent lighting, was observed with a 72 h-IC50 being 124 mg/L. However, Joonas et al. (2019) reported that the growth of freshwater benthic diatom *Fistulifera pelliculosa* was not affected by the presence of nano-TiO_2 at concentrations up to 100 mg/L. Although it is recognized that there may be considerable variations in protocols used in different laboratories in terms of growth conditions, these varied results suggest that diatoms might show a species-specific response to the presence of nano-TiO_2. This survey reveals a knowledge gap regarding to what extent, estuarine benthic diatoms, which are believed to be associated with a high exposure of nano-TiO_2, may be affected by the presence of nano-TiO_2.

This chapter is divided into two Sections. The Section 1 focused on the impact of nano-TiO_2 on the growth of three estuarine benthic diatoms in the presence of fluorescent lighting, and the Section 2 explored the possible mechanisms that may account for the findings observed in Section 1.

Section 1: The impact of nano-TiO_2 on the growth of three estuarine benthic diatoms in the presence of fluorescent lighting

To address the knowledge gap, the impact of nano-TiO_2 on the growth of estuarine benthic diatoms isolated from the Severn Estuary was investigated under laboratory conditions. Three different species were tested to see if there was a species-specific response.

Aim 1: To investigate whether the presence of nano-TiO_2 poses a risk to the estuarine benthic diatoms, the growth of three estuarine benthic diatoms in the presence of 100 mg/L nano-TiO_2 was followed after 72 h of cultivation. The concentration of 100 mg/L was tested because it is the highest concentration suggested for testing the toxicity of a chemical by OECD (2011). The 100 mg/L is also the threshold suggested by the United Nations to distinguish toxic and non-toxic substances in "Globally harmonized system of classification and labelling of chemicals (GHS)" (United Nations 2015).

Hypothesis 1.1: Evidences from the previous studies indicate a negative impact of nano-TiO_2 on the growth of marine planktonic diatoms. It was hypothesized that the growth of estuarine benthic diatoms exposed to 100 mg/L nano-TiO_2 would be negatively affected, manifested as a lower biomass yield and a lower growth

rate after 72 h, compared to control samples (in absence of TiO_2 particles).

Hypothesis 1.2: It was hypothesized, based on the recorded responses of diatom species, that the three species tested in the present study would have varied responses to the presence of nano-TiO_2.

Aim 2: It has been reported that particle size played an importance role in determining the impact of TiO_2 on marine planktonic diatoms (Clement et al. 2013; Xia et al. 2015; Sendra et al. 2017a). For example, Sendra et al. (2017a) reported that the growth inhibition of nano-TiO_2 on *Phaeodactylum tricornutum* (72 h-IC50 = 132 mg/L) was greater than the growth inhibition of bulk-TiO_2 (72 h-IC50 = 185 mg/L). To investigate whether the impact of nano-TiO_2 on selected species of estuarine benthic diatoms was related to the particle size, the growth of estuarine benthic diatoms in the presence of 100 mg/L micro-TiO_2 (TiO_2 particles with size in the micrometer range) was measured for comparison.

Hypothesis 2.1: It was hypothesized that the growth of selected species of estuarine benthic diatoms would be less negatively affected by the presence of micro-TiO_2, compared to the presence of nano-TiO_2.

Hypothesis 2.2: It was hypothesized that different species may have varied sensitivity to particle size.

4.2 Method

4.2.1 Estuarine benthic diatoms

Three estuarine benthic diatom clones (*Nitzschia* cf. *clausii*, *Navicula gregaria*, *Cylindrotheca closterium*) isolated from the Severn Estuary, UK were tested. Information about these three clones was detailed in Section 3.2.1 in Chapter 3. Cells at exponential growth phase were harvested for experiments.

4.2.2 TiO_2 particles

Micro-TiO_2 (product no. T8141) and nano-TiO_2 (Aeroxide® P25, product no.718467) were purchased from Sigma-Aldrich. The properties of TiO_2 were measured following the methods described in section 2.2.1 in Chapter 2, including particle size (see section 2.2.1.1), surface area (see section 2.2.1.3) and crystal structure

(see section 2.2.1.4).

The elements present in the two TiO_2 particles were examined by the energy-dispersive X-ray (EDX) spectroscopy analysis, with Sigma HD VP Field Emission scanning electron microscope and its embedded SmartEDX component (∑IGMA^{TM}, Zeiss). This examination was done by Dr. Chong Liu, School of Physics, University of Bristol, UK.

The hydrodynamic diameter of TiO_2 (100 mg/L) in the f/2 medium was measured via dynamic light scattering (DLS) through a Zetasizer Nano-S90 (Malvern-ZEN-1690, Malvern Instruments) at < 10 min, 1 h, 2 h, 4 h and 24 h, following the method described in the section 2.2.4 in Chapter 2.

TiO_2 stocks were prepared with Milli-Q water immediately before experiments began. Specifically, TiO_2 powder (0.0200 g) was weight into a 5 mL sterile plastic tube in a glove box. Milli-Q water (2 mL) was added into the tube containing TiO_2 by transferring 1 mL of water each time using a 1 mL micropipette. The stocks (10 g/L) were ultra-sonicated for 15 min in a water bath (110W, 40 kHz, Bransonic CPX3800H-E ultrasonic bath, Emerson) before dispersing into f/2 medium to create particle suspensions at concentration of 100 mg/L. The particle suspensions were exposed to cells within 10 min of preparation.

4.2.3 The impact of TiO_2 particle type on the growth of estuarine benthic diatoms in the presence of fluorescent lighting

To investigate whether the presence of nano-TiO_2 affected the growth of estuarine benthic diatoms (aim 1), and to find out whether estuarine benthic diatoms responded differently to the presence of nano-TiO_2 and micro-TiO_2 (aim 2), the growth of three estuarine benthic diatom cultures grown with and without TiO_2 was followed. The impact of TiO_2 was indicated by the difference in the algal biomass yield, growth rate and chlorophyll *a* concentration per cell between the treatment group (with TiO_2) and the control group (without TiO_2).

Algal cultures were exposed to 100 mg/L nano-TiO_2 (nano-TiO_2 treatment) or 100 mg/L micro-TiO_2 (micro-TiO_2 treatment) for 72 h as stated in section 3.2.3.1. A blank control group was setup by growing cells without

nano-TiO_2. Twelve replicates were prepared for each group and randomly allocated to microplate wells. The initial biomass in the algal sample was 1.3×10^4 cells/mL for *Nitzschia* cf. *clausii* and *Cylindrotheca closterium* and was 1.7×10^4 cells/mL for *Navicula gregaria*. Microplates were incubated statically under fluorescent lighting as stated in section 3.2.3.1. After 72 h of cultivation, cells and TiO_2 particles were harvested from the microplate and transferred into 5 mL clean test tubes. After thoroughly vortex mixing the sample in the test tube for 20s, a 0.5 mL subsample was taken for cell density measurement, and the remaining 4 mL was used for chlorophyll *a* measurement.

4.2.4 Cell density measurement

The subsample for cell density measurement was preserved in Lugol's iodine solution (final concentration of 1%) and stored in the dark prior to enumeration. For cell enumeration, preserved cells were re-suspended with a vortex mixer for 30 seconds and then loaded into a haemocytometer chamber (Mod-Fuchs Rosenthal BS748, Weber, 0.2 mm deep). Issues relating to heteroaggregation observed during preliminary tests were considered (see section 3.3.1.1 in Chapter 3); for *Navicula gregaria* only, the subsamples preserved for cell density measurement were sonicated with H_2SO_4 (final concentration of 0.067 M) for 2 min in a water bath (110W, 40 KHz), before loading into a haemocytometer chamber for counting. Preliminary test indicated sonication with H_2SO_4 had negligible impact on the control cells (Section 3.3.1.2).

Cells were left to settle for 2 min and then examined under a magnification of × 400 with a light microscope (Olympus CH, Japan). Cells being transparent without a clear protoplast were considered as dead and were not counted.

The biomass yield (Y) and the average specific growth rate (μ, day^{-1}) between 0 and 72 h was calculated according to equation 4.1 and equation 4.2, respectively (OECD 2011).

$$Y = C_{72} - C_0 \qquad \text{(eq 4.1)}$$

$$\mu\ (\text{day}^{-1}) = \frac{\ln C_{72} - \ln C_0}{3} \qquad \text{(eq 4.2)}$$

where C_{72} and C_0 are the cell density (cells/ml) at time 72 h and 0 h.

4.2.5 Chlorophyll *a* content measurement

The 4 mL subsamples were centrifuged for chlorophyll *a* content measurement was stated in section 3.2.4. The chlorophyll *a* (chl *a*) content in the algal culture was determined by equation 3.3 and the chlorophyll *a* per cell was calculated by equation 4.3.

$$\text{chl a per cell (pg)} = \frac{\text{chl } a\ (\text{mg/L})}{\text{cell density (cells/ml)}} \times 10^6 \qquad \text{(eq 4.3)}$$

4.2.6 Data analysis

Tests for the statistical significance between values were performed using SPSS software (version 24.0 of SPSS for Windows). After checking the normality of the data or the residuals by Kolmogorov-Smirnov test, parametric tests (e.g. independent-samples T tests, ANOVA tests) were applied to determine the difference between groups. Results were shown as mean values ± standard deviation. The significance level was set at < 0.05.

4.3 Results

4.3.1 Characteristics of TiO_2 particles

The images of the two TiO_2 particles (nano-TiO_2 and micro-TiO_2), which are different in size, are shown in Figure 4.1.

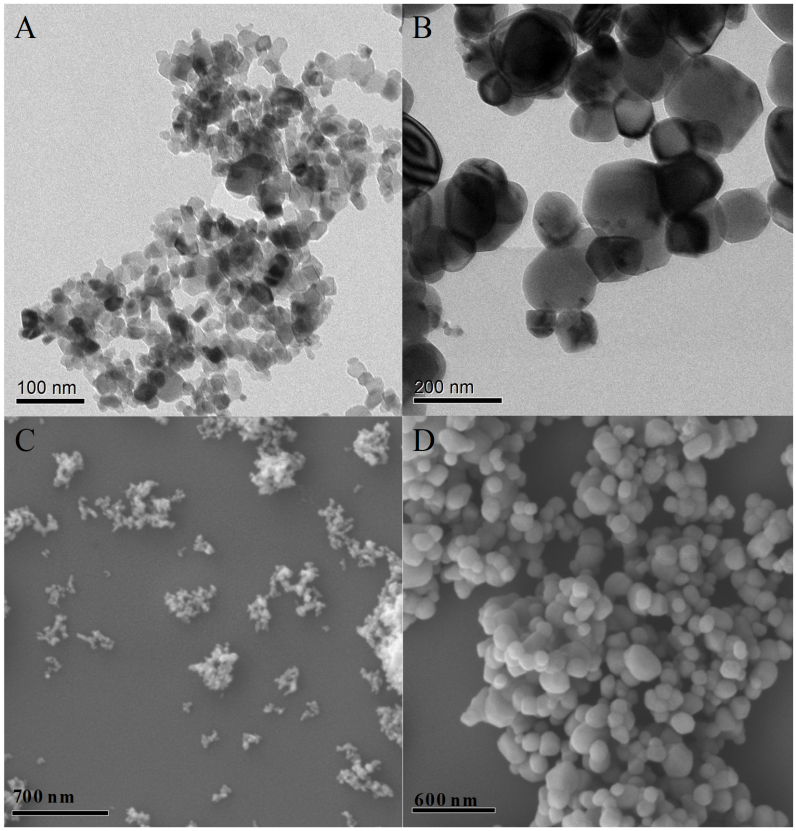

Figure 4.1 (A, B) Transmission electron microscopy (TEM) images and (C, D) scanning electron microscopy (SEM) images of (A, C) nano-TiO_2 and (B, D) micro-TiO_2. The TEM images were taken by Dr Ian Griffiths, School of Physics, University of Bristol, UK.

The characteristics of two TiO_2 particles are summarized in Table 4.2. Compared to nano-TiO_2, the micro-TiO_2 had a larger primary particle size and a smaller surface area per gram. The average primary particle size of micro-TiO_2 was 5.4 times greater than that of nano-TiO_2. The surface area per gram of nano-TiO_2 was 4.5 times greater than that of micro-TiO_2.

Table 4.1 Characteristics of the TiO_2 particles in the powder form.

	Nano-TiO_2	**Micro-TiO_2**
Primary particle size (nm)[a]	24.4 ± 1.4	131.0 ± 1.4
Surface area (m^2/g)[b]	44.83 ± 0.93	9.97 ± 0.27
Crystal structure	85.8 % anatase; 14.2 % rutile	97.8 % anatase; 2.2 % rutile
Colour	white	white

a) Results are shown as geometric mean ± standard deviation (n = 120).

b) Results are shown as arithmetic mean ± standard deviation (n = 3).

The elements present in the two TiO_2 particles were examined by energy-dispersive X-ray spectroscopy

analysis (Figure 4.2). The EDX spectra confirmed the presence of elements titanium (Ti, marked by peaks at 4.512 keV and 4.933 keV), oxygen (O, marked by peak at 0.525 keV) and chlorine (Cl, marked by peak at 2.622 keV and 2.822 keV) in the two TiO_2 particles.

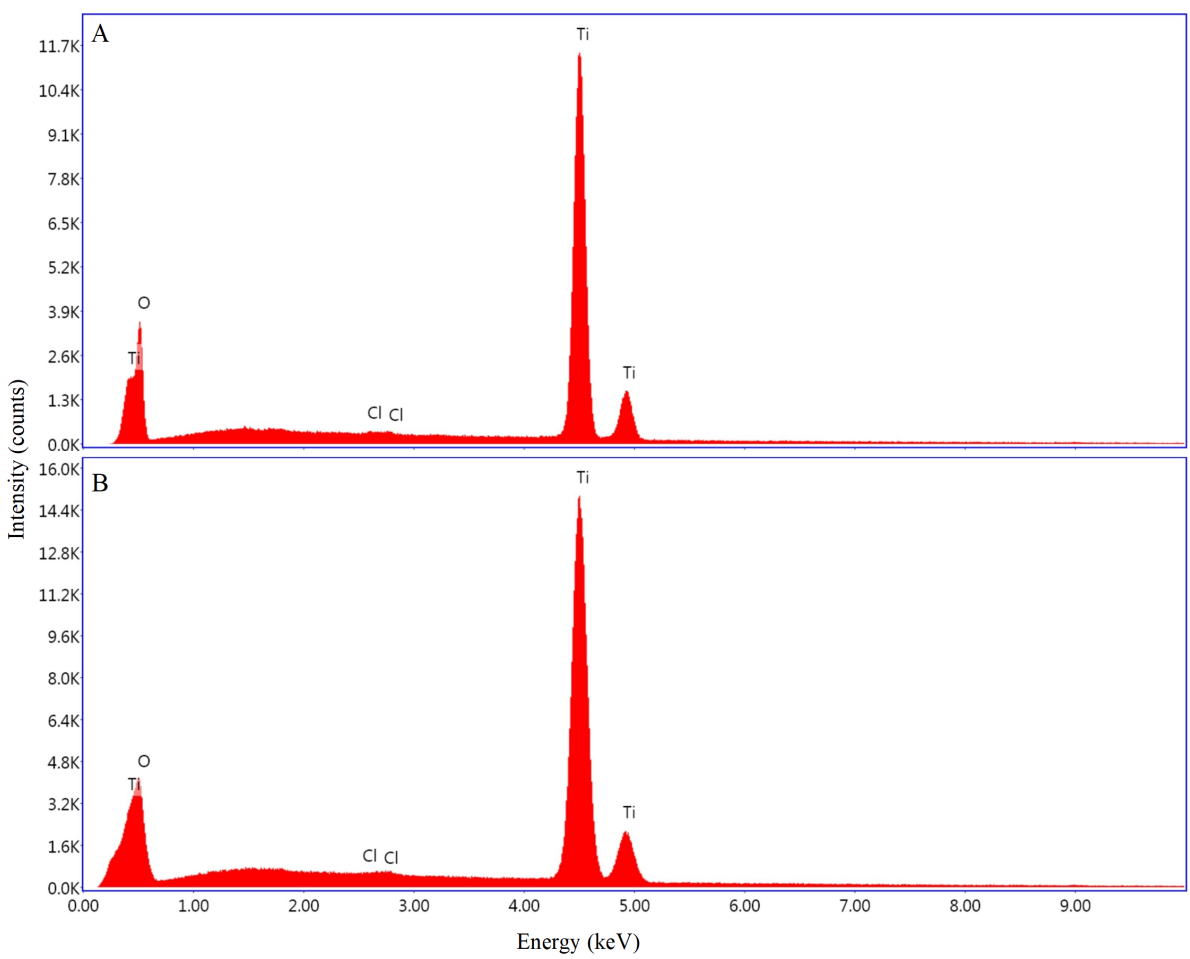

Figure 4.2 Energy-dispersive X-ray (EDX) spectra of (A) micro-TiO_2 and (B) nano-TiO_2.The presence of element titanium (Ti), oxygen (O) and chlorine (Cl) respond to the peaks are marked in the figure. The EDX spectra were taken by Dr Chong Liu, School of Physics, University of Bristol, UK.

The hydrodynamic size of two TiO_2 particles in the f/2 medium are shown in Figure 4.3. Both particles were found be unstable in the f/2 medium. Nano-TiO_2 aggregated to 1130.0 ± 160.8 nm within 10 min, which was 46 times greater than the primary particle size of nano-TiO_2. The nano-TiO_2 aggregates continued to increase and reached a maximum of 1793.3 ± 260.4 nm at 4 h. Micro-TiO_2 immediately (< 10 min) aggregated to 464.0 ± 88.6 nm, which was 3.5 times greater than the primary particle size of micro-TiO_2. The size of micro-TiO_2 aggregates reached a maximum of 1806.0 ± 82.7 nm at 4 h. Though the initially-formed nano-TiO_2

aggregates were significantly larger than the initially-formed micro-TiO_2 aggregates ($F_{1,4}$ = 39.471, p = 0.003), the hydrodynamic diameter of the aggregates of the two TiO_2 were not significantly different after 1 h incubation in the f/2 medium, according to one-way ANOVA tests (1 h, $F_{1,4}$ = 0.968, p = 0.381; 2 h, $F_{1,4}$ = 0.002, p = 0.970; 4 h, $F_{1,4}$ = 0.006, p = 0.940; 24 h, $F_{1,4}$ = 0.387, p = 0.568).

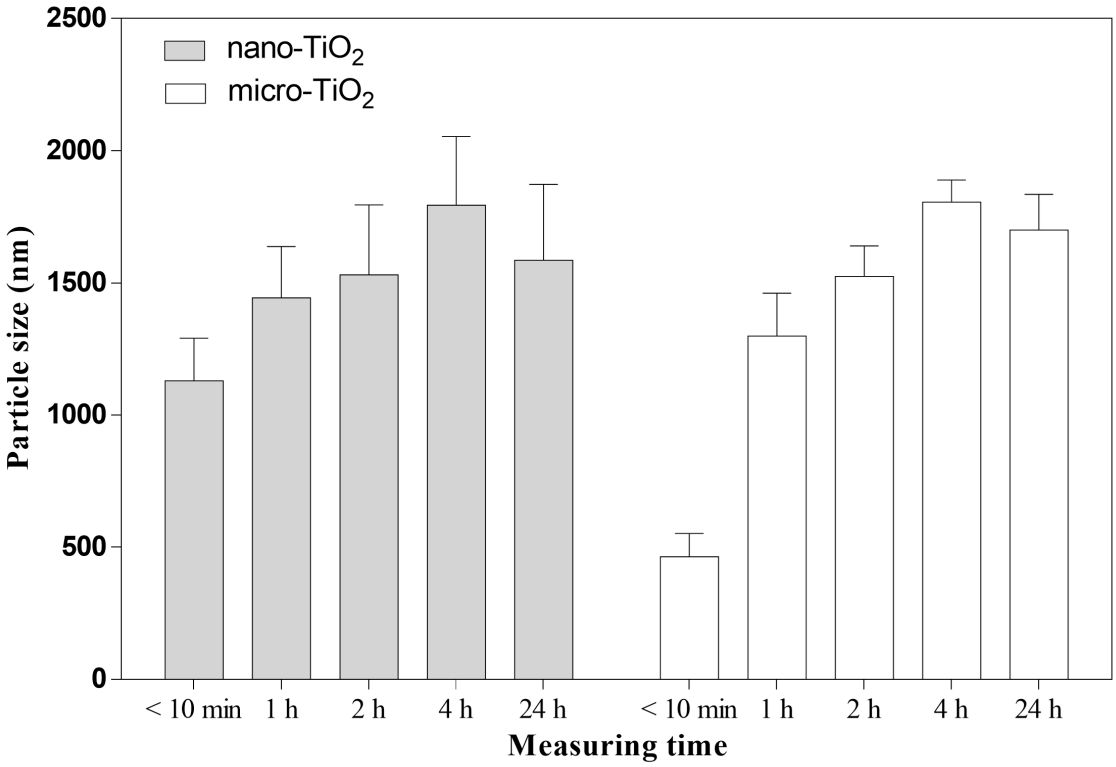

Figure 4.3 Z-average hydrodynamic size (measured by Zetasizer Nano-S90) of nano-TiO_2 and micro-TiO_2 (100 mg/L) aggregates in the f/2 medium at 5 different time points. Results are shown as mean ± standard deviation (n = 3).

4.3.2 The impact of TiO_2 particle type on the biomass yield of three estuarine benthic diatoms in the presence of fluorescent lighting

To find out the impact of TiO_2 on the growth of three estuarine benthic diatoms, their biomass yields were measured following cultivation with and without TiO_2 particles, after 72 h of cultivation in the presence of fluorescent lighting (Figure 4.4). Their cell density was used as an indicator of biomass. Though started from a similar initial biomass ($1 – 2 \times 10^4$ cells/ml), the biomass yield at 72 h varied distinctly among three species, with *Nitzschia* c.f. *clausii* cultures being the lowest and *Cylindrotheca closterium* being the highest.

In the *Nitzschia* c.f. *clausii* cultures, the biomass yield in the control group was 5.9×10^4 cells/ml, after 72 h of cultivation. Higher biomass yields were recorded after 72 h in the treatment groups with the presence of micro-TiO_2 (increased by 28.3%) and nano-TiO_2 (increased by 64.2 %), compared to the control group. A one-way ANOVA test indicated that the biomass yields at 72 h in the three groups (1 control + 2 treatments) were significantly different ($F_{2, 33} = 40.835$, $p < 0.001$). A TukeyHSD *post-hoc* test confirmed that the biomass yield in the three groups followed a statistically significant order of "control group < micro-TiO_2 treatment < nano-TiO_2 treatment".

In the *Navicula gregaria* cultures, the biomass yield in the control group was 12.2×10^4 cells/ml, after 72 h of cultivation. A slightly lower biomass yield was recorded after 72 h in the micro-TiO_2 treatment group (lower by 4.1%), compared to the control group. A higher biomass yield was recorded after 72 h in the nano-TiO_2 treatment group (increased by 23.3%), compared to the control group. A one-way ANOVA test indicated that the biomass yields at 72 h in the three groups were significantly different ($F_{2, 33} = 11.473$, $p < 0.001$). A TukeyHSD *post-hoc* test confirmed that the biomass yield in three groups followed a statistically significant order of "control group = micro-TiO_2 treatment < nano-TiO_2 treatment".

In the *Cylindrotheca closterium* cultures, the biomass yield in the control group was 71.1×10^4 cells/ml, after 72 h of cultivation. A lower biomass was recorded at 72 h in the micro-TiO_2 treatment group (lower by 2%), compared to the control group. A higher biomass yield was recorded at 72 h in the nano-TiO_2 treatment group (higher by 7.3%), compared to the control group. A one-way ANOVA test indicated that the biomass yields at 72 h in the three groups were significantly different ($F_{2, 33} = 6.289$, $p = 0.005$). A TukeyHSD *post-hoc* test confirmed that the biomass yield in three groups followed a statistically significant order of "control group = micro-TiO_2 treatment < nano-TiO_2 treatment".

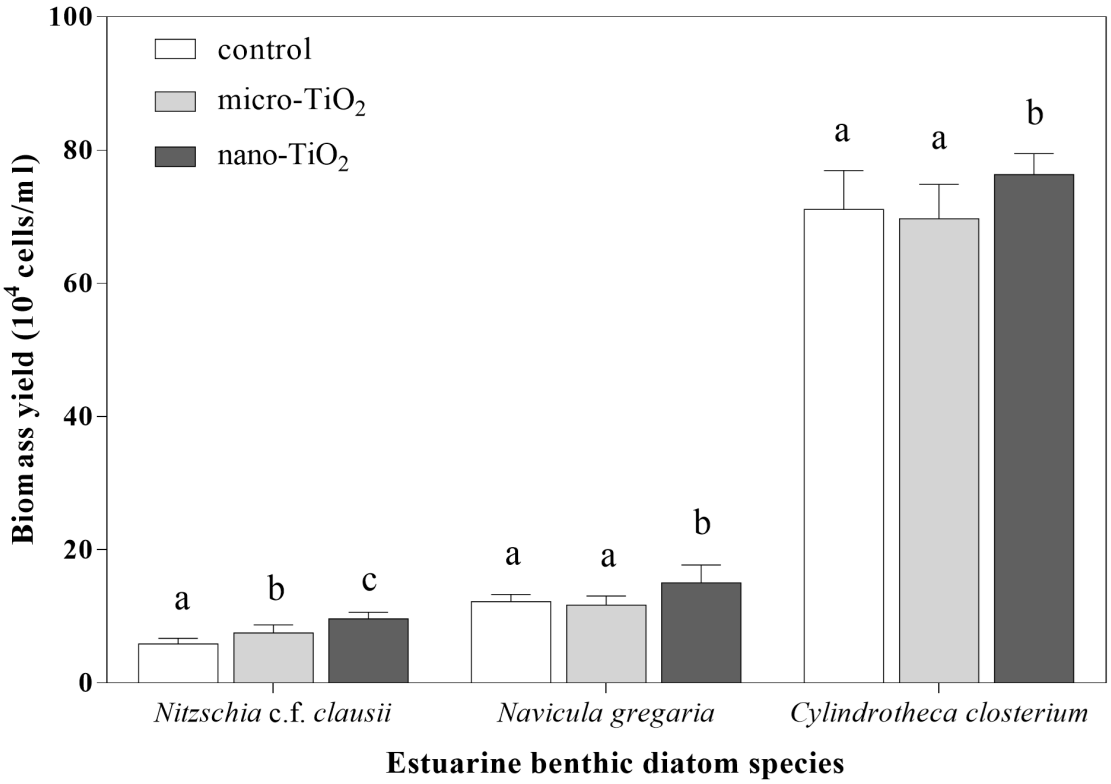

Figure 4.4 The biomass yield of diatom cultures grown with no TiO_2 (control), 100 mg/L micro-TiO_2 and 100 mg/L nano-TiO_2, after 72 h of cultivation in the presence of fluorescent lighting. Three different species (*Nitzschia* c.f. *clausii*, *Navicula gregaria* and *Cylindrotheca closterium*) were tested. Results are shown as mean ± standard deviation (n = 12). Within each species, bars with the same letter are not significantly different (Tukey HSD *post-hoc* test).

4.3.3 The impact of TiO_2 particles on the growth rate of three estuarine benthic diatoms in the presence of fluorescent lighting

The average specific growth rate of the diatoms within 72 h was calculated for each group (Table 4.2). Variable growth rates were recorded in the control groups, with an order of *Nitzschia* c.f. *clausii* (μ = 0.57 day^{-1}) < *Navicula gregaria* (μ = 0.70 day^{-1}) < *Cylindrotheca closterium* (μ = 1.34 day^{-1}).

A significantly higher growth rate was recorded for each species when grown with 100 mg/L nano-TiO_2 (Table 4.2). The greatest increase of growth rate was noticed in *Nitzschia* c.f. *clausii* (increased by 25%), followed by *Navicula gregaria* (increased by 8.5%) and *Cylindrotheca closterium* (increased by 1.5%).

A significantly higher growth rate was recorded in the treatment with 100 mg/L micro-TiO_2 for *Nitzschia* c.f. *clausii* only (increased by 12.3%) (Table 4.2). As for *Navicula gregaria* and *Cylindrotheca closterium*, the growth rate in the treatment with 100 mg/L micro-TiO_2 was not significantly different from the control group (Table 4.2).

Table 4.2 The average specific growth rate (μ, day^{-1}) within 72 h for diatom cultures grown with no TiO_2 (control), 100 mg/L micro-TiO_2 and 100 mg/L nano-TiO_2, in the presence of fluorescent lighting. Results are shown as mean ± standard deviation (n = 12). Within each species, numbers with the same letter was not significantly different (Tukey HSD *post-hoc* test).

Group	*Nitzschia* c.f. *clausii*	*Navicula gregaria*	*Cylindrotheca closterium*
Control	0.57 ± 0.04 [a]	0.70 ± 0.03 [a]	1.34 ± 0.03 [a]
Micro-TiO_2	0.64 ± 0.04 [b]	0.69 ± 0.03 [a]	1.33 ± 0.02 [a]
Nano-TiO_2	0.71 ± 0.03 [c]	0.76 ± 0.05 [b]	1.36 ± 0.01 [b]

4.3.4 The impact of TiO_2 particles on the chlorophyll *a* concentration per cell of three estuarine benthic diatoms in the presence of fluorescent lighting

The chlorophyll *a* concentration per cell in each group after 72 h of cultivation was calculated and illustrated in Figure 4.5. In the control groups, the chl *a* per cell was 2.75 pg, 2.44 pg and 1.67 pg for *Nitzschia* c.f. *clausii*, *Navicula gregaria* and *Cylindrotheca closterium*, respectively.

In the *Nitzschia* c.f. *clausii* culture, lower chlorophyll *a* concentration per cell values were recorded in the micro-TiO_2 treatment (lower by 6.7%) and nano-TiO_2 treatment (lower by 3.2%), compared to the control group. A one-way ANOVA test indicated that differences in the chlorophyll *a* concentration per cell between the three groups were not significant ($F_{2, 33} = 0.801$, $p = 0.457$).

In the *Navicula gregaria* culture, a relatively higher chlorophyll *a* concentration per cell was recorded in the micro-TiO_2 treatment (increased by 7.1%). A lower chlorophyll *a* concentration per cell was recorded in the nano-TiO_2 treatment (lower by 5.9%). A one-way ANOVA test indicated that differences in the chlorophyll *a* concentration per cell between the three groups were not significant ($F_{2, 33} = 2.697$, $p = 0.082$).

In the *Cylindrotheca closterium* culture, lower chlorophyll *a* concentration per cell values were recorded in the micro-TiO_2 treatment (lower by 9.5%) and nano-TiO_2 treatment (lower by 3.8%). A one-way ANOVA

test indicated that differences in the chlorophyll *a* concentration per cell between the three groups were not significant ($F_{2, 33} = 0.872$, $p = 0.427$).

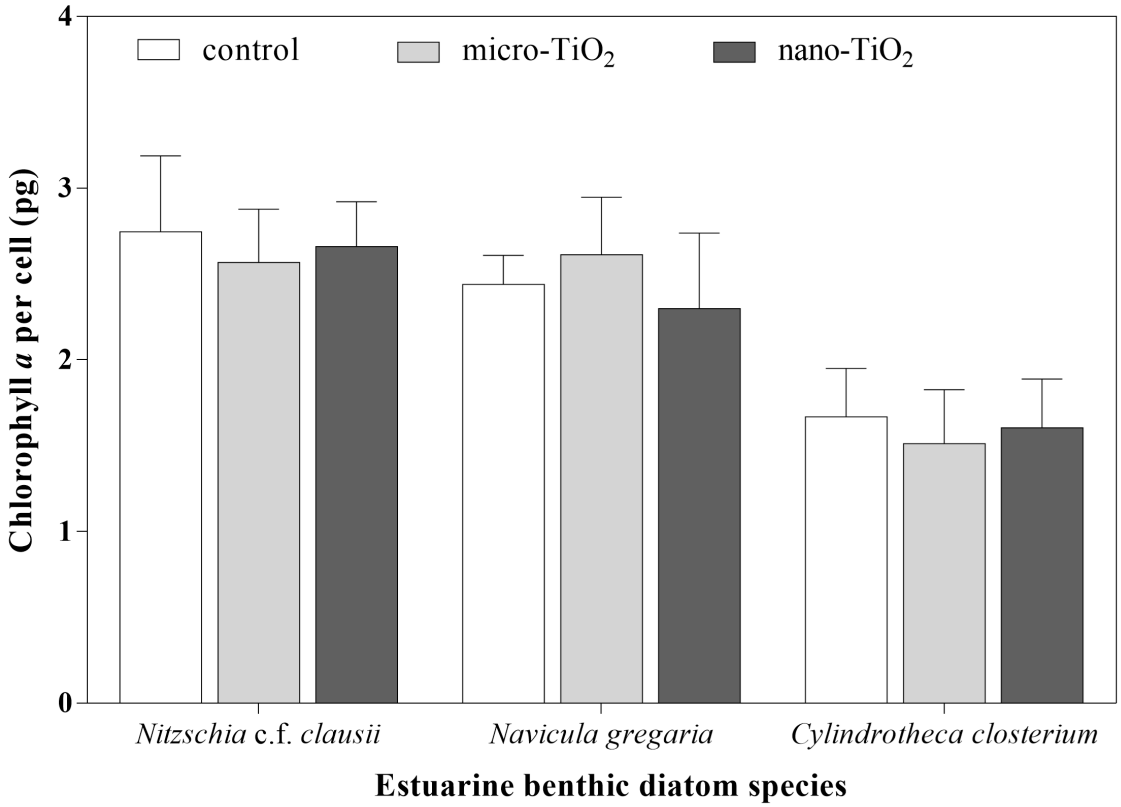

Figure 4.5 The chlorophyll *a* concentration per cell of diatoms grown with no TiO_2 (control), 100 mg/L micro-TiO_2 and 100 mg/L nano-TiO_2, in the presence of fluorescent lighting. Three different species (*Nitzschia* c.f. *clausii*, *Navicula gregaria* and *Cylindrotheca closterium*) were tested. Results are shown as mean ± standard deviation (n = 12).

4.3.5 Summary of results

- When grown under laboratory conditions with fluorescent lighting, significantly higher biomass yields (assessed by cell density) and significantly higher growth rates were recorded in the three estuarine benthic diatom cultures in the presence of 100 mg/L nano-TiO_2, compared to the control samples, after 72 h of exposure. Species-specific responses were recorded, with the greatest increases observed for *Nitzschia* c.f. *clausii*, followed by *Navicula gregaria*, and the lowest increases observed for *Cylindrotheca closterium*,
- A significantly higher biomass yield and higher growth rate was recorded in the *Nitzschia* c.f. *clausii*

culture in the presence of 100 mg/L micro-TiO_2, compared the control group, after 72 h of cultivation. The biomass yield and growth rate in *Navicula gregaria* and *Cylindrotheca closterium* cultures with the presence of 100 mg/L micro-TiO_2 was not significantly different from the corresponding control group.

- Significantly higher biomass yield and growth rate was recorded in all three species with the presence of nano-TiO_2, compared to that with the presence of micro-TiO_2.
- Chlorophyll *a* concentration per cell was not significantly influenced by the presence of both types of TiO_2 for all three species.

Section 2: Investigation on the possible mechanisms for the stimulated growth of estuarine benthic diatoms in the presence of nano-TiO_2 and fluorescent lighting

Introduction

Results obtained from earlier work (Section 1) revealed significantly higher growth rates of estuarine benthic diatoms when exposed to 100 mg/L nano-TiO_2, compared to the controls without nano-TiO_2. The stimulated growth in the presence of nano-TiO_2 has been previously recorded in a marine planktonic diatom species *Phaeodactylum tricornutum*, a marine tychoplanktonic diatom species *Nitzschia closterium* (also named as *Cylindrotheca closterium* or *Ceratoneis closterium*) and two freshwater green algae species (*Chlamydomonas reinhardtii* and *Pseudokirchneriella subcapitata*), yet generally at particle concentrations much lower than 100 mg/L (Table 4.3). In five out of six studies summarized in Table 4.3, the stimulation effect of nano-TiO_2 was measured after 72 h of exposure with particle concentrations no greater than 20mg/L, and the impact of nano-TiO_2 reverted to an inhibitory response at concentrations of 100 mg/L or higher. In one study conducted with *Nitzschia closterium*, the stimulation effect of nano-TiO_2 on the algal growth rate was recorded at 2 h only, with particle concentration no greater than 20 mg/L; after prolonged exposure (≥ 4 h), an inhibitory effect, instead of a stimulation effect, was recorded (Xia et al. 2015).

Table 4.3 Studies recording the growth stimulation effect of nano-TiO_2 in the presence of fluorescent lighting. **SP =** Stimulation percentage of growth rate. **IP =** Inhibition percentage of growth rate. Studies with diatoms are marked in bold and shown first, followed by studies with green algae. "–" denotes the information is not available.

Taxonomic group	Species	Primary particle size (nm)	Crystal structure	Particle concentration (mg/L)	Cultivation time (h)	SP or IP	Reference
Estuarine benthic Bacillariophyceae	***Nitzschia* c.f. *clausii***	24.4	85.8% anatase 14.2% rutile	100	72	SP = 25%	The present study
	Navicula gregaria			100	72	SP = 8.5%	
	Cylindrotheca closterium			100	72	SP = 1.5%	
Marine planktonic Bacillariophyceae	***Phaeodactylum tricornutum***	15	100% anatase	0.01	72	SP = 5%	Clement et al. (2013)
				1 – 100	72	IP = 5 – 100%	
		25	100% anatase	0.01	72	SP = 5%	
				1 – 100	72	IP = 5 – 100%	
		32	100% anatase	0.01 – 1	72	SP = 5 – 15%	
				10 – 100	72	IP = 30 – 100%	
		38	79% anatase 21% rutile	0.1 – 1	72	SP < 5%	Sendra et al. (2017a)
				100 – 400	72	IP > 0	
	Nitzschia closterium	21	98.6% anatase 1.4% rutile	5 – 20	2	SP = 5 – 8%	Xia et al. (2015)
					4 – 24	IP = 10 – 35%	
				5 – 100	72	IP = 5 – 45%	
Freshwater planktonic Chlorophyceae	*Chlamydomonas reinhardtii*	38	79% anatase 21% rutile	0.1 – 1	72	SP < 5%	Sendra et al. (2017a)
				100 – 400	72	IP > 0	
	Pseudokirchneriella subcapitata	< 25	–	16 – 20	72	SP = 5 – 10%	Nogueira et al. (2015)
		30	–	0.6 – 8	72	SP = 2 –10%	Hartmann et al. (2010)
				20 – 250	72	IP = 10 – 80%	

It has been well recognized that algal growth rate may be affected by light intensity (Juneja et al. 2013). Because TiO_2 particles are not considered to be soluble in water, the adsorption of nano-TiO_2 onto the cell surface or the entrapment of cells by particle aggregates may lead to a "shading effect", which may contribute to a lowered light received by cells exposed to nano-TiO_2 (Hund-Rinke and Simon 2006; Aruoja et al. 2009; Morelli et al. 2018). It was considered that if the estuarine benthic diatoms in the control group were receiving too much light, the lower light condition in the nano-TiO_2 treatment may result in a higher algal growth rate, compared to the control group (without nano-TiO_2), accounting for the results obtained in the Section 1.

In addition, it has been reported that the uptake rate of nutrients can play an important role in regulating algal growth rate (Juneja et al. 2013). It was also considered that if the presence of nano-TiO_2 may somehow induce a faster uptake rate of nutrients, the algal growth rate in the nano-TiO_2 treatment group may be higher, compared to that in the control group, accounting for the results obtained in the Section 1.

Aim 3: To investigate whether the light shading effect was contributing to the higher growth rate of estuarine benthic diatoms, experiments were conducted to test the responses of estuarine benthic diatoms to lowered light intensity, which simulated the light shading effect of nano-TiO_2.

Hypothesis 3: In Section 1, estuarine benthic diatoms were cultivated under fluorescent lighting with PAR of 80 μmol m^{-2} s^{-1}. It was hypothesized that the estuarine benthic diatoms would grow quicker at light intensities lower than 80 μmol m^{-2} s^{-1}.

Aim 4: It has been reported that the uptake rate of nutrients is positively related to the concentration of nutrient in the medium until reaching saturation (Paasche 1973; Xin et al. 2010). Algal growth rate may be controlled by the type of nutrient, of which the uptake rate is the lowest (Juneja et al. 2013). To investigate which type of nutrient in the f/2 medium was the controlling nutrient for the growth of estuarine benthic diatoms, experiments were conducted to test the responses of estuarine benthic diatoms to increased concentrations of different type of nutrients.

Hypothesis 4: It was hypothesized that increasing the concentration of a certain type of nutrient in the culture medium would increase algal growth rate.

4.4 Methods

4.4.1 The impact of light intensity on the growth rate of estuarine benthic diatoms in the presence of fluorescent lighting

To investigate whether the estuarine benthic diatoms grew better under lower light intensity (aim 3), which simulating the effects of light shading by nano-TiO_2, the growth rates of three estuarine benthic diatoms under several light intensities were compared after a period of 72 h.

Algal cultures were resuspended in fresh f/2 medium. Six groups of algal samples were prepared for each species, with 6 replicates per group. Each replicate contained 4.5 mL algal culture and occupied a well in the 12-well microplate. Each group occupied one 12-well microplate and was incubated under one of the six light conditions (PAR= 30, 40, 50, 60, 70 or 80 μmol m^{-2} s^{-1}, cool white fluorescent lighting, F58W/840, T8 Luxline® Plus, Sylvania). In the experiments conducted in Section 1 (section 4.2.3), estuarine benthic diatoms were cultivated under fluorescent lighting with PAR of 80 μmol m^{-2} s^{-1}. Therefore, diatoms in the control group were grown under 80 μmol m^{-2} s^{-1} in the present experiment. The light intensities lower than 80 μmol m^{-2} s^{-1} were obtained by applying different types of neutral density filters (LEE filters, http://www.leefilters.com/lighting/technical-list.html) on top of the microplate. The initial biomass in the algal sample was 1.3×10^4 cells/mL for *Nitzschia* cf. *clausii* and *Cylindrotheca closterium* and was 1.7×10^4 cells/mL for *Navicula gregaria*, in accordance to the starting states in the experiments conducted in Section 1. All microplates were incubated in static conditions at 18 ± 1 ℃ with a cycle of 14 h-light and 10 h-dark in a growth room (Reftech Climate Room). After 72 h of cultivation, samples in each microplate well were harvested for cell density measurement as described in section 4.2.3 and average growth rate was calculated according to section 4.2.4.

4.4.2 The impact of nutrient availability on the growth of *Nitzschia* cf. *clausii* in the presence of fluorescent lighting

To investigate which type of nutrients in the f/2 medium was controlling the growth of the estuarine benthic diatoms (aim 4), the growth rate of estuarine benthic diatoms in amended culture media enriched with different types of nutrients were compared to the growth rate in the unamended culture medium after a period of 72 h. *Nitzschia* c.f. *clausii* had the lowest biomass yield among the three species (Figure 4.4), in the experiments conducted in Section 1, suggesting its growth in the f/2 medium should not to be nutrient limited. Therefore, this species was tested to address aim 4, so that the any difference in the growth rates between the amended medium and the original medium could only be linked to a lower nutrient uptake rate in the original medium, but not be linked to a nutrient depletion in the original medium.

Four modified f/2 media sets were prepared by doubling the concentration of (i) nitrate (corresponding to stock 1); (ii) phosphate (corresponding to stock 2); (iii) silicate (corresponding to stock 3); and (iv) trace metals (corresponding to stock 4), respectively, compared to the concentration in the normal f/2 medium (see section 2.2.3.1 for the details). Algal cultures at the exponential stage were harvested and centrifuged at 2000 rpm (805 *g*) for 5 min to remove the old medium. The cell pellets were resuspended in fresh unamended f/2 medium (control) or four enriched f/2 media (treatments). Five groups (1 control + 4 treatments) of algal samples were prepared. Each replicate contained 4.5 mL algal culture and occupied a well in the 12-well microplate (polystyrene, growth area of 3.8 cm^2/well). The initial biomass in the algal sample was 1.3×10^4 cells/ml, in accordance to the starting states in the experiments conducted in Section 1. Microplates were incubated as described in section 4.2.3. Samples were harvested for cell density measurement at 72 h as described in section 4.2.3 and growth rate was calculated according to section 4.2.4. All assays were run in four replicates.

4.4.3 Data analysis

Data were analyzed according to section 4.2.6.

4.5 Results

4.5.1 The impact of light intensity on the growth of estuarine benthic diatoms in the presence of fluorescent lighting

To find out whether the estuarine benthic diatoms grew better under lower light intensity (simulating the light shading effect of nano-TiO_2), the growth rates of estuarine benthic diatom cultures cultivated under light intensities of 30 – 70 μmol m^{-2} s^{-1} were compared to their growth rates at 80 μmol m^{-2} s^{-1}, the light intensity used in the experiments conducted in Section 1 (Figure 4.6). One-way ANOVA tests indicated that the average growth rates of diatoms cultivated under the six selected light intensities were not significantly different for each test species (*Nitzschia* c.f. *clausii*, $F_{5,30} = 0.633$, $p = 0.676$; *Navicula gregaria*, $F_{5,30} = 0.714$, $p = 0.618$; and *Cylindrotheca closterium*, $F_{5,30} = 0.816$, $p = 0.548$).

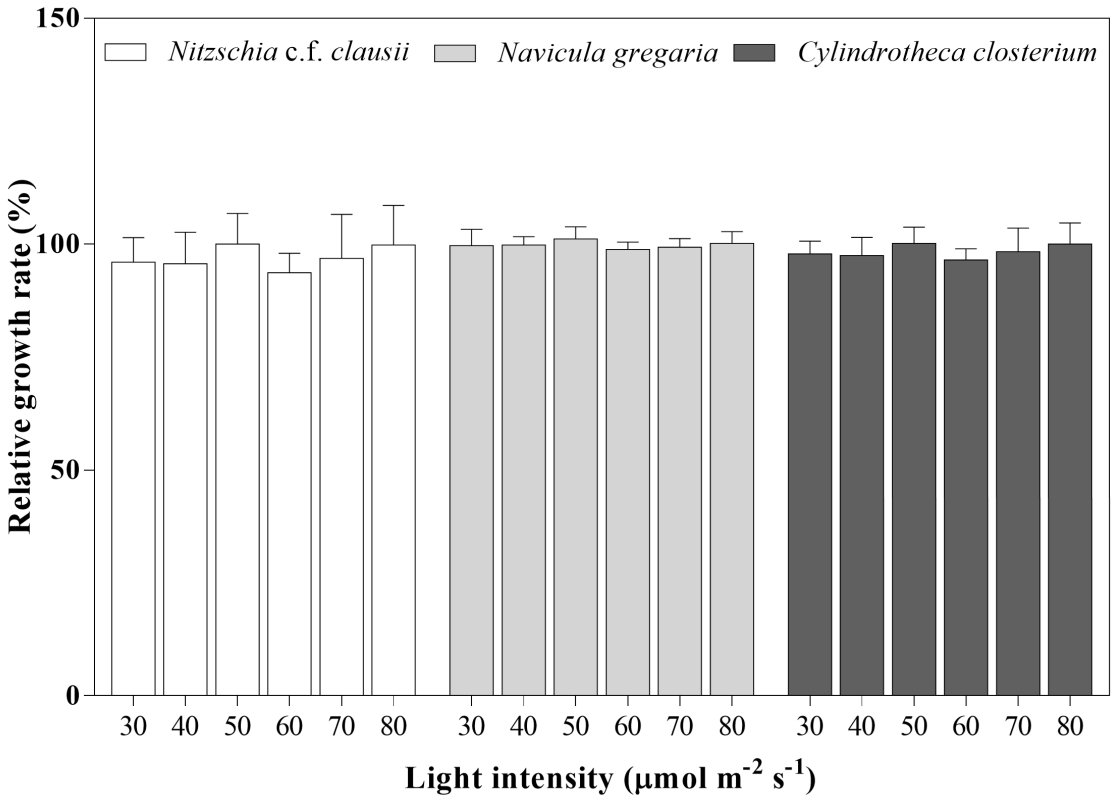

Figure 4.6 The relative growth rate (μ) of diatom cultures cultivated under a series of light intensities (30 – 70 μmol m^{-2} s^{-1}), compared to the growth rate of the control group cultivated at 80 μmol m^{-2} s^{-1} in the presence of fluorescent lighting. Three different species (*Nitzschia* c.f. *clausii*, *Navicula gregaria* and *Cylindrotheca closterium*) are marked by the colour of the bars. Results are shown as mean ± standard deviation (n = 6).

4.5.2 The impact of nutrient concentration on the growth of *Nitzschia* cf. *clausii* in the presence of fluorescent lighting

To investigate which type of nutrients in the f/2 medium was controlling the growth of t *Nitzschia* cf. *clausii* (simulating the presence of nano-TiO_2 that may facilitate nutrient acquisition), the growth rates of *Nitzschia* cf. *clausii* cultivated with enriched f/2 media were compared to the growth rate in unamended f/2 medium (Figure 4.7).

The growth rate of *Nitzschia* c.f. *clausii* within 72 h in the five culture media were: 0.56 day^{-1} (control medium); 0.57 day^{-1} (enriched with nitrate); 0.59 day^{-1} (enriched with phosphate); 0.74 day^{-1} (enriched with silicate) and 0.55 day^{-1} (enriched with trace metal). A one-way ANOVA test indicated that the growth rates

in the five different media were significantly different ($F_{4, 15} = 61.375$, $p < 0.001$). A TukeyHSD *post-hoc* test confirmed that the growth rate in the medium enriched with silicate was significantly higher than that in the other four media, while the growth rates in the other four media were not significantly different from each other.

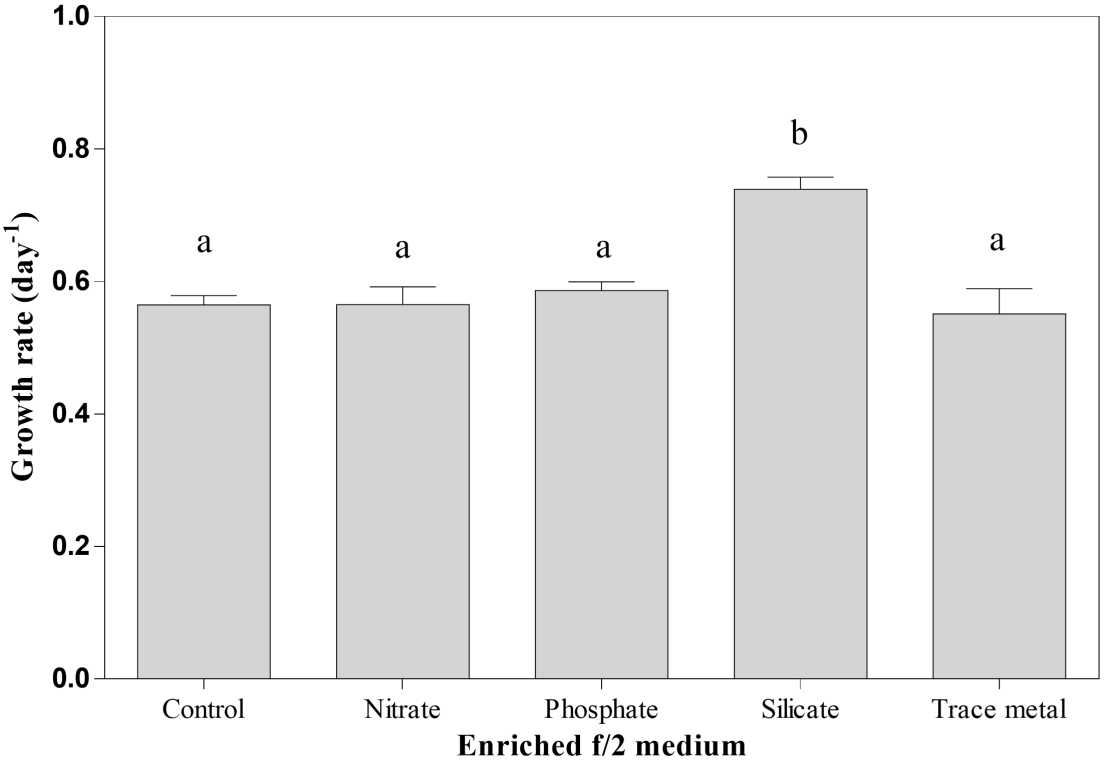

Figure 4.7 The average growth rate within 72 h of *Nitzschia* c.f. *clausii* grown in the normal f/2 medium (control) and nitrate, phosphate, silicate and trace metal enriched f/2 media, in the presence of fluorescent lighting. Results are shown as mean ± standard deviation (n = 4). Bars with the same letter are not significantly different (Tukey HSD *post-hoc* test).

4.5.3 Summary of results

- The growth rates of three estuarine benthic diatoms cultivated under light intensities lower than 80 µmol m^{-2} s^{-1} was not significantly different from their growth rate measured at 80 µmol m^{-2} s^{-1}.
- The growth rate of *Nitzschia* cf. *clausii* cultures cultivated with doubled concentration of nitrate, phosphate and trace metal was not significantly different from its growth rate in the unamended f/2 medium. The growth rate of *Nitzschia* cf. *clausii* cultivated with doubled concentration of silicate was significantly higher, compared to its growth rate in the unamended f/2 medium.

4.6 Discussion

4.6.1 The impact of nano-TiO_2 on the growth of estuarine benthic diatom in the presence of fluorescent lighting

It was hypothesized that the growth of estuarine benthic diatoms would be negatively impacted by the presence of nano-TiO_2. Significantly higher biomass yields after 72 h of cultivation (increased by 7.3 – 64.2%) and significantly higher average growth rates over 72 h (increased by 1.5 – 25%) were recorded in three estuarine benthic diatom cultures when they were exposed to100 mg/L nano-TiO_2 in the presence of fluorescent lighting, compared to the control group, which was not in agreement with the hypothesis. The stimulated growth observed in the estuarine benthic diatom cultures with the presence of 100 mg/L nano-TiO_2 was unexpected, because most of the previous studies has reported a growth inhibition effect of nano-TiO_2 at concentrations ≤ 100 mg/L and even at concentrations ≤ 10 mg/L (Table 4.4).

The same type of nano-TiO_2 (P25) used in the present study has been tested in several freshwater green algae including *Chlorella* sp., *Pseudokirchneriella subcapitata*, *Scenedesmus* sp. and *Chlamydomonas reinhardtii* with fluorescent lighting (marked by underlined species names in Table 4.4). Five out of seven studies reported 72 h-IC50 values between 2.16 mg/L and 71.1 mg/L, which was lower than 100 mg/L, suggesting that the growth inhibition of 100 mg/L nano-TiO_2 would be greater than 50%. Hartmann et al. (2013), testing the freshwater green alga *Pseudokirchneriella subcapitata*, reported a 72 h-IC10 value (the concentration of nano-TiO_2 at which the inhibition percentage on the growth rate is 10%) of 38 mg/L and a 72 h-IC50 value of 160 mg/L, indicating that the growth inhibition in the presence of 100 mg/L nano-TiO_2 would be within the range of 10 – 50%. A 100% inhibition of algal growth was reported by Chen et al. (2012) in freshwater green alga *Chlamydomonas reinhardtii*, in the presence of 100 mg/L nano-TiO_2. On the contrary, results in the present investigation revealed that the growth rate of three estuarine benthic diatoms exposed to 100 mg/L nano-TiO_2 in the presence of fluorescent lighting were significantly higher than the control group (in absence of nano-TiO_2). Comparably, the estuarine benthic diatom species tested in the present study would appear to be less susceptible to nano-TiO_2 than those freshwater planktonic green algae species.

The impact of other types of nano-TiO_2 on algal growth have also been tested with fluorescent lighting. Studies conducted with diatoms have been marked by highlighting species names in bold in Table 4.4. The

growth inhibition of nano-TiO_2 were recorded in three marine diatom species (*Phaeodactylum tricornutum*, *Skeletonema costatum* and *Nitzschia closterium*) with 72 h-IC50 values ranging from 7.37 to 167.79 mg/L, and in two freshwater diatom species (*Nitzschia frustulum* and *Nitzschia palea*) with 72 h-IC50 values ranging from 28.98 to 124 mg/L. To be noted, one of the species tested in the present study, *Cylindrotheca closterium* (also named as *Nitzschia closterium* or *Ceratoneis closterium*), was previously investigated by Xia et al. (2015). They reported that the growth rate of *Nitzschia closterium* was inhibited by 45% after a 72 h exposure to 100 mg/L nano-TiO_2 with primary particle size of 21 nm (Xia et al. 2015), which was in contrast to that obtained in the present study where the growth rate of *Cylindrotheca closterium* was found to be significantly stimulated though only by a small margin of 1.5% in the presence of 100 mg/L nano-TiO_2 (primary particle size of 24.4 nm). *Cylindrotheca closterium* is a tychopelagic diatom, which shows a half-planktonic and half-benthic existence in nature (Round 1981). The clone used in the present study was isolated from the mudflats of the Severn Estuary and was assumed to be growing primarily as an epipelic species, which grows in the muds as opposed to the water column (Round 1981). The *Cylindrotheca closterium* culture tested by Xia et al. (2015) was described and cultivated as a planktonic species. The contrasting results obtained between the present investigation and the study by Xia et al. (2015), as well as studies with other diatoms, suggested that the estuarine benthic diatom species test in the present study may have a higher tolerance to the presence of nano-TiO_2 than the diatom species from habitats other than the mudflats in intertidal areas.

Growth inhibition in response to the exposure of nano-TiO_2 has also been recorded in green algae and red algae (Table 4.4). In those studies, 55% of them reported 72 h-IC50 values ranging between 9.72 – 21.2 mg/L, which is far lower than the concentration of 100 mg/L at which stimulatory responses were recorded in the present study. In the other studies, the inhibition percentage on the growth rate (IP) in the presence of 100 mg/L was recorded to be within 30 – 100% (Table 4.4).

In summary, the estuarine benthic diatom species tested in the present investigation appeared to be more tolerant to nano-TiO_2 than those species previously tested, in the presence of fluorescent lighting. A further discussion about the potential reasons for the higher resistance of estuarine benthic diatom species to nano-TiO_2 is presented in section 7.2 in Chapter 7.

Table 4.4 Impact of nano-TiO_2 on the growth rate of different algal species cultivated under laboratory conditions with fluorescent lighting. Studies with nano-TiO_2 (P25, the type of particles used in the present investigation) are shown first, marked by underlined species names. For the other studies, studies with diatoms are shown first with species names marked in bold. Within the same species, studies with smaller nano-TiO_2 are shown first. **IC50** (mg/L) = the concentration of nano-TiO_2 at which the inhibition percentage on growth rate is 50%. **IC10** (mg/L) = the concentration of nano-TiO_2 at which the inhibition percentage on growth rate is 10%. **SP (X)** = Stimulation percentage of growth rate with the presence of **X** mg/L nano-TiO_2**. IP (X)** = Inhibition percentage of growth rate with the presence of **X** mg/L nano-TiO_2. "–" denotes the information is not available.

Taxonomic group	**Species name**	**Primary particle size (nm)**	**Crystal structure**	**Medium type**	**Impact of nano-TiO_2**	**Reference**
Estuarine benthic Bacillariophyceae	***Nitzschia* c.f. *clausii***	24.4	85.8% anatase 14.2% rutile	f/2	72 h-SP = 25% (100)	The present study
	Navicula gregaria			f/2	72 h-SP = 8.5% (100)	
	Cylindrotheca closterium			f/2	72 h-SP = 1.5% (100)	
Freshwater planktonic Trebouxiophyceae	*Chlorella* sp.	21 nm	–	BG11	72 h-IC50: 2.16	Roy et al. (2016)
Freshwater planktonic Chlorophyceae	*Pseudokirchneriella subcapitata*	–	–	OECD	72 h-IC50: 2.53	Lee and An (2013)
		30	–	ISO	72 h-IC50 = 71.1	Hartmann et al. (2010)
		23	–	OECD	72 h-IC10: 38 72 h-IC50: 200	Hartmann et al. (2013)
	Scenedesmus sp.	21	–	BG11	72 h-IC50: 4.139	Roy et al. (2016)
	Chlamydomonas reinhardtii	21	–	CM	72 h-IC50: 10	Wang et al. (2008)
		21	–	SE	72 h-IP = 100% (100)	Chen et al. (2012)
Marine planktonic Bacillariophyceae	***Phaeodactylum tricornutum***	5 – 10	100% anatase	f/2	48 h-IP = 50% (40) 96 h-IP = 27% (40)	Deng et al. (2017)
		15	99.8% anatase	f/2	72 h-IC50: 167.79 72 h-IP = 40% (100)	Wang et al. (2016)
		15	100% anatase	Synthetic seawater	72 h-IC50: 10.91	Clement et al. (2013)
		25	100% anatase	Synthetic seawater	72 h-IC50: 11.30	Clement et al. (2013)
		32	100% anatase	Synthetic seawater	72 h-IC50: 14.30	Clement et al. (2013)

		38	79% anatase, 21% rutile	f/2	72 h-IC50: 132.0	Sendra et al. (2017b)
	Skeletonema costatum	5 – 10	100% anatase	f/2	72 h-IC50: 7.37	Li et al. (2015)
	Nitzschia closterium	21	98.6% anatase, 1.4% rutile	f/2	72 h-IP = 45% (100)	Xia et al. (2015)
Freshwater planktonic diatom	***Nitzschia frustulum***	20	–	CSI	72 h-IC50: 28.98	Jia et al. (2019)
Freshwater benthic diatom	***Nitzschia palea***	50	100% anatase	OECD	72 h-IC50: 124 72 h-IP = 21% (50)	Ockenden (2019)
	Fistulifera pelliculosa	< 5	mainly anatase	OECD	72 h-IP = 0 (100)	Joonas et al. (2019)
Marine planktonic Dinophyceae	*Karenia brevis*	5 – 10	100% anatase	f/2	72 h-IC50: 10.69	Li et al. (2015)
Marine planktonic Chlorophycease	*Dunaliella tertiolecta*	25	100% anatase	f/2	72 h-IP = 100% (100)	Manzo et al. (2016)
Freshwater planktonic Trebouxiophyceae	*Chlorella pyrenoidosa*	12.0	mainly anatase	OECD	96 h-IC50: 9.1	Middepogu et al. (2018)
	Chlorella sp.	5 – 10	100% anatase	SE	48 h-IP = 60% (100) 96 h-IP = 80% (100)	Ji et al. (2011)
		17	mainly anatase	BB	72 h-IC50: 16.12	Sadiq et al. (2011)
Freshwater planktonic Chlorophyceae	*Pseudokirchneriella subcapitata*	< 5	mainly anatase	OECD	72 h-IC50: 14.8	Joonas et al. (2019)
		< 10 nm	67.2% anatase 32.8% amorphous	ISO	72 h-IP = 30% (100)	Hartmann et al. (2010)
		25 – 70	–	OECD	72 h-IC50: 9.72	Aruoja et al. (2009)
	Scenedesmus sp.	17	mainly anatase	BB	72 h-IC50: 21.2	Sadiq et al. (2011)
	Scenedesmus obliquus	42	–	BG11	72 h-IP = 50% (100)	Iswarya et al. (2017)
	Chlamydomonas reinhardtii	< 5	mainly anatase	OECD	72 h-IC50: 13.7	Joonas et al. (2019)

4.6.2 The possible mechanisms to account for the stimulated growth of estuarine benthic diatoms observed in the presence of 100 mg/L nano-TiO_2 and fluorescent lighting

In the investigation conducted in Section 1, significantly higher biomass yields and significantly higher growth rates were recorded in three estuarine benthic diatoms (*Nitzschia* cf. *clausii*, *Navicula gregaria*, *Cylindrotheca closterium*), after 72 h exposure to 100 mg/L nano-TiO_2 in the presence of fluorescent lighting with PAR of 80 µmol m^{-2} s^{-1}. It was hypothesized that the light intensity of 80 µmol m^{-2} s^{-1} (PAR) may be too high for the growth of estuarine benthic diatoms and these diatoms would grow quicker at light intensity lower than 80 µmol m^{-2} s^{-1}. The growth rates of three estuarine benthic diatoms cultivated under PAR of 30 – 70 µmol m^{-2} s^{-1} were not significantly different from the control group cultivated under PAR of 80 µmol m^{-2} s^{-1} (the light intensity used in the experiments conducted in Section 1), which was not in agreement with the hypothesis. These results revealed that the stimulated growth in the presence of nano-TiO_2 was not likely to be linked to the light shading effect of nano-TiO_2.

A second hypothesis was that the presence of nano-TiO_2 may somehow accelerate the nutrient uptake rate and thus the estuarine benthic diatoms would grow quicker. An investigation with *Nitzschia* c.f. *clausii* culture indicated that silicate could be a likely candidate as the controlling nutrient for the growth of *Nitzschia* c.f. *clausii* in the f/2 medium. This result suggested that if the presence of nano-TiO_2 in some way has led to an increased uptake of silicate, the growth rate of *Nitzschia* c.f. *clausii* in the nano-TiO_2 treatment would be higher than that in the control group. Increasing the concentration of silicate worked effectively in stimulating the growth of *Nitzschia* c.f. *clausii*. One possible explanation for higher growth rate in the nano-TiO_2 treatment may be associated with a higher silicate availability, compared to that in the control group, possibly from impurities associated with the nano-TiO_2. However, an EDX spectrum of nano-TiO_2 revealed that element silicon (Si) was not present in the nano-TiO_2 particles (Figure 4.2), implying that no additional Si could have been introduced into algal culture from the nano-TiO_2 particles. The adsorption of nano-TiO_2 onto the cell surface and/or the entrapment of diatom cells by particle aggregates were observed with three estuarine benthic diatoms (Figure 3.3). Studies showed that ions may adsorb onto the surface of nanoparticles (Hotze et al. 2010; Engates and Shipley 2011). It is possible that silicate adsorbed onto the surface of nanoparticles and thus created a microenvironment within the NP-cell matrix where the silicate concentration

inside was higher than that outside (e.g. in the surrounding medium). For those cells within the microenvironment, the uptake rate of silicate could therefore have been much higher than the other cells, contributing to a higher growth rate in the nano-TiO_2 treatment, compared to the control group.

Another possible explanation was that it could have been possible that nano-TiO_2 reduced the demand for silicate for diatom cells, as they could utilize a substitute substance. It has been reported that nano-TiO_2 was incorporated into diatom valve during frustule, by forming the lining base of the frustule pore (Jeffryes et al. 2008). There is a possibility that diatom cells may have utilized nano-TiO_2 as a substitute for SiO_2 during frustule synthesis, and thus have reduced the demand for silicate on a per cell basis. Another possibility is that thinner walls were synthesized when cells were exposed to nano-TiO_2, which may also lead to a reduced demand for silicate. However, the silicon (Si) content and titanium (Ti) content in the cell frustules were not measured, so it is not possible to confirm whether there were any alterations in frustules synthesis.

In addition, the stimulated growth in the presence of nano-TiO_2 may also be a result of enhanced photosynthetic performance. A significantly higher maximum electron transport rate ($rETR_{max}$) and maximum light use coefficient for PSII (α) was recorded in a freshwater benthic diatom *Nitzschia palea* exposed to 5 and 10 mg/L nano-TiO_2, compared to the control group without nano-TiO_2, yet the increase in $rETR_{max}$ and α values were not significantly different to those in the control group when nano-TiO_2 concentration increased to 50 mg/L (Ockenden 2019). It has been reported that the nano-TiO_2 inside spinach cells could stimulate photochemical reactions through increasing electron transport rate and oxygen evolution rate (Hong et al. 2005) and could induce faster carbon assimilation through promoting Rubisco carboxylation (Gao et al. 2008). Carboxylation refers to the chemical reaction in which the carbon dioxide is fixed into glucose during the process of photosynthesis. Rubisco refers to the enzyme ribulose 1,5-bisphosphate carboxylase, which plays a key role in promoting the carboxylation reaction (Karcher 1995). It has previously been recorded that nano-TiO_2 can pass into algal cells in a few species including freshwater green algae *Pseudokirchneriella subcapitata* (Hartmann et al. 2010), *Scenedesmus obliquus* (Dalai et al. 2013), *Chlorella pyrenoidosa* (Middepogu et al. 2018) and the marine diatom *Skeletonema costatum* (Li et al. 2015), *Nitzschia closterium* (Xia et al. 2015), *Phaeodactylum tricornutum* (Wang et al. 2016b; Sendra et al. 2017b). It is possible that the internalization of nano-TiO_2 into estuarine benthic diatom cells occurred in the experiments undertaken in the current study, which may have enhanced the photosynthetic efficiency of

the estuarine benthic diatom cells in a similar way to that found on spinach cells (Hong et al. 2005; Gao et al. 2008), resulting in higher algal growth rates. However, the photosynthetic performance of these diatom cells was not measured in the present study.

The hormetic response of algal cells to the presence of nano-TiO_2 may contribute to a stimulated growth. This mechanism has been suggested by a number of researchers who observed a stimulation effect of nano-TiO_2 on algal growth rate with particle concentrations no greater than 20 mg/L (Hartmann et al. 2010; Xia et al. 2015; Sendra et al. 2017b). A hormetic effect is considered to occur due to an overcompensation to the disruption of homeostasis, through the adaptive response of cells (Calabrese and Baldwin 2002; Calabrese and Mattson 2017). A stimulatory hormetic response has been widely recorded in toxicological tests, yet the exact mechanism for the hormesis effect remains unclear (Agutter 2008; Calabrese 2013; Calabrese and Mattson 2017). A possible mechanism for the hormetic response may be linked to a slightly elevated ROS level. A modest increase of ROS has been reported to promote cell proliferation in cancer cells and plant cells, through modulating redox signaling and the transcription process (Fehér et al. 2008; Mittler 2017). Evidence suggested that the presence of nano-TiO_2 could increase the ROS level in algal cultures in the presence of fluorescent lighting (Li et al. 2015; Xia et al. 2015; Deng et al. 2017). It is speculated that the ROS level in the estuarine benthic diatom cultures grown in the presence of nano-TiO_2 may have fallen within the range which could have led to a stimulated cell division. No measurements were taken during this study to identify the level of ROS. However, the hormetic response is typically observed at relatively low concentrations of toxicant only, and thus it possibly did not have a marked contribution to the stimulated growth observed in the present study.

4.6.3 The impact of TiO_2 on estuarine benthic diatoms in the presence of fluorescent lighting: was primary particle size a key factor for the stimulation impact of TiO_2?

It was hypothesized that the algal growth would be more negatively affected in the presence of nano-TiO_2 compared to the presence of micro-TiO_2. The presence of both TiO_2 particles showed no adverse impact on the growth of all three estuarine benthic diatoms, in contrast to the hypothesis. Yet, the stimulation effect of nano-TiO_2 was found to be stronger than micro-TiO_2, manifested as greater increase in the growth rate in the

presence of nano-TiO_2, compared to the lack of a significant increase or a lower increase in the presence of micro-TiO_2.

Relative to the micro-TiO_2 (131 nm), nano-TiO_2 (24.4 nm) had a smaller particle size and greater surface area per mass basis. In relation to the possible mechanisms discussed in the above section, the smaller particle size of nano-TiO_2 may facilitate its incorporation into diatom frustules and its internalization into algal cells. To be noted, although nano-TiO_2 and micro-TiO_2 had different primary particle size, the hydrodynamic size of their aggregates in the culture medium was not found to be significantly different, after a short-time incubation (Section 4.3.1). It was recorded that both nano-TiO_2 and micro-TiO_2 formed large aggregates once added into algal culture (f/2 medium) (Figure 4.3). The size of the initial aggregates of nano-TiO_2 was recorded to be 1130.0 nm, which was significantly larger than the size of the initial aggregates of micro-TiO_2 at 464.0 nm, within the first 10 min. However, after 1 h of incubation in the absence of cells, the size of nano-TiO_2 aggregates and micro-TiO_2 aggregates were not significantly different and remained not significantly different over the next few hours (2 – 24 h), with size of aggregates being approximately 1600 – 1800 nm. Preliminary experiments suggested that the size of particle aggregates further increased in the presence of cells, with size being tens and even hundreds of micrometers (Figure 3.3). Nevertheless, results from the present investigation would indicate that despite their aggregation behavior, the particle form of TiO_2 with a smaller primary particle size had a greater impact on the growth of estuarine benthic diatoms, compared to the particle form with a larger primary particle size, indicating the important influence that particle size may have on the impact of TiO_2 on these algae in the presence of fluorescent lighting.

4.6.4 The impact of TiO_2 on estuarine benthic diatoms in the presence of fluorescent lighting: was there a species-specific response?

It was hypothesized that the three estuarine benthic diatoms would respond differently to the presence of nano-TiO_2 and micro-TiO_2. The extent of the stimulation in the presence of nano-TiO_2 varied between species, with the greatest increase observed for *Nitzschia* c.f. *clausii*, followed by *Navicula gregaria*, and the least increase observed for *Cylindrotheca closterium*, in accordance to the hypothesis. The impact of micro-TiO_2 also varied across species, with a stimulated effect on *Nitzschia* c.f. *clausii* only and no significant impact on *Navicula gregaria* and *Cylindrotheca closterium*, partly in accordance to the hypothesis.

The different response among three species implied that there was a species-specific sensitivity to the presence of nano-TiO_2 and micro-TiO_2. The species-specific responses might be linked to species-specific differences between their performance (e.g. growth rate, carbon assimilation rate) under the particular cultivation conditions adopted for these experiments; conditions may have not been optimal for all species. The highest growth rate was recorded in the control group of *Cylindrotheca closterium* culture ($\mu = 1.34$ day^{-1}), together with the lowest increase of growth rate (1.5%) in the nano-TiO_2 treatment. The lowest growth rate was recorded in the control group of *Nitzschia* cf. *clausii* culture ($\mu = 0.57$ day^{-1}), together with the highest increase of growth rate (25%) in the nano-TiO_2 treatment. It is possible that the current experimental setup did not provide the optimal growth condition for *Nitzschia* cf. *clausii* cells, and thus it had a higher potential to grow quicker when suitable conditions arise. Comparatively, the current experimental setup might have provided conditions that were close to the optimal growth condition required by *Cylindrotheca closterium* cells. In the field, it is common that species are growing sub-optimally. Results from the present investigation suggested the presence of nano-TiO_2 (or micro-TiO_2) might have created an environment which was more favorable for *Nitzschia* c.f. *clausii*, compared to *Navicula gregaria* and *Cylindrotheca closterium*. Such a species-specific response to the presence of nano-TiO_2 may have an impact on species composition in areas where deposition of nanoparticles is high and could knock on consequences for their grazers and the structure of the food web.

4.6.5 **Limitations and suggestions**

The volumetric flask was not used to prepare TiO_2 stocks because TiO_2 tend to adsorb onto the glass (Handy 2012). The procedure of making TiO_2 stocks in the present study (by suspending 0.02 g TiO_2 in 2 mL water) was likely to result in a lower exposure of TiO_2 compared to the nominal 100 mg/L. For nano-TiO_2 with a density of 4.26 g/mL (https://www.sigmaaldrich.com/catalog/product/aldrich/718467?lang=en&region=GB), 0.02 g nano-TiO_2 would occupy a volume of 0.0047 mL (= 0.02/4.26). Therefore, the particle concentration of nano-TiO_2 stock was estimated to be 9.977 g/L (= 0.02 g / (2 mL + 0.0047 mL), As a result, the cultures were exposed to 99.77 mg/L nano-TiO_2, which was 2.3% lower than the nominal 100 mg/L. As for micro-TiO_2 with a density of 3.9 g/mL (https://www.sigmaaldrich.com/catalog/product/sigma/t8141?lang=en&region=GB), the particle concentration of micro-TiO_2 stock was estimated to be 9.974 mg/L. As a result, the cultures

were exposed to 99.74 mg/L micro-TiO_2, which was 2.6% lower than the nominal 100 mg/L.

One limitation is that the experiments were not carried out with the presence of UVR. TiO_2 is a photocatalytic substance. Studies have reported that TiO_2 could be photoactivated by ultraviolet radiation (UVR) and the presence of UVR has been shown to play an important role in determining the impact of nano-TiO_2 on algae (Miller et al. 2012; Graziani et al. 2013; Sendra et al. 2017a). Even the presence of a low level of UVR (1.65 W/m^2) has been shown to significantly enhance the negative impact of nano-TiO_2 on algal growth (Graziani et al. 2013). The present investigation, along with other previous research work (e.g. studies listed in Table 4.4) have been conducted under laboratory conditions with fluorescent lighting which only contains a negligible level of UVR. It is possible that nano-TiO_2 was not fully activated under fluorescent lighting. For a better understanding of the risk of nano-TiO_2 on the estuarine benthic diatoms in the field where UVR is commonly present, the responses of estuarine benthic diatoms to the presence of nano-TiO_2 under UVR were investigated and results were presented in Chapter 5.

4.7 **Conclusion**

To my knowledge, this is the first study investigating the growth response of estuarine benthic mud-dwelling epipelic diatoms when exposed to nano-TiO_2 in the presence of fluorescent lighting. Three clones of benthic diatoms including *Nitzschia* c.f. *clausii*, *Navicula gregaria* and *Cylindrotheca closterium* were isolated from the Severn Estuary, UK and tested for their responses to the presence of nano-TiO_2 and micro-TiO_2.

- Significantly higher biomass yield and growth rates were recorded in all three species in the presence of 100 mg/L nano-TiO_2 and fluorescent lighting, compared to the control group. The stimulation effect was species-specific.
- The stimulation effect of nano-TiO_2 observed in the present investigation was not linked to a light shading effect of nano-TiO_2.
- The stimulation effect of nano-TiO_2 on the estuarine benthic diatoms might possibly be linked to an increased uptake rate of silicate or a reduced consumption of Si for frustule synthesis on a per cell basis or the incorporation of nano-TiO_2 into cell wall as a substitute of SiO_2. Other mechanisms such as enhanced photosynthesis and a hormetic response, may also contribute to the growth

stimulation observed in the presence of nano-TiO_2.

- The stimulation effect of micro-TiO_2 was found to be weaker than nano-TiO_2.

Chapter 5 Investigation on the response of estuarine benthic diatom *Cylindrotheca closterium* exposed to nano-TiO_2 in the presence of ultraviolet radiation

5.1 Introduction

The negative impacts of nano-TiO_2 on algae have been widely recorded. Increased oxidative stress, due to the production of excessive reactive oxygen species (ROS), is considered by many researchers to be the main reason for the observed negative impact of nano-TiO_2 (Chen et al. 2012; Miller et al. 2012; Dalai et al. 2013; Li et al. 2015; Xia et al. 2015; Roy et al. 2016; Deng et al. 2017; Sendra et al. 2017b; Sendra et al. 2017a; Middepogu et al. 2018; Jia et al. 2019; Wu et al. 2019). ROS may be produced biologically by algal cells in response to the presence of nano-TiO_2 (Li et al. 2015), or produced chemically on the surface of TiO_2 particles (Chong et al. 2010). TiO_2 is a photocatalytic substance. When irradiated by light with enough energy, photoreactions would occur on the surface of TiO_2 particles and induce the production of ROS (see section 1.6.2.2 in Chapter 1 for more details). In general, ultraviolet radiation (UVR) contains enough energy to photoactivate TiO_2 particles and to induce the production of ROS (Chong et al. 2010; Skocaj et al. 2011). Some studies have reported that the impact of nano-TiO_2 was highly dependent on the UVR level (Miller et al. 2012; Graziani et al. 2013; Roy et al. 2016; Sendra et al. 2017b; Sendra et al. 2017a). The presence of a relatively low level of UVR (1.65 W/m^2, compared to 70 – 110 W/m^2 in a clear sky on a sunny day) was shown to significantly enhance the negative impact of nano-TiO_2 on the growth of green alga *Chlorella mirabilis* (Graziani et al. 2013). Miller et al. (2012) reported that the growth of marine planktonic algae including *Thalassiosira pseudonana*, *Dunaliella tertiolecta* and *Isochrysis galbana* were significantly inhibited by the presence of 3 – 7 mg/L nano-TiO_2 under visible light (400 – 700 nm) together with UVR (8.6 W/m^2), while their growth was not affected in the presence of the same amount of nano-TiO_2 under visible light with a much lower level of UVR (0.17 W/m^2).

In addition to the growth inhibition, some studies have investigated the impact of nano-TiO_2 on the algal photophysiology. This is generally followed with use of pulse amplitude modulated (PAM) fluorometry, through the measurement of chlorophyll fluorescence (Maxwell and Johnson 2000; Consalvey et al. 2005).

The maximum quantum yield of photosystem II (PSII) after dark-adaption (Fv/Fm) has been one of the most commonly selected endpoints (Chen et al. 2012; Deng et al. 2017; Middepogu et al. 2018; Ockenden 2019), because it indicates algal photosynthetic potential and is considered to be a sensitive endpoint to environment stressors (Maxwell and Johnson 2000; Consalvey et al. 2005). Rapid light response curves (RLCs) are also increasingly applied to study algal photosynthetic performance in response to various stressors (Ralph and Gademann 2005; Perkins et al. 2006; Williamson et al. 2014). From the RLC, maximum electron transport rate ($rETR_{max}$), maximum light use coefficient (α) and light saturation coefficient (E_k) can be calculated, which can indicate any change in the algal photosynthetic activity (Consalvey et al. 2005). Although PAM measurements have been applied to study the algal photosynthetic performance in response to various stressors including heavy metal, UVR, pesticides and herbicides (Peterson et al. 1994; Juneau et al. 2001; Juneau et al. 2002; Schreiber et al. 2007; Baumann et al. 2009; Magnusson et al. 2010; Schmidt et al. 2015; Hu et al. 2016; Howe et al. 2017; Shi et al. 2017; de Baat et al. 2018; Cabrerizo et al. 2019), there have been a very limited number of studies where this method has been adopted to address the impact of nano-TiO_2 (Chen et al. 2012; Deng et al. 2017; Middepogu et al. 2018; Ockenden 2019). Chen et al. (2012) investigated the impact of nano-TiO_2 on the Fv/Fm of freshwater green alga *Chlamydomonas reinhardtii* and found decreased Fv/Fm values within 12 h when cells were exposed to 10 – 100 mg/L nano-TiO_2. However, after prolonged exposure time, the Fv/Fm in the treatment groups with nano-TiO_2 recovered and remained not significantly different from the control group until the end of exposure at 72 h. In contrast, Deng et al. (2017) found that the Fv/Fm of the marine planktonic diatom *Phaeodactylum tricornutum* exposed to nano-TiO_2 was not significant affected within 48 h of exposure, yet significantly lower Fv/Fm values were recorded at 72 h and 96 h, in the presence of 5 – 40 mg/L nano-TiO_2, compared to the control group with nano-TiO_2.

Most previous studies investigating the impact of nano-TiO_2 to date were carried out with planktonic species, with little focus on benthic species. Estuarine benthic diatoms inhabiting the intertidal area might be particularly impacted by the presence of nano-TiO_2 as they may be subjected to a higher and longer UVR exposure period compared with species in the water column, assuming they remain at the surface when the tide goes out. To my knowledge, there are no published studies on the impact of nano-TiO_2 on the estuarine benthic diatoms in the presence of UVR. Previously it was demonstrated that *Cylindrotheca closterium* grew well under laboratory conditions and its growth was only slightly stimulated by 1.5% in the presence of 100

mg/L nano-TiO_2 in the presence of fluorescent lighting (Chapter 4). Therefore, the potential stimulation effect of nano-TiO_2 may only have a marginal influence on the response of *Cylindrotheca closterium* to nano-TiO_2 in the presence of UVR. As a result, *Cylindrotheca closterium* was selected as the test species to investigate the potential impact of nano-TiO_2 in the presence of a lighting containing PAR as well as UVR (hereafter refers as UV lighting). It has been reported that a high level of UVR may inhibit algal growth (Rijstenbil 2003). Therefore, in the present study, a relatively low level of UVR (6 W/m^2), which showed no significant impact on the growth of *Cylindrotheca closterium* was applied, to assure algal growth was not stressed by UVR alone.

Aim 1: To investigate whether nano-TiO_2 posed a risk to the estuarine benthic diatom *Cylindrotheca closterium* in the presence of UV lighting, a preliminary test was conducted to test whether the growth of *Cylindrotheca closterium* was affected by the presence of 100 mg/L nano-TiO_2. This concentration of 100 mg/L was selected because it is the highest concentration suggested for testing the toxicity of a chemical by OECD (2011). The 100 mg/L concentration is also the threshold suggested by United Nations to distinguish toxic and non-toxic substances in "Globally harmonized system of classification and labelling of chemicals (GHS)" (United Nations 2015). Concerns about the possible risk(s) of the accidental release of nano-TiO_2 on organisms are mainly related to its extremely small particle size (Wigginton et al. 2007; Handy et al. 2008a; Menard et al. 2011). To investigate whether the impact of nano-TiO_2 on *Cylindrotheca closterium* in the presence of UV lighting was related to the particle size, the growth rate of *Cylindrotheca closterium* in the presence of 100 mg/L micro-TiO_2 was investigated for comparison with the impact of nano-TiO_2.

Hypothesis 1.1: Growth inhibition of nano-TiO_2 in the presence of UVR has been recorded in planktonic algae. Therefore, it was hypothesized that the growth of *Cylindrotheca closterium* would be inhibited by the presence of 100 mg/L nano-TiO_2 in the presence of UV lighting, manifested as a lower growth rate compared to the control samples (in absence of TiO_2 particles).

Hypothesis 1.2: It was hypothesized that the diatom exposed to nano-TiO_2 would be more impaired than the diatom exposed to micro-TiO_2, in the presence of UV lighting.

Aim 2: To investigate whether the growth inhibition of nano-TiO_2 on the estuarine benthic diatom *Cylindrotheca closterium* in the presence of UV lighting was a function of particle concentration, the growth of *Cylindrotheca closterium* with varying concentrations of nano-TiO_2 was followed.

Hypothesis 2: It was hypothesized that the growth inhibition of nano-TiO_2 in the presence of UV lighting would increase as particle concentration increases, until reaching the maximum inhibition of 100%.

Aim 3: To investigate whether the growth inhibition of nano-TiO_2 on the estuarine benthic diatom *Cylindrotheca closterium* in the presence of UV lighting was affected by cultivation time, the growth of *Cylindrotheca closterium* in the presence of nano-TiO_2 was followed every 24 h within the period of 72 h.

Hypothesis 3: In common with other motile benthic diatoms, *Cylindrotheca closterium* would be expected secrete extracellular polymeric substances (EPS) during growth (Smith and Underwood 1998; Smith and Underwood 2000). The presence of EPS has been reported to contribute to the detoxification and enhance the resistance of the marine planktonic diatom *Phaeodactylum tricornutum* cells to the presence of nano-TiO_2 (Sendra et al. 2017a). Therefore, it was hypothesized that the growth inhibition of nano-TiO_2 in the presence of UV lighting would decrease as cultivation time increases.

Aim 4: To investigate the impact of nano-TiO_2 on the photophysiology of the estuarine benthic diatom *Cylindrotheca closterium* in the presence of UV lighting, the photophysiology of *Cylindrotheca closterium* was assessed by PAM measurements after 72 h of exposure.

Hypothesis 4: It was hypothesized that the photosynthetic performance of *Cylindrotheca closterium* would be impaired by nano-TiO_2 in the presence of UV lighting.

5.2 Methods

5.2.1 Culture condition

A clone of the epipelic estuarine benthic diatom *Cylindrotheca closterium* was isolated from the Severn

Estuary, UK). Information about the clonal culture was detailed in Section 3.2.1 in Chapter 3. Cells at exponential growth phase were harvested for experiments.

5.2.2 TiO_2 particles

Micro-TiO_2 (product no. T8141) and nano-TiO_2 (Aeroxide® P25, product no.718467) particles were bought from Sigma-Aldrich. Their characteristics were shown in section 4.3.1 in Chapter 4.

Stocks of TiO_2 were prepared Milli-Q water immediately before experiments. The TiO_2 stocks were ultrasonicated for 15 min in a water bath (110W, 40 kHz) before dispersing into fresh f/2 medium to achieve the desired concentrations. The particle suspensions were exposed to cells within 10 minutes of preparation.

5.2.3 The impact of TiO_2 particle type on the growth of *Cylindrotheca closterium* in the presence of UV lighting

To find out whether *Cylindrotheca closterium* responded differently to the presence of nano-TiO_2 and micro-TiO_2 (aim 1), the growth rates of *Cylindrotheca closterium* exposed to different type of TiO_2 were determined after a period of 72 h. A negative control was set up at the same time to test the impact of UVR on the growth rate of *Cylindrotheca closterium*.

Algal cultures were exposed to 100 mg/L nano-TiO_2 (nano-TiO_2 treatment) or 100 mg/L micro-TiO_2 (micro-TiO_2 treatment) for 72 h as stated in section 3.2.3.1. Two blank control groups were setup by growing cells in f/2 medium without nano-TiO_2. Each group occupied a well in the 12-well microplate. The initial biomass in the algal sample was 1.0×10^4 cells/ml. One control group and 2 treatments were incubated in static condition illuminated by Repti-Glo 5.0 bulbs (Exo Terra, Rolf C. Hagen Inc). The light emitted by Repti-Glo 5.0 PAR (400 – 700 nm) of 80 µmol m^{-2} s^{-1}, UVA (320 – 400 nm) of 16.7 µmol m^{-2} s^{-1} and UVB (280 – 320 nm) of 1.1 µmol m^{-2} s^{-1} (measured by Ocean Optics Flame Spectrometer, Model Flame-S-UV-VIS-ES, Ocean Optics, Inc), and thereafter referred to as UV lighting. The negative control group was incubated in under fluorescent lighting with PAR of 80 µmol m^{-2} s^{-1}, which was the illumination used in experiments reported in Chapter 4. After 72 h, samples were harvested for cell density measurement at 72 h as described in section 4.2.3 and growth rate was calculated according to section 4.2.4. All assays were run in six

replicates.

5.2.4 The impact of nano-TiO_2 on the growth of *Cylindrotheca closterium* in relation to particle concentration and cultivation time in the presence of UV lighting

To investigate whether the growth inhibition of nano-TiO_2 on *Cylindrotheca closterium* was related to particle concentration (aim 2) and exposure time (aim 3), the growth of *Cylindrotheca closterium* with varying concentrations of nano-TiO_2 was followed every 24 h within the period of 72 h.

Algal cultures were exposed to varying concentrations of nano-TiO_2 (2, 5, 10 and 20 mg/L) for 72 h as stated in section 3.2.3.1. A blank control groups was setup by growing cells in f/2 medium without nano-TiO_2. The initial biomass in the algal sample was 2.3×10^4 cells/ml. This biomass was selected to ensure the initial chlorophyll *a* content in the *Cylindrotheca closterium* culture was higher than the detection limit. Microplates were incubated under UV lighting as described in section 5.2.3. *Cylindrotheca closterium* samples was harvested at 24, 48 and 72 h for cell density measurement and chlorophyll *a* measurement as described in section 4.2.3. All assays were run in four replicates.

5.2.5 The impact of nano-TiO_2 on the photophysiology of *Cylindrotheca closterium* in the presence of UV lighting

To investigate whether the presence of nano-TiO_2 affected the photophysiology of *Cylindrotheca closterium* (aim 4), the photosynthetic performance of *Cylindrotheca closterium* was measured with a water-PAM after a period of 72 h.

Five groups (1 control + 4 treatments) of algal samples were prepared according to section 5.2.4, with nano-TiO_2 concentration being 0, 2, 5, 10 and 20 mg/L. Each replicate contained 4.5 mL algal culture and occupied a 35 mm vented petri dishes (polystyrene, Corning®). The 12-well microplates were not used in this experiment, because samples may be affected during the measurement of another sample within the same microplate due to light scattering. The initial biomass in the algal sample was 2.3×10^4 cells/ml, in accordance to the starting states in the experiment conducted in section 5.2.4. All the petri dishes containing *Cylindrotheca closterium* were incubated as described in section 5.2.4. The PAM measurements were

conducted after 72 h of cultivation. All assays were run in four replicates.

5.2.6 Growth measurements and calculations

5.2.6.1 Cell density measurement

For cell enumeration, preserved cells were re-suspended with a vortex mixer for 30 seconds and then loaded into a haemocytometer chamber (Mod-Fuchs Rosenthal BS748, Weber, 0.2 mm deep). Cells were left to settle for 2 min and then examined under a magnification of ×400 with a light microscope (Olympus CH, Japan). Cells being transparent without a clear protoplast were considered as dead and were not counted.

5.2.6.2 Calculation of growth rate inhibition and IC50 value

The growth rate was calculated based on the cell density according to the equation 5.1 (OECD 2011).

$$\mu_{i-j}\ (\mathrm{day}^{-1}) = \frac{\ln C_j - \ln C_i}{t_i - t_i} \qquad \text{(eq 5.1)}$$

where $\mu_{i\text{-}j}$ is the average growth rate from time *i* to time *j*, C_i and C_j is the cell density at time *i* and time *j*, t_i and t_j is the time *i* (day) and time *j* (day).

The inhibition percentage on growth rate (IP) was calculated according to equation 5.2 (OECD 2011).

$$\mathrm{IP}_{i-j}\ (\%) = \begin{cases} 100 \times \dfrac{\mu_{i-j\ control} - \mu_{i-j\ treatment}}{\mu_{i-j\ control}}, \mu_{i-j\ treatment} > 0 \\ 100\quad, \mu_{i-j\ treatment} \leq 0 \end{cases} \qquad \text{(eq 5.2)}$$

where $\mu_{i\text{-}j\ control}$ is average growth rate of the control group (without TiO_2) from time *i* to time *j*, $\mu_{i\text{-}j\ treatment}$ is growth rate of a treatment replicate from time *i* to time *j*.

Dose-response curves were constructed by plotting IP against the log value of the particle concentrations. IC50 values (the concentration at which the inhibition percentage on growth rate is 50%) were calculated by fitting the dose-response curve with a log-logistic mode (Seefeldt et al. 1995).

5.2.6.3 Chlorophyll *a* measurement

Chlorophyll *a* content in the samples and the chlorophyll *a* content per cell were determined as described in section 4.2.5.

5.2.7 PAM measurements and calculations

5.2.7.1 Rapid light curve measurements

The rapid light response curve (RLC) method was followed to indicate the photosynthetic performance of *Cylindrotheca closterium*. After 72 h of exposure, *Cylindrotheca closterium* grew closely attached to the bottom of the petri dish, forming a layer of biofilm. The RLC of *Cylindrotheca closterium* was measured with a water-PAM (FIBER version, Walz, Germany), which is best suited for examinations with biofilms. For each sample, the upper 3.7 mL of medium was carefully removed, in order to expose cells for the PAM measurements without drying them. Cells in the petri dish was dark adapted for 15 min before measurement (Defew et al. 2004). The purpose of the dark adaptation was to obtain the maximum quantum yield of PSII after dark-adaption ($Fv/Fm = 1 – F_0/F_m$), which requires the measurement of minimal fluorescence (F_0) and the maximal fluorescence (F_m) after dark adaption. After dark adaption, the FIBRE probe of the water-PAM was placed at a set distance of 0.2 mm above the cells, to avoid the direct contact of the probe with the cells, and the fibre probe was fixed in position to ensure the same area of the biofilm was measured during the measurement. The inbuilt light curve function in the water-PAM was performed by applying the saturation pulse technique (a saturating light pulse of 3000 µmol quanta m^{-2} s^{-1} was applied for 600 ms) to the culture sample every 20 s after exposing the culture to each of 9 gradually increased actinic light levels (0 – 250 µmol m^{-2} s^{-1}). The effective quantum efficiency of PSII (Y(II)) was recorded at each light level (PAR, µmol m^{-2} s^{-1}). Rapid light curves (RLCs) were constructed by plotting relative electron transport rate ($rETR = 0.5 \times PAR \times Y(II)$) values against light level (PAR).

5.2.7.2 Calculation of photophysiological parameters

The maximum quantum yield of PSII after dark adaption (Fv/Fm) was obtained immediately after dark adaption. It was directly derived from the Wincontrol Software for the water-PAM.

The maximum electron transport rate ($rETR_{max}$), maximum light use coefficient (α) and light saturation coefficient ($E_k = rETR_{max}/\alpha$) were obtained by fitting the RLCs with the model of Eilers and Peeters (1988) (equation 5.3, Figure 5.1).

$$rETR = rETR_{max}\left(1 - \exp\left(\frac{-\alpha E}{rETR_{max}}\right)\right) \quad \text{(eq 5.3)}$$

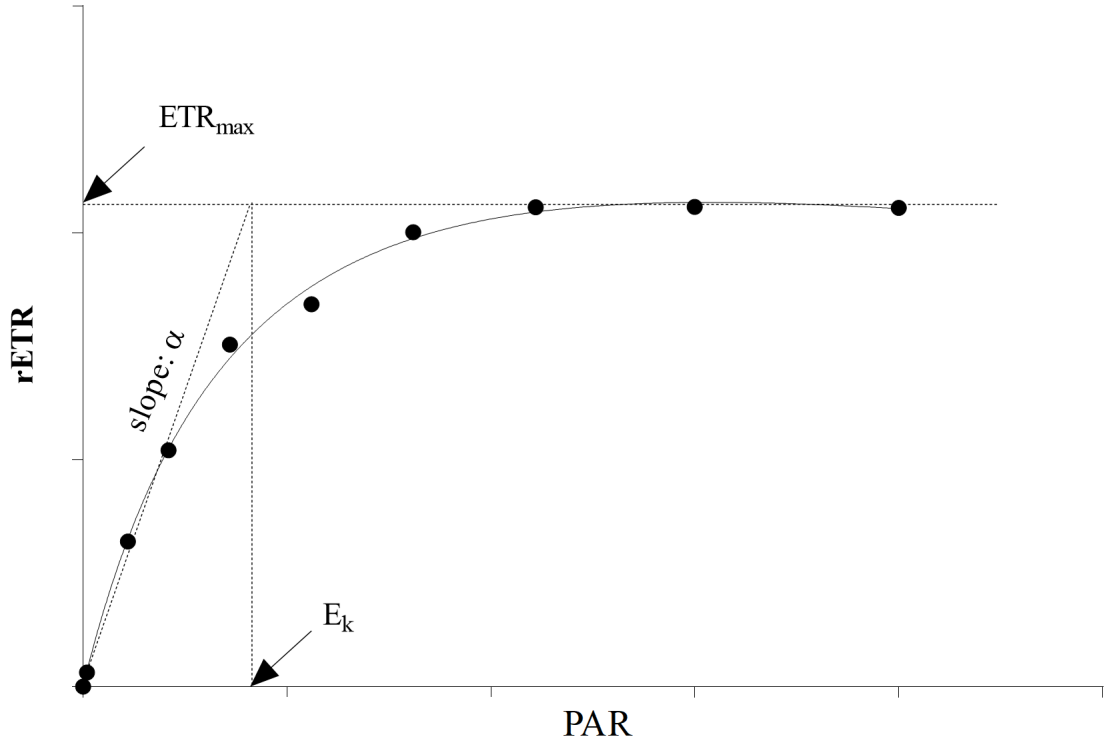

Figure 5.1 An example of a typical rapid light curve.

5.2.8 **Data analyses**

Tests for the statistical significance between values were performed using SPSS software (version 24.0 of SPSS for Windows). After checking the normality of the residuals by Kolmogorov-Smirnov test, parametric tests (e.g. ANOVA tests) were applied to determine the difference between groups. Data were transformed by the Box-Cox method before analysis where necessary. The dose-response curves and rapid light curves were fitted in GraphPad Prism 6.0 software (https://www.graphpad.com/, GraphPad Software). The IC50 values (mean and 95% confidence interval) and the significance of the differences between two IC50 values (assessed by Extra sum-of-squares F test) were determined by GraphPad Prism 6.0. The values of $rETR_{max}$,

α and E_k were also determined by GraphPad Prism 6.0. The significance level was set at < 0.05.

5.3 Results

5.3.1 Impact of TiO_2 particle type on the growth of *Cylindrotheca closterium* in the presence of UV lighting

The average growth rate within 72 h was calculated to indicate the impact of two TiO_2 particle types on the growth of *Cylindrotheca closterium* (Figure 5.2). In the presence of UV lighting, the growth rate of *Cylindrotheca closterium* exposed to 100 mg/L micro-TiO_2 was 82% lower than that in the control group; in the treatments with 100 mg/L nano-TiO_2, the biomass (assessed by cell density) at 72 h was lower than the starting biomass, such that there was a negative growth rate ($\mu = -0.76$ day^{-1}). The average growth rate in the negative control group cultivated in the presence of fluorescent lighting ($\mu = 1.33 \pm 0.02$ day^{-1}) was not significantly different from the control group cultivated in the presence of UV lighting ($\mu = 1.34 \pm 0.02$ day^{-1}), according to a one-way ANOVA test ($F_{1,10} = 0.275$, $p = 0.249$).

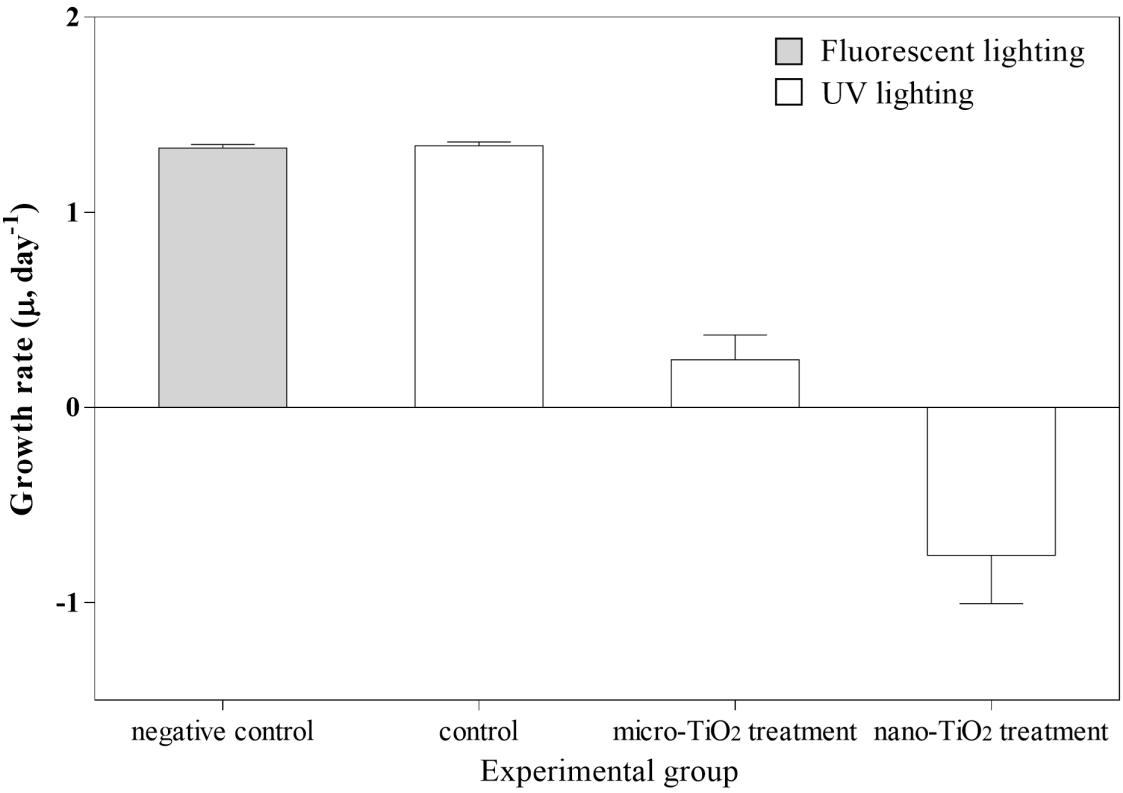

Figure 5.2 The average growth rate within 72 h for *Cylindrotheca closterium* cultures in the control group (without TiO_2) and treatments with 100 mg/L micro-TiO_2 and 100 mg/L nano-TiO_2, in the presence of fluorescent lighting (grey bar) or UV lighting (white bars). Results are shown as mean ± standard deviation (n = 6).

5.3.2 The impact of nano-TiO_2 on the growth of *Cylindrotheca closterium* in relation to particles concentration and cultivation time in the presence of UV lighting

5.3.2.1 Growth curve of *Cylindrotheca closterium* with varying concentrations of nano-TiO_2 in the presence of UV lighting

The cell density in the *Cylindrotheca closterium* cultures with varying concentrations of nano-TiO_2 in the presence of UV lighting were measured every 24 h and the results are plotted as growth curves in Figure 5.3. The cell density in the control group grown without TiO_2 increased as cultivation time increased, from 2.3×10^4 cells/mL at time zero to 1.3×10^6 cells/mL at 72 h. Treatment with 2 mg/L nano-TiO_2 had almost the same growth profile as the control group, with cell density being not significantly different from the control

group at each measuring point. The treatments with 5 and 10 mg/L nano-TiO_2 showed similar growth profiles to the control group, but the cell density in these two groups were significantly lower than that in the control group. The cell density in the treatment with 5 mg/L nano-TiO_2 at selected time points were 36.7% (at 24 h), 58.3% (at 48 h) and 27.8% (at 72 h) lower than that in the control group. The cell density in the treatment with 10 mg/L nano-TiO_2 at selected time points were 62.5% (24 h), 91.0% (48 h) and 92.6% (72 h) lower than that measured in the control group. The treatment with 20 mg/L nano-TiO_2 exhibited a different growth profile compared with the other four groups. The cell density in the treatment with 20 mg/L nano-TiO_2 increased by 17% in the first 24 h and then decreased in the next 48 h, with the cell density at 72 h being 30% lower than the starting cell density at time zero.

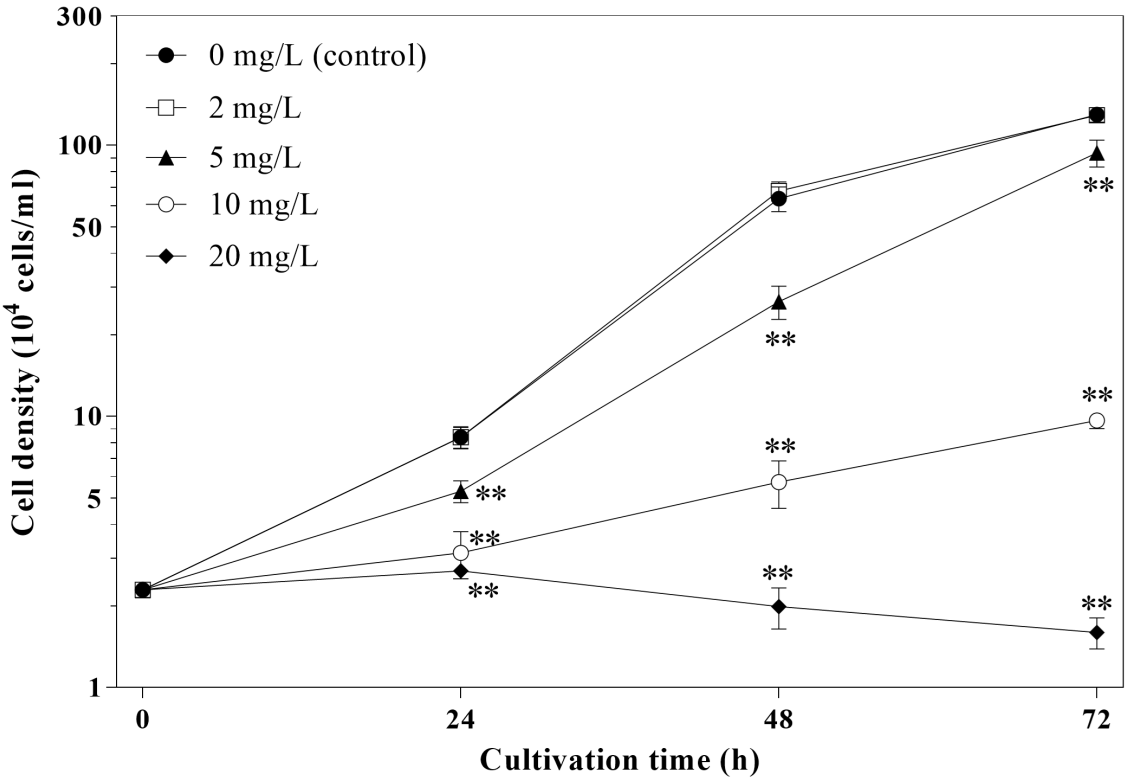

Figure 5.3 The growth curves of *Cylindrotheca closterium* cultures with varying concentrations of nano-TiO_2 in the presence of UV lighting, indicated by temporal change in cell density. The concentration of nano-TiO_2 is denoted by different symbols. Results are shown as mean ± standard deviation (n = 4). The Y-axis is shown in log-scale. Significant difference compared to the control group was marked as * ($0.01 \leq p < 0.05$) and ** ($p < 0.01$) next to the symbol, based on TukeyHSD *post-hoc* test, at each measuring time point.

It was evident that there was a temporal variation in the growth rates, hence growth rates were determined for each day. The daily growth rates of *Cylindrotheca closterium* with varying concentrations of nano-TiO_2 within the period of 3 days (72 h) were calculated (Table 5.1). Temporal changes of growth rate were noted in all groups. In the control group, the highest growth rate was recorded on day 2 (24 – 48 h, $\mu = 2.02$ day^{-1}) and the lowest growth rate was noted on day 3 (48 – 72 h, $\mu = 0.71$ day^{-1}). Similar temporal patterns were also recorded in the treatments nano-TiO_2 (Table 5.1).

As shown in Table 5.1, the growth rate in the treatment with 2 mg/L nano-TiO_2 was not significantly different from the control group, at each selected measuring time; the growth rate in the treatment with 5 mg/L nano-TiO_2 was significantly lower on the first two days, but reverted to be significantly higher on the third day, compared to the control group; the growth rate in the treatments with 10 and 20 mg/L nano-TiO_2 was significantly lower than the control group, at each selected measuring time.

Table 5.1 The daily growth rate of *Cylindrotheca closterium* with varying concentrations of nano-TiO_2 in the presence of UV lighting. Results are shown as mean ± standard deviation (n = 4). Significant differences compared to the control group are marked as * ($0.01 \leq p < 0.05$) and ** ($p < 0.01$), based on TukeyHSD *post-hoc* test.

Particle concentration (mg/L)	**Daily growth rate (day^{-1})**		
	0 – 24 h	**24 – 48 h**	**48 – 72 h**
0 (control)	1.29 ± 0.09	2.02 ± 0.10	0.71 ± 0.06
2	1.29 ± 0.09	2.09 ± 0.08	0.64 ± 0.06
5	0.84 ± 0.09 **	1.60 ± 0.14 **	1.26 ± 0.11 **
10	0.30 ± 0.20 **	0.58 ± 0.21 **	0.52 ± 0.07 *
20	0.16 ± 0.06 **	-0.32 ± 0.19 **	-0.23 ± 0.13 **

5.3.2.2 IC50 values of nano-TiO_2 for *Cylindrotheca closterium* in the presence of UV lighting

The inhibition percentage on growth rate (IP) at 24 h (for the period of 0 – 24 h), 48 h (for the period of 0 – 48 h) and 72 h (for the period of 0 – 72 h) was calculated and plotted against nano-TiO_2 concentration in Figure 5.4. The log-logistic model provided a good fit of the dose-response curves with $R^2 \geq 0.93$. The 24 h-IC50 value (6.48 mg/L) and the 48 h-IC50 (7.09 mg/L) was not significantly different (Extra sum-of-squares F test, $F_{1,28} = 1.688$, $p = 0.205$). The 72 h-IC50 (8.73 mg/L) was significantly higher than the 24 h-IC50 and 48 h-IC50 (Extra sum-of-squares F test, $F_{1,28} \geq 23.26$, $p < 0.001$).

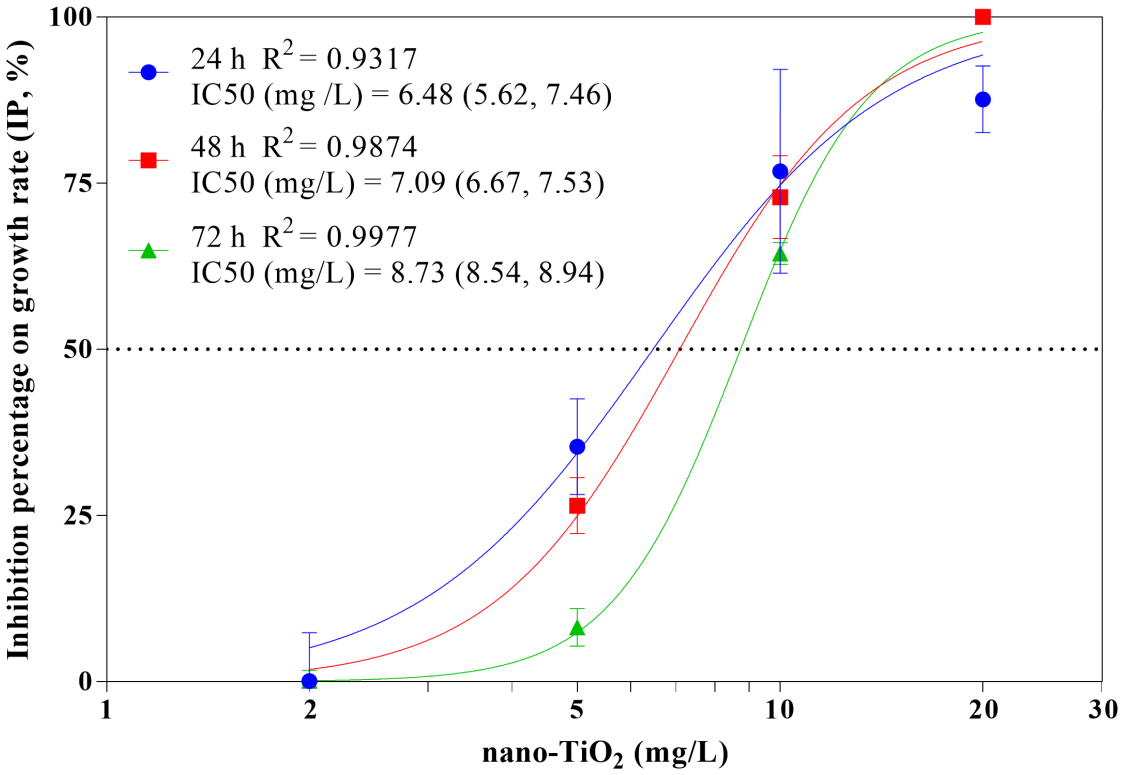

Figure 5.4 Dose-response curves of *Cylindrotheca closterium* to the presence of nano-TiO_2 after different periods of cultivation (denoted by colour), in the presence of UV lighting. Responses are defined as the inhibition percentage on growth rate (IP) in the treatment group compared to the control group grown without TiO_2. Results are shown as mean ± standard deviation (n = 4). Curves were fitted with a log-logistic model. The R^2 values indicate the goodness of curve fitting are shown in the figure. The IC50 values are shown as mean and 95% confidence interval in the parentheses in the figure.

5.3.2.3 Cellular chlorophyll *a* concentration of *Cylindrotheca closterium* with varying concentrations of nano-TiO_2 in the presence of UV lighting

The cellular chlorophyll *a* concentrations of *Cylindrotheca closterium* with varying concentrations of nano-TiO_2 at 24 h, 48 h and 72 h were calculated (Table 5.2). The cellular chl *a* content in the control group was not significantly changed within the period of 72 h, according to a one-way ANOVA test ($F_{2,9} = 0.183$, $p = 0.836$). Temporal changes of cellular chl *a* were noted in treatments with the presence of nano-TiO_2. A decrease trend in the cellular chl *a* concentration was recorded in the treatment with 2 mg/L nano-TiO_2. On contrast, increase trends in the cellular chl *a* concentration was recorded in the treatment with 5 – 20 mg/L nano-TiO_2.

As shown in Table 5.2, the chl *a* per cell in the treatment with 2 or 5 mg/L nano-TiO_2 was not significantly different from the control group, at each selected measuring time; the chl *a* per cell in the treatment with 10 mg/L nano-TiO_2 was significantly lower than the control group on the first day only; the chl *a* per cell in the treatment with 20 mg/L nano-TiO_2 was significantly lower than the control group at the first day, and was significantly higher than the control group on the third day.

Table 5.2 The chlorophyll *a* concentration (pg per cell) of *Cylindrotheca closterium* with varying concentrations of nano-TiO_2 in the presence of UV lighting, after different cultivation time. Results are shown as mean ± standard deviation (n = 4). Significant difference compared to the control group was marked as * ($0.01 \leq p < 0.05$) and ** ($p < 0.01$), based on TukeyHSD *post-hoc* test.

Particle concentration (mg/L)	24 h	48 h	72 h
0 (control)	0.78 ± 0.02	0.78 ± 0.05	0.76 ± 0.07
2	0.82 ± 0.06	0.80 ± 0.03	0.68 ± 0.08
5	0.75 ± 0.06	0.80 ± 0.03	0.84 ± 0.03
10	0.50 ± 0.19 *	0.88 ± 0.17	0.93 ± 0.13
20	0.34 ± 0.23 **	0.64 ± 0.09	1.18 ± 0.14 **

5.3.3 Impact of nano-TiO_2 on the photophysiology of *Cylindrotheca closterium*

The photosynthetic performance of *Cylindrotheca closterium* was determined by rapid light curve (RLC) measurement with a water-PAM. The RLCs of the control and the treatments with 2 and 5 mg/L nano-TiO_2 are illustrated in Figure 5.5. Unfortunately, due to the low fluorescence signal (because of the relatively low concentration of chlorophyll *a*), the RLC measurements could not be performed for treatments with 10 and 20 mg/L nano-TiO_2. The RLCs from the control and the treatment with 2 mg/L nano-TiO_2 followed a similar pattern, which was different to the RLC of the treatment with 5 mg/L nano-TiO_2.

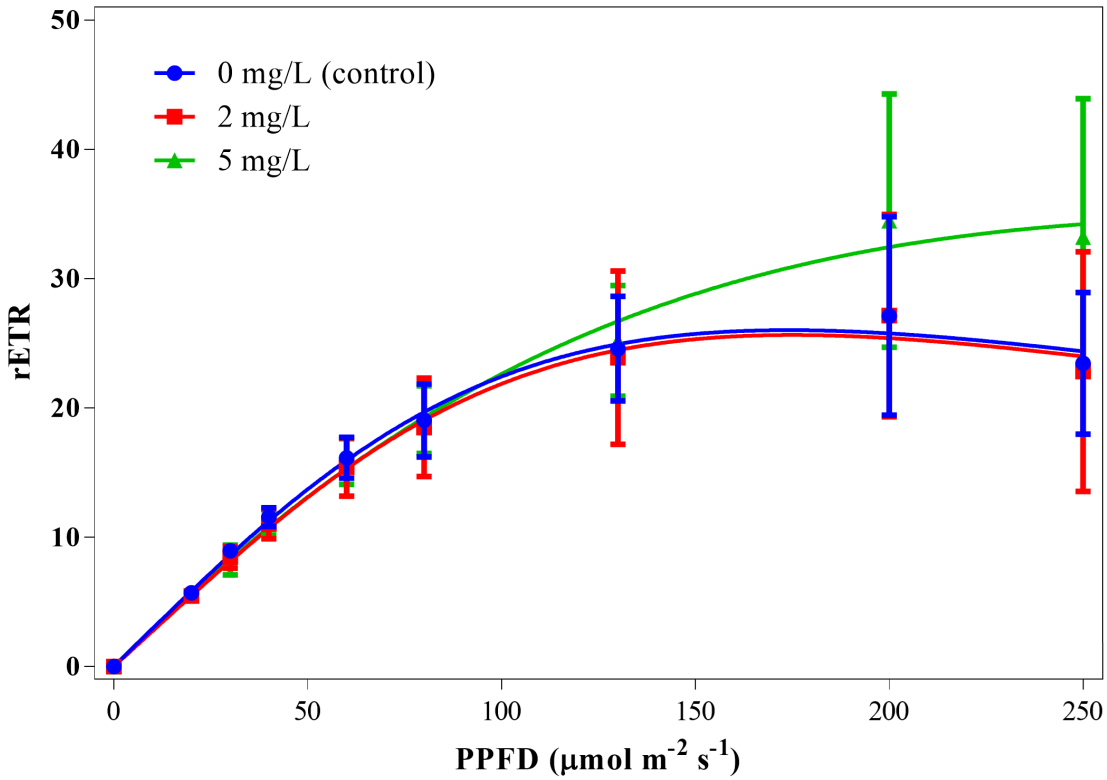

Figure 5.5 Rapid light curves (RLCs) of *Cylindrotheca closterium* cultures with varying concentrations of nano-TiO_2 (denoted by different symbols), in the presence of UV lighting. Results are shown as mean ± standard deviation (n = 4). The RLC curve was fitted with the model of Eilers and Peeters (1988).

Four photophysiological parameters including the maximum quantum yield of PSII after dark-adaption (Fv/Fm), maximum electron transport rate ($rETR_{max}$), maximum light use coefficient (α) and light saturation coefficient (E_k) were derived from the RLC measurements (Table 5.3). Considerable variations were recorded among replicates. According to one-way ANOVA tests, the difference between three groups were not significant, for all four parameters (Fv/Fm, $F_{2, 9} = 0.844$, $p = 0.461$; $rETR_{max}$, $F_{2, 9} = 1.300$, $p = 0.319$; α, $F_{2, 9} = 0.285$, $p = 0.759$; E_k, $F_{2, 9} = 0.887$, $p = 0.445$).

Table 5.3 The maximum quantum yield of PSII after dark-adaption (Fv/Fm), maximum electron transport rate ($rETR_{max}$), maximum light use coefficient (α) and light saturation coefficient (E_k) of *Cylindrotheca closterium* with varying concentration of nano-TiO_2 in the presence of UV lighting, after 72 h of cultivation. Results are shown as mean ± standard deviation (n = 4).

Particle concentration (mg/L)	Fv/Fm	$rETR_{max}$	α	E_k (μmol m^{-2} s^{-1})
0 (control)	0.621 ± 0.034	26.8 ± 6.1	0.297 ± 0.025	91.7 ± 26.9
2	0.579 ± 0.051	26.3 ± 8.4	0.276 ± 0.019	95.3 ± 29.1
5	0.604 ± 0.053	35.1 ± 10.7	0.291 ± 0.063	128.3 ± 62.8

5.3.4 Summary of results

- In the presence of UV lighting, the growth rate of *Cylindrotheca closterium* was significantly inhibited by 100 mg/L nano-TiO_2 and micro-TiO_2, with greater inhibition recorded in the presence of nano-TiO_2. The amount of UVR in the UV lighting showed no significant impact on the growth of *Cylindrotheca closterium*, in absence of nano-TiO_2.
- The growth inhibition of nano-TiO_2 in the presence of UV lighting on the *Cylindrotheca closterium* increased as particle concentration increased from 5 to 20 mg/L, with IC50 values being approximately 6 – 8 mg/L.
- In the presence of UV lighting, the photophysiology of *Cylindrotheca closterium* exposed to 2 and 5 mg/L nano-TiO_2 was not significant different from the control, after 72 h of exposure.

5.4 Discussion

5.4.1 The impact of TiO_2 on estuarine benthic diatoms in the presence of UV lighting: was primary particle size a key factor for the growth inhibition of TiO_2?

It was hypothesized that the growth rate of *Cylindrotheca closterium* exposed to 100 mg/L nano-TiO_2 would be inhibited compared to the control group, and the inhibition recorded with nano-TiO_2 would be greater than that recorded with micro-TiO_2, in the presence of UV lighting. In the present investigation, the growth rate of *Cylindrotheca closterium* was 82% inhibited by the presence of 100 mg/L micro-TiO_2 and was 100% inhibited by the presence of 100 mg/L nano-TiO_2, compared to the control group, in accordance with the hypothesis.

The amount of UVR in the UV lighting did not significantly affect the growth rate of *Cylindrotheca*

closterium, in the absence of TiO_2. Results from Chapter 4 revealed that the presence of 100 mg/L nano-TiO_2 and micro-TiO_2 did not negatively affect the growth rate of *Cylindrotheca closterium*, in the presence of fluorescent lighting with a negligible amount of UVR. Therefore, the negative impact of nano-TiO_2 and micro-TiO_2 on the growth rate of *Cylindrotheca closterium* observed in the present study was considered to result from the interaction between UVR and TiO_2 particles, which was likely be linked to the photoactivation of TiO_2 particles in the presence of UVR.

When activated by UVR, photoreactions would happen on the surface of TiO_2 particles and induce the production of ROS (reviewed in section 1.6.2.2 in Chapter 1). The elevated oxidative stress as a result of excessive production of ROS is considered to be the main reason for the observed growth inhibition effect on algae in the presence of nano-TiO_2 and UVR (Miller et al. 2012; Roy et al. 2016; Sendra et al. 2017b). Results from the present investigation indicated ROS production in the nano-TiO_2 treatment may have been higher than that in the micro-TiO_2 treatment, based on the differences in growth inhibition. Because ROS are generated at the surface of TiO_2 particles (Chong et al. 2010), the ROS production is expected to be positively correlated with total particle surface area. With a smaller particle size, the surface area of nano-TiO_2 per mass basis (44.83 m^2/g) was measured to be 4.5 times higher than micro-TiO_2 (9.97 m^2/g). However it is noted that both particles formed large aggregates once added into the culture medium (f/2 medium). The immediately formed aggregates (i.e. those forming within 10 min) of the smaller nano-TiO_2 in the f/2 medium was found to be larger, at 1130.0 ± 160.8 nm, while the aggregates of the larger micro-TiO_2 was found to be smaller, at 464.0 ± 88.6 nm (Figure 4.3). Preliminary experiments suggested that the size of particle aggregates may further increase over time. The aggregation may result in a decreased available particle surface area compared to the theoretical value. Nevertheless, results from the present investigation would indicate that despite their significant aggregation behavior, the particle form of TiO_2 with a smaller primary particle size may possibly have induced a greater ROS production compared to the particle form of TiO_2 with a larger primary particle size, confirming the influence of particle size on the impact of TiO_2 in the presence of UV lighting.

5.4.1 The IC50 value of nano-TiO_2 for *Cylindrotheca closterium* in the presence of UV lighting

It was hypothesized that the growth inhibition of nano-TiO_2 in the presence of UV lighting would increase as particle concentration increases, until reaching the maximum inhibition of 100%. In the present investigation, a positive relationship between particle concentration and the IP for *Cylindrotheca closterium* was observed in the presence of UV lighting, in accordance with the hypotheses. The 72 h-IC50 value of nano-TiO_2 for *Cylindrotheca closterium* was calculated to be 8.73 mg/L with 95% confidence interval of 8.54 – 8.94 mg/L.

Previous studies that investigated the impact of nano-TiO_2 with the presence of UVR are summarized in Table 5.4. Studies conducted with diatoms have been marked by highlighting species names in bold. The 72 h-IC50 of nano-TiO_2 for marine planktonic diatom *Phaeodactylum tricornutum* was found to be 1.98 mg/L, which was 4.4 times lower than the 72 h-IC50 value for *Cylindrotheca closterium*. Results from the present investigation indicated that IP tend to decrease over time (see discussion in section 5.4.2), suggesting that the IP value of nano-TiO_2 for *Cylindrotheca closterium* at 96 h may not be greater than that observed at 72 h. Comparably, the growth of marine planktonic diatom *Thalassiosira pseudonana* was completely inhibited by the presence of 5 mg/L nano-TiO_2, while the IP of 5 mg/L nano-TiO_2 of *Cylindrotheca closterium* was no greater than 8.2%. Together, these results suggested that the estuarine benthic diatoms species tested in the present study may have a higher tolerance to nano-TiO_2, compared to the marine planktonic species in the water column.

The inhibition effect of nano-TiO_2 in the presence of UVR has also been recorded in other types of planktonic algae, and mainly in green algae (Table 5.4). The 72 h-IC50 values obtained with freshwater planktonic green algae ranged between 1.565 – 2.3 mg/L, which was 3.8 – 5.6 times lower than the 72 h-IC50 value for *Cylindrotheca closterium*. In two studies with *Isochrysis galbana* (marine Prymnesiophyceae) and *Amphidinium carterae* (marine Dinophyceae), a significant inhibition was recorded in the presence of 1 mg/L nano-TiO_2, while the growth of *Cylindrotheca closterium* was not significantly affected by the presence of 2 mg/L nano-TiO_2. In another study with *Dunaliella tertiolecta* (marine green alga), a 100% inhibition was recorded in the presence of 5 mg/L nano-TiO_2, while the IP of 5 mg/L nano-TiO_2 of

Cylindrotheca closterium was anticipated to be no greater than 8.2%, after 96 h of exposure.

These comparisons suggested the estuarine benthic diatom *Cylindrotheca closterium* might be more tolerant to nano-TiO_2 in the presence of UVR, compared to those planktonic species. A further discussion about the possible reasons for the higher tolerance of *Cylindrotheca closterium* is presented in section 7.2 in Chapter 7.

Table 5.4 Impact of nano-TiO_2 on different algae cultivated with the presence of UVR. Studies with marine species are shown first, followed by studies with freshwater species. Studies with diatoms were marked in bold. **IC50** (mg/L) = the concentration of nano-TiO_2 at the inhibition on the growth rate is 50%. **IP (X)** = Inhibition percentage of growth rate in the presence of **X** mg/L nano-TiO_2.

Algal species		**Primary particle size (nm)**	**Crystal structure**	**Culture medium**	**UVR (W/m^2)**	**IC50 or IP**	**Reference**
Estuarine benthic Bacillariophyceae	***Cylindrotheca closterium***	24.4	85.8 % anatase 14.2 % rutile	f/2	5.6 (UVA) 0.4 (UVB)	**72 h-IC50: 8.73** 72 h-IP = 0 (2) 72 h-IP = 8.2% (5)	The present study
Marine planktonic Bacillariophyceae	***Thalassiosira pseudonana***	15 – 30	81% anatase 19% rutile	f/2	4.5 (UVA) 4.1 (UVB)	96 h-IP = 100% (5)	Miller et al. (2012)
	Phaeodactylum tricornutum	38	79% anatase 21% rutile	f/2	2 (UVA)	**72 h-IC50: 1.98**	Sendra et al. (2017a)
Marine planktonic Dinophyceae	*Amphidinium carterae*	38	79% anatase 21% rutile	f/2	Solar light	72 h-IP > 0 (1)	Sendra et al. (2017b)
Marine planktonic Chlorophyceae	*Dunaliella tertiolecta*	10 – 50	mainly anatase	f/2	4.5 (UVA) 4.1 (UVB)	96 h-IP = 100% (5)	Miller et al. (2012)
Marine planktonic Prymnesiophyceae	*Isochrysis galbana*	10 – 50	mainly anatase	f/2	4.5 (UVA) 4.1 (UVB)	96 h-IP > 0 (1)	Miller et al. (2012)
Freshwater planktonic Chlorophyceae	*Scenedesmus obliquus*	10 – 50	mainly anatase	BG11	4.4 (UVR)	**72 h-IC50: 1.76**	Dalai et al. (2013)
	Scenedesmus sp.	20.65	81.1% anatase 18.9 % rutile	BG11	10 (UVA)	**72 h-IC50: 2.275**	Roy et al. (2016)
	Chlamydomonas reinhardtii	38	79% anatase 21% rutile	Freshwater medium	2 (UVA)	**72 h-IC50: 2.30**	Sendra et al. (2017a)
Freshwater planktonic Trebouxiophyceae	*Chlorella* sp.	20.65	81.1% anatase 18.9 % rutile	BG11	10 (UVA)	**72 h-IC50: 1.565**	Roy et al. (2016)

5.4.2 The temporal change of growth inhibition of nano-TiO_2 in the presence of UV lighting

It was hypothesized that the growth inhibition of nano-TiO_2 on *Cylindrotheca closterium* would decrease over time, due to the detoxification of EPS. The IC50 values of nano-TiO_2 for *Cylindrotheca closterium* followed an order of 24 h-IC50 (6.48 mg/L) ≈ 48 h-IC50 (7.09 mg/L) < 72 h-IC50 (8.73 mg/L), partly in accordance with the hypothesis. To my knowledge, this is the first study which reported the temporal change of IC50 value of nano-TiO_2 in the presence of UV lighting. For those studies shown in Table 5.4, only the growth inhibition at the end of exposure (72 h or 96 h) was reported.

The increase of IC50 value over time was mainly attributed to the decreased of IP in the presence of 5 mg/L nano-TiO_2 (Figure 5.4). It was calculated that IP of 5 mg/L nano-TiO_2 on *Cylindrotheca closterium* in the presence of UV lighting was significantly lower at 72 h (8.2 ± 2.8%), compared to the IP values at 24 h (35.3 ± 7.2%) and 48 h (26.5 ± 4.2%). The IP was calculated based on the difference between the growth rate in the treatment and in the control group. Therefore, the decreased IP of 5 mg/L nano-TiO_2 at 72 h might come from an increased growth rate ("accelerated growth") in the treatment, or a decreased growth rate ("decelerated growth") in the control. The growth rate of the control group at 48 – 72 h was 65% lower than its growth rate within 24 – 48 h. A decrease in the growth rate was also observed in the treatment with 5 mg/L nano-TiO_2, from 24 – 48 h to 48 – 72 h, yet by a much smaller extent of 21%. Unexpectedly, the algal growth rate in the treatment with 5 mg/L nano-TiO_2 on the last day (1.26 day^{-1}) was 78% higher than that in the control group (0.71 day^{-1}). These results indicated that the accelerated growth in the treatment and the decelerated growth in the control group may jointly contribute to the lower IP in the treatment with 5 mg/L nano-TiO_2 at 72 h.

The decelerated growth in the control group may be a result of the control group approaching the stationary growth phase. The accelerated growth in the treatment may be a result of decreased reactivity of nano-TiO_2 over time. As a motile benthic diatom, *Cylindrotheca closterium* secretes EPS during growth. The EPS is a mixture of sugars, uronic acids and proteins, which could become bound to nano-TiO_2 and form a coat, which could potentially decrease the reactivity of nano-TiO_2 (Gao et al. 2018). It has been reported that the growth rate of green alga *Chlorella pyrenoidosa* in the presence of nano-TiO_2 was significantly higher with the

presence of EPS compare to the absence of EPS (Gao et al. 2018), which lends support to this explanation. The EPS content in the *Cylindrotheca closterium* culture was anticipated to accumulate over time from release during motility, and potentially from further exudation in response to the presence of nano-TiO_2 (Sendra et al. 2017a). Due to the increased EPS content, the reactivity of the nano-TiO_2 in the treatment may decrease over time, resulting in a reduced stress and thus a recovered growth (accelerated growth). Another possible reason for the accelerated growth may be linked to the increased cell density. As cell density increases, the ROS quota per cell may be reduced, which may lead to a lower oxidative stress on a per cell basis and therefore a recovered growth.

5.4.3 The impact of nano-TiO_2 on the photophysiology of *Cylindrotheca closterium* in the presence of UV lighting

It was hypothesized that the presence of nano-TiO_2 would impair the photophysiology of *Cylindrotheca closterium* in the presence of UV lighting. However, no negative impacts were recorded in any photophysiological parameters in the presence of 2 and 5 mg/L nano-TiO_2, compared to the control, which was not in agreement with the hypothesis.

Fv/Fm is considered to be a sensitive indicator to the presence of stress (Maxwell and Johnson 2000; Consalvey et al. 2005). For healthy algal cells, reported Fv/Fm values are generally around 0.6 – 0.65 (Chen et al. 2012; Deng et al. 2017; Middepogu et al. 2018). In the present study, the Fv/Fm values were 0.58 – 0.62 for *Cylindrotheca closterium* with varying concentrations of nano-TiO_2 (0 – 5 mg/L), suggesting cells in all three groups were in a healthy condition. The impact of nano-TiO_2 with the presence of UVR on the Fv/Fm of algae has rarely been reported. Ockenden (2019) reported that the Fv/Fm of riverine biofilm (dominated by freshwater benthic diatoms) exposed to 5 mg/L nano-TiO_2 under natural daylight was not significantly different from the control, after 72 h of exposure, suggesting that freshwater benthic diatoms may respond in a similar way to their estuarine benthic counterparts to the presence of nano-TiO_2.

The maximum electron transport rate ($rETR_{max}$), maximum light use coefficient (α) and light saturation coefficient (E_k) has not been commonly measured in previous studies investigating the impact of nano-TiO_2. In the present investigation, all three parameters were not significantly altered in *Cylindrotheca closterium*

exposed to 2 and 5 mg/L nano-TiO_2, after 72 h of exposure in the presence of UV lighting. Similar results were obtained by Ockenden (2019), who found that the $rETR_{max}$, α and E_k of the riverine biofilm exposed to 5 mg/L nano-TiO_2 in field experiments in natural daylight were not significantly different from the control after 72 h of exposure. Yet to be noted, Ockenden (2019) recorded significantly lower values of $rETR_{max}$, α and E_k in the riverine biofilm exposed to 5 mg/L nano-TiO_2, compared to the control, after a shorter period of 24 h. This suggested that algal cells might quickly adapt to nano-TiO_2 with a fast recovery. Because the photosynthetic response of *Cylindrotheca closterium* after a shorter exposure time was not measured in the current study, it is not clear whether nano-TiO_2 posed an acute impact on the photophysiology *Cylindrotheca closterium*, in the presence of UV lighting.

In the present investigation, a significantly lower biomass yield (lower by 27.8%) and a significantly lower average growth rate (lower by 8.2%) were recorded in *Cylindrotheca closterium* exposed to 5 mg/L nano-TiO_2, despite there was no significant alterations in the photophysiological parameters including Fv/Fm, $rETR_{max}$, α and E_k, compared to the control group. Cardinale et al. (2012) presented evidence that there was no clear relationship between the photosynthetic performance and algal growth rate, in three freshwater green algae *Scenedesmus quadricauda, Chlamydomonas moewusii* and *Chlorella vulgaris*, in the presence of nano-TiO_2. They reported that the gross primary production (i.e. photosynthetic performance) and the respiration conjointly determined the growth rate (Cardinale et al. 2012). It is possible that the photophysiology of *Cylindrotheca closterium* was not affected by 5 mg/L nano-TiO_2, but the respiration rate of diatom cells was increased, which led to a reduced algal growth.

5.4.4 Limitations and suggestions

An initial biomass of 2.3×10^4 cells/mL was adopted in the present study, to ensure the initial chlorophyll *a* content in the algal culture was higher than the detection limit. In the control group of *Cylindrotheca closterium*, a significantly lower growth rate was measured on the third day, compared to the first two days, suggesting that the control group may be approaching the stationary growth stage on the third day. Possibly some density-dependent factors have led to the decreased growth when algae are grown in the static condition as biofilms e.g. pH and oxygen gradients, though these algae being motile may prevent such gradients forming. This implied that the initial biomass adopted in the present study may be too high for the

fast-growing *Cylindrotheca closterium*. It is suggested that, for those fast-growing species, it may be necessary adopt a shorter exposure time or a lower inoculum biomass, to avoid issues related to the decelerated growth in the control group.

In the present investigation, the FIBER-version of the Water-PAM was adopted for RLC measurements. Compared with the other types of PAM instruments, the FIBER-version is best suited for biofilms, as *in-situ* measurements can be done without disturbing the biofilms. The diatom *Cylindrotheca closterium* grew closely attached to the microplate surface, making the FIBER-version a good option for PAM measurement. However, the FIBER-version is less sensitive than the other types of PAM, and requires a relatively higher chlorophyll (> 0.1 mg/L) to provide detectable results (https://www.walz.com/products/chl_p700/water-pam/fiber_version.html, accessed 16/08/2019). Due to the detection limit, no results could be obtained when conducting PAM measurements with the treatments with 10 and 20 mg/L nano-TiO_2. It might be better to use a more sensitive PAM, such as the Cuvette version of the Water-PAM or the DIVING-PAM, for a better understanding of the photophysiological response of estuarine benthic diatoms cells to the presence of nano-TiO_2. The impact of nano-TiO_2 on the photophysiology at 24 h was not measured, due to the low fluorescence signal as a result of low concentration of chlorophyll *a*. The lack of early measurements meant that any possible initial inhibition would have been missed. In the further studies, an improvement would be to make measurements more frequently, for a better understanding of the impact of nano-TiO_2 on algal photophysiology over time.

Previous studies suggested that the tolerance of algae to nano-TiO_2 may be species-specific. The current study investigated the response of *Cylindrotheca closterium* to the presence of nano-TiO_2 in a monoculture. To the best of my knowledge, it provides some of the first measurements of impacts of nano-TiO_2 on an intertidal estuarine benthic diatom, with the presence of UVR. However, the response of a single species may not provide a clear indication of the risk of nano-TiO_2 in the environment, as the community generally contains a number of different species which may have varied tolerance. Therefore, in Chapter 6, an investigation was carried out to examine the responses of estuarine benthic diatoms at the community level, to the presence of nano-TiO_2 and UV lighting, to gain further insights into the ecological risk of nano-TiO_2.

5.5 **Conclusion**

In the present study, for the first time, the response of an intertidal estuarine benthic diatom to the presence of nano-TiO_2 was investigated in the presence of UVR. The test species, *Cylindrotheca closterium*, was isolated from the mudflats of the Severn Estuary, UK. The amount of UVR showed no negative impact on the growth of *Cylindrotheca closterium,* under the test conditions in absence of TiO_2. A number of negative impacts on the growth of *Cylindrotheca closterium* were recorded when the alga was exposed to nano-TiO_2 and UV lighting.

- The smaller size of nano-TiO_2 was considered to contribute to a greater growth inhibition, as the growth inhibition effect of micro-TiO_2 on *Cylindrotheca closterium* was significantly lower than nano-TiO_2. The varied negative impacts on algal growth were considered to be linked to the different potential in generating ROS between the two sizes of TiO_2.
- The 72 h-IC50 values of nano-TiO_2 for *Cylindrotheca closterium* was 8.73 mg/L with 95% confidence interval of 8.54 – 8.94 mg/L.
- Results obtained in the present investigation demonstrated that growth endpoints (i.e. changes in biomass yield or growth rate) of *Cylindrotheca closterium* provided a better indication of impact of nano-TiO_2 in the presence of UV lighting, compared to photophysiology endpoints.

Chapter 6 Investigation on the response of an estuarine microphytobenthic community dominated by benthic diatoms exposed to nano-TiO_2 in the presence of ultraviolet radiation

6.1 Introduction

6.1.1 The importance of microphytobenthic biofilms in the estuarine ecosystem

Microphytobenthic biofilms, which are widely found on the surface sediments of estuarine intertidal areas, comprise a matrix of sediments, microphytobenthos (MPB), heterotrophic bacteria and extracellular polymeric substances (EPS) (Underwood and Paterson 1993a; Underwood and Kromkamp 1999; Méléder et al. 2003), together with a range of meiofauna (e.g. nematodes, ciliates, Boyden and Little 1973; Nicholas et al. 1992). The MPB within the biofilms have been reported to make a large contribution to the global estuarine primary production (Admiraal et al. 1983; MacIntyre et al. 1996; Underwood and Kromkamp 1999). The MPB also play an important role in supporting estuarine secondary production as a direct food source (Pinckney and Zingmark 1991; MacIntyre et al. 1996). Moreover, they have been found to serve several other functions including enhancing the survival of microorganisms under harsh environmental conditions (Decho 1990), increasing sediment stability and thereby reducing sediment erosion (Little et al. 1992; Underwood and Paterson 1993a; Yallop et al. 1994; Miller et al. 1996; Stal and de Brouwer 2003), and promoting nutrient cycling (Underwood and Kromkamp 1999; Decho 2000; Catarina et al. 2003).

6.1.2 The presence of benthic diatoms in the intertidal MPB

Benthic diatoms are the key primary producers in many intertidal MPB with epipelic species dominating mudflats. The diatoms play an especially important role for estuaries with high turbidity, as they may not be able to support a high biomass of phytoplankton in the water column (Underwood and Paterson 1993a). As the key primary producers in the estuaries, the quantity of benthic diatoms and their composition may have great impacts on the structure and the stability of the estuarine ecosystem. Field observations showed that benthic diatom communities can display temporal, spatial, and vertical variations in terms of biomass and composition (Colijn and Dijkema 1981; Admiraal et al. 1984; Pinckney et al. 1994; Underwood 1994;

Underwood et al. 1998; Underwood and Kromkamp 1999; Consalvey et al. 2004a; Zacher et al. 2005). The variability in communities of benthic diatoms have been found to be related to environmental abiotic variables including temperature, irradiance, day length, sediment type, water level, salinity, nutrient gradient and tidal cycle (Admiraal and Peletier 1980; Colijn and Dijkema 1981; Admiraal et al. 1982; Zong and Horton 1998; Thornton et al. 2002; Consalvey et al. 2004a; Underwood et al. 2005; McQuatters-Gollop et al. 2007; Waring et al. 2007; McKew et al. 2011). In addition, a number of anthropogenic stressors, such as the release of pollutants including sulphide, oil, biocide, pesticide, and heavy metals have been reported to superimpose variations in the biomass and composition of these estuarine benthic diatom communities (Admiraal and Peletier 1979; Underwood and Paterson 1993b; Chronopoulou et al. 2013).

6.1.3 The impact of nano-TiO_2 on the intertidal MPB

The dramatically escalating in the production and application of NPs have raised concerns regarding their environmental risk, due to their extremely small size and high surface area to volume ratio, especially for the most widely used nano-TiO_2 (Boxall et al. 2007; Nowack and Bucheli 2007; Handy et al. 2008a; Handy et al. 2008b; Miller et al. 2012; Jain et al. 2018; Maurizi et al. 2018). Water is the ultimate sink for most of the chemicals (Koumanova 2006). The nano-TiO_2 released into the environment may accumulate in the aquatic environment through atmospheric deposition, surface run-off, sewage, wastewater discharge and direct input (Boxall et al. 2007; Klaine et al. 2008; Koelmans et al. 2009; Donia and Carbone 2019). Studies have highlighted that nano-TiO_2 in the aquatic environment is likely to sediment within a few hours once in the saline environment (Keller et al. 2010; Sillanpää et al. 2011; Li et al. 2016). Estuaries, where seawater and freshwater merge together, may be the first place where nano-TiO_2 encounter a saline environment. Therefore, nano-TiO_2 particles carried by the water are anticipated to settle out to benthic environments in estuaries. It has been reported that the majority of NPs added into the estuarine mesocosms would accumulate in the estuarine biofilm (Ferry et al. 2009), making it an important sink for the NPs. However, to the best of my knowledge, to date, there are no published studies on the impact of nano-TiO_2 on the MPB in estuarine biofilms.

Some studies have been conducted to explore the impact of nano-TiO_2 on the MPB in biofilms formed in

river and streams (Binh et al. 2016; Hough et al. 2017; Wright et al. 2018, Ockenden 2019), yet diverse responses were obtained in terms of their impact to photosynthetic organisms. Hough et al. (2017) measured a higher biomass (assessed by chlorophyll *a* content) in stream biofilms with the presence of 1.5 mg/L nano-TiO_2 after 22 days. Wright et al. (2018) reported a significantly lower biomass (assessed by chlorophyll *a* content) in a stream biofilm when grown with 5 mg/L nano-TiO_2 after 28 days. Ockenden (2019) reported that the biomass (assessed by chlorophyll *a* content) in a rive biofilm was negatively affected by the presence of 5 mg/L nano-TiO_2 after a much shorter period of 3 days. In Chapter 4, the impact of nano-TiO_2 on three estuarine benthic diatoms was investigated. Results obtained in Chapter 4, together with the results from other researches, provided strong evidence of species-specific responses to the presence of nano-TiO_2. Therefore, it was hypothesized that one possible reason for the differences in response obtained in the freshwater biofilms may be related to the differential response of species within biofilms, to the presence of nano-TiO_2.

It remains unknown, apart from the knowledge gained during the single species testing in the current research, whether particular species within the estuarine microphytobenthic community would be more or less affected by the presence of nano-TiO_2, which represents a knowledge gap. In the present study, the impact of nano-TiO_2 on intertidal MPB was investigated under UV lighting containing a considerable amount of UVR in addition to the PAR, which best mimics the natural condition. The response of MPB, collected from the Severn Estuary, exposed to varying concentrations of nano-TiO_2 was investigated. Three hypotheses were proposed.

Hypothesis 1: In Chapter 5, a significant growth inhibition effect of nano-TiO_2 on the estuarine benthic diatom *Cylindrotheca closterium* was recorded in the presence of UV lighting. Therefore it was hypothesized that the growth of the intertidal MPB may be inhibited, manifested as a lower biomass (measured as chlorophyll *a* content) compared to the control samples.

Hypothesis 2: The negative impact of nano-TiO_2 on the intertidal MPB biomass would increase as particle concentration increased.

Hypothesis 3: The MPB may contain species with varied tolerance. It was hypothesized that the composition of the diatom community would be altered in the presence of nano-TiO_2 due to species-specific responses.

6.2 Methods

6.2.1 Test nanoparticles

Nano-TiO_2 (Aeroxide® P25, product no.718467) was bought from Sigma-Aldrich. Particle characteristics were detailed in section 4.3.1 in Chapter 4.

6.2.2 Intertidal MPB preparation

On 10th July 2016, surface sediments with visible presence of benthic diatoms (Figure 6.1A) were removed from the mudflat at Portishead, the Severn Estuary in the United Kingdom (51°29'34"N 2°46'26"W). The sediments were transferred into sterile petri dishes together with some estuarine water to keep samples moist. Samples were brought back to the laboratory within 2 h and kept in the growth room (18 ^{0}C, PAR = 80 μmol m^{-2} s^{-1}, fluorescent lighting on a 14 h-light and 10 h-dark cycle). The MPB organisms were isolated from the surface using the lens-tissue technique (Eaton and Moss 1966; Yallop et al. 1994). In order to avoid sediment particles and tissue fibers in the later rising process, cover glasses (cleaned with ethanol) were placed on the top of two layers of lens-tissue (Figure 6.1B). After 4 h, cover glasses were carefully lifted up and the attached MPB were gently scraped down with a cell scraper and suspended in fresh culture medium. The diatom assemblage was well mixed and equally divided into seven 12-well microplates. All the microplates were cultivated in the Reftech temperature-controlled growth room (18 ^{0}C, PAR = 80 μmol m^{-2} s^{-1}, fluorescent lighting, 14-h light and 10-h dark) to allow the growth of MPBs at the bottom of the microplate well. Microplates were places on the table individually without stacking. After 3 days of cultivation, a distinct colour was observed on the bottom of the microplate by eye, indicating a healthy growing MPB biofilm was developing (Figure 6.1C) and this observation was confirmed by viewing plates using an inverted microscope. The upper 4 mL medium in each microplate well was carefully removed and the remaining 0.5 mL was used for experiments and the MPBs in each well as considered as an individual replicate. To be noted, the biomass and species composition of the

MPBs may inevitably be slightly varied in each replicate, in terms of relative abundance and species composition reflecting the heterogeneous assemblages that develop on mudflats (Underwood 1994).

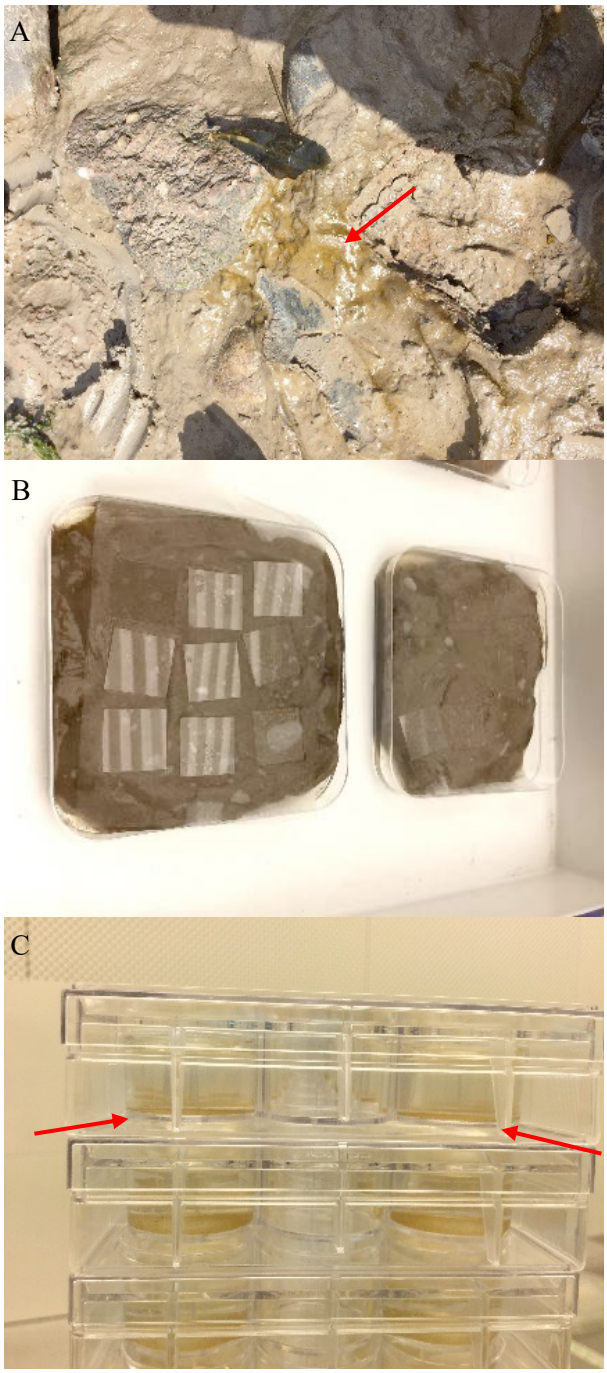

Figure 6.1 (A) An example of the MPBs from the Severn Estuary (brown colour, located with red arrows) on the surface of the mudflat. (B) MPB isolation process with lens-tissue method and additional cover glasses (10 mm in diameter). (C) Visualization of MPBs biofilms grown at the bottom of microplate wells (brown colour, located with red arrows).

The medium used for cultivating the MPB was made up according to section 2.2.3.1 with natural seawater, instead of artificial seawater made of seasalts. The natural seawater was used so that culture medium would be more representative of the environment where the MPB had been growing, given the relatively short acclimation period. Seawater was collected from the Marine Lake, Clevedon, adjacent to Portishead in the United Kingdom (51°26'08"N 2°52'08"W) on 2nd July 2016, after a high tide which topped up the lake with seawater. After brought back to the laboratory, the seawater (salinity = 26 ‰, pH = 8.75) was immediately filtered through 1 μm cellulose nitrate membrane filter and was used for making up culture medium. The final culture medium had a salinity of 26 ‰ with pH being 8.0.

6.2.3 **Experimental setup**

Fresh culture medium (4 mL) containing varying concentrations of nano-TiO_2 was added into the microplate wells which contained 0.5 mL intertidal MPB, with the final nano-TiO_2 concentrations set to be 0, 50, 100 and 200 mg/L. This process was done with extreme care by slowly adding new medium through the well side to avoid the suspension of MPB. The final volume in each well was 4.5 mL. All microplates were incubated under UV lighting as described in section 5.2.3. With the period of 2 weeks, the upper 3.6 mL medium in each microplate well were replaced by the 3.6 mL fresh culture medium every 24 h, to minimize the nutrient limitation for MPB growth. The medium replacing process was done with extreme care to avoid MPB resuspension, though inevitably some algae may have been removed by this process, yet number of cells removed were considered to be negligible. Microscopy examination confirmed that the cell density in the removed old medium was lower than the detection limit. According to the results in Chapter 2, the majority of the nano-TiO_2 (> 99%) settled down to the bottom of each well within 24 h. Therefore, the medium replacing process was considered to have a negligible impact on removing cells as well as NPs from the microplate well.

At the starting point, six randomly selected replicates were harvested for measuring the initial state of the MPB. After 1 week or 2 weeks of cultivation, the MPBs exposed to varying concentrations of nano-TiO_2, were harvested for measurements. For each sample in the microplate well, the MPB was harvested with a cell scraper (19 mm blade, Corning) and transferred to a 5 mL test tube. After thoroughly vortex mixing the sample in the test tube for 20s, a 1.5 mL subsample was taken for diatom composition analysis

(preserved in Lugol's iodine solution with final concentration of 1% and stored in the dark prior to analysis) and the remaining 3 mL was used for biomass measurement (processed immediately). All assays were run in six replicates.

6.2.4 **Biomass measurements**

To investigate whether the biomass of MPB was affected by the presence of nano-TiO_2, the chlorophyll *a* content as well as the phaeopigment content in the MPB was measured. Phaeopigments are degradation products of chl *a* and an increased degradation of chl *a* generally implies that organisms have encountered adverse growth conditions (Hendry et al. 1987). The concentration of phaeopigment in the MPB was therefore measured to indicate whether MPB was stressed in the presence of nano-TiO_2.

The 3 mL subsamples for biomass measurement were processed by the method described in section 4.2.5. The content of chlorophyll *a* and phaeopigment in the MPB was calculated by equation 6.1 and equation 6.2, respectively (Lorenzen 1967).

$$\text{chlorophyll } a \ (\mu g/cm^2) = \frac{k \times F \times \left(E_{665_0} - E_{665_a}\right) \times v \times V_1}{l \times V_2 \times s} \qquad \text{(eq 6.1)}$$

$$\text{phaeopigments } (\mu g/cm^2) = \frac{k \times F \times \left(R \times E_{665_a} - E_{665_0}\right) \times v \times V_1}{l \times V_2 \times s} \qquad \text{(eq 6.2)}$$

where k (= 11.9035 µg·cm/ml, Ritchie 2006) is the absorption coefficient of chlorophyll *a* in the pure ethanol, F (= 2.0) is the factor to equate the reduction in absorbance after acidification to the initial chlorophyll *a* concentration, R (= 2.0) is the maximum ratio of E_{665_0} and E_{665_a} in the absence of phaeopigment, E_{665_0} and E_{665_a} are adjusted absorbance values of pigment extracts at 665 nm (turbidity-adjusted absorbance by deducting absorbance at 750 nm (A_{750}) from absorption at 665 nm (A_{665})) before and after acidification, v (= 1.8 mL) is the volume of ethanol used for pigment extraction, V_1 (= 4.5 mL) is the volume of the original cell culture, l (= 1 cm) is the path length of the cuvette, V_2 (= 3 mL) is the volume of cell culture used for chlorophyll *a* measurement and s (= 3.8 cm^2) is the growth area of one 12-well microplate well.

6.2.5 **Diatom composition analysis**

To investigate the whether diatom composition in the MPB had altered after exposure to nano-TiO_2, the composition of the diatom community in the MPB was determined. The 1.5 mL subsample for diatom composition analysis was processed with the following two steps before being examined with scanning electron microscopy (SEM) for identification.

Initially, the clumps of cells and nano-TiO_2 aggregates were broken up. The heteroaggregation of nano-TiO_2 and algal cells severely hindered the identification of diatoms, as some of the cells were entrapped or encapsulated by the particles. It has been reported that the presence of EPS facilitates the heteroaggregation of nano-TiO_2 and cells (Gao et al. 2018), corroborated with the findings of this research (Section 3.3.1 in Chapter 3). Therefore, an acid digestion process, which was found to be efficient for extracting EPS from biofilms (Barranguet et al. 2004), was applied to dissolve the bound EPS. The samples preserved in the Lugol's iodine were first centrifuged at 4000 rpm (3220 *g*) for 15 min. For each sample, the pellet was rinsed with Milli Q water for 3 times to remove the salts. Each time the pellet was resuspended in 10 mL Milli-Q water, vortexed and then centrifuged at 4000 rpm (3220 *g*) for 5 min. Afterwards, the pellet was heated in a water bath with 10 mL 0.1 M HCl for an hour. After heating, the sample was centrifuged down at 4000 rpm (3220 *g*) and the pellet was rinsed 3 times with Milli Q water (10 mL water each time) to remove all traces of the acid.

Diatoms were then cleaned to remove organic matter to enable frustules to be identified. The method recommended by Jiang et al. (2015) was followed. The cell pellet after acid digestion was gradually cleaned with 15, 50 and 100% (*v/v*) ethanol. Each time 5 mL of ethanol was used to resuspend the pellet and then the mixture was centrifuged at 4000 rpm (3220 *g*) for 3 min. After the last centrifugation with 100% ethanol, 4 mL of supernatant was removed. The remaining 1 mL sample was vigorously vortex mixed to resuspend the diatom valves or frustules. A subsample of 10 µl was spread on a 12 mm round cover glass (cleaned with ethanol), which was mounted on an SEM stub with carbon tape. The sample was left to air dry and then sputter coated (Edwards Scancoat Gold Sputter Coater) for 40 seconds before examination by SEM.

The examination of diatoms was conducted with SEM at 5 KV with SE2 detector and a standard aperture of 30 μm. Due to the presence of TiO_2 particles, the key features of some frustules were obscured, making the identification at species level associated with uncertainty. In addition, some frustules were present in the lateral position (i.e. girdle view), making the identification at the species level impossible. Therefore, the diatom valves were identified at genus level. At least 400 valves were identified per sample.

6.2.6 **Diatom community diversity index calculation**

The diversity of the diatom community in the intertidal MPB was indicated by the Shannon diversity index (H'), which was calculated by equation 6.3 (Shannon and Weaver 1949).

$$H' = -\sum_{i=1}^{R} p_i \ln p_i \qquad \text{(eq 6.3)}$$

where p_i is the relative abundance of genus i and R is the total number of identified genera.

6.2.7 **Data analysis**

Tests for the statistical significance between values were performed using SPSS software (version 24.0 of SPSS for Windows). After checking the homogeneity of variance by Levene's test and the normality of the residuals by Kolmogorov-Smirnov test, parametric tests (e.g. independent-samples T tests, ANOVA tests) were applied to determine the difference between groups. For the Shannon diversity indices (H'), non-parametric tests (Mann-Whitney test, Kruskal-Wallis test) were used. Data are shown as mean ± standard deviation unless otherwise stated. The significance level was set at < 0.05.

Tests for the similarity between diatom composition were performed using PAST V3 software (Hammer et al. 2001). A 2D non-metric multidimensional scaling (NMDS) plot was made to illustrate the difference in diatom composition between groups, using a Bray-Curtis similarity index, based on the relative genus abundance of the diatom communities. Spearman' rank correlations were applied to determine the correlation between NMDS Axis values and the relative abundance of each genus, to find out the influence of each genus on the separation of diatom communities along each Axis in the NMDS plot. Bubble plots

were made to visualize the difference in the relative abundance of each genus between groups. Analysis of similarities (ANOSIM) tests were applied to determine if there were significant differences in community composition between groups, using a Bray-Curtis similarity index with permutation N being 999. The significance level was set at < 0.05.

6.3 Results

6.3.1 The impact of nano-TiO_2 on the chlorophyll *a* content of the intertidal MPB in the presence of UV lighting

To investigation whether the biomass of intertidal MPB was affected by the presence of nano-TiO_2 and UV lighting, the chlorophyll *a* content was measured to indicate the change of biomass. The biomass of the MPBs cultivated under varying concentrations of nano-TiO_2 are illustrated in Figure 6.2. At the starting point (time 0), the variation of biomass between 6 randomly selected intertidal MPB was relatively small (coefficient of variation = 3%). After 1 week and 2 weeks of cultivation, considerable variation of biomass was obtained between the 6 replicates within each group (coefficient of variation = 20 – 37%).

After 1 week of cultivation, the average biomass in the three groups exposed to nano-TiO_2 was 8% (50 mg/L), 27% (100 mg/L) and 12% (200 mg/L) higher than the control group (1.55 ± 0.39 μg/cm^2). However, the difference between four groups was not significant, according to a one-way ANOVA test ($F_{3, 20} = 0.973$, $p = 0.425$). From time 0 to week 1, the change of biomass was not significantly altered in all groups, according to independent-samples T tests (control, $t_{10} = 0.150$, $p = 0.884$; 50 mg/L, $t_{5.182} = -0.769$, $p = 0.475$; 100 mg/L, $t_{5.063} = -1.653$, $p = 0.158$; 200 mg/L, $t_{5.14} = -0.968$, $p = 0.376$).

After 2 weeks of cultivation, the biomass in the three groups exposed to nano-TiO_2 was 46% (50 mg/L), 4% (100 mg/L) and 50% (200 mg/L) higher than the control group (2.01 ± 0.74 μg/cm^2). A significant difference was found between the four groups, according to the one-way ANOVA test ($F_{3, 20} = 3.942$, $p = 0.023$). However, the difference between any two groups was not significant, according to the TukeyHSD *post-hoc* test ($p \geq 0.074$). According to one-way ANOVA tests, from week 1 to week 2, the change of biomass was not significantly in the control group ($F_{1, 10} = 1.785$, $p = 0.211$) and in the treatment with 100

mg/L nano-TiO_2 ($F_{1, 10}$ = 0.075, p = 0.790); yet there was a significant increase of biomass in the treatment with 50 mg/L nano-TiO_2 (increased by 75 ± 48%, $F_{1, 10}$ = 19.849, p = 0.001) and 200 mg/L nano-TiO_2 (increased by 73 ± 40%, $F_{1, 10}$ = 15.464, p = 0.003).

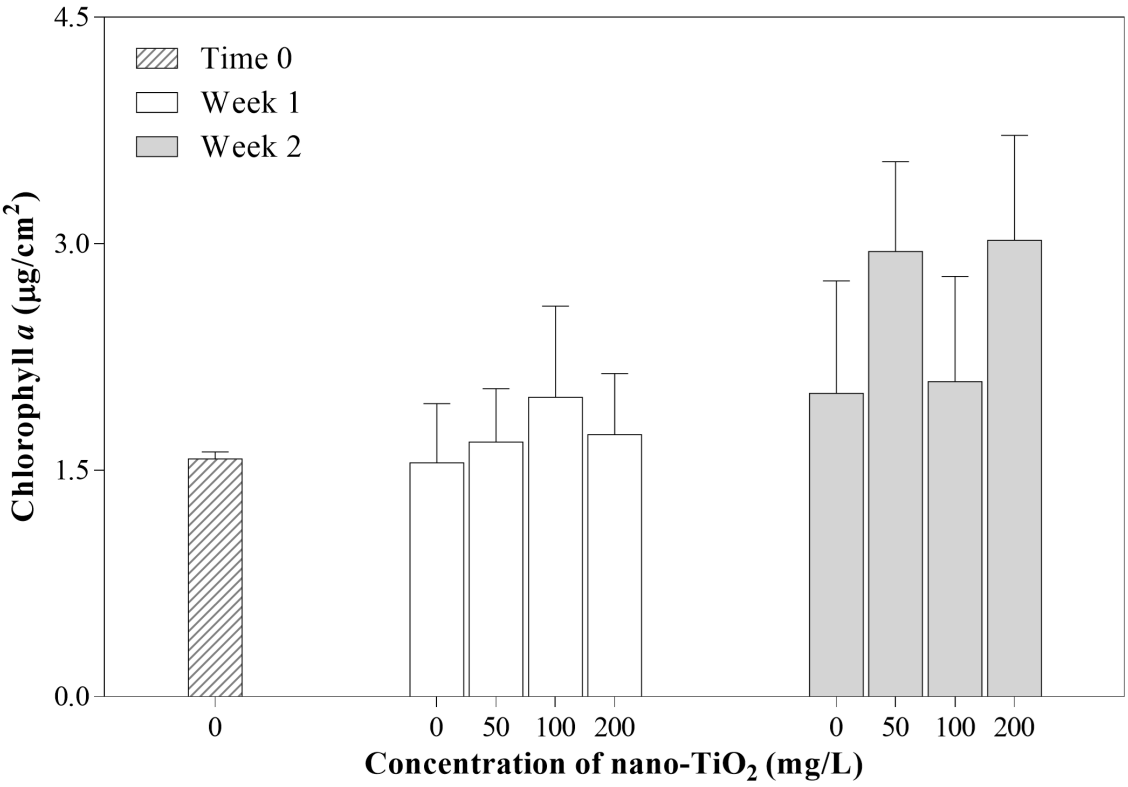

Figure 6.2 The biomass (indicated by chlorophyll *a* concentration) in the initial intertidal MPB (denoted as Time 0) and in MPBs following cultivation with varying concentrations of nano-TiO_2 for 1 week (denoted as Week 1) and 2 weeks (denoted as Week 2), in the presence of UV lighting. Results are shown as mean ± standard deviation (n = 6).

6.3.2 The impact of nano-TiO_2 on the phaeopigment content of the intertidal MPB in the presence of UV lighting

The content of phaeopigment was measured to indicate the degradation of chlorophyll *a* in the intertidal MPB. The phaeopigment contents of MPB cultivated under varying concentrations of nano-TiO_2 in the presence of UV lighting are illustrated in Figure 6.3. Considerable variation of phaeopigment was obtained between the 6 replicates within each group (coefficient of variation = 13 – 34%).

After 1 week of cultivation, the average phaeopigment content in the three treatments exposed to nano-TiO_2 was 62% (50 mg/L), 77% (100 mg/L) and 98% (200 mg/L) higher than the control group (0.52 ± 0.14 μg/cm^2). Significant differences were found between the four groups, according to a one-way ANOVA test ($F_{3, 20} = 5.212$, $p = 0.008$). A TukeyHSD *post-hoc* test indicated that the phaeopigment concentration in the treatments with 50 – 200 mg/L nano-TiO_2 were all significantly higher than the control, yet the difference between the three treatments was not significant. From time 0 to week 1, there was a significant increase of phaeopigment concentration in all 4 groups, according to independent-samples T tests (control, $t_{5.8} = -6.615$, $p = 0.001$; 50 mg/L, $t_{5.582} = -10.945$, $p < 0.001$; 100 mg/L, $t_{5.269} = -7.799$, $p < 0.001$; 200 mg/L, $t_{10} = -15.789$, $p < 0.001$). The concentration of phaeopigment at Week 1 was 4.4 – 8.6 times higher than that at Time 0.

After 2 weeks of cultivation, the average phaeopigment concentration in the three treatments exposed to nano-TiO_2 was 62% (50 mg/L), 53% (100 mg/L) and 151% (200 mg/L) higher than the control group (0.87 ± 0.18 μg/cm^2). Significant differences were found between the four groups, according to a one-way ANOVA test ($F_{3, 20} = 6.605$, $p = 0.003$). A TukeyHSD *post-hoc* test indicated that the phaeopigment concentrations in the treatments with 50 and 200 mg/L nano-TiO_2 were significantly higher than that in the control. According to one-way ANOVA tests, from week 1 to week 2, the change of phaeopigment concentration was not significant in the treatment with 100 mg/L nano-TiO_2 ($F_{1, 10} = 3.961$, $p = 0.075$); however, there was a significant increase of phaeopigment in the control group (increased by 67 ± 35%, $F_{1, 10} = 13.879$, $p = 0.004$) and in the treatments with 50 mg/L nano-TiO_2 (increased by 68 ± 32%, $F_{1, 10} = 20.787$, $p = 0.001$) and 200 mg/L nano-TiO_2 (increased by 112 ± 34%, $F_{1, 10} = 55.506$, $p < 0.001$).

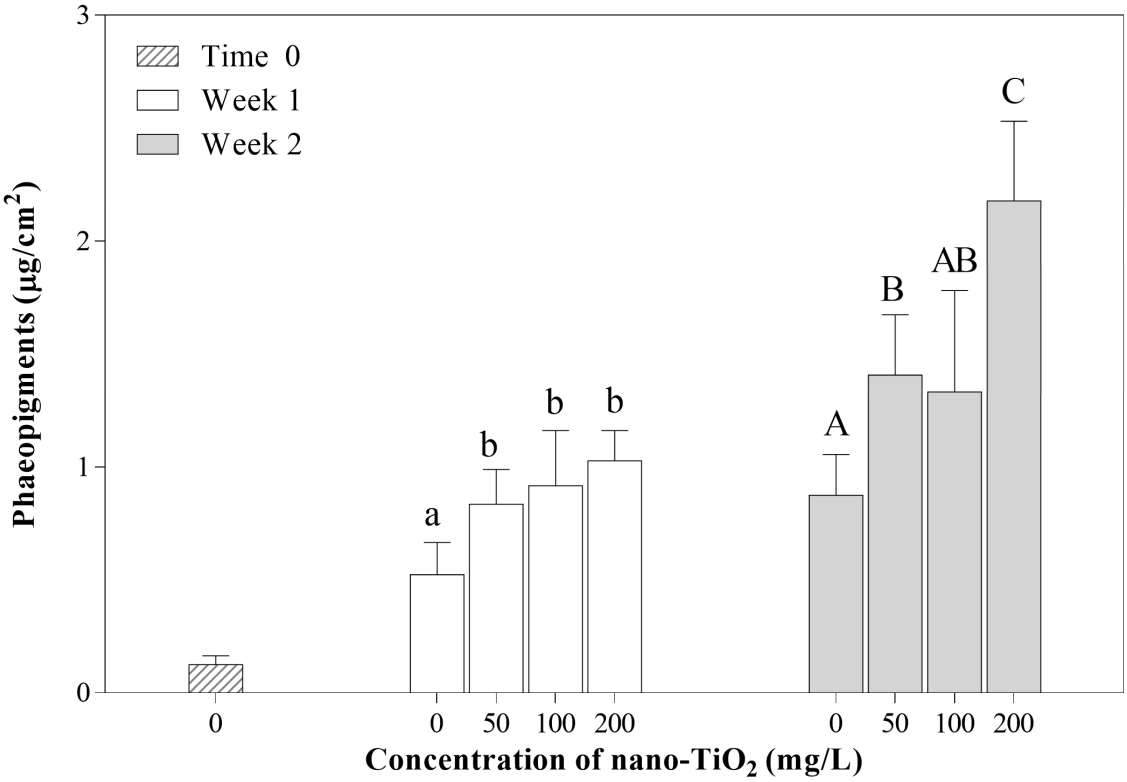

Figure 6.3 The phaeopigment concentration in the initial intertidal MPB (denoted as Time 0) and in MPBs following cultivation with varying concentrations of nano-TiO_2 after 1 week (denoted as Week 1) and 2 weeks (denoted as Week 2), in the presence of UV lighting. Results are shown as mean ± standard deviation (n = 6). Bars sharing a same lowercased-letter or uppercased-letter are not significantly different (TukeyHSD *post-hoc* test).

6.3.3 The impact of nano-TiO_2 on the richness of the diatom community in the intertidal MPB in the presence of UV lighting

The richness of the diatom community in the intertidal MPB was assessed by the number of diatom genera in the MPB. A total of 6 diatom genera were recorded in each MPB biofilm. A representative frustule for each genus is shown in Figure 6.4. The presence of nano-TiO_2 showed no impact on the genus richness of the diatom community at both week 1 and week 2.

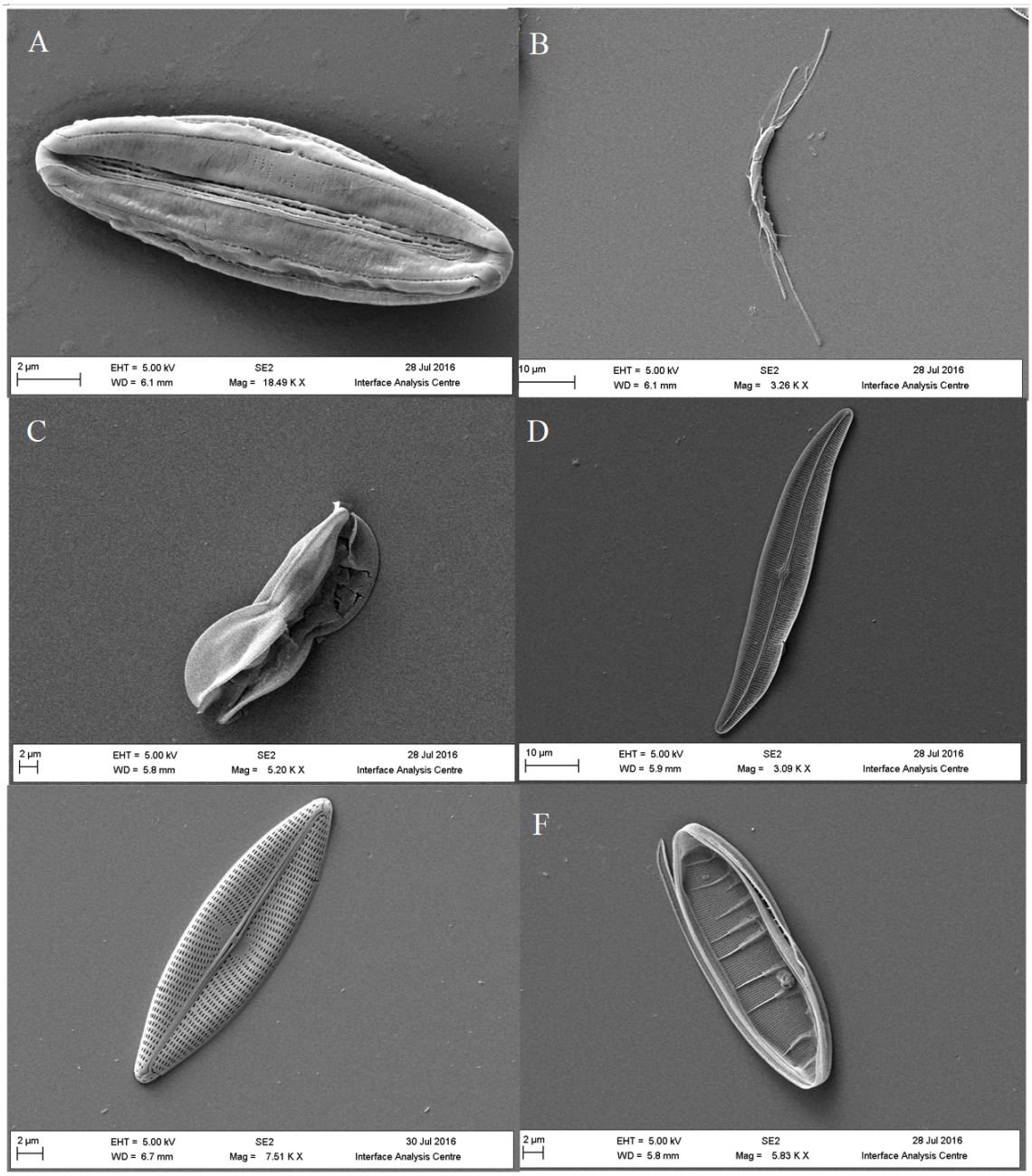

Figure 6.4 Scanning electron microscopy images of frustules belongs to genus (A) *Amphora*, (B) *Cylindrotheca*, (C) *Entomoneis*, (D) *Gyrosigma*, (E) *Navicula*, (F) *Nitzschia*, in the intertidal MPB.

6.3.4 The impact of nano-TiO_2 on the diversity of the diatom community in the intertidal MPB in the presence of UV lighting

The diversity of the diatom community in the intertidal MPB was assessed by the Shannon diversity index H', based on the relative abundance of each genus. The average relative abundance (RA) of each genus in the groups are illustrated in Figure 6.5. At the starting point (Time 0), the diatom community in the MPB

was dominated by *Cylindrotheca* spp. with a RA of 69.2% and *Navicula* spp. being common (RA = 22.0%) and very low abundance of other genera (RA < 5%). A distinct decrease in the RA of *Cylindrotheca* spp. and increases in the RA of *Entomoneis* spp. and *Navicula* spp. was recorded in the MPBs after 1 week and 2 weeks of cultivation, regardless of the concentration of nano-TiO_2. After week 1 and week 2, all the diatom community in the MPB were dominated by *Navicula* spp. (up to 64.3% in RA) and *Entomoneis* spp. (up to 53.1% in RA), with low RA of other genera.

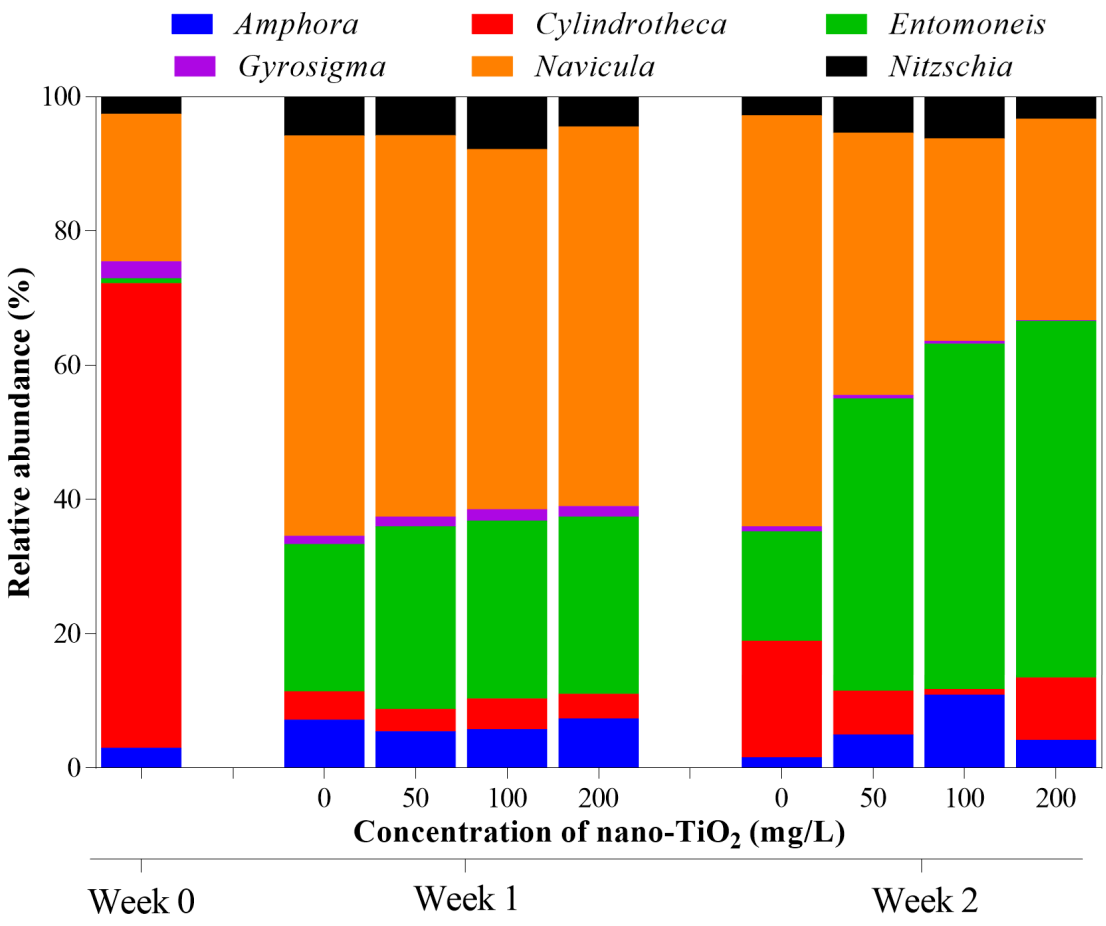

Figure 6.5 The relative abundance of each diatom genus (marked by colour) in the initial intertidal MPBs (Time 0) and in the MPBs cultivated with varying concentrations of nano-TiO_2, after 1 week (Week 1) and 2 weeks of cultivation (Week 2), in the presence of UV lighting. Results are shown as the mean value of 6 replicates.

The Shannon diversity index (H') of the diatom community in the intertidal MPBs cultivated with varying concentrations of nano-TiO_2 in the presence of UV lighting is illustrated in Figure 6.6. Considerable

variation of H' values were obtained between the 6 replicates within each group (coefficient of variation = 12 – 27%).

After 1 week of cultivation, the average H' values in the treatments exposed to nano-TiO_2 were 1.11 (0 mg/L), 1.13 (50 mg/L), 1.16 (100 mg/L) and 1.09 (200 mg/L). The difference between the four groups was not significant, according to the Kruskal-Wallis test (χ^2 = 1.086, d.f. = 3, asymptotic p = 0.780). According to Mann-Whitney tests, from time 0 to week 1, the diversity of the epipelic diatom community in the treatment with 50 mg/L nano-TiO_2 was significantly increased from 0.88 ± 0.17 to 1.13 ± 0.14 (U = 4, N_1 = 6, N_2 = 6, exact p = 0.026); the diversity of the diatom community in the other 3 groups was not significantly changed (N_1 = 6, N_2 = 6, control, U = 7, exact p = 0.093; 100 mg/L, U = 7, exact p = 0.093; 200 mg/L, U = 8, exact p = 0.132).

After 2 weeks of cultivation, the average H' values in the treatments with the presence of nano-TiO_2 was 0.97 (0 mg/L), 1.18 (50 mg/L), 1.02 (100 mg/L) and 1.08 (200 mg/L). The difference between the four groups was not significant, according to the Kruskal-Wallis test (χ^2 = 3.980, d.f. = 3, asymptotic p = 0.264). From week 1 to week 2, the diversity of the diatom community in all four groups had not significantly changed, according to Mann-Whitney tests (N_1 = 6, N_2 = 6, control, U = 15, exact p = 0.699; 50 mg/L, U = 12, exact p = 0.394; 100 mg/L, U = 12, exact p = 0.394; 200 mg/L, U = 17, exact p = 0.937).

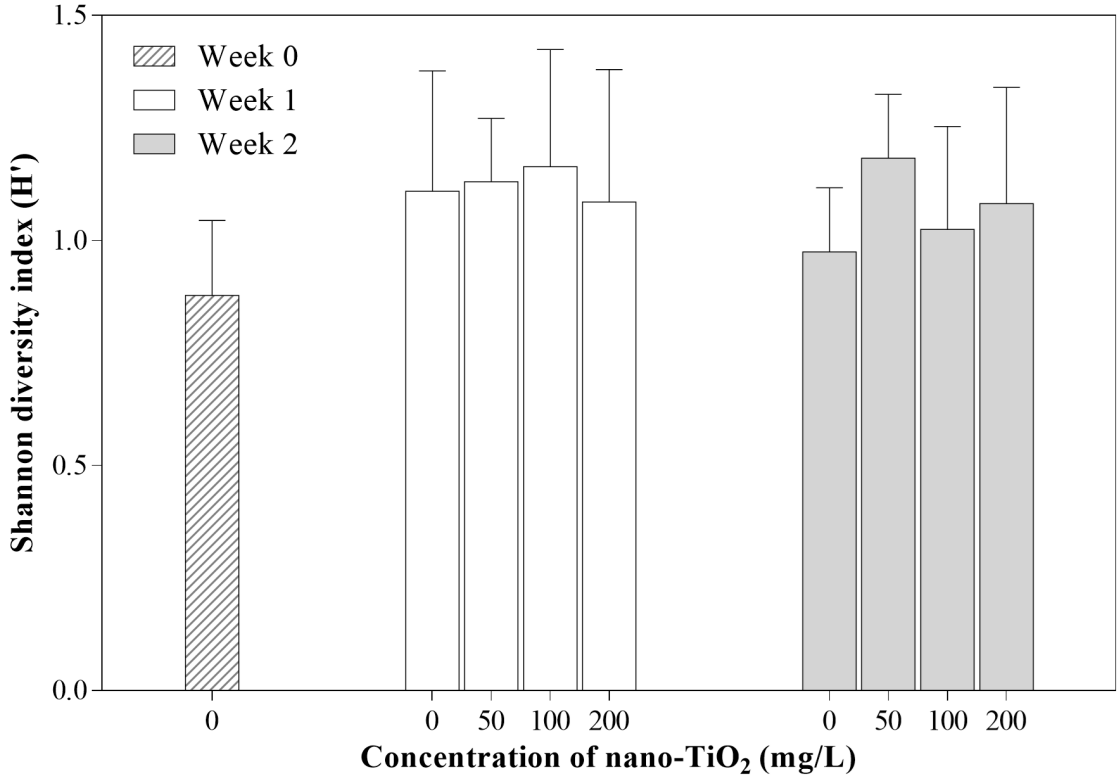

Figure 6.6 The diversity of diatom community in the initial intertidal MPB (Time 0) and in MPBs cultivated with varying concentrations of nano-TiO_2 for 1 week (Week 1) and 2 weeks (Week 2) in the presence of UV lighting. The diversity of diatom community was indicated by Shannon diversity index (H'). Results are shown as mean ± standard deviation (n = 6).

6.3.5 The impact of nano-TiO_2 on the diatom composition in the intertidal MPB in the presence of UV lighting

The differences between the diatom composition of each group were analyzed by ANOSIM test and illustrated by NMDS plots.

6.3.5.1 The impact of nano-TiO_2 on the diatom composition at week 1 in the presence UV lighting

A non-metric multidimensional scaling (NMDS) plot was used to indicate the difference of diatom composition in the MPBs cultivated for 1 week with varying concentrations of nano-TiO_2 in the presence of UV lighting. The stress value for the NMDS plot was 0.0799, suggesting a very good representation of

the difference in the diatom composition by the ordination distances. As shown in Figure 6.7, the control group and the three treatments overlapped with each other.

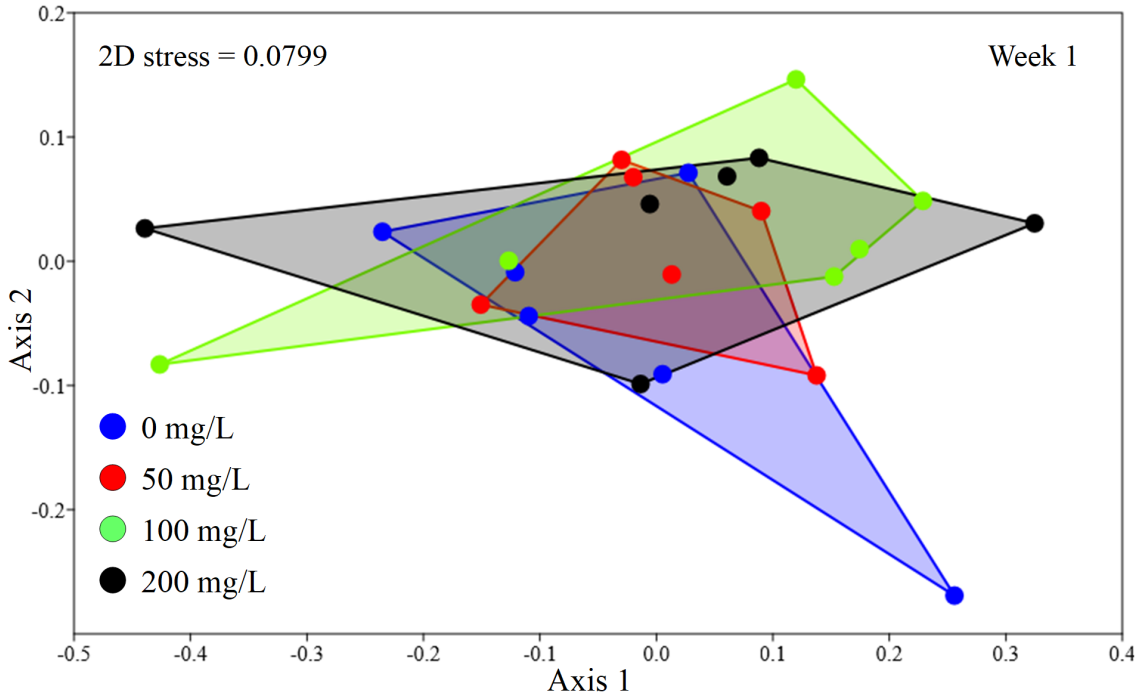

Figure 6.7 NMDS plot based on the relative abundance of 6 diatom genera in intertidal MPBs cultivated with varying concentration of nano-TiO_2 (marked by colour) for 1 week in the presence of UV lighting. Each point indicates an individual replicate in the group.

Figure 6.8 shows the change in diatom composition from time 0 to week 1. The stress value for the NMDS plot was 0.1141, suggesting a good representation of the diatom communities by the ordination distances. Considerable variation between the replicates within each group was noted. The diatom composition in the samples harvested at week 1 were completely separated from those harvested at time 0 on Axis 1. An ANOSIM test confirmed that the diatom composition in all four groups at week 1 were significantly different to the diatom composition at the start ($R = 1$, $p \leq 0.005$). Spearman's rank correlations between the Axis 1 value and the RA of each genus were calculated to indicate the influence of each genus on the separation of diatom communities along Axis 1. A significant negative Spearman's Rank correlation was obtained between the Axis 1 value and the RA of genus *Cylindrotheca* (SR = -0.911, $p < 0.001$). A significant positive Spearman's Rank correlation was obtained between the Axis 1 value and the RA of genus *Navicula* (SR = 0.626, $p = 0.004$). According to the bubble plots (Figure 6.8), the separation of the

group at time 0 and the groups at week 1 was mainly attributed to the difference in the RA of genus *Cylindrotheca* and *Navicula*. Compared with the initial RA of genus *Cylindrotheca* at time 0 (RA = 69.2 ± 5.2%), decreases in the RA of genus *Cylindrotheca* were recorded in all 4 groups at week 1 (RA = 3.3 – 4.6%). Compared with the initial RA of genus *Navicula* at time 0 (RA = 22.0 ± 5.7%), increases in the RA of genus *Navicula* were recorded in all 4 groups at week 1 (RA = 53.6 – 59.6%).

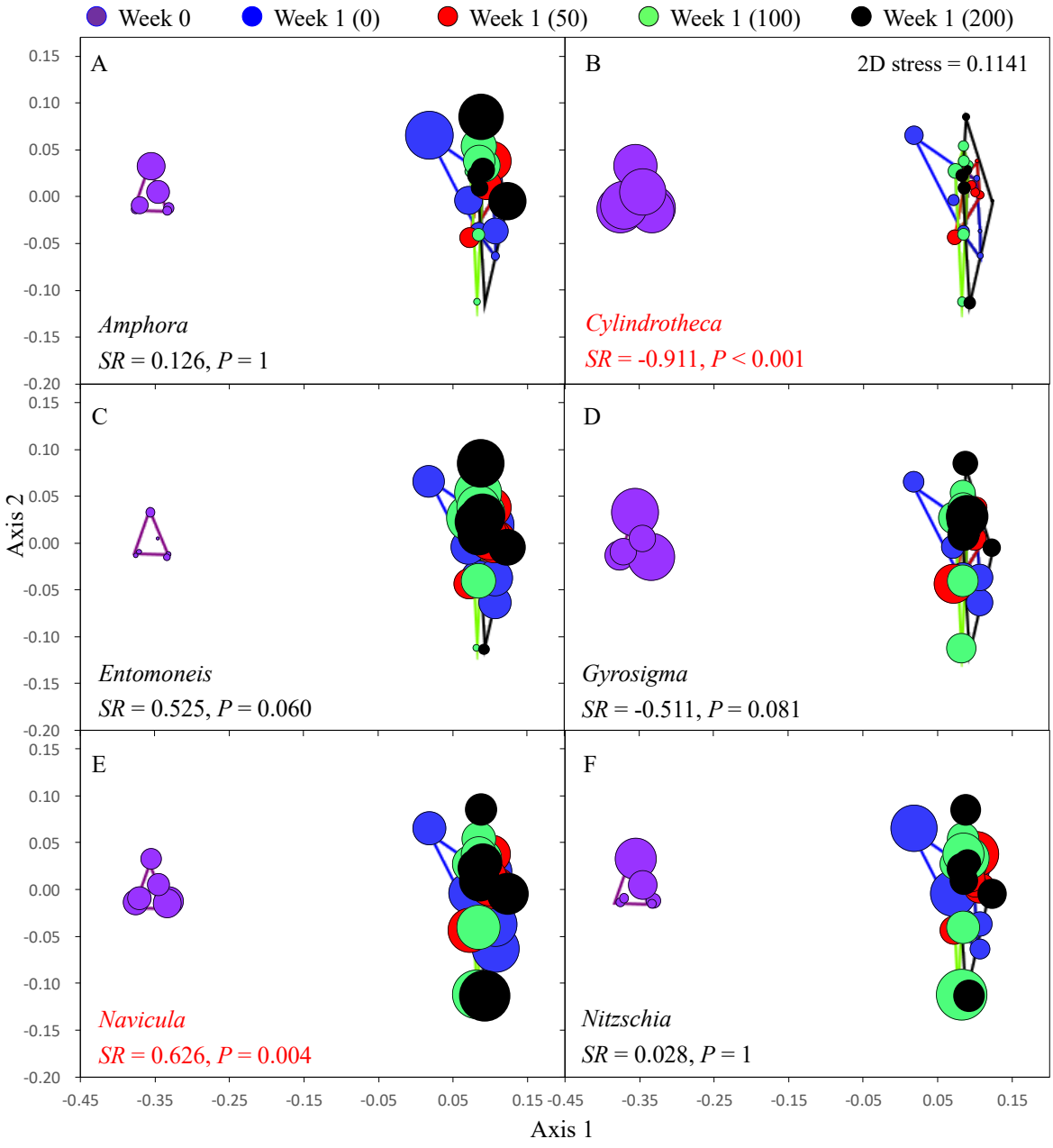

Figure 6.8 Bubble NMDs plots showing the relative abundance of genus (A) *Amphora*, (B) *Cylindrotheca*, (C) *Entomoneis*, (D) *Gyrosigma*, (E) *Navicula*, (F) *Nitzschia* in the initial intertidal MPB (Time 0) and in the MPBs cultivated with varying concentration of nano-TiO_2 (mg/L) for 1 week (Week 1) in the presence of UV lighting. The concentration of nano-TiO_2 are denoted by numbers in the parentheses in the legend. Each point indicates an individual replicate in the group. Within each genus, larger bubbles indicate a relatively higher relative abundance. Bubble sizes are not comparable between genera. The Spearman's rank correlation coefficient (SR) and *P* value between Axis 1 values and the RA of each genus are shown in the Figure.

6.3.5.2 The impact of nano-TiO_2 on the diatom composition in the second week

A NMDS plot was used to indicate the difference of diatom composition in the MPBs cultivated for 2 weeks with varying concentrations of nano-TiO_2 in the presence of UV lighting (Figure 6.9). The stress value for the NMDS plot was 0.0594, suggesting a very good representation of the diatom communities by the ordination distances. Considerable variations were noted within the replicates of each group. A clear separation was noticed between the control group and the treatments with nano-TiO_2 along Axis 1. One-way ANOSIM (factor: nano-TiO_2 concentration) confirmed that the differences in the diatom community composition between the 4 groups were greater than the differences within each group (Global R = 0.404, p = 0.001). A Spearman's rank correlation between the Axis 1 value and the RA of each genus was calculated to indicate the influence of each genus on the separation of the control group and the treatments with nano-TiO_2 along Axis 1. A significant negative Spearman's Rank (SR) correlation was obtained between Axis 1 value and the RA of genus *Cylindrotheca* (SR = -0.7302, $p < 0.001$), and between Axis 1 value and the genus *Navicula* (SR = -0.904, $p < 0.001$). A significant positive Spearman's Rank (SR) correlation was obtained between the Axis 1 value and the RA of genus *Entomoneis* (SR= 0.928, $p < 0.001$). According to the bubble plots (Figure 6.9), the separation of the control group and the treatments with nano-TiO_2 was mainly attributed to the differences in the RA of genus *Entomoneis*, *Navicula* and *Cylindrotheca*. After 2 weeks of cultivation, significant increases in the RA of genus *Entomoneis* was recorded in 3 treatments with nano-TiO_2 (RA = 43.5 – 53.1%), compared to the control group (RA = 16.2%); significant decreases in the RA of genus *Navicula* was recorded in 3 treatments with nano-TiO_2 (RA = 30.0 – 39.0%), compared to the control group (RA = 64.3%); significant decreases in the RA of genus *Cylindrotheca* was recorded in 3 treatments with nano-TiO_2 (RA = 0.8 – 9.3%), compared to the control group (RA = 14.0%).

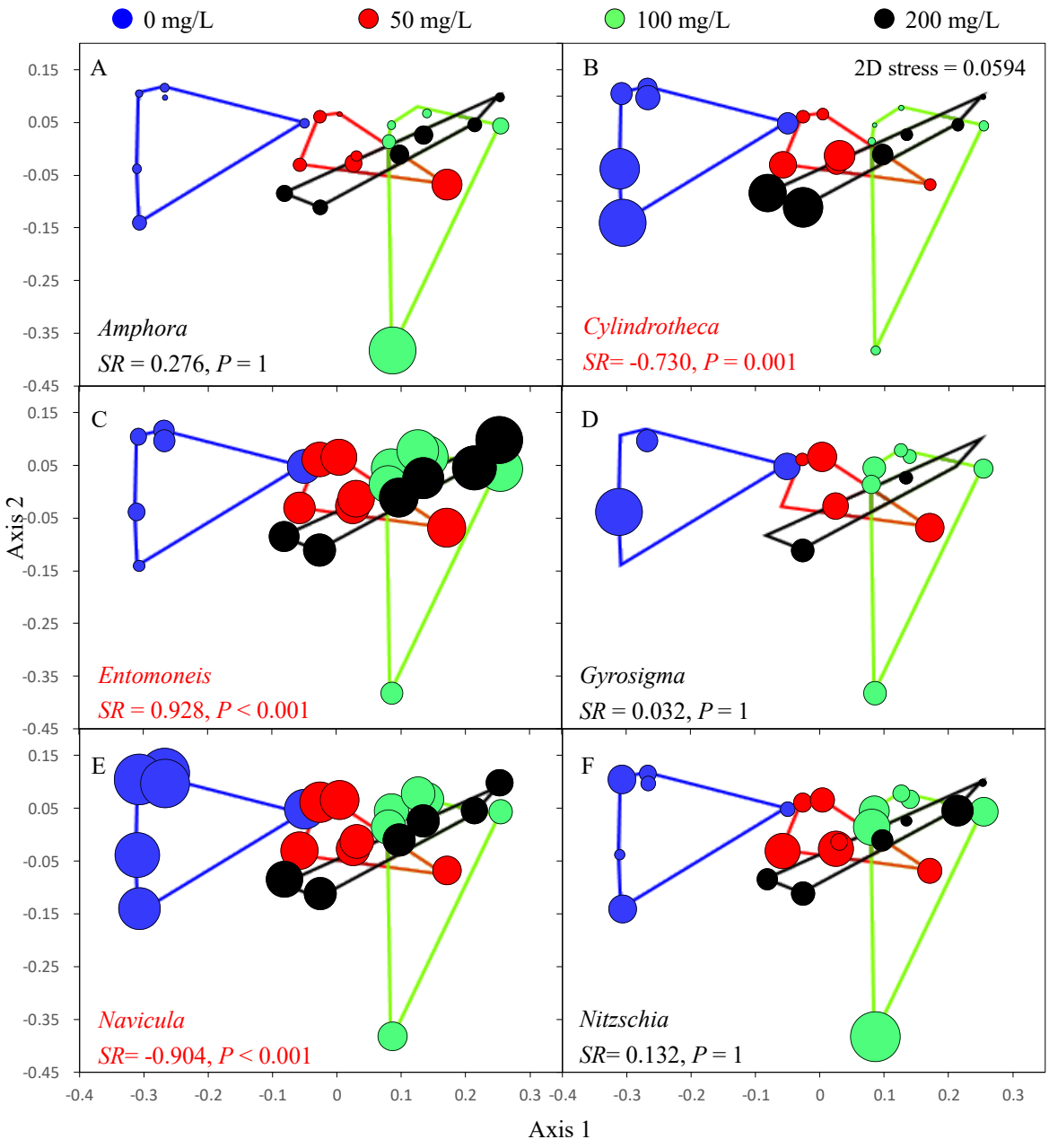

Figure 6.9 Bubble NMDS plots showing the relative abundance (RA) of genus (A) *Amphora*, (B) *Cylindrotheca*, (C) *Entomoneis*, (D) *Gyrosigma*, (E) *Navicula*, (F) *Nitzschia* in the intertidal MPBs cultivated with varying concentration of nano-TiO_2 (denoted by colour) for 2 weeks in the presence of UV lighting. Each point indicates an individual replicate in the group. Within each genus, larger bubbles indicate a relatively higher RA. Bubble sizes are not comparable between genera. The Spearman's rank correlation coefficient (SR) and *P* value between Axis 1 values and the RA of each genus are shown in each figure.

Figure 6.10 shows the change of diatom composition from week 1 to week 2. The stress value for the NMDS plot was 0.097, suggesting a good representation of the diatom communities by the ordination distances. The control groups at week 1 and week 2 overlapped, and ANOSIM test confirmed that the difference between them was not significant ($R = 0.139$, $p = 0.106$). Complete separation was noted in the treatment with 50 mg/L nano-TiO_2 at week 1 and week 2 along Axis 1, and ANOSIM test confirmed that the difference between them was significant ($R = 0.567$, $p = 0.006$). Complete separation was also noted in the treatment with 100 mg/L nano-TiO_2 at week 1 and week 2 along Axis 1, and ANOSIM test confirmed that the difference between them was significant ($R = 0.419$, $p = 0.006$). A slightly overlap was noted in the treatment with 200 mg/L nano-TiO_2 at week 1 and week 2 along Axis 1, and an ANOSIM test confirmed that the difference between them was significant ($R = 0.467$, $p = 0.009$). A two-way ANOSIM (factor 1: particle concentration: 50, 100 or 200 mg/L; factor 2: cultivation time: week 1 or week 2) was applied to investigate the impact of particle concentration and cultivation time on the diatom composition. The main effect of particle concentration was not significant on the diatom composition ($R = 0.053$, $p = 0.146$), but the main effect of cultivation time was significant ($R = 0.484$, $p = 0.001$).

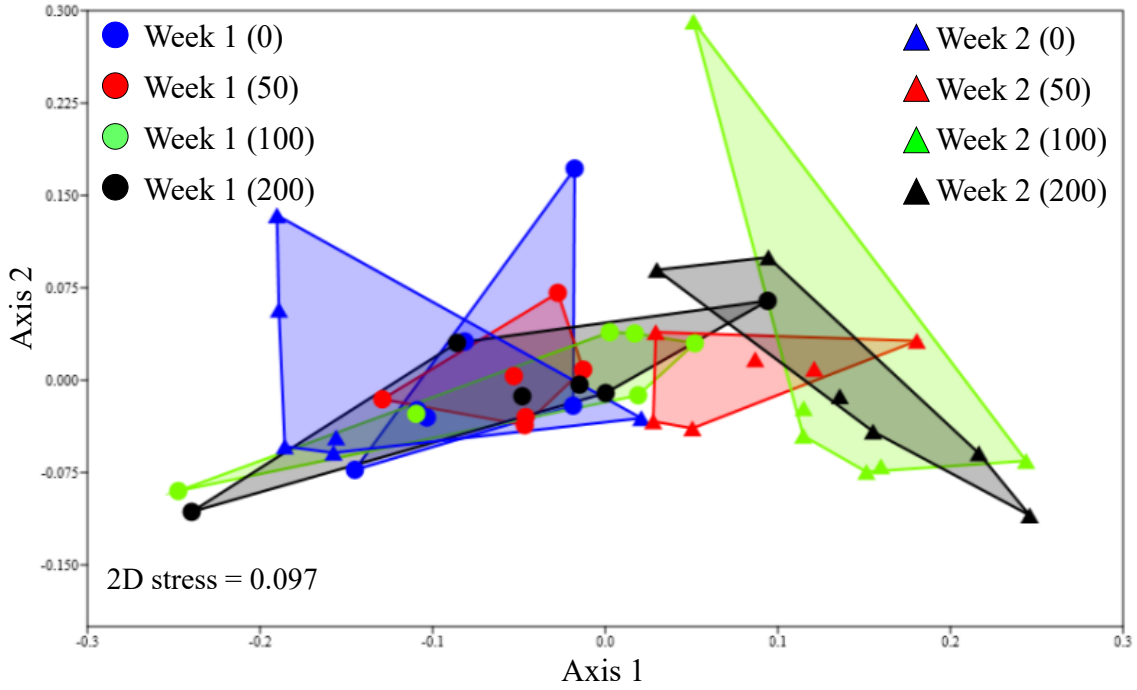

Figure 6.10 NMDS plot based on the relative abundance of 6 diatom genera in the intertidal MPBs cultivated with varying concentration of nano-TiO_2 (mg/L) for 1 week (Week 1) and 2 weeks (Week 2). The concentration of nano-TiO_2 are denoted by numbers in the parentheses in the legend. Each point indicates an individual replicate in the group.

A Spearman's rank correlation between the Axis 1 values and the RA of each genus was calculated to indicate the influence of each genus on the separation of diatom communities at week 1 and week 2 along Axis 1. A significant positive Spearman's Rank correlation was obtained between the Axis 1 value and the RA of genus *Entomoneis* (SR = 0.919, $p < 0.001$). A significant negative Spearman's Rank correlation was obtained between the Axis 1 value and the RA of genus *Navicula* (SR = -0.951, $p < 0.001$). According to the bubble plots (Figure 6.11), the separation of the groups with nano-TiO_2 at week 1 and week 2 was mainly attributed to the difference in the RA of genus *Entomoneis* and *Navicula*. Compared with the RA of genus *Entomoneis* at week 1 (RA = 26.4 – 27.2%), significant increases in the RA of genus *Entomoneis* were recorded in the treatments with nano-TiO_2 at week 2 (RA = 43.5 – 53.1%). Compared with the RA of genus *Navicula* at week 1 (RA = 53.6 – 56.8%), significant decreases in the RA of genus *Navicula* were recorded in the treatments with nano-TiO_2 at week 2 (RA = 30.0 – 39.0%).

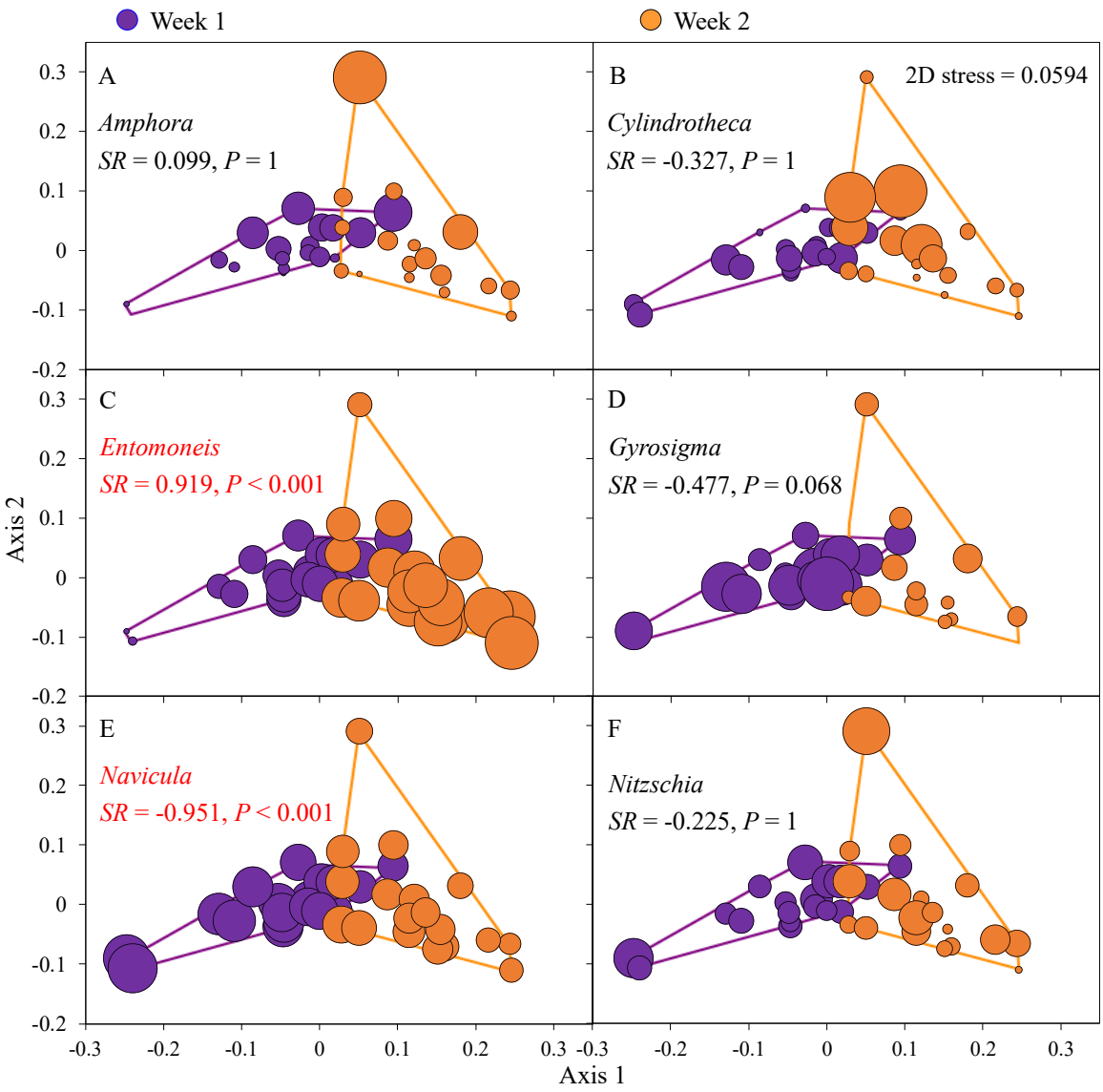

Figure 6.11 Bubble plots showing the relative abundance of genus (A) *Amphora*, (B) *Cylindrotheca*, (C) *Entomoneis*, (D) *Gyrosigma*, (E) *Navicula*, (F) *Nitzschia* in the intertidal MPBs cultivated after 1 week or 2 weeks of cultivation (marked by different colour). Each point indicates an individual replicate in the group. Within each genus, larger bubbles indicate a relatively higher relative abundance. Bubble sizes are not comparable between genera. The Spearman's rank correlation coefficient (SR) and *P* value between Axis 1 values and the RA of each genus are shown in the figure.

6.3.6 Summary of results

- At both week 1 and week 2, the presence of nano-TiO_2 showed no significant impacts on the biomass (measured as chl *a* content) of intertidal MPB, compared to the control group, in the

presence of UV lighting.

- At week 1, significantly higher phaeopigment was obtained in the treatments with 50 – 200 mg/L nano-TiO_2, compared to the control group, in the presence of UV lighting. At week 2, significantly higher phaeopigment were obtained in the treatments with 50 mg/L nano-TiO_2 and 200 mg/L nano-TiO_2, compared to the control group, in the presence of UV lighting.
- At both week 1 and week 2, the genus richness and diversity of the diatom community was not significantly affected by the presence of nano-TiO_2 and UV lighting.
- At week 1, the presence of nano-TiO_2 showed no significant impacts on the diatom composition in the intertidal MPB, in the presence of UV lighting. At week 2, a significant shift in the diatom composition was recorded in the presence of nano-TiO_2, with a higher RA of genus *Entomoneis* and a lower RA of genus *Navicula* and *Cylindrotheca*, compared to the control group, in the presence of UV lighting.

6.4 Discussion

6.4.1 The impact of nano-TiO_2 on the biomass of the intertidal MPB in the presence of UV lighting

It was hypothesized that nano-TiO_2 in the presence of UV lighting would negatively affect the intertidal MPB and result in a decreased biomass (assessed by chlorophyll *a* content) and the decrease of biomass would be greater in the presence of higher concentration of nano-TiO_2. The chlorophyll *a* content in the intertidal MPB was not significantly altered by the presence of 50 – 200 mg/L nano-TiO_2, compared to the control, at both week 1 and week 2, which was contrary to the hypothesis, though high variation within replicates was noted. Although the chl *a* content was not significantly different between treatments with nano-TiO_2 and the control group without nano-TiO_2, the phaeopigment content was significantly higher (increased by 62 – 151%) in the treatments with nano-TiO_2, compared to the control. Phaeopigments are degradation products of chl *a* and an increased degradation of chl *a* generally implies that organisms have encountered adverse growth conditions (Hendry et al. 1987). For example, a decrease of chl *a* content and a coincident increase in the phaeopigment content were recorded in an estuarine benthic diatom assemblage after biocide treatment with formaldehyde spray within 1 day (Underwood and Paterson

1993b). Therefore, the higher phaeopigment concentration recorded in the present study in the treatments with nano-TiO_2 was considered to be an indicator that some or all intertidal MPB species were negatively affected by the presence of nano-TiO_2.

The similar chl *a* between the treatment groups and the control group may indicate a recovery of some or all species in the nano-TiO_2 treatments and it is possible to draw upon information from the species composition to support this theory (see section 6.4.2). The biofilms were growing for a period of two weeks in the present investigation. A decreased growth inhibition effect of nano-TiO_2 over time has been reported in a few studies with monocultures (Hazeem et al. 2016; Li et al. 2019; Ockenden 2019), though these studies were conducted in the presence of fluorescent lighting. It is possible that after prolonged cultivation time, the MPB exposed to the nano-TiO_2 have recovered from any initial inhibition. Due to the lack of measurements at shorter intervals, it is unknown whether the biomass of intertidal MPB was acutely affected or not.

The similar chl *a* content between the treatment groups and the control group recorded in the whole intertidal MPB may also be linked to the shading effect of nano-TiO_2, which could cause an increase of cellular chlorophyll *a* content. Due to its insolubility, the presence of nano-TiO_2 has been suggested to decrease the availability of light received by cells, known as a shading effect, through their direct adsorption onto the surface of algal cells or entrapment of algal cells by particle aggregates (Aruoja et al. 2009; Hartmann et al. 2010; Wang et al. 2016b). A higher cellular chlorophyll *a* content has been found to be a response of algal cells when encountering lower light conditions (Pan et al. 1996; Ferreira et al. 2016). Hough et al. (2017) recorded an increased chl *a* content (increased by 75 – 128%) in a stream biofilm after 18 days exposure to 100 – 300 mg/L nano-TiO_2, compared to the control without nano-TiO_2, and they suggested that shading effect caused by the presence of nano-TiO_2 might have contributed to the increase of chl *a*. In the present study, the presence of nano-TiO_2 could have led to a similar effect, through reducing the light received by the intertidal MPB and therefore triggering an algal response of increasing cellular chl *a* concentration. However, cell enumeration was not carried out in the current investigation, so it is not possible to confirm if the cellular pigment concentration did increase in treated MPB, or if cell numbers were different between treatments.

The similar chl *a* between the treatment groups and the control group may also be related to the alteration of MPB composition. In the present investigation, after 2 weeks of cultivation, a significant shift in the diatom composition in the MPB was recorded in the presence of nano-TiO_2, with a higher relative abundance of the genus *Entomoneis* and a lower relative abundance of the genus *Navicula* and *Cylindrotheca*, compared to the control. It is possible that the cellular chl *a* content in the *Entomoneis* spp. was higher than that in the *Navicula* spp. and *Cylindrotheca* spp., which could therefore have compensated for any increase in the degradation of chl *a* and result in a similar overall chl *a* in the MPB. The alteration of MPB composition may also have happened at the class level. The alteration of the freshwater MPB composition when exposed to nano-TiO_2 has been previously recorded. Binh et al. (2016) found decreases of diatom and cyanobacteria and an increase of green algae in a stream biofilm after a 22-week exposure to nano-TiO_2. A similar result was reported by Wright et al. (2018), who discovered that after a 22-day exposure to nano-TiO_2 (the same type of nano-TiO_2 used in the current study), the MPB composition in the stream biofilm significantly changed, with increases of *Oscillatoria* spp. (filamentous cyanobacteria), *Chaetophora* sp. (a filamentous green alga) and decreases of *Acutodesmus dimorphus* (green algae), *Gomphonema clavatum* (diatom) and *Gomphonema lagenula* (diatom). In the present investigation, in addition to the predominant benthic diatoms, the presence of cyanobacteria and euglenoids, though with a low abundance, were also observed in the intertidal MPB. However, the quantification of each type of algae was not carried out in the current study, so it is not possible to confirm whether there was any alternation of MPB composition at class level in treated MPB.

6.4.2 The impact of nano-TiO_2 on the diatom composition in the intertidal MPB in the presence of UV lighting

It was hypothesized that the presence of nano-TiO_2 would alter the diatom composition in the intertidal MPB. The evidence shown in the present investigation indicated that the diatom composition was not significantly affected by 50 – 200 mg/L nano-TiO_2, compared to the control group, after 1 week of cultivation in the presence of UV lighting, in contrast to the hypothesis. However, after 2 weeks of cultivation in the presence of UV lighting, a significant shift in the diatom composition in the intertidal MPB was recorded in the treatments with 50 – 200 mg/L nano-TiO_2, compared to the control, in accordance with the hypothesis. The alteration of diatom composition was mainly attributed to the

increased RA of the genus *Entomoneis* and the decreased RA of the genera *Navicula* and *Cylindrotheca* in the presence of nano-TiO_2, compared to the control.

Wright et al. (2018) reported a significant increase in the RA of *Oscillatoria* spp. (a heavy metal and organic pollution tolerant genus) and decreases in the RA of *Acutodesmus dimorphus*, *Gomphonema clavatum* and *Gomphonema lagenula* (three typically pollution-sensitive algae) in a stream biofilm in response to the presence of nano-TiO_2. The result observed by Wright et al. (2018) suggested that the species with a high tolerance to pollutants may also have a relatively high tolerance to the presence of nano-TiO_2. Results from the current investigation suggested that *Entomoneis* spp. may have a higher tolerance to the presence of nano-TiO_2, compared to *Navicula* spp. and *Cylindrotheca* spp. This conclusion was consistent with previously published findings on the sensitivity of *Entomoneis* spp., *Navicula* spp. and *Cylindrotheca* spp. to the presence of pollutants. *Entomoneis* spp. (synonym *Amphiprora*) is a genus that has been reported to be highly tolerant to adverse growth conditions, including environmental extremes (e.g. pH and salinity), pollutants and toxic substances (e.g. copper, zinc, polycyclic aromatic hydrocarbons (PAHs), ammonia, sulfide) (French and Evans 1988; Zargiel et al. 2011; Ben Othman et al. 2018). For example, Zargiel et al. (2011) recorded that *Entomoneis* was the dominant genus in the biofilm grown on a ship panel which was coated with copper biocide. According to Underwood et al. (1993a), the most commonly present *Navicula* species in Portishead mudflats on the Severn estuary (the sampling site of the estuarine biofilm test in the present study) is *N. pargemina*, *N. phyllepta* and *N. flanatica*. These *Navicula* species have been reported to be sensitive to the presence of ammonia and sulphide (Admiraal and Peletier 1980; Underwood et al. 1998; Underwood and Provot 2000). *Cylindrotheca closterium*, a species identified in the intertidal MPB in the current investigation, is a species sensitive to toxicants and has been proposed as a model species for toxicity tests (Moreno-Garrido et al. 2003; Araújo et al. 2010b; Araújo et al. 2010a). The growth of *Cylindrotheca closterium* in monoculture, one of the isolated diatom species from the Portishead mudflats on the Severn estuary for this study, was shown to be completely inhibited in the presence of 100 mg/L nano-TiO_2 in the presence of UVR (section 5.3.1 in Chapter 5), which matches observations made in the community experiment described here, where a significantly lower RA of genus *Cylindrotheca* was recorded in the treatments compared with the control, after 2 weeks of exposure.

The higher tolerance of *Entomoneis* spp. may be associated with their complex structure and relatively higher surface area relative to volume (Figure 6.4). It has been reported that benthic diatoms are normally embedded in a matrix of EPS (Hoagland et al. 1993). The EPS attached to the diatom cells could adsorb nano-TiO_2, preventing the direct interaction nano-TiO_2 with the cell wall and therefore increase the cell's tolerance to the presence of nano-TiO_2 (Geo et al. 2018). Assuming a similar nano-TiO_2 quota per unit volume, cells with a higher surface area to volume ratio, such as *Entomoneis* cells, may have a higher potential of binding nano-TiO_2 and thus *Entomoneis* cells may be better protected. Further investigations would be required to verify this. As for *Cylindrotheca* spp., their long needle shaped ends might be not be fully covered by the EPS and thus they may be associated with a higher risk of physical interaction with NPs and a higher possibility of cell wall damage, which may facilitate greater interaction between nano-TiO_2 with the cell membrane and increases the possibility of particle internalization.

To be noted, the change in the RA of each diatom genus only provided information regarding the response of a genus in relative to the response of other genera, to the presence of nano-TiO_2. This information should not be interpreted as the response of a genus to the presence of nano-TiO_2. For example, an increased RA of *Entomoneis* should not be interpreted as the growth of *Entomoneis* was stimulated by the presence of nano-TiO_2. There is a possibility that the growth of all cells were inhibited by the presence of nano-TiO_2 but inhibition percentage of *Entomoneis* was lower than those of other genera.

6.4.3 Environmental relevance and implications of the present study

It is important to note that the concentration of nano-TiO_2 (50 – 200 mg/L) added to the intertidal MPB in the present study was considerably higher than estimated environmental concentrations. The highest concentration of nano-TiO_2 in the water column in the UK was predicted to be 0.25 – 24.5 µg/L (see Table 1.2 in Chapter 1 for details). However, more information is needed on the concentrations of nano-TiO_2 that may be associated with sediments. Considering the dramatically increased production and application of nano-TiO_2 over the past 10 years, the release of nano-TiO_2 and thus the concentration of nano-TiO_2 in the environment may be higher. The concentration of nano-TiO_2 exposed to the estuarine biofilm was anticipated to be remarkably higher than that in the water column, due to the possible sedimentation and accumulation effect (Battin et al. 2009; Ferry et al. 2009; Gao et al. 2018). Ferry et al. (2009) investigated

the partitioning of gold NPs (nano-Au) within artificial estuarine mesocosms, which contained seawater, sediments, flora (biofilm and sea grass) and fauna (snail, clam, shrimp and fish), after adding a single dose of nano-Au (6 µg/L). The concentration of nano-Au added into the estuarine mesocosms was believed to be environmentally relevant (Ferry et al. 2009). After 12 days of interaction, approximately 8.6% of nano-Au remained in seawater, 24.5% of nano-Au was detected in the sediments, and the biofilm accumulated the most nano-Au by 61%. The concentration of nano-Au in the biofilm was found to be 1.53×10^4 times higher than that in the water on a per mass basis (Ferry et al. 2009). A similar accumulation effect was anticipated to have occurred for nano-TiO_2 in the intertidal MPB biofilm experiment conducted for the present study. The concentration of nano-TiO_2 applied in the present study ranged from 50 – 200 mg/L, which was $0.2 – 0.8 \times 10^4$ times higher than the highest predicted concentration in the water column (24.5 µg/L, Boxall et al. 2007), and therefore was considered to be realistic scenarios assuming nano-TiO_2 partition in a similar fashion to the nano-Au.

To the best of my knowledge, this is the first study to have revealed that some species in the MPB in estuarine biofilms could be impaired by the presence of nano-TiO_2. Although chl *a* content, the commonly used biomass indicator, was not significantly different in the presence of nano-TiO_2 in the intertidal MPB, the increased phaeopigment provided evidence to support the hypothesis that the intertidal MPB was impaired in the presence of nano-TiO_2. The potential shading effect of nano-TiO_2 might have 'masked' the negative impact of nano-TiO_2 and thus result in an underestimation of their risk, if chl *a* content was the only endpoint selected to indicate the impact of nano-TiO_2. It is recommended that such tests should be accompanied with viable cell counts where practicable, or measurements of the degradation of chl *a*. The cell counts should be done on a species-specific basis to inform about differing species' responses. As demonstrated here, when species compositional change was used as an endpoint, the impact of nano-TiO_2 became significant. The shift in the diatom composition in the presence of nano-TiO_2 may have notable ecological significance, for organisms in the higher levels of the food chain, when the consumers exhibit a genus-specific dietary preference. As an important finding, this study highlighted nano-TiO_2 as a potential risk to the healthy functioning of estuarine organisms in food webs relying on intertidal MPB as a significant part of their diet.

6.4.4 **Limitations and suggestions**

The response of intertidal MPB to the presence of nano-TiO_2 recorded in the present study provided insights into the potential risk of nano-TiO_2 to the estuarine biota. However, to be noted, the traditional type of toxicity testing carried out in the well-controlled laboratory conditions are often far different from the conditions to which algae are exposed in field conditions. For example, the illumination in the lab was set to be 80 μmol m^{-2} s^{-1} (PAR) throughout the day in the present study, while the light intensity and spectrum in the field may vary dramatically at dawn and dusk. In addition, the UVR level was set at a constant level throughout the day in the present study, while the UVR could vary dramatically within a day under natural conditions in exposed intertidal mudflats. The biofilms were also grown in constant temperature. Further, it is often the case that certain species may grow better under lab conditions that the others and thus it is possible that only a sub-set of the MPB community was targeted in the present study. As a result, the intertidal MPB grown in the lab might behave differently compared to that grown in the field. However, the present tests may offer more realism than single species testing and provide further insights into the long-term impacts of nano-TiO_2.

Motility is a unique feature of many benthic diatoms. They may respond to various environmental conditions such as light intensity, UVR exposure, tidal cycle by migrating up and down in the sediments (Round and Palmer 1966; Consalvey et al. 2004a; Underwood et al. 2005). It would be interesting to investigate whether the presence of nano-TiO_2 has a negative impact on the diatom motility in the further studies.

6.5 **Conclusion**

In the present study, for the first time, to the best of my knowledge, the response of intertidal MPB to the presence of nano-TiO_2 was investigated.

- Chlorophyll *a* concentration, as a measure of biomass in the intertidal MPB was not significantly affected by the presence of 50 – 200 mg/L nano-TiO_2, after 1 week or 2 weeks of cultivation in the presence of UV lighting. However, an increase in the phaeopigment was recorded, suggesting

that intertidal MPB was negatively impacted by the presence of 50 – 200 mg/L nano-TiO_2.

- The genera richness and diversity of the diatom community was not significantly altered by the presence of 50 – 200 mg/L nano-TiO_2 and UV lighting.
- The diatom composition was significantly altered after 2 weeks of exposure to 50 – 200 mg/L nano-TiO_2 in the presence of UV lighting. A decrease in the relative abundance of genus *Navicula* and *Cylindrotheca*, and an increase in the relative abundance of genus *Entomoneis*, relative to the control, was recorded in the presence of nano-TiO_2.

Chapter 7 Synthesis and recommendations for future studies

7.1 The importance of illumination type when determining the impact of nano-TiO_2

TiO_2 is a photocatalytic substance, which could accelerate a chemical reaction when activated by light. One of the aims of the present thesis was to investigate whether the type of illumination played a role in determining the impact of nano-TiO_2 on the growth of intertidal estuarine benthic diatoms and if so, how much of a difference that would make. It was recorded that the growth rate of *Cylindrotheca closterium* showed a slight but significant increase of 1.5% in the presence of 100 mg/L nano-TiO_2 under fluorescent lighting but was significantly inhibited by 100% in the presence of 100 mg/L nano-TiO_2 under UV lighting, after 72 h of exposure, hence major differences were recorded. The growth rates of *Cylindrotheca closterium* under two light regimes in the absence of nano-TiO_2 were found to be not significantly different, so the presence of UVR alone did not inhibit algal growth in the absence of the nanoparticles.

Importantly, up until now, most of the published laboratory investigations to quantify the impacts of nano-TiO_2 have been performed with fluorescent lighting, which is recommended by the OECD guideline (OECD 2011), and these fluorescent lighting are reported to emit a negligible level of UVR. To the best of my knowledge, circa 5% of the previous studies had explored the impact of nano-TiO_2 in the presence of UVR. Results from the present investigation, and evidence from previous studies which were conducted with the presence of UVR, highlighted that the UVR level in the illumination may play a crucial role in determining the impact of nano-TiO_2 on the algae. The environmental risk of nano-TiO_2 may be underestimated under laboratory investigations where lighting contained little or negligible levels of UVR had been used for illumination, though it is acknowledged that not all algae will grow in locations with considerable amount of UVR. It is suggested that the influence of different wavelengths of light, with a specific focus on the range of UVR (< 400 nm), should not be neglected in future studies when investigating the impact of photocatalytic nano-TiO_2. The influence of illumination should also be considered when investigating the impact of other types of photocatalytic substances, such as ZnO, SnO_2, CeO_2, Fe_2O_3, CdS (Khan et al. 2015; Zhu et al. 2019).

Considering the greater negative impact in the presence of UVR than that in the absence of UVR, the algae

inhabiting within the areas where a considerable amount of UVR may be present, such as very shallow areas of wind-washed littoral regions in lakes, the intertidal areas in estuaries, polar and alpine areas where ozone reduction is significant and in water bodies where the dissolve organic matters (DOM) is low, might be under a much higher risk from the release of nano-TiO_2, compared with algae inhabiting other regions with relatively low level of UVR penetration. As a result, it is suggested that future regulations regarding the application of nano-TiO_2 should take into account their possible releasing sites to consider their impacts to local algal assemblages.

7.2 **Species-specific sensitivity to the presence of nano-TiO_2**

Benthic diatoms are the dominant species in intertidal areas of estuaries, which may be regions where a higher exposure of nano-TiO_2 might be expected. Up to date, no investigations have been carried out to explore the response of estuarine benthic diatoms to the presence of nano-TiO_2. One of the aims of this thesis was to investigate the impact of estuarine benthic diatom species to the presence of nano-TiO_2 and to see if they have different sensitivity compared to other species.

Here it was demonstrated that the growth rates of the estuarine benthic diatoms were stimulated when exposed to 100 mg/L nano-TiO_2 in the presence of fluorescent lighting, in species including *Nitzschia* c.f. *clausii* (increased by 25%), *Navicula gregaria* (increased by 8.5%) and *Cylindrotheca closterium* (increased by 1.5%), compared to controls grown without nano-TiO_2. These results are in contrast to a number of other studies, which found negative impacts of nano-TiO_2 under the same light condition and particle concentration, in species including a few freshwater planktonic species (e.g. *Pseudokirchneriella subcapitata*, *Chlamydomonas reinhardtii*, *Chlorella* sp., *Scenedesmus* sp.), freshwater benthic diatom species (e.g. *Nitzschia palea*) and marine planktonic diatom species (e.g. *Phaeodactylum tricornutum*, *Skeletonema costatum*) (Table 4.4 in Chapter 4). These results add to the evidence which demonstrates a wide variation in the algal response to a single type of nanoparticle, supporting the view that there is a considerable degree of species-specific response to nano-TiO_2. Comparatively, the three estuarine benthic diatom species seemed to have a higher tolerance to nano-TiO_2, compared with other planktonic species and freshwater benthic species, in the presence of fluorescent lighting. In addition to the species-specific sensitivity, this wide variation may partly link to the differences in the experimental protocol and the

differences in the particle properties as summarized in section 1.6.1 in Chapter 1.

It was also demonstrated that the growth rate of an estuarine benthic diatom species, *Cylindrotheca closterium*, was inhibited by the presence of nano-TiO_2 under UV lighting, with 72 h-IC50 of 8.73 mg/L nano-TiO_2. Similarly, growth inhibition of nano-TiO_2 has also been recorded by other researchers in the presence of illumination containing a considerable amount of UVR, in a few freshwater planktonic species (e.g. *Chlamydomonas reinhardtii, Chlorella* sp.) and marine planktonic species (e.g. *Thalassiosira pseudonana, Phaeodactylum tricornutum, Dunaliella tertiolecta*). However, the reported 72 h-IC50 values were no greater than 3 mg/L nano-TiO_2, which was significantly lower than the 8.73 mg/L obtained in the present thesis (Table 5.4 in Chapter 5). These comparisons also supported that there is a considerable degree of species-specific response to nano-TiO_2, suggesting that the estuarine benthic diatom species tested in the presence thesis may have a higher tolerance to nano-TiO_2, compared to other freshwater and marine planktonic species, in the presence of UV lighting.

It is highly likely that the sampling site (Portishead, Severn Estuary, UK) where the estuarine benthic diatoms were isolated, might have already accumulated a notable amount of nano-TiO_2. The sampling site is 200 meters downstream of a popular swimming pool, named Portishead Open Air Pool. As a common additive in sunscreens, the release of nano-TiO_2 into the water due to the wash-off of sunscreen during bathing activities has been recorded (Botta et al. 2011; Johnson et al. 2011; Jeon et al. 2016). The water in the pool is constantly filtered through recycled glass filters and released into the Seven Estuary directly. These recycled glass filters may only filter particles larger than 1 μm (https://eagleleisure.co.uk/swimming-pool-filters-benefits-glass-media/, accessed 13/09/2019). According to Botta et al. (2011), the particles containing nano-TiO_2 released from the 4 commercial sunscreens were mainly smaller than 1 μm, suggesting the nano-TiO_2 deposited into the pool may be released into the Seven Estuary directly. Approximately 50,000 people visit Portishead pool every year (http://www.portisheadopenairpool.org.uk/about-us/history/). Assuming people applied 0.8 mg/cm^2 sunscreen to half of their body area (2 m^2) (Narbutt et al. 2019), the total sunscreen used by the swimmers at Portishead pool is estimated to be 800 kg per year. Assuming half of the commercial sunscreen contains nano-TiO_2 with a typical content of 4.6% (Botta et al. 2001), the nano-TiO_2 released from the Portishead pool may reach 18.4 kg per year. These released nano-TiO_2 may accumulate in the downstream estuary. Under this circumstance, the estuarine benthic diatom species isolated

from the Portishead, Severn Estuary might have already been exposed the nano-TiO_2 and this pre-acclimation might have rendered them less susceptible.

The relatively high tolerance of estuarine benthic diatoms may also be linked to their unique feature of secreting EPS during moving. Compared to the other species which only produce EPS in response to environmental stress, EPS production by motile diatoms is deemed to be much higher, as it is an integral process during growth to support diatoms' locomotion (Smith and Underwood 1998). Preliminary observations indicated that these estuarine benthic diatoms could be firmly adhered to the surface during cultivation, owing to the secretion of EPS. The presence of EPS has been reported to play an importance role in reducing the availability of nano-TiO_2, by adsorbing or trapping nano-TiO_2 and preventing the direct physical interaction of nano-TiO_2 with the cell membrane (Gao et al. 2018; Zhu et al. 2019), providing protection to the diatom cells. Relative to planktonic species, the benthic diatoms are generally embedded in a matrix of EPS (Hoagland et al. 1993). Therefore, benthic diatom species, compared to other species, may be better protected by an EPS film and by the EPS released into their immediate environment, thus having a higher tolerance to the presence of nano-TiO_2 due to reduced contact with the nanoparticles.

7.3 Is *Cylindrotheca closterium* a good model species for investigating the impact of nano-TiO_2?

Investigations on the changes in the diatom composition in the MPB assemblage indicated that some species did better than other species under exposure to nano-TiO_2 in the presence of UV lighting, providing some insights into the potentially different responses of individuals in a mixed assemblage. After a two-week exposure to 50 – 200 mg/L nano-TiO_2 in the presence of UV lighting, the diatom composition in the MPB assemblage was significantly altered, suggesting that different genera of benthic diatoms could have responded differently to the presence of nano-TiO_2 (section 6.3.5.2 in Chapter 6). The significantly higher RA of genus *Entomoneis* and the lower RA of genus *Navicula* and *Cylindrotheca* recorded in the treatment with nano-TiO_2, compared to the control group, implied that genera *Navicula* and *Cylindrotheca* appeared to be less tolerant to the presence of nano-TiO_2 and suggested that *Entomoneis* may be more tolerant. This suggested *Navicula* spp. and *Cylindrotheca* spp. may be better indicators for the risk of nano-TiO_2, compared to the *Entomoneis* spp., due to their relatively higher sensitivity. Amongst the three estuarine benthic diatom

species investigated during this research (*Navicula gregaria*, *Nitzschia* cf. *clausii*, and *Cylindrotheca closterium*), *Cylindrotheca closterium* had the highest growth rate of 1.34 day^{-1}, suggesting this species could be easily maintained under laboratory conditions (section 4.3.3 in Chapter 4). In the single species testing, a clear dose-response curve to the increased concentration of nano-TiO_2 was obtained with *Cylindrotheca closterium* (section 5.3.2.2 in Chapter 5), with IC50 values within 6 – 9 mg/L. In addition, *Cylindrotheca closterium* is a common species present in many parts of the world (Araújo et al. 2010a). Previously, *Cylindrotheca closterium* has been proposed as a model species for toxicity tests with heavy metal (Moreno-Garrido et al. 2003; Araújo et al. 2010a). Results from this these suggested that *Cylindrotheca closterium* may also be a good model species for investigating the impact and the risk of nano-TiO_2.

7.4 Considerations for selecting suitable endpoints to address the risk of nano-TiO_2

In the present thesis, several endpoints were used to address the risk of nano-TiO_2, including endpoints related to biomass such as cell density yield, growth rate, chlorophyll *a* content, chlorophyll *a* concentration per cell, and endpoints related to photophysiology such as maximum quantum yield of PSII after dark-adaption (Fv/Fm), the maximum electron transport rate ($rETR_{max}$), maximum light use coefficient (α) and light saturation coefficient (E_k). Varied responses were recorded when using different endpoints, under exposure to nano-TiO_2.

Investigations in the current research revealed that cell density measurements using traditional light microscopy may be compromised by the presence of nano-TiO_2, due to the heteroaggregation between particles and algal cells which entrapped cells and obscured their recognition (section 3.3.1.1 in Chapter 3). For the three estuarine benthic diatoms species test in the present thesis, the interference of nano-TiO_2 on the cell density measurement was recorded with *Navicula gregaria* cultures only. This suggested that the interference may be species-specific, possibly related to differences in EPS production, cell wall properties, or other aspects of cell morphology. Interference of nano-TiO_2 caused a 49% underestimation of cell density of *Navicula gregaria*. Such a large underestimation was found to be sufficient to reverse the conclusion regarding the impact of nano-TiO_2 on the growth of *Navicula gregaria*, from a stimulation effect (without the interference) to an inhibitory effect (with the interference) (section 3.3.1.2 in Chapter 3). Therefore, it is

suggested that if cell density measurement via cell enumeration under light microscopy was the selected endpoint, preliminary investigations must be carried out with each test species to find out if the presence of nano-TiO_2 interferes with this measurement. If the interference exists, additional modifications should be applied to the protocol to eliminate the interference. In the present study, a sonication method with H_2SO_4 was found to work effectively in eliminating the interference of nano-TiO_2 recorded with *Navicula gregaria*, by breaking up the clumps of TiO_2 particles and cells (section 3.3.1.2 in Chapter 3). This method might work well in other species which are not sensitive to sonication treatment, and could be considered in the future studies.

Investigations revealed that the presence of nano-TiO_2 would not interfere with chlorophyll *a* content measurement using spectrophotometry (section 3.3.2 in Chapter 3). However, both increased and decreased chlorophyll *a* concentrations per cell were recorded in *Cylindrotheca closterium* in the presence of nano-TiO_2 (section 5.3.2.3 in Chapter 5). The increase of cellular chlorophyll *a* concentration may be linked to the shading effect of nano-TiO_2 so that the cells accumulated more pigments to increase their light capturing capacity (Pan et al. 1996; Ferreira et al. 2016). The increase of cellular chlorophyll *a* concentration may also be linked to the inhibition on the cell division so that the cells were growing bigger with more pigments but were not able to divide. The decrease of cellular chlorophyll *a* concentration may be linked to the degradation of chlorophyll *a*. As a result, it would be impossible to know whether any change in the chlorophyll *a* content is attributed to the difference in the algal biomass or the differences in the cellular chlorophyll *a* content, in the absence of additional measurements on cell numbers. Therefore, it is suggested that the chlorophyll *a* concentration measurement should be accompanied by cell density measurement wherever possible. If cell density measurement could not be achieved, it is recommended that the concentration of phaeopigment should be measured at the same time, which may provide some insights into whether the cells were under growth stress.

Investigations in the current research also revealed that the presence of nano-TiO_2 may interfere with *in vivo* fluorescence results (section 3.3.3.2 in Chapter 3). Therefore, *in vivo* fluorescence measurement was not recommended for quantification of the biomass in the presence of nano-TiO_2.

Photophysiological endpoints including Fv/Fm, $rETR_{max}$, α and E_k measured for *Cylindrotheca. closterium* were not significantly affected after 72 h exposure to 5 mg/L nano-TiO_2 in the presence of UV lighting, which was not in agreement with the growth inhibition (indicated by biomass yield) observations in the same culture. Previous studies indicated that algal photosynthetic performance may be enhanced (Ockenden, 2019), or inhibited (Deng et al. 2017), while algal growth was significantly inhibited by the presence of nano-TiO_2. These results implied that the endpoints related to response of photophysiological endpoints may not provide a definite indication for the potential impact of nano-TiO_2 on algal growth, which is normally the major concern in the risk assessment. Cardinale et al. (2012) presented evidence that algal growth rate was determined by the difference bewteen the gross primary production (i.e. photosynthetic performance) and the respiration. Therefore, the photophysiological endpoints alone, might not be good endpoints for addressing the impact of nano-TiO_2.

Overall, it is recommended that in future investigations, (i) priority should be given to the endpoints related to the cell density when investigating the impact of nano-TiO_2, (ii) the response of chlorophyll *a* content, should not be used to interpret the impact of nano-TiO_2, in absence of the response of cell density, (iii) where cell density can not be easily measured, the concentration of phaeopigment should be measured concurrently with the measurement of chlorophyll *a* concentration, to address the impact of nano-TiO_2, (iv) the response of photophysiological endpoints alone, should be treated with caution when interpreting the risk of nano-TiO_2.

Abbreviations

AEW: artificial estuarine water

Alpha (α): maximum light use coefficient

ANOSIM: analysis of similarities

ANOVA: analysis of variance

BET: Brunauer, Emmett, Teller

DLS: dynamic light scattering

DOC: dissolve organic carbon

DOM: dissolve organic matters

EDX: energy-dispersive X-ray

E_k: light saturation coefficient

ENP: engineered nanoparticle

EPS: extracellular polymeric substances

FESEM: Field Emission scanning electron microscope

Fv/Fm: maximum quantum yield of PSII after dark-adaption

GHS: globally harmonized system of classification and labelling of chemicals

H_2O_2: hydrogen peroxide

IC10: concentration of a substance at which the inhibition on the growth rate is 10%

IC50: concentration of a substance at which the inhibition on the growth rate is 50%

INP: incidental nanoparticle

IP: Inhibition percentage on growth rate

LM: light microscope

MPB: microphytobenthos/ microphytobenthic

Nano-TiO_2: titanium dioxide nanoparticles

NMDS: non-metric multidimensional scaling

NNP: natural nanoparticle

NOM: natural organic matters

NP: nanoparticle

$O_2^{-}\bullet$: superoxide radical anions

OECD: Organization for Economic Cooperation and Development

OH•: OH radicals

PAM: pulse amplitude modulated

PAR: photosynthetically active radiation

pH_{PZC}: the pH value at which the zeta-potential of the NP dispersion is zero

PSII: photosystem II

RA: relative abundance

$rETR_{max}$: maximum electron transport rate

RLC: rapid light curve

ROS: reactive oxygen species

SEM: scanning electron microscope/microscopy

SP: stimulation percentage on growth rate

SR: Spearman's Rank

TEM: transmission electron microscope/microscopy

UV: ultraviolet

UVR: ultraviolet radiation

XRD: X-ray powder diffraction

Reference

Abou-Waly H, Abou-Setta MM, Nigg HN et al. (1991) Growth response of freshwater algae, *Anabaena flosaquae* and *Selenastrum capricornutum* to atrazine and hexazinone herbicides. Bulletin of Environmental Contamination and Toxicology 46 (2):223-229.

Adam N, Schmitt C, Galceran J et al. (2014) The chronic toxicity of ZnO nanoparticles and $ZnCl_2$ to *Daphnia magna* and the use of different methods to assess nanoparticle aggregation and dissolution. Nanotoxicology 8 (7):709-717.

Adam V, Loyaux-Lawniczak S, Labille J et al. (2016) Aggregation behaviour of TiO_2 nanoparticles in natural river water. Journal of Nanoparticle Research 18 (1):13.

Admiraal W (1977) Tolerance of estuarine benthic diatoms to high concentrations of ammonia, nitrite ion, nitrate ion and orthophosphate. Marine Biology 43 (4):307-315.

Admiraal W, Bouwman LA, Hoekstra L et al. (1983) Qualitative and quantitative interactions between microphytobenthos and herbivorous meiofauna on a brackish intertidal mudflat. Internationale Revue der gesamten Hydrobiologie und Hydrographie 68 (2):175-191.

Admiraal W, Peletier H (1979) Sulfide tolerance of benthic diatoms in relation to their distribution in an estuary. British Phycological Journal 14 (2):185-196.

Admiraal W, Peletier H (1980) Distribution of diatom species on an estuarine mud flat and experimental analysis of the selective effect of stress. Journal of Experimental Marine Biology and Ecology 46 (2):157-175.

Admiraal W, Peletier H, Brouwer T (1984) The seasonal succession patterns of diatom species on an intertidal mudflat: an experimental analysis. Oikos 42 (1):30-40.

Admiraal W, Peletier H, Zomer H (1982) Observations and experiments on the population-dynamics of epipelic diatoms from an estuarine mudflat. Estuarine, Coastal and Shelf Science14 (5):471-487.

Agutter PS (2008) Elucidating the mechanism(s) of hormesis at the cellular level: the universal cell response. American Journal of Pharmacology and Toxicology 3 (1):100-110.

Aitken R, Creely K, Tran C et al. (2004) Nanoparticles: An occupational hygiene review. HSE Books.

Al-Kattan A, Wichser A, Zuin S et al. (2014) Behavior of TiO_2 released from nano-TiO_2-containing paint and comparison to pristine nano-TiO_2. Environmental science & technology 48 (12):6710-6718.

Allouni ZE, Cimpan MR, Hol PJ et al. (2009) Agglomeration and sedimentation of TiO_2 nanoparticles in cell culture medium. Colloid Surface B 68 (1):83-87.

Almusallam AS, Abdulraheem YM, Shahat M et al. (2012) Aggregation behavior of titanium dioxide nanoparticles in aqueous environments. Journal of Dispersion Science and Technology 33 (5):728-738.

American Society for Testing and Materials (2012) Standard terminology relating to nanotechnology. ASTM E2456-06(2012) American Society for Testing and Materials.

Amiano I, Olabarrieta J, Vitorica J et al. (2012) Acute toxicity of nanosized TiO_2 to *Daphnia magna* under UVA

irradiation. Environmental Toxicology and Chemistry 31 (11):2564-2566.

Andersen RA (2005) Algal culturing techniques. Elsevier academic press.

Araújo CVM, Diz FR, Lubián LM et al. (2010a) Sensitivity of *Cylindrotheca closterium* to copper: influence of three test endpoints and two test methods. Science of The Total Environment 408 (17):3696-3703.

Araújo CVM, Blasco J, Moreno-Garrido I (2010b) Microphytobenthos in ecotoxicology: a review of the use of marine benthic diatoms in bioassays. Environment International 36 (6):637-646.

Aruoja V, Dubourguier H-C, Kasemets K et al. (2009) Toxicity of nanoparticles of CuO, ZnO and TiO_2 to microalgae *Pseudokirchneriella subcapitata*. Science of the Total Environment 407 (4):1461-1468.

Ast M, Gruber A, Schmitz-Esser S et al. (2009) Diatom plastids depend on nucleotide import from the cytosol. Proceedings of the National Academy of Sciences 106 (9):3621-3626.

Atkinson M, Bingman C (1997) Elemental composition of commercial seasalts. Journal of Aquariculture and Aquatic Sciences 8 (2):39.

Auguste M, Lasa A, Pallavicini A et al. (2019) Exposure to TiO_2 nanoparticles induces shifts in the microbiota composition of *Mytilus galloprovincialis* hemolymph. Science of The Total Environment 670:129-137.

Auten RL, Davis JM (2009) Oxygen toxicity and reactive oxygen species: the devil Is in the details. Pediatric Research 66:121.

Baalousha M (2017) Effect of nanomaterial and media physicochemical properties on nanomaterial aggregation kinetics. NanoImpact 6:55-68.

Baalousha M, Nur Y, Romer I et al. (2013) Effect of monovalent and divalent cations, anions and fulvic acid on aggregation of citrate-coated silver nanoparticles. Science of the Total Environment 454:119-131.

Ball AS, Williams M, Vincent D et al. (2001) Algal growth control by a barley straw extract. Bioresource Technology 77 (2):177-181.

Barranguet C, van Beusekom SAM, Veuger B et al. (2004) Studying undisturbed autotrophic biofilms: still a technical challenge. Aquatic Microbial Ecology 34 (1):1-9.

Batley GE, Kirby JK, McLaughlin MJ (2013) Fate and risks of nanomaterials in aquatic and terrestrial environments. Accounts of Chemical Research46 (3):854-862.

Battin TJ, Kammer Fvd, Weilhartner A et al. (2009) Nanostructured TiO_2: Transport behavior and effects on aquatic microbial communities under environmental conditions. Environmental Science & Technology 43 (21):8098-8104.

Baumann HA, Morrison L, Stengel DB (2009) Metal accumulation and toxicity measured by PAM—chlorophyll fluorescence in seven species of marine macroalgae. Ecotoxicology and Environmental Safety 72 (4):1063-1075.

Baun A, Justesen KB, Nyholm N (2002) Algal tests with soil suspensions and elutriates: a comparative evaluation for PAH-contaminated soils. Chemosphere 46 (2):251-258.

Beer C, Foldbjerg R, Hayashi Y et al. (2012) Toxicity of silver nanoparticles—nanoparticle or silver ion? Toxicology Letters 208 (3):286-292.

Ben Othman H, Lanouguère É, Got P et al. (2018) Structural and functional responses of coastal marine phytoplankton communities to PAH mixtures. Chemosphere 209:908-919.

Binh CTT, Adams E, Vigen E et al. (2016) Chronic addition of a common engineered nanomaterial alters biomass, activity and composition of stream biofilm communities. Environmental Science: Nano 3 (3):619-630.

Blaise C, Gagne F, Ferard JF et al. (2008) Ecotoxicity of selected nano-materials to aquatic organisms. Environmental Toxicology 23 (5):591-598.

Blaylock BG, Frank ML, McCarthy JF (1985) Comparative toxicity of copper and acridine to fish, Daphnia and algae. Environmental Toxicology and Chemistry: An International Journal 4 (1):63-71.

Botta C, Labille J, Auffan M et al. (2011) TiO_2-based nanoparticles released in water from commercialized sunscreens in a life-cycle perspective: structures and quantities. Environmental Pollution 159 (6):1543-1550.

Bowman DM, May ND, Maynard AD (2018) Nanomaterials in cosmetics: regulatory aspects. In: Analysis of cosmetic products. Elsevier, pp 289-302

Boxall A, Chaudhry Q, Sinclair C et al. (2007) Current and future predicted environmental exposure to engineered nanoparticles. Central Science Laboratory, York, UK.

Boyden CR, Little C (1973) Faunal distributions in soft sediments of the Severn Estuary. Estuarine and Coastal Marine Science 1 (3):203-223.

Brami C, Glover AR, Butt KR et al. (2017) Effects of silver nanoparticles on survival, biomass change and avoidance behaviour of the endogeic earthworm *Allolobophora chlorotica*. Ecotoxicology environmental safety 141:64-69.

British Standards Institution (2007) Terminology for nanomaterials. PAS 136:2007. London, UK.

Brunauer S, Emmett PH, Teller E (1938) Adsorption of gases in multimolecular layers. Journal of the American chemical society 60:309-319.

Brunelli A, Pojana G, Callegaro S et al. (2013) Agglomeration and sedimentation of titanium dioxide nanoparticles (n-TiO_2) in synthetic and real waters. Journal of Nanoparticle Research 15 (6):1684.

Bundschuh M, Seitz F, Rosenfeldt RR et al. (2016) Effects of nanoparticles in fresh waters: risks, mechanisms and interactions. Freshwater Biologyogy 61 (12):2185-2196.

Cabrerizo MJ, González-Olalla JM, Hinojosa-López VJ et al. (2019) A shifting balance: responses of mixotrophic marine algae to cooling and warming under UVR. New Phytologist 221 (3):1317-1327.

Calabrese EJ (2013) Hormetic mechanisms. Critical Reviews in Toxicology 43 (7):580-606.

Calabrese EJ, Baldwin LA (2002) Defining hormesis. Human & Experimental Toxicology 21 (2):91-97.

Calabrese EJ, Mattson MP (2017) How does hormesis impact biology, toxicology, and medicine? NPJ Aging and Mechanisms of Disease 3 (1):13.

Carbone M, Donia DT, Sabbatella G et al. (2016) Silver nanoparticles in polymeric matrices for fresh food packaging. Journal of King Saud University-Science 28 (4):273-279.

Cardinale BJ, Bier R, Kwan C (2012) Effects of TiO_2 nanoparticles on the growth and metabolism of three species

of freshwater algae. Journal of Nanoparticle Research 14 (8).

Caruso G, Caffo M, Alafaci C et al. (2011) Could nanoparticle systems have a role in the treatment of cerebral gliomas? Nanomedicine: Nanotechnology, Biology and Medicine 7 (6):744-752.

Catarina MMÂe, Adriano AB, William JW (2003) Intertidal biofilms on rocky substratum can play a major role in estuarine carbon and nutrient dynamics. Marine Ecology Progress Series 258:275-281.

Cedergreen N, Kudsk P, Mathiassen SK et al. (2007) Combination effects of herbicides on plants and algae: do species and test systems matter? Pest Management Science: formerly Pesticide Science 63 (3):282-295.

Chekli L, Zhao YX, Tijing LD et al. (2015) Aggregation behaviour of engineered nanoparticles in natural waters: characterising aggregate structure using on-line laser light scattering. Journal of Hazardous Materials 284:190-200.

Chen F, Xiao Z, Yue L et al. (2019) Algae response to engineered nanoparticles: current understanding, mechanisms and implications. Environmental Science: Nano 6 (4):1026-1042.

Chen JY, Fang JF, Wei XZ (2013) Studies on the dispersion and deposition behavior of nano-TiO2 in aquatic system (in Chinese). Environmental Science 34 (10):3933-3939.

Chen KL, Elimelech M (2007) Influence of humic acid on the aggregation kinetics of fullerene (C60) nanoparticles in monovalent and divalent electrolyte solutions. Journal of Colloid and Interface Science 309 (1):126-134.

Chen LZ, Zhou LN, Liu YD et al. (2012) Toxicological effects of nanometer titanium dioxide (nano-TiO_2) on *Chlamydomonas reinhardtii*. Ecotoxicology and Environmental Safety 84:155-162.

Chen YS, Frey W, Kim S, et al. Silica-coated gold nanorods as photoacoustic signal nanoamplifiers[J]. Nano letters, 2011, 11(2): 348-354.

Cheng N-S (1997) Simplified settling velocity formula for sediment particle. Journal of hydraulic engineering 123 (2):149-152.

Chhipa, H. Nanofertilizers and nanopesticides for agriculture. *Environ Chem Lett* **15,** 15–22 (2017). https://xs.scihub.ltd/https://doi.org/10.1007/s10311-016-0600-4

Chong MN, Jin B, Chow CWK et al. (2010) Recent developments in photocatalytic water treatment technology: a review. Water Researchearch 44 (10):2997-3027.

Chronopoulou PM, Fahy A, Coulon F et al. (2013) Impact of a simulated oil spill on benthic phototrophs and nitrogen-fixing bacteria in mudflat mesocosms. Environmental Microbiology 15 (1):242-252.

Clement L, Hurel C, Marmier N (2013) Toxicity of TiO_2 nanoparticles to cladocerans, algae, rotifers and plants - effects of size and crystalline structure. Chemosphere 90 (3):1083-1090.

Colijn F, Dijkema KS (1981) Species composition of benthic diatoms and distribution of chlorophyll *a* on an inter tidal flat in the dutch wadden sea. Marine Ecology Progress Series 4 (1):9-21.

Commission staff working paper (2012b) EUROPEAN COMMISSION. SWD(2012) 288 final http://ec.europa.eu/health//sites/health/files/nanotechnology/docs/swd_2012_288_en.pdf. Accessed 22.12.2016

Consalvey M, Paterson DM, Underwood GJC (2004a) The ups and downs of life in a benthic biofilm: migration of benthic diatoms. Diatom Research 19 (2):181-202.

Consalvey M, Jesus B, Perkins RG et al. (2004b) Monitoring migration and measuring biomass in benthic biofilms: the effects of dark/far-red adaptation and vertical migration on fluorescence measurements. Photosynthesis Research 81 (1):91-101.

Consalvey M, Perkins RG, Paterson DM et al. (2005) PAM fluorescence: a beginners guide for benthic diatomists. Diatom Research 20 (1):1-22.

Cosgrove T (2010) Colloid science: principles, methods and applications. John Wiley & Sons.

Cox A, Venkatachalam P, Sahi S et al. (2016) Silver and titanium dioxide nanoparticle toxicity in plants: a review of current research. Plant Physiology and Biochemistry 107:147-163.

Dalai S, Pakrashi S, Kumar RSS et al. (2012) A comparative cytotoxicity study of TiO_2 nanoparticles under light and dark conditions at low exposure concentrations. Toxicology Research 1 (2):116-130.

Dalai S, Pakrashi S, Nirmala MJ et al. (2013) Cytotoxicity of TiO_2 nanoparticles and their detoxification in a freshwater system. Aquatic Toxicology 138:1-11.

Das R, Sarkar S, Chakraborty S et al. (2014) Remediation of antiseptic components in wastewater by photocatalysis using TiO_2 nanoparticles. Industrial & Engineering Chemistry Research 53 (8):3012-3020.

Dash A, Singh AP, Chaudhary BR et al. (2012) Effect of silver nanoparticles on growth of eukaryotic green algae. Nano-Micro Letters 4 (3):158-165.

de Baat ML, Bas DA, van Beusekom SAM et al. (2018) Nationwide screening of surface water toxicity to algae. Science of The Total Environment 645:780-787.

Decho AW (1990) Microbial exopolymer secretions in ocean environments: their role(s) in food webs and marine processes. Oceanography and Marine Biology: An Annual Review 28:73-153.

Decho AW (2000) Microbial biofilms in intertidal systems: an overview. Continental Shelf Research 20 (10-11):1257-1273.

Defew EC, Perkins RG, Paterson DM (2004) The influence of light and temperature interactions on a natural estuarine microphytobenthic assemblage. Biofilms 1 (1):21-30.

Deluchat V, Bollinger J-C, Serpaud B et al. (1997) Divalent cations speciation with three phosphonate ligands in the pH-range of natural waters. Talanta 44 (5):897-907.

Deng X-Y, Cheng J, Hu X-L et al. (2017) Biological effects of TiO_2 and CeO_2 nanoparticles on the growth, photosynthetic activity, and cellular components of a marine diatom *Phaeodactylum tricornutum*. Science of The Total Environment 575:87-96.

Dhasmana A, Uniyal S, Kumar V et al. (2019) Scope of nanoparticles in environmental toxicant remediation. In: Sobti RC, Arora NK, Kothari R (eds) Environmental Biotechnology: For Sustainable Future. Springer Singapore, Singapore, pp 31-44. doi:10.1007/978-981-10-7284-0_2

Domingos RF, Tufenkji N, Wilkinson KJ (2009) Aggregation of titanium dioxide nanoparticles: role of a fulvic acid. Environmental Science & Technology 43 (5):1282-1286.

Donia DT, Carbone M (2019) Fate of the nanoparticles in environmental cycles. International Journal of Environmental Science and Technology16 (1):583-600.

Du W, Tan W, Peralta-Videa JR et al. (2017a) Interaction of metal oxide nanoparticles with higher terrestrial plants: physiological and biochemical aspects. Plant Physiology and Biochemistry 110:210-225.

Du W, Gardea-Torresdey JL, Xie Y et al. (2017b) Elevated CO_2 levels modify TiO_2 nanoparticle effects on rice and soil microbial communities. Science of The Total Environment 578:408-416.

Dupont Report (2015) DuPont™ Ti-Pure® titanium dioxide. http://www2.dupont.com/Titanium_Technologies/en_US/tech_info/literature/Coatings/CO_B_H_65969_Coatings_Brochure.pdf. Accessed 0303 2015

Eaton JW, Moss B (1966) Estimation of numbers and pigment content in epipelic algal populations. Limnology and Oceanography 11 (4):584-&.

Eilers PHC, Peeters JCH (1988) A model for the relationship between light-intensity and the rate of photosynthesis in phytoplankton. Ecological Modelling 42 (3-4):199-215.

El Jay A (1996) Toxic effects of organic solvents on the growth of *Chlorella vulgaris* and *Selenastrum capricornutum*. Bulletin of Environmental Contamination Toxicology 57 (2):191-198.

Engates KE, Shipley HJ (2011) Adsorption of Pb, Cd, Cu, Zn, and Ni to titanium dioxide nanoparticles: effect of particle size, solid concentration, and exhaustion. Environmental Science and Pollution Research 18 (3):386-395.

EPA (2010) Nanomaterial case studies: nanoscale titanium dioxide in water treatment and in topical sunscreen (Final). U.S. Environmental Protection Agency, Washington, DC.

Erdem A, Metzler D, Cha D et al. (2015) Inhibition of bacteria by photocatalytic nano-TiO_2 particles in the absence of light. International Journal of Environmental Science and Technology 12 (9):2987-2996.

Esakkimuthu T, Durairaj S, S.Akila (2014) Application of nanoparticles in wastewater treatment. Pollution Research 33:567-571.

Espitia PJP, Soares NdFF, dos Reis Coimbra JS et al. (2012) Zinc oxide nanoparticles: synthesis, antimicrobial activity and food packaging applications. Food Bioprocess Technology 5 (5):1447-1464.

Fan W, Liu T, Li X et al. (2016) Nano-TiO_2 affects Cu speciation, extracellular enzyme activity, and bacterial communities in sediments. Environmental Pollution 218:77-85.

Farkas J, Booth AM (2017) Are fluorescence-based chlorophyll quantification methods suitable for algae toxicity assessment of carbon nanomaterials? Nanotoxicology 11 (4):569-577.

Federici G, Shaw BJ, Handy RD (2007) Toxicity of titanium dioxide nanoparticles to rainbow trout (*Oncorhynchus mykiss*): gill injury, oxidative stress, and other physiological effects. Aquatic Toxicology 84 (4):415-430.

Fehér A, Otvös K, Pasternak TP et al. (2008) The involvement of reactive oxygen species (ROS) in the cell cycle activation (G(0)-to-G(1) transition) of plant cells. Plant Signaling & Behavior 3 (10):823-826.

Fekete-Kertész I, Maros G, Gruiz K et al. (2016) The effect of TiO_2 nanoparticles on the aquatic ecosystem: a comparative ecotoxicity study with test organisms of different trophic levels. Periodica Polytechnica Chemical

Engineering 60 (4):231-243.

Ferreira VS, Pinto RF, Sant'Anna C (2016) Low light intensity and nitrogen starvation modulate the chlorophyll content of *Scenedesmus dimorphus*. Journal of Applied Microbiology 120 (3):661-670.

Ferry JL, Craig P, Hexel C et al. (2009) Transfer of gold nanoparticles from the water column to the estuarine food web. Nature Nanotechnology 4 (7):441-444.

Fisher NS (1977) On the differential sensitivity of estuarine and open-ocean diatoms to exotic chemical stress. The American Naturalist 111 (981):871-895.

Fleury C, Mignotte B, Vayssière J-L (2002) Mitochondrial reactive oxygen species in cell death signaling. Biochimie 84 (2–3):131-141.

Franklin NM, Rogers NJ, Apte SC et al. (2007) Comparative toxicity of nanoparticulate ZnO, bulk ZnO, and $ZnCl_2$ to a freshwater microalga (*Pseudokirchneriella subcapitata*): the importance of particle solubility. Environmental Science & Technology 41 (24):8484-8490.

Franklin NM, Stauber JL, Markich SJ et al. (2000) pH-dependent toxicity of copper and uranium to a tropical freshwater alga (*Chlorella* sp.). Aquatic Toxicology 48 (2):275-289.

French MS, Evans LV (1988) The effects of copper and zinc on growth of the fouling diatoms *Amphora* and *Amphiprora*. Biofouling 1 (1):3-18.

French RA, Jacobson AR, Kim B et al. (2009) Influence of ionic strength, pH, and cation valence on aggregation kinetics of titanium dioxide nanoparticles. Environmental Science & Technology 43 (5):1354-1359.

Friend PL, Lucas CH, Holligan PM et al. (2008) Microalgal mediation of ripple mobility. Geobiology 6 (1):70-82.

Gandamalla D, Lingabathula H, Yellu N (2019) Nano titanium exposure induces dose- and size-dependent cytotoxicity on human epithelial lung and colon cells. Drug and Chemical Toxicology 42 (1):24-34.

Gao F, Liu C, Qu C et al. (2008) Was improvement of spinach growth by nano-TiO_2 treatment related to the changes of Rubisco activase? BioMetals 21 (2):211-217.

Gao X, Zhou K, Zhang L et al. (2018) Distinct effects of soluble and bound exopolymeric substances on algal bioaccumulation and toxicity of anatase and rutile TiO_2 nanoparticles. Environmental Science: Nano 5 (3):720-729.

Ge YG, Schimel JP, Holden PA (2011) Evidence for negative effects of TiO_2 and ZnO nanoparticles on soil bacterial communities. Environmental Science & Technology 45 (4):1659-1664.

Geng H, Peng Y, Qu L, et al. Structure Design and Composition Engineering of Carbon-Based Nanomaterials for Lithium Energy Storage[J]. Advanced Energy Materials, 1903030.

Gerbersdorf SU, Bittner R, Lubarsky H et al. (2009) Microbial assemblages as ecosystem engineers of sediment stability. Journal of Soils and Sediments 9 (6):640-652.

Giordano M, Beardall J, Raven JA (2005) CO_2 concentrating mechanisms in alage: mechanisms, environmental modulation, and evolution. Annual Review of Plant Biology 56 (1):99-131.

Golanski L, Gaborieau A, Guiot A et al. Characterization of abrasion-induced nanoparticle release from paints into liquids and air. In: Journal of Physics: Conference Series, 2011. vol 1. IOP Publishing, p 012062

Gondikas AP, Kammer Fvd, Reed RB et al. (2014) Release of TiO_2 nanoparticles from sunscreens into surface waters: a one-year survey at the old danube recreational lake. Environmental Science & Technology 48 (10):5415-5422.

Gong N, Shao K, Feng W et al. (2011) Biotoxicity of nickel oxide nanoparticles and bio-remediation by microalgae *Chlorella vulgaris*. Chemosphere 83 (4):510-516.

Gottschalk F, Sonderer T, Scholz RW et al. (2009) Modeled environmental concentrations of engineered nanomaterials (TiO_2, ZnO, Ag, CNT, fullerenes) for different regions. Environmental Science & Technology 43 (24):9216-9222.

Graziani L, Quagliarini E, Osimani A et al. (2013) Evaluation of inhibitory effect of TiO_2 nanocoatings against microalgal growth on clay brick facades under weak UV exposure conditions. Building and Environment 64:38-45.

Guillard RRL, Ryther JH (1962) Studies of marine planktonic diatoms. I. *Cyclotella nana* Hustedt and *Detonula confervaceae* (Cleve). Canadian Journal of Microbiology 8 (2):229-239.

Hammer Ø, Harper DA, Ryan PD (2001) PAST: paleontological statistics software package for education and data analysis. Palaeontologia electronica 4 (1):9.

Han L, Zhai Y, Liu Y et al. (2017) Comparison of the in vitro and in vivo toxic effects of three sizes of zinc oxide (ZnO) particles using flounder gill (FG) cells and zebrafish embryos. Journal of Ocean University of China 16 (1):93-106.

Handy RD, Owen R, Valsami-Jones E (2008a) The ecotoxicology of nanoparticles and nanomaterials: current status, knowledge gaps, challenges, and future needs. Ecotoxicology 17 (5):315-325.

Handy RD, von der Kammer F, Lead JR et al. (2008b) The ecotoxicology and chemistry of manufactured nanoparticles. Ecotoxicology 17 (4):287-314.

Hao Y, Ma C, Zhang Z et al. (2018) Carbon nanomaterials alter plant physiology and soil bacterial community composition in a rice-soil-bacterial ecosystem. Environmental Pollution 232:123-136.

Hartmann NB, Engelbrekt C, Zhang JD et al. (2013) The challenges of testing metal and metal oxide nanoparticles in algal bioassays: titanium dioxide and gold nanoparticles as case studies. Nanotoxicology 7 (6):1082-1094.

Hartmann NB, Von der Kammer F, Hofmann T et al. (2010) Algal testing of titanium dioxide nanoparticles-testing considerations, inhibitory effects and modification of cadmium bioavailability. Toxicology 269 (2-3):190-197.

Hazeem LJ, Bououdina M, Rashdan S et al. (2016) Cumulative effect of zinc oxide and titanium oxide nanoparticles on growth and chlorophyll a content of *Picochlorum* sp. Environmental Science and Pollution Research 23 (3):2821-2830.

He YT, Wan JM, Tokunaga T (2008) Kinetic stability of hematite nanoparticles: the effect of particle sizes. Journal of Nanoparticle Research 10 (2):321-332.

Heinlaan M, Ivask A, Blinova I et al. (2008) Toxicity of nanosized and bulk ZnO, CuO and TiO_2 to bacteria *Vibrio*

fischeri and crustaceans *Daphnia magna* and *Thamnocephalus platyurus*. Chemosphere 71 (7):1308-1316.

Hendry GAF, Houghton JD, Brown SB (1987) Tansley review No-11 - the degradation of chlorophyll - a niological enigma. New Phytologist 107 (2):255-302.

Hett A (2004) Nanotechnology: small matter, many unknowns. Swiss Reinsurance Company.

Hoagland KD, Rosowski JR, Gretz MR et al. (1993) Diatom extracellular polymeric substances - function, fine-structure, chemistry, and physiology. Journal of Phycology 29 (5):537-566.

Holm-Hansen O, Lorenzen CJ, Holmes RW et al. (1965) Fluorometric determination of chlorophyll. ICES Journal of Marine Science 30 (1):3-15.

Hong F, Zhou J, Liu C et al. (2005) Effect of nano-TiO_2 on photochemical reaction of chloroplasts of spinach. Biological Trace Element Research 105 (1):269-279.

Hong J, Zhang Y-Q (2016) Murine liver damage caused by exposure to nano-titanium dioxide. Nanotechnology 27 (11):112001.

Horst AM, Vukanti R, Priester JH et al. (2013) An assessment of fluorescence- and absorbance-based assays to study metal-oxide nanoparticle ROS production and effects on bacterial membranes. Small 9 (9-10):1753-1764.

Hotze EM, Phenrat T, Lowry GV (2010) Nanoparticle aggregation: challenges to understanding transport and reactivity in the environment. Journal of Environmental Quality 39 (6):1909-1924.

Hou J, Wang L, Wang C et al. (2019) Toxicity and mechanisms of action of titanium dioxide nanoparticles in living organisms. Journal of Environmental Sciences 75:40-53.

Hough ZJ, Walters HS, Bechtold HA (2017) Titanium dioxide (TiO_2) nanoparticles more strongly affect bacteria compared to algae in stream ecosystems. Journal of Student Research 6(1): 103-108

Howe PL, Reichelt-Brushett AJ, Clark MW et al. (2017) Toxicity estimates for diuron and atrazine for the tropical marine cnidarian Exaiptasia pallida and in-hospite *Symbiodinium* spp. using PAM chlorophyll-a fluorometry. Journal of Photochemistry and Photobiology B: Biology 171:125-132.

Hu H, Deng Y, Fan Y et al. (2016) Effects of artificial sweeteners on metal bioconcentration and toxicity on a green algae *Scenedesmus obliquus*. Chemosphere 150:285-293.

Hu J, Wang J, Liu S et al. (2017) Effect of TiO_2 nanoparticle aggregation on marine microalgae *Isochrysis galbana*. Journal of Environmental Sciences 66: 208-215

Huang G, Bai Z, Dai S et al. (1993) Accumulation and toxic effect of organometallic compounds on algae. 7 (6):373-380.

Hudson N, Baker A, Reynolds D (2007) Fluorescence analysis of dissolved organic matter in natural, waste and polluted waters—a review. River Research and Applications 23 (6):631-649.

Hund-Rinke K, Simon M (2006) Ecotoxic effect of photocatalytic active nanoparticles (TiO_2) on algae and daphnids Environmental Science and Pollution Research 13 (4):225-232.

Huynh KA, Chen KL (2011) Aggregation kinetics of citrate and polyvinylpyrrolidone coated silver nanoparticles in monovalent and divalent electrolyte solutions. Environmental Science & Technology 45 (13):5564-5571.

Iavicoli I, Leso V, Fontana L et al. (2011) Toxicological effects of titanium dioxide nanoparticles: a review of in vitro mammalian studies. European Review for Medical and Pharmacological Sciences 15 (5):481-508.

Ikuma K, Decho AW, Lau BLT (2015) When nanoparticles meet biofilms—interactions guiding the environmental fate and accumulation of nanoparticles. Frontiers in Microbiology 6:591.

International Organization for Standardization (2008) Nanotechnologies - terminology and definitions for nano-objects - nanoparticle, nanofibre and nanoplate. ISO/TS 27687. International Organization for Standardization.

Iswarya V, Sharma V, Chandrasekaran N et al. (2017) Impact of tetracycline on the toxic effects of titanium dioxide (TiO_2) nanoparticles towards the freshwater algal species, *Scenedesmus obliquus*. Aquatic Toxicology 193:168-177.

Jain A, Ranjan S, Dasgupta N et al. (2018) Nanomaterials in food and agriculture: an overview on their safety concerns and regulatory issues. Critical Reviews in Food Science and Nutrition 58 (2):297-317.

Jeffryes C, Gutu T, Jiao J et al. (2008) Metabolic insertion of nanostructured TiO_2 into the patterned biosilica of the diatom *Pinnularia* sp. by a two-stage bioreactor cultivation process. Acs Nano 2 (10):2103-2112.

Jeon S-k, Kim E-j, Lee J et al. (2016) Potential risks of TiO_2 and ZnO nanoparticles released from sunscreens into outdoor swimming pools. Journal of hazardous materials 317:312-318.

Ji J, Long ZF, Lin DH (2011) Toxicity of oxide nanoparticles to the green algae *Chlorella* sp. Chemical Engineering Journal 170 (2-3):525-530.

Jia K, Sun C, Wang Y et al. (2019) Effect of TiO_2 nanoparticles and multiwall carbon nanotubes on the freshwater diatom *Nitzschia frustulum*: evaluation of growth, cellular components and morphology. Chemistry and Ecology 35 (1):69-85.

Jiang J, Oberdrster G, Elder A et al. (2008) Does nanoparticle activity depend upon size and crystal phase? Nanotoxicology 2 (1):33-42.

Jiang WK, Pan HQ, Wang FX et al. (2015) A rapid sample processing method to observe diatoms via scanning electron microscopy. Journal of Applied Phycology 27 (1):243-248.

Johnson AC, Bowes MJ, Crossley A et al. (2011) An assessment of the fate, behaviour and environmental risk associated with sunscreen TiO_2 nanoparticles in UK field scenarios. Science of The Total Environment 409 (13):2503-2510.

Joonas E, Aruoja V, Olli K et al. (2019) Environmental safety data on CuO and TiO_2 nanoparticles for multiple algal species in natural water: filling the data gaps for risk assessment. Science of The Total Environment 647:973-980.

Juneau P, Dewez D, Matsui S et al. (2001) Evaluation of different algal species sensitivity to mercury and metolachlor by PAM-fluorometry. Chemosphere 45 (4):589-598.

Juneau P, El Berdey A, Popovic R (2002) PAM fluorometry in the determination of the sensitivity of *Chlorella vulgaris, Selenastrum capricornutum*, and *Chlamydomonas reinhardtii* to copper. Archives of Environmental Contamination and Toxicology 42 (2):155-164.

Juneja A, Ceballos MR, Murthy SG (2013) Effects of environmental factors and nutrient availability on the

biochemical composition of algae for biofuels production: a review. Energies 6 (9).

Kaegi R, Ulrich A, Sinnet B et al. (2008) Synthetic TiO_2 nanoparticle emission from exterior facades into the aquatic environment. Environmental Pollution 156 (2):233-239.

Kakinoki K, Yamane K, Teraoka R et al. (2004) Effect of relative humidity on the photocatalytic activity of titanium dioxide and photostability of famotidine. Journal of Pharmaceutical Sciences 93 (3):582-589.

Kandasamy G, Maity D. Recent advances in superparamagnetic iron oxide nanoparticles (SPIONs) for in vitro and in vivo cancer nanotheranostics. International Journal of Pharmaceutics, 2015, 496(2): 191-218.

Karcher SJ (1995) 4 - Plant genomic southern blotting with probes for low- and high-copy-number genes. In: Karcher SJ (ed) Molecular Biology. Academic Press, San Diego, pp 193-201. doi:https://doi.org/10.1016/B978-012397720-5.50038-4

Karmakar S, Kumar S, Rinaldi R et al. Nano-electronics and spintronics with nanoparticles. In: Journal of Physics: Conference Series, 2011. vol 1. IOP Publishing, p 012002

Keller AA, Wang HT, Zhou DX et al. (2010) Stability and aggregation of metal oxide nanoparticles in natural aqueous matrices. Environmental Science & Technology 44 (6):1962-1967.

Khan MM, Adil SF, Al-Mayouf A (2015) Metal oxides as photocatalysts. Journal of Saudi Chemical Society 19 (5):462-464.

Kim M-J, Ko D, Ko K et al. (2018) Effects of silver-graphene oxide nanocomposites on soil microbial communities. Journal of Hazardous Materials 346:93-102.

Kimura H, Sawada T, Oshima S et al. (2005) Toxicity and roles of reactive oxygen species. Current Drug Targets - Inflammation & Allergy 4 (4):489-495.

Kiser MA, Westerhoff P, Benn T et al. (2009) Titanium nanomaterial removal and release from wastewater treatment plants. Environmental Science & Technology 43 (17):6757-6763.

Kitahara A (1973) Zeta potential in nonaqueous media and its effect on dispersion stability. Progress in organic coatings 2 (2):81-98.

Klaine SJ, Alvarez PJJ, Batley GE et al. (2008) Nanomaterials in the environment: behavior, fate, bioavailability, and effects. Environmental Toxicology and Chemistry 27 (9):1825-1851.

Koelmans AA, Nowack B, Wiesner MR (2009) Comparison of manufactured and black carbon nanoparticle concentrations in aquatic sediments. Environmental Pollution 157 (4):1110-1116.

Kokura S, Handa O, Takagi T et al. (2010) Silver nanoparticles as a safe preservative for use in cosmetics. Nanomedicine: Nanotechnology, Biology and Medicine 6 (4):570-574.

Koumanova B Fate of chemicals in the aquatic environment. In: Simeonov L, Chirila E (eds) Chemicals as Intentional and Accidental Global Environmental Threats, Dordrecht, 2006// 2006. Springer Netherlands, pp 93-103

Kroll A, Behra R, Kaegi R et al. (2014) Extracellular polymeric substances (EPS) of freshwater biofilms stabilize and modify CeO2 and Ag nanoparticles. Plos One 9 (10):e110709.

Kulacki KJ, Cardinale BJ (2012) Effects of nano-titanium dioxide on freshwater algal population dynamics. Plos One 7 (10).

Kumari J, Kumar D, Mathur A et al. (2014) Cytotoxicity of TiO_2 nanoparticles towards freshwater sediment microorganisms at low exposure concentrations. Environmental Research 135:333-345.

Lagally CD, Reynolds CCO, Grieshop AP et al. (2012) Carbon nanotube and fullerene emissions from spark-ignited engines. Aerosol Science and Technology 46 (2):156-164.

Lam PKS, Wut PF, Chan ACW et al. (1999) Individual and combined effects of cadmium and copper on the growth response of *Chlorella vulgaris*. Environmental Toxicology: An International Journal 14 (3):347-353.

Larsson M, Hill A, Duffy JJATNRS (2012) Suspension stability; why particle size, zeta potential and rheology are important. Annual Transactions of the Nordic Rheology Society 20:209-214.

Larue C, Veronesi G, Flank AM et al. (2012) Comparative uptake and impact of TiO_2 nanoparticles in wheat and rapeseed. Journal of Toxicology and Environmental Health, Part A 75 (13-15):722-734.

Lebrette S, Pagnoux C, Abélard P (2004) Stability of aqueous TiO_2 suspensions: influence of ethanol. Journal of Colloid and Interface Science 280 (2):400-408.

Lee SH, Richards RJ (2004) Montserrat volcanic ash induces lymph node granuloma and delayed lung inflammation. Toxicology 195 (2-3):155-165.

Lee WM, An YJ (2013) Effects of zinc oxide and titanium dioxide nanoparticles on green algae under visible, UVA, and UVB irradiations: No evidence of enhanced algal toxicity under UV pre-irradiation. Chemosphere 91 (4):536-544.

Lee Y, Choi J-r, Lee KJ et al. (2008) Large-scale synthesis of copper nanoparticles by chemically controlled reduction for applications of inkjet-printed electronics. Nanotechnology 19 (41):415604.

Li F, Liang Z, Zheng X et al. (2015) Toxicity of nano-TiO_2 on algae and the site of reactive oxygen species production. Aquatic Toxicology 158:1-13.

Li L, Sillanpää M, Risto M (2016) Influences of water properties on the aggregation and deposition of engineered titanium dioxide nanoparticles in natural waters. Environmental Pollution 219:132-138.

Li M, Jiang Y, Chuang C-Y et al. (2019) Recovery of *Alexandrium tamarense* under chronic exposure of TiO_2 nanoparticles and possible mechanisms. Aquatic Toxicology 208:98-108.

Lichtenthaler HK, Buschmann C (2001) Chlorophylls and carotenoids: measurement and characterization by UV-VIS spectroscopy. In: Current Protocols in Food Analytical Chemistry. John Wiley & Sons, Inc. doi:10.1002/0471142913.faf0403s01

Lin D, Story SD, Walker SL et al. (2017) Role of pH and ionic strength in the aggregation of TiO_2 nanoparticles in the presence of extracellular polymeric substances from *Bacillus subtilis*. Environmental Pollution 228:35-42.

Lin DH, Ji J, Long ZF et al. (2012) The influence of dissolved and surface-bound humic acid on the toxicity of TiO_2 nanoparticles to *Chlorella* sp. Water Researchearch 46 (14):4477-4487.

Lin Q-B, Li H, Zhong H-N et al. (2014) Migration of Ti from nano-TiO_2-polyethylene composite packaging into food simulants. Food Additives & Contaminants: Part A 31 (7):1284-1290.

Little C, Paterson DM, Crawford RM et al. (1992) Algal stabilization of estuarine sediment. Report (May 1992) to the Energy Technology Support Unit, United Kingdom Department of Trade and Industry.

Liu H, Ma L, Liu J et al. (2010) Toxicity of nano-anatase TiO_2 to mice: liver injury, oxidative stress. Toxicological & Environmental Chemistry 92 (1):175-186.

Liu W, An R, Wang C et al. (2018) Recent progress in rapid sintering of nanosilver for electronics applications. Micromachines 9 (7):346.

Liu Y, Tourbin M, Lachaize S et al. (2014a) Nanoparticles in wastewaters: hazards, fate and remediation. Powder Technology 255:149-156.

Liu Y, Zhang J, Gao B et al. (2014b) Combined effects of two antibiotic contaminants on *Microcystis aeruginosa*. Journal of Hazardous Materials 279:148-155.

Loosli F, Le Coustumer P, Stoll S (2015) Effect of electrolyte valency, alginate concentration and pH on engineered TiO_2 nanoparticle stability in aqueous solution. Science of The Total Environment 535:28-34.

Lorenzen C (1967) Determination of chlorophyll and pheopigments:spectrophotometric equations. Limnology and Oceanography 12 (2):343-346.

Lorenzen CJ (1966) A method for the continuous measurement of *in vivo* chlorophyll concentration. Deep Sea Research and Oceanographic Abstracts 13 (2):223-227.

Luo M, Huang Y, Zhu M et al. (2018) Properties of different natural organic matter influence the adsorption and aggregation behavior of TiO_2 nanoparticles. Journal of Saudi Chemical Society 22 (2):146-154.

Luttrell T, Halpegamage S, Tao J et al. (2014) Why is anatase a better photocatalyst than rutile? - model studies on epitaxial TiO_2 films. Scientific Reports 4:4043.

Ma X, Geiser-Lee J, Deng Y et al. (2010) Interactions between engineered nanoparticles (ENPs) and plants: phytotoxicity, uptake and accumulation. Science of The Total Environment 408 (16):3053-3061.

MacIntyre H, Geider R, Miller D (1996) Microphytobenthos: the ecological role of the “secret garden” of unvegetated, shallow-water marine habitats. I. distribution, abundance and primary production. Estuaries 19 (2):186-201.

Magnusson M, Heimann K, Quayle P et al. (2010) Additive toxicity of herbicide mixtures and comparative sensitivity of tropical benthic microalgae. Marine Pollution Bulletin 60 (11):1978-1987.

Makoto E, Norihiro K, Masato N et al. (2010) Reproductive and developmental toxicity studies of manufactured nanomaterials. Reproductive Toxicology 30 (3):343-352.

Manangama G, Migault L, Audignon-Durand S et al. (2019) Maternal occupational exposures to nanoscale particles and small for gestational age outcome in the French longitudinal study of children. Environment International 122:322-329.

Manivannan A, Soundararajan P, Jeong BR (2017) Role of reactive oxygen species signaling in cell proliferation and differentiation. In: Reactive Oxygen Species in Plants. pp 319-329. doi:10.1002/9781119324928.ch17

Manzo S, Buono S, Rametta G et al. (2015) The diverse toxic effect of SiO_2 and TiO_2 nanoparticles toward the marine microalgae *Dunaliella tertiolecta*. Environmental Science and Pollution Research 22 (20):15941-15951.

Marker AFH (1972) The use of acetone and methanol in the estimation of chlorophyll in the presence of phaeophytin. Freshwater Biology 2 (4):361-385.

Martin CR, Mitchell DT (1998) Peer reviewed: nanomaterials in analytical chemistry. Analytical chemistry 70 (9):322A-327A.

Maurizi L, Papa A-L, Boudon J et al. (2018) Toxicological risk assessment of emerging nanomaterials: cytotoxicity, cellular uptake, effects on biogenesis and cell organelle activity, acute toxicity and biodistribution of oxide nanoparticles. In: Unraveling the Safety Profile of Nanoscale Particles and Materials-From Biomedical to Environmental Applications. IntechOpen,

Maxwell K, Johnson GN (2000) Chlorophyll fluorescence - a practical guide. Journal of Experimental Botany 51 (345):659-668.

Mayer P, Cuhel R, Nyholm N (1997) A simple in vitro fluorescence method for biomass measurements in algal growth inhibition tests. Water Research 31 (10):2525-2531.

McKew BA, Taylor JD, McGenity TJ et al. (2011) Resistance and resilience of benthic biofilm communities from a temperate saltmarsh to desiccation and rewetting. The ISME journal 5 (1):30-41.

McQuatters-Gollop A, Raitsos DE, Edwards M et al. (2007) Spatial patterns of diatom and dinoflagellate seasonal cycles in the NE Atlantic Ocean. Marine Ecology Progress Series 339:301-306.

Méléder V, Barillé L, Launeau P et al. (2003) Spectrometric constraint in analysis of benthic diatom biomass using monospecific cultures. Remote Sensing of Environment 88 (4):386-400.

Menard A, Drobne D, Jemec A (2011) Ecotoxicity of nanosized TiO_2. Review of in vivo data. Environmental Pollution 159 (3):677-684.

Metzler DM, Erdem A, Huang CP (2018) Influence of algae age and population on the response to TiO_2 nanoparticles. International Journal of Environmental Research and Public Health 15 (4):585.

Metzler DM, Li MH, Erdem A et al. (2011) Responses of algae to photocatalytic nano-TiO_2 particles with an emphasis on the effect of particle size. Chemical Engineering Journal 170 (2-3):538-546.

Mezni A, Alghool S, Sellami B et al. (2018) Titanium dioxide nanoparticles: synthesis, characterisations and aquatic ecotoxicity effects. Chemistry and Ecology 34 (3):288-299.

Miao A-J, Wang W-X, Juneau P (2005) Comparison of Cd, Cu, and Zn toxic effects on four marine phytoplankton by pulse-amplitude-modulated fluorometry. Environmental Toxicology and Chemistry: An International Journal 24 (10):2603-2611.

Miao AJ, Zhang XY, Luo ZP et al. (2010) Zinc oxide engineered nanoparticles dissolution and toxicity to marine phytoplankton. Environmental Toxicology and Chemistry 29 (12):2814-2822.

Middepogu A, Hou J, Gao X et al. (2018) Effect and mechanism of TiO_2 nanoparticles on the photosynthesis of *Chlorella pyrenoidosa*. Ecotoxicology and Environmental Safety 161:497-506.

Miller D, Geider R, MacIntyre H (1996) Microphytobenthos: the ecological role of the “secret garden” of unvegetated, shallow-water marine habitats. II. role in sediment stability and shallow-water food webs. Estuaries 19 (2):202-212.

Miller RJ, Bennett S, Keller AA et al. (2012) TiO_2 nanoparticles are phototoxic to marine phytoplankton. Plos One 7 (1).

Miller RJ, Lenihan HS, Muller EB et al. (2010) Impacts of metal oxide nanoparticles on marine phytoplankton. Environmental Science & Technology 44 (19):7329-7334.

Minetto D, Libralato G, Marcomini A et al. (2017) Potential effects of TiO_2 nanoparticles and $TiCl_4$ in saltwater to *Phaeodactylum tricornutum* and *Artemia franciscana*. Science of The Total Environment 579:1379-1386.

Minetto D, Libralato G, Volpi Ghirardini A (2014) Ecotoxicity of engineered TiO_2 nanoparticles to saltwater organisms: an overview. Environment International 66:18-27.

Mitrano DM, Rimmele E, Wichser A et al. (2014) Presence of nanoparticles in wash water from conventional silver and nano-silver textiles. Acs Nano 8 (7):7208-7219.

Mittler R (2017) ROS are good. Trends in Plant Science 22 (1):11-19.

Morelli E, Gabellieri E, Bonomini A et al. (2018) TiO_2 nanoparticles in seawater: aggregation and interactions with the green alga *Dunaliella tertiolecta*. Ecotoxicology and Environmental Safety 148:184-193.

Moreno-Garrido I, Hampel M, Lubián LM et al. (2003) Sediment toxicity tests using benthic marine microalgae *Cylindrotheca closterium* (Ehremberg) Lewin and Reimann (Bacillariophyceae). Ecotoxicology and Environmental Safety 54 (3):290-295.

Moreno-Garrido I, Lubián LM, Soares AMVM (2000) Influence of cellular density on determination of EC50 in microalgal growth inhibition tests. Ecotoxicology and Environmental Safety 47 (2):112-116.

Morris JE (2018) Nanopackaging: nanotechnologies and electronics packaging. In: Nanopackaging. Springer, pp 1-44

Mu L, Sprando RL (2010) Application of nanotechnology in cosmetics. Pharmaceutical research 27 (8):1746-1749.

Mueller NC, Nowack B (2008) Exposure modeling of engineered nanoparticles in the environment. Environmental Science & Technology 42 (12):4447-4453.

Munkegaard M, Abbaspoor M, Cedergreen N (2008) Organophosphorous insecticides as herbicide synergists on the green algae *Pseudokirchneriella subcapitata* and the aquatic plant *Lemna minor*. Ecotoxicology 17 (1):29-35.

Murr LE, Esquivel EV, Bang JJ et al. (2004) Chemistry and nanoparticulate compositions of a 10,000 year-old ice core melt water. Water Research 38 (19):4282-4296.

Musee N (2010) Simulated environmental risk estimation of engineered nanomaterials: a case of cosmetics in Johannesburg City. Human & Experimental Toxicology 30 (9):1181-1195.

Nagai T, Taya K, Annoh H et al. (2013) Application of a fluorometric microplate algal toxicity assay for riverine periphytic algal species. Ecotoxicology and Environmental Safety 94:37-44.

Nagaveni K, Sivalingam G, Hegde MS et al. (2004) Photocatalytic degradation of organic compounds over combustion-synthesized Nano-TiO_2. Environmental Science & Technology 38 (5):1600-1604.

Narbutt J, Philipsen P A, Harrison G I, et al. Sunscreen applied at≥ 2 mg cm− 2 during a sunny holiday prevents

erythema, a biomarker of ultraviolet radiation-induced DNA damage and suppression of acquired immunity. British Journal of Dermatology, 2019, 180(3): 604-614.

Navarro E, Baun A, Behra R et al. (2008) Environmental behavior and ecotoxicity of engineered nanoparticles to algae, plants, and fungi. Ecotoxicology 17 (5):372-386.

Neal C, Jarvie H, Rowland P et al. (2011) Titanium in UK rural, agricultural and urban/industrial rivers: geogenic and anthropogenic colloidal/sub-colloidal sources and the significance of within-river retention. Science of The Total Environment 409 (10):1843-1853.

Nicholas WL, Bird AF, Beech TA et al. (1992) The nematode fauna of the Murray River estuary, South Australia; the effects of the barrages across its mouth. Hydrobiologia 234 (2):87-101.

Nicolas M, Séverine LM, Anne B-N et al. (2016) Effect of two TiO_2 nanoparticles on the growth of unicellular green algae using the OECD 201 test guideline: influence of the exposure system. Toxicological & Environmental Chemistry 98 (8):860-876.

Nogueira V, Lopes I, Rocha-Santos TAP et al. (2015) Assessing the ecotoxicity of metal nano-oxides with potential for wastewater treatment. Environmental Science and Pollution Research 22 (17):13212-13224.

Nordberg J, Arner ESJ (2001) Reactive oxygen species, antioxidants, and the mammalian thioredoxin system. Free Radical Biology and Medicine 31 (11):1287-1312.

Notter T, Aengenheister L, Weber-Stadlbauer U et al. (2018) Prenatal exposure to TiO_2 nanoparticles in mice causes behavioral deficits with relevance to autism spectrum disorder and beyond. Translational Psychiatry 8 (1):193.

Nowack B, Bucheli TD (2007) Occurrence, behavior and effects of nanoparticles in the environment. Environmental Pollution 150 (1):5-22.

Nur Y, Lead JR, Baalousha M (2015) Evaluation of charge and agglomeration behavior of TiO_2 nanoparticles in ecotoxicological media. Science of The Total Environment 535:45-53.

Nusch EA (1980) Comparison of different methods for chlorophyll and phaeopigment determination. Archiv fUr Hydrobiologie 14:14-36.

Nuzzo A, Hosseinkhani B, Boon N et al. (2017) Impact of bio-palladium nanoparticles (bio-Pd NPs) on the activity and structure of a marine microbial community. Environmental Pollution 220:1068-1078.

O'Brien N, Cummins E (2010) Nano-scale pollutants: fate in Irish surface and drinking water regulatory systems. Human and Ecological Risk Assessment: An International Journal 16 (4):847-872.

Obernosterer I, Catala P, Reinthaler T et al. (2005) Enhanced heterotrophic activity in the surface microlayer of the Mediterranean Sea. Aquatic Microbial Ecology 39 (3):293-302.

Ockenden A (2019) Investigating the effects of titanium nanoparticles on freshwater benthic algae. University of Bristol, Unpublised thesis

Odling G, Robertson N (2015) Why is anatase a better photocatalyst than rutile? The importance of free hydroxyl radicals. ChemSusChem 8 (11):1838-1840.

OECD (1984) Alga, growth inhibition test. OECD guidelines for testing of chemicals 201.

OECD (2010) Preliminary guidance notes on sample preparation and dosimetry for the safety testing of manufactured nanomaterials.

OECD (2011) Test No. 201: freshwater alga and cyanobacteria, growth inhibition test. OECD Publishing, Paris. doi:http://dx.doi.org/10.1787/9789264069923-en

Ong KJ, MacCormack TJ, Clark RJ et al. (2014) Widespread nanoparticle-assay interference: Implications for nanotoxicity testing. Plos One 9 (3).

Ottofuelling S, Von Der Kammer F, Hofmann T (2011) Commercial titanium dioxide nanoparticles in both natural and synthetic Water: comprehensive multidimensional testing and prediction of aggregation nehavior. Environmental Science & Technology 45 (23):10045-10052.

Ozkaleli M, Erdem A (2018) Biotoxicity of TiO_2 nanoparticles on *Raphidocelis subcapitata* microalgae exemplified by membrane deformation. International Journal of Environmental Research and Public Health 15 (3):416.

Paasche E (1973) Silicon and the ecology of marine plankton diatoms. II. Silicate-uptake kinetics in five diatom species. Marine Biology 19 (3):262-269.

Pan YL, Rao DVS, Mann KH (1996) Acclimation to low light intensity in photosynthesis and growth of *Pseudo-nitzschia multiseries* Hasle, a neurotoxigenic diatom. Journal of Plankton Research 18 (8):1427-1438.

Peng XH, Palma S, Fisher NS et al. (2011) Effect of morphology of ZnO nanostructures on their toxicity to marine algae. Aquatic Toxicology 102 (3-4):186-196.

Perkins RG, Mouget JL, Lefebvre S et al. (2006) Light response curve methodology and possible implications in the application of chlorophyll fluorescence to benthic diatoms. Marine Biology 149 (4):703-712.

Petersen EJ, Henry TB, Zhao J et al. (2014) Identification and avoidance of potential artifacts and misinterpretations in nanomaterial ecotoxicity measurements. Environmental Science & Technology 48 (8):4226-4246.

Peterson HG, Boutin C, Martin PA et al. (1994) Aquatic phyto-toxicity of 23 pesticides applied at expected environmental concentrations. Aquatic Toxicology 28 (3):275-292.

Pinckney J, Piceno Y, Lovell CR (1994) Short-term changes in the vertical distribution of benthic microalgal biomass in intertidal nuddy sediments. Diatom Research 9 (1):143-153.

Pinckney J, Zingmark RG (1991) Effects of tidal stage and sun angles on intertidal benthic microalgal productivity. Marine Ecology Progress Series 76 (1):81-89.

Pitt JA, Kozal JS, Jayasundara N et al. (2018) Uptake, tissue distribution, and toxicity of polystyrene nanoparticles in developing zebrafish (*Danio rerio*). Aquatic Toxicology 194:185-194.

Pokhrel LR, Dubey B (2013) Evaluation of developmental responses of two crop plants exposed to silver and zinc oxide nanoparticles. Science of The Total Environment 452-453:321-332.

Popov AP, Priezzhev AV, Lademann J et al. (2005) TiO_2 nanoparticles as an effective UV-B radiation skin-protective compound in sunscreens. Journal of Physics D: Applied Physics38 (15):2564-2570.

Prathna TC, Saroj Kumar S, Maria K (2018) Nanoparticles in household level water treatment: an overview.

Separation and Purification Technology 199:260-270.

Priyanka KP, Kurian A, Balakrishna KM et al. (2018) Toxicological impact of TiO_2 nanoparticles on *Eudrilus euginiae*. IET Nanobiotechnology 12 (5):579-584.

Rajkumar K, Kanipandian N, Thirumurugan R (2016) Toxicity assessment on haemotology, biochemical and histopathological alterations of silver nanoparticles-exposed freshwater fish *Labeo rohita*. Applied Nanoscience 6 (1):19-29.

Ralph PJ, Gademann R (2005) Rapid light curves: a powerful tool to assess photosynthetic activity. Aquatic Botany 82 (3):222-237.

Rawski DP, Bhuiyan MSH (2017) Pulp and paper: nonfibrous components. In: Reference Module in Materials Science and Materials Engineering. Elsevier. doi:https://doi.org/10.1016/B978-0-12-803581-8.10289-9

Relier C, Dubreuil M, Garcia OL et al. (2017) Study of TiO_2 P25 nanoparticles genotoxicity on lung, blood, and liver cells in lung overload and non-overload conditions after repeated respiratory exposure in rats. Toxicological Sciences 156 (2):527-537.

Rijstenbil JW (2003) Effects of UVB radiation and salt stress on growth, pigments and antioxidative defence of the marine diatom Cylindrotheca closterium. Marine Ecology Progress Series 254:37-47.

Ritchie R (2006) Consistent sets of spectrophotometric chlorophyll equations for acetone, methanol and ethanol solvents. Photosynthesis Research 89 (1):27-41.

Ritchie RJ (2008) Universal chlorophyll equations for estimating chlorophylls a, b, c, and d and total chlorophylls in natural assemblages of photosynthetic organisms using acetone, methanol, or ethanol solvents. Photosynthetica 46 (1):115-126.

Robichaud CO, Uyar AE, Darby MR, Zucker LG, Wiesner MR (2009) Estimates of upper bounds and trends in nano-TiO_2 production as a basis for exposure assessment. Environmental Science & Technology 43 (12):4227-4233.

Round F (1981) The ecology of algae. Cambridge University Press.

Round FE, Palmer J (1966) Persistent, vertical-migration rhythms in benthic microflora. J Marine Biol Assoc UK 46:191-214.

Roy R, Parashar A, Bhuvaneshwari M et al. (2016) Differential effects of P25 TiO_2 nanoparticles on freshwater green microalgae: *Chlorella* and *Scenedesmus* species. Aquatic Toxicology 176:161-171.

Royal Society (2004) Nanoscience and nanotechnologies: opportunities and uncertainties: summary and recomendations. Royal Society.

Rudramurthy GR, Swamy MK (2018) Potential applications of engineered nanoparticles in medicine and biology: an update. Journal of Biological Inorganic Chemistry 23 (8):1185-1204.

Sadiq IM, Dalai S, Chandrasekaran N et al. (2011) Ecotoxicity study of titania (TiO_2) NPs on two microalgae species: *Scenedesmus* sp. and *Chlorella* sp. Ecotoxicology and Environmental Safety 74 (5):1180-1187.

Salata O (2004) Applications of nanoparticles in biology and medicine. Journal of Nanobiotechnology 2 (1):3.

Salieri B, Pasteris A, Baumann J et al. (2015) Does the exposure mode to ENPs influence their toxicity to aquatic species? A case study with TiO_2 nanoparticles and *Daphnia magna*. Environmental Science and Pollution Research 22 (7):5050-5058.

Samadani M, Perreault F, Oukarroum A et al. (2018) Effect of cadmium accumulation on green algae *Chlamydomonas reinhardtii* and acid-tolerant *Chlamydomonas* CPCC 121. Chemosphere 191:174-182.

Sapkota A, Symons JM, Kleissl J et al. (2005) Impact of the 2002 Canadian forest fires on particulate matter air quality in Baltimore City. Environmental Science & Technology 39 (1):24-32.

Sartory DP (1982) Spectrophotometric analysis of chlorophyll a in freshwater phytoplankton.

Saxena P, Harish (2018) Nanoecotoxicological reports of engineered metal oxide nanoparticles on algae. Current Pollution Reports 4 (2):128-142.

Schieber M, Chandel NS (2014) ROS function in redox signaling and oxidative stress. Current Biology 24 (10):R453-R462.

Schmidt ÉC, Kreusch M, Felix MRdL et al. (2015) Effects of ultraviolet radiation (UVA+UVB) and copper on the morphology, ultrastructural organization and physiological responses of the red alga *Pterocladiella capillacea*. Photochem Photobiol 91 (2):359-370.

Schreiber U, Quayle P, Schmidt S et al. (2007) Methodology and evaluation of a highly sensitive algae toxicity test based on multiwell chlorophyll fluorescence imaging. Biosensors and Bioelectronics 22 (11):2554-2563.

Second regulatory review on nanomaterials (2012a) EUROPEAN COMMISSION. COM(2012) 572 final, http://ec.europa.eu/nanotechnology/pdf/second_regulatory_review_on_nanomaterials_-_staff_working_paper_accompanying_com(2012)_572.pdf. Accessed 26.02.2014

Seefeldt SS, Jensen JE, Fuerst EP (1995) Log-logistic analysis of herbicide dose-response relationships. Weed Technology 9 (2):218-227.

Sendra M, Sánchez-Quiles D, Blasco J et al. (2017a) Effects of TiO_2 nanoparticles and sunscreens on coastal marine microalgae: Ultraviolet radiation is key variable for toxicity assessment. Environment International 98:62-68.

Sendra M, Moreno-Garrido I, Yeste MP et al. (2017b) Toxicity of TiO_2, in nanoparticle or bulk form to freshwater and marine microalgae under visible light and UV-A radiation. Environmental Pollution 227:39-48.

Shannon CE, Weaver W (1949) The mathematical theory of communication. The University of Illinois Press, Urbana

Sharifi S, Behzadi S, Laurent S et al. (2012) Toxicity of nanomaterials. Chemical Society Reviews 41 (6):2323-2343.

Shehata SA, Lasheen MR, Ali GH et al. (1999) Toxic effect of certain metals mixture on some physiological and morphological characteristics of freshwater algae. Water, Air, and Soil Pollution 110 (1):119-135.

Shi H, Magaye R, Castranova V et al. (2013) Titanium dioxide nanoparticles: a review of current toxicological data. Particle and Fibre Toxicology, 10 (1):15.

Shi K, Yu J, Liu C et al. (2017) Impacts of enhanced UVB radiation on photosynthetic characteristics of the marine

diatom *Phaeodactylum tricornutum* (Bacillariophyceae, Heterokontophyta). Journal of Applied Phycology 29 (3):1287-1296.

Shi X, Li Z, Chen W et al. (2016) Fate of TiO_2 nanoparticles entering sewage treatment plants and bioaccumulation in fish in the receiving streams. NanoImpact 3-4:96-103.

Shih Y-H, Liu W-S, Su Y-F (2012) Aggregation of stabilized TiO_2 nanoparticle suspensions in the presence of inorganic ions. Environmental Toxicology and Chemistry 31 (8):1693-1698.

Sillanpää M, Paunu T-M, Sainio P (2011) Aggregation and deposition of engineered TiO_2 nanoparticles in natural fresh and brackish waters. Journal of Physics: Conference Series 304 (1):012018.

Simeonidis K, Mourdikoudis S, Kaprara E et al. (2016) Inorganic engineered nanoparticles in drinking water treatment: a critical review. Environmental Science: Water Researchearch Technology 2 (1):43-70.

Simon H-U, Haj-Yehia A, Levi-Schaffer F (2000) Role of reactive oxygen species (ROS) in apoptosis induction. Apoptosis 5 (5):415-418.

Sinang SC, Daud N, Kamaruddin N et al. (2019) Potential growth inhibition of freshwater algae by herbaceous plant extracts. Acta Ecologica Sinica 39 (3):229-233.

Singh AK (2016) Engineered nanoparticles: structure, properties and mechanisms of toxicity. Cambridge University Press.

Skocaj M, Filipic M, Petkovic J et al. (2011) Titanium dioxide in our everyday life; is it safe? Radiology and Oncology 45 (4):227-247.

Smith DJ, Underwood GJ (1998) Exopolymer production by intertidal epipelic diatoms. Limnology and Oceanography 43 (7):1578-1591.

Smith DJ, Underwood GJC (2000) The production of extracellular carbohydrates by estuarine benthic diatoms: the effects of growth phase and light and dark treatment. Journal of Phycology 36 (2):321-333.

Sondi I, Salopek-Sondi B (2004) Silver nanoparticles as antimicrobial agent: a case study on E-coli as a model for Gram-negative bacteria. Journal of Colloid and Interface Science 275 (1):177-182.

Souza VGL, Fernando AL (2016) Nanoparticles in food packaging: biodegradability and potential migration to food—a review. Food Packaging Shelf Life 8:63-70.

Stal L, de Brouwer J (2003) Biofilm formation by benthic diatoms and their influence on the stabilization of intertidal mudflats. Berichte – Forschungszentrum TERRAMARE 12:109-111.

Stauber JL, Florence TMJMB (1987) Mechanism of toxicity of ionic copper and copper complexes to algae. Marine biology 94 (4):511-519.

Stauber JL, Franklin NM, Adams MS (2002) Applications of flow cytometry to ecotoxicity testing using microalgae. Trends in Biotechnology 20 (4):141-143.

Suh WH, Suslick KS, Stucky GD et al. (2009) Nanotechnology, nanotoxicology, and neuroscience. Progress in neurobiology 87 (3):133-170.

Taboada-Serrano P, Chin C-J, Yiacoumi S et al. (2005) Modeling aggregation of colloidal particles. Current

Opinion in Colloid & Interface Science 10 (3):123-132.

Tang J-X, Hoagland KD, Siegfried BD (1997) Differential toxicity of atrazine to selected freshwater algae. Bulletin of Environmental Contamination Toxicology 59 (4):631-637.

Tang Y, Xin H, Yang F et al. (2018) A historical review and bibliometric analysis of nanoparticles toxicity on algae. Journal of Nanoparticle Research 20 (4):92.

Taylor SR (1964) Abundance of chemical elements in the continental crust: a new table. Geochimica et Cosmochimica Acta28 (8):1273-1285.

Tegart G (2004) Nanotechnology: the technology for the twenty-first century. Foresight 6 (6):364-370.

Thill A, Zeyons O, Spalla O et al. (2006) Cytotoxicity of CeO_2 nanoparticles for *Escherichia coli.* Physico-chemical insight of the cytotoxicity mechanism. Environmental Science & Technology 40 (19):6151-6156.

Thornton DCO, Dong LF, Underwood GJC et al. (2002) Factors affecting microphytobenthic biomass, species composition and production in the Colne Estuary (UK). Aquatic Microbial Ecology 27 (3):285-300.

Tiwari DK, Behari J, Sen P (2008) Application of nanoparticles in waste water treatment. World Applied Sciences Journal 3 (3):417-433.

Tong TZ, Shereef A, Wu JS et al. (2013) Effects of material morphology on the phototoxicity of nano-TiO_2 to bacteria. Environmental Science & Technology 47 (21):12486-12495.

Tsuji JS, Maynard AD, Howard PC et al. (2005) Research strategies for safety evaluation of nanomaterials, part IV: risk assessment of nanoparticles. Toxicological sciences 89 (1):42-50.

Tsuzuki T (2009) Commercial scale production of inorganic nanoparticles. International Journal of Nanotechnology 6 (5):567-578.

Tunzi MG, Chu MY, Bain Jr RC (1974) *In vivo* fluorescence, extracted fluorescence, and chlorophyll concentrations in algal mass measurements. Water Research 8 (9):623-635.

Underwood GJC (1994) Seasonal and spatial variation in epipelic diatom assemblages in the Severn Estuary. Diatom Research 9 (2):451-472.

Underwood GJC (2010) Microphytobenthos and phytoplankton in the Severn estuary, UK: present situation and possible consequences of a tidal energy barrage. Marine Pollution Bulletin 61 (1-3):83-91.

Underwood GJC, Kromkamp J (1999) Primary production by phytoplankton and microphytobenthos in estuaries. Advances in Ecological Research 29:93-153.

Underwood GJC, Paterson DM (1993a) Seasonal changes in diatom biomass, sediment stability and biogenic stabilization in the Severn Estuary. Journal of the Marine Biological Association of the United Kingdom 73 (4):871-887.

Underwood GJC, Paterson DM (1993b) Recovery of intertidal benthic diatoms after biocide treatment and associated sediment dynamics. Journal of the Marine Biological Association of the United Kingdom73 (1):25-45.

Underwood GJC, Perkins RG, Consalvey MC et al. (2005) Patterns in microphytobenthic primary productivity: species-specific variation in migratory rhythms and photosynthetic efficiency in mixed-species biofilms.

Limnology and Oceanography 50 (3):755-767.

Underwood GJC, Phillips J, Saunders K (1998) Distribution of estuarine benthic diatom species along salinity and nutrient gradients. European Journal of Phycology 33 (2):173-183.

Underwood GJC, Provot L (2000) Determining the environmental preferences of four estuarine epipelic diatom taxa: growth across a range of salinity, nitrate and ammonium conditions. European Journal of Phycology 35 (2):173-182.

Underwood GJC, Yallop ML (1994) *Navicula pargemina* sp. nov.—a small epipelic species from the Severn Estuary, U.K. Diatom Research 9 (2):473-478.

UNEP (2007) Emerging challenges: nanotechnology and the environment.

United Nations (2015) Globally harmonized system of classification and labelling of chemicals (GHS). Sixth revised edition edn., New York and Geneva.

Urrestarazu Ramos E, Vaes WHJ, Mayer P et al. (1999) Algal growth inhibition of *Chlorella pyrenoidosa* by polar narcotic pollutants: toxic cell concentrations and QSAR modeling. Aquatic Toxicology 46 (1):1-10.

Venugopal G, Hunt A, Alamgir F. Nanomaterials for energy storage in lithium-ion battery applications[J]. Material Matters, 2010, 5(2): 42.

Voltolina D (1991) A comparison of methods for the dispersion of cultures of benthic diatoms. Cryptogamie Algologie 12 (3):183-187.

Wagner S, Gondikas A, Neubauer E et al. (2014) Spot the difference: engineered and natural nanoparticles in the environment—release, behavior, and fate. Angewandte Chemie International Edition 53 (46):12398-12419.

Wang H, Burgess RM, Cantwell MG et al. (2014a) Stability and aggregation of silver and titanium dioxide nanoparticles in seawater: role of salinity and dissolved organic carbon. Environmental Toxicology and Chemistry 33 (5):1023-1029.

Wang H, Qi J, Keller AA et al. (2014b) Effects of pH, ionic strength and humic acid on the removal of TiO_2 nanoparticles from aqueous phase by coagulation. Colloids and Surfaces A: Physicochemical and Engineering Aspects 450:161-165.

Wang JX, Zhang XZ, Chen YS et al. (2008) Toxicity assessment of manufactured nanomaterials using the unicellular green alga *Chlamydomonas reinhardtii*. Chemosphere 73 (7):1121-1128.

Wang Y, Sun C, Zhao X et al. (2016a) The application of nano-TiO_2 photo semiconductors in agriculture. Nanoscale Research Letters 11 (1):529.

Wang Y, Zhu X, Lao Y et al. (2016b) TiO_2 nanoparticles in the marine environment: physical effects responsible for the toxicity on algae *Phaeodactylum tricornutum*. Science of The Total Environment 565: 818-826.

Warheit DB, Hoke RA, Finlay C et al. (2007) Development of a base set of toxicity tests using ultrafine TiO_2 particles as a component of nanoparticle risk management. Toxicology letters 171 (3):99-110.

Waring J, Baker NR, Underwood GJC (2007) Responses of estuarine intertidal microphytobenthic algal assemblages to enhanced ultraviolet B radiation. Global Change Biol 13 (7):1398-1413.

Wei L, Thakkar M, Chen Y et al. (2010) Cytotoxicity effects of water dispersible oxidized multiwalled carbon nanotubes on marine alga, *Dunaliella tertiolecta*. Aquatic Toxicology 100 (2):194-201.

Weir A, Westerhoff P, Fabricius L et al. (2012) Titanium dioxide nanoparticles in food and personal care products. Environmental Science & Technology 46 (4):2242-2250.

Westerhoff P, Atkinson A, Fortner J et al. (2018) Low risk posed by engineered and incidental nanoparticles in drinking water. Nature Nanotechnology 13 (8):661-669.

Wigginton NS, Haus KL, Hochella MF (2007) Aquatic environmental nanoparticles. J Environ Monitor 9 (12):1306-1316.

Williamson CJ, Brodie J, Goss B et al. (2014) *Corallina* and *Ellisolandia* (Corallinales, Rhodophyta) photophysiology over daylight tidal emersion: interactions with irradiance, temperature and carbonate chemistry. Marine Biology 161 (9):2051-2068.

Windler L, Lorenz C, von Goetz N et al. (2012) Release of titanium dioxide from textiles during washing. Environmental Science & Technology 46 (15):8181-8188.

Wright MV, Matson CW, Baker LF et al. (2018) Titanium dioxide nanoparticle exposure reduces algal biomass and alters algal assemblage composition in wastewater effluent-dominated stream mesocosms. The Science of the total environment 626:357-365.

Wu D, Yang S, Du W et al. (2019) Effects of titanium dioxide nanoparticles on *Microcystis aeruginosa* and microcystins production and release. Journal of Hazardous Materials 377: 1-7.

Xia B, Chen BJ, Sun XM et al. (2015) Interaction of TiO_2 nanoparticles with the marine microalga *Nitzschia closterium*: growth inhibition, oxidative stress and internalization. Science of the Total Environment 508:525-533.

Xiao YL, Vijver MG, Chen GC et al. (2015) Toxicity and accumulation of Cu and ZnO nanoparticles in *Daphnia magna*. Environmental Science & Technology 49 (7):4657-4664.

Xin L, Hong-ying H, Ke G et al. (2010) Effects of different nitrogen and phosphorus concentrations on the growth, nutrient uptake, and lipid accumulation of a freshwater microalga Scenedesmus sp. Bioresource Technology 101 (14):5494-5500.

Xiong DW, Fang T, Yu LP et al. (2011) Effects of nano-scale TiO_2, ZnO and their bulk counterparts on zebrafish: acute toxicity, oxidative stress and oxidative damage. Science of the Total Environment 409 (8):1444-1452.

Yallop ML, Dewinder B, Paterson DM et al. (1994) Comparative structure, primary production and biogenic stabilization of cohesive and noncohesive marine sediments inhabited by microphytobenthos. Estuarine, Coastal and Shelf Science S 39 (6):565-582.

Yallop ML, Paterson DM, Wellsbury P (2000) Interrelationships between rates of microbial production, exopolymer production, microbial biomass, and sediment stability in biofilms of intertidal sediments. Microbial Ecology 39 (2):116-127.

Yang WW, Miao AJ, Yang LY (2012) Cd^{2+} toxicity to a green alga *Chlamydomonas reinhardtii* as influenced by its ddsorption on TiO_2 engineered nanoparticles. Plos One 7 (3).

Yentsch CS, Menzel DW (1963) A method for the determination of phytoplankton chlorophyll and phaeophytin

by fluorescence. Deep Sea Research and Oceanographic Abstracts 10 (3):221-231.

Yin C, Meng F, Meng Y et al. (2016) Differential ultraviolet–visible absorbance spectra for characterizing metal ions binding onto extracellular polymeric substances in different mixed microbial cultures. Chemosphere 159:267-274.

Yue Y, Behra R, Sigg L et al. (2015) Toxicity of silver nanoparticles to a fish gill cell line: role of medium composition. Nanotoxicology 9 (1):54-63.

Zacher K, Wulff A, Hanelt D et al. (2005) Impact of UV radiation on the succession of intertidal benthic primary producers in Antarctica. Phycologia 44 (4):114-115.

Zargiel KA, Coogan JS, Swain GW (2011) Diatom community structure on commercially available ship hull coatings. Biofouling 27 (9):955-965.

Zhang L, Gu FX, Chan JM et al. (2008) Nanoparticles in medicine: therapeutic applications and developments. Clinical pharmacology & Therapeutics 83 (5):761-769.

Zhang S, Deng R, Lin D et al. (2017) Distinct toxic interactions of TiO_2 nanoparticles with four coexisting organochlorine contaminants on algae. Nanotoxicology 11 (9-10):1115-1126.

Zhang Wx, Elliott DW (2006) Applications of iron nanoparticles for groundwater remediation. Remediation Journal 16 (2):7-21.

Zhang X, Li W, Yang Z (2015) Toxicology of nanosized titanium dioxide: an update. Archives of Toxicology 89 (12):2207-2217.

Zheng L, Hong F, Lu S et al. (2005) Effect of nano-TiO_2 on strength of naturally aged seeds and growth of spinach. Biological Trace Element Research 104 (1):83-91.

Zhou DX, Ji ZX, Jiang XM et al. (2013) Influence of material properties on TiO_2 nanoparticle agglomeration. Plos One 8 (11).

Zhou DX, Keller AA (2010) Role of morphology in the aggregation kinetics of ZnO nanoparticles. Water Research 44 (9):2948-2956.

Zhu M, Wang H, Keller AA et al. (2014) The effect of humic acid on the aggregation of titanium dioxide nanoparticles under different pH and ionic strengths. Science of The Total Environment 487:375-380.

Zhu N, Wang S, Tang C et al. (2019) Protection mechanisms of periphytic biofilm to photocatalytic nanoparticle exposure. Environmental Science & Technology 53 (3):1585-1594.

Zi FY, Long W, Hua GY et al. (2013) Recent progress in biomedical applications of titanium dioxide. Physical Chemistry Chemical Physics 15 (14):4844-4858.

Zong Y, Horton BP (1998) Diatom zones across intertidal flats and coastal saltmarshes in Britain. Diatom Research 13 (2):375-394.